UNIVERSITAT POLITÈCNICA DE CATALUNYA

PhD program in:
AUTOMATIC CONTROL, ROBOTICS AND COMPUTER VISION

Contributions to LPV control under time-varying saturations

Doctoral thesis by:
Adrián Ruiz Royo

Thesis advisors:
Dr. Bernardo Morcego Seix
Dr. Damiano Rotondo

September, 2023

To my parents,
to my sister,
to my family.

Abstract

This thesis presents contributions to the state-of-the-art in the field of gain-scheduling control, with special emphasis on linear parameter-varying (LPV) systems and the presence of time-varying saturations. In this area, solutions are formulated to design gain-scheduling controllers based on linear matrix inequalities (LMIs), thus offering a systematic way to efficiently solve the problems below using the available solvers under a finite number of conditions.

First of all, the problem of designing state-feedback controllers with the capability to take into account both the possible inherent physical variations of the system and those that may affect the actuators over time is considered. For this purpose, it is proposed to use the shifting paradigm concept and a convex representation for the description of the instantaneous saturation limit values. Additionally, an optimization procedure is suggested for selecting the desired specifications, such as the maximization of the system's closed-loop convergence speed when the largest saturation limit is available. As a result, the designed controller is able to adjust its performance considering the amount of available control action while ensuring closed-loop system stability under saturation avoidance. When state information is not directly available through the sensors, the suggested methodology is adapted to the utilization of a dynamic output-feedback controller structure.

Then, the problem of the feedback linearization of nonlinear systems subject to actuator saturations is addressed. As a consequence of the nonlinear transformation of the state, the feedback linearized system is affected by the presence of state-dependent saturations, making it difficult to design controllers using linear techniques. In order to guarantee the stability of the linearized system under saturation avoidance, the idea of establishing a control strategy based on the combination of a linearization law and a gain planning controller is explored. Hence, the total control action will remain in the linearity region of the actuator. In addition, the controller is designed using the developed methodology, thus ensuring its adaptability to changes in the saturation limits. The effectiveness of the proposed methodology is demonstrated using the Quanser 3-DoF hover platform.

Finally, the problem of designing switching controllers for linear systems subject to asymmetric saturations is considered. The presented solution transforms the asymmetrically saturated linear system into an equivalent switched system with symmetric saturations. In contrast to existing results in the literature, a switching rule is established based on the achievable closed-loop system performance, which allows the selection of the controller with the largest closed-loop system convergence speed among all non-saturating controllers.

Resumen

Esta tesis presenta diversas contribuciones en el ámbito del control por planificación de ganancia, con especial énfasis en sistemas lineales de parámetros variantes (LPV, del inglés *linear parameter-varying*) y la presencia de saturaciones variables en el tiempo. En esta área, se formulan soluciones para diseñar controladores por planificación de ganancia basadas en desigualdades lineales matriciales (LMI, del inglés *linear matrix inequality*), ofreciendo así una forma sistemática de resolver eficientemente los problemas descritos más adelante a través de los algoritmos numéricos disponibles bajo un número finito de condiciones.

En primer lugar, se plantea el problema de diseñar controladores por realimentación del estado con la capacidad de tener en cuenta tanto las posibles variaciones físicas inherentes del sistema como las que pueden afectar a los actuadores a lo largo del tiempo. Para ello se propone utilizar el paradigma *shifting LPV* y una representación convexa para describir los cambios instantáneos de los límites de la saturación. Además, se propone un procedimiento de optimización para seleccionar las especificaciones deseadas, como por ejemplo la maximización de la velocidad de convergencia del sistema en lazo cerrado cuando se dispone del mayor límite de saturación. Como resultado, el controlador diseñado es capaz de ajustar su rendimiento teniendo en cuenta la cantidad de acción de control disponible, al mismo tiempo que garantiza la estabilidad del sistema en lazo cerrado evitando la saturación. Cuando la información del estado no está disponible directamente a través de los sensores, la metodología sugerida se adapta a la utilización de una estructura de control dinámica por realimentación de salida.

Posteriormente, se aborda la linealización por realimentación de sistemas no lineales sujetos a saturación del actuador. Como consecuencia de la transformación no lineal del estado, el sistema linearizado se ve afectado por la presencia de saturaciones que dependen del estado, dificultando así el diseño de controladores mediante el uso de técnicas lineales. Con el fin de garantizar la estabilidad del sistema y evitar su saturación, se explora la idea de establecer una estrategia de control basada en la combinación de una ley de linealización con un controlador por planificación de ganancia. Por consiguiente, la acción de control permanecerá en la región de linealidad del actuador. Además, el control está diseñado utilizando la metodología desarrollada, asegurando así su adaptabilidad a los cambios en los límites de la saturación. La efectividad de la metodología propuesta se demuestra utilizando la plataforma experimental: *Quanser 3-DoF hover*.

Finalmente, se considera el problema de diseño de controladores de conmutación para sistemas lineales sujetos a saturaciones asimétricas. La solución presentada transforma el sistema lineal saturado asimétricamente en un sistema conmutado equivalente con saturación simétrica. A diferencia de los resultados existentes en la literatura, se establece una regla de conmutación basada en el rendimiento que puede lograr el sistema en lazo cerrado. Concretamente, la regla de conmutación permite seleccionar el controlador con la velocidad de convergencia del sistema en lazo cerrado más grande entre todos los controladores disponibles que aseguren evitar la saturación.

Resum

Aquesta tesi presenta diverses contribucions en l'àmbit del control per planificació del guany, amb especial èmfasi en sistemes lineals de paràmetres variants (LPV, de l'anglès *linear parameter-varying*) i la presència de saturacions variables en el temps. En aquesta àrea, es formulen solucions per dissenyar controladors per planificació de guany basats en desigualtats lineals matricials (LMIs, de l'anglès *linear matrix inequalities*), oferint així una forma sistemàtica de resoldre eficientment els problemes que es descriuen més endavant a través dels algorismes numèrics disponibles sota un nombre finit de condicions.

En primer lloc, es planteja el problema de dissenyar controladors per realimentació d'estat amb la capacitat de tenir en compte tant les possibles variacions físiques inherents del sistema com les que poden afectar els actuadors al llarg del temps. Amb aquesta finalitat, es proposa utilitzar el paradigma *shifting LPV* i una representació convexa per a la descripció dels valors límit de saturació instantània. A més, es suggereix un procediment d'optimització per seleccionar les especificacions desitjades, com ara la maximització de la velocitat de convergència del sistema en llaç tancat quan es disposa del límit de saturació més gran. Com a resultat, el controlador dissenyat és capaç d'ajustar el seu rendiment tenint en compte la quantitat d'acció de control disponible, alhora que garanteix l'estabilitat del sistema en llaç tancat evitant la saturació. Quan la informació de l'estat no està disponible directament a través dels sensors, la metodologia suggerida s'adapta a la utilització d'una estructura de control dinàmica per realimentació de sortida.

Posteriorment, s'aborda la linealització per realimentació de sistemes no lineals afectats per la saturació de l'actuador. A conseqüència de la transformació no lineal de l'estat, el sistema linealitzat es veu afectat per la presència de saturacions que depenen de l'estat, dificultant així el disseny de controladors mitjançant tècniques lineals. Per tal de garantir l'estabilitat del sistema linealitzat i evitar la seva saturació, s'explora la idea d'establir una estratègia de control basada en la combinació d'una llei de linealització amb un controlador per planificació de guany. Per tant, l'acció de control romandrà a la regió de linealitat de l'actuador. A més, el controlador està dissenyat utilitzant la metodologia desenvolupada, assegurant així la seva adaptabilitat als canvis en els límits de la saturació. L'eficàcia de la metodologia proposada es demostra mitjançant la plataforma experimental: *Quanser 3-DoF hover*.

Finalment, es considera el problema de dissenyar controladors de commutació per a sistemes lineals afectats per saturacions asimètriques. La solució presentada transforma el sistema lineal saturat asimètricament en un sistema commutat equivalent amb saturació simètrica. A diferència dels resultats existents a la literatura, s'estableix una regla de commutació basada en el rendiment que pot aconseguir el sistema en llaç tancat. Concretament, la regla de commutació permet seleccionar el controlador amb la velocitat de convergència del sistema en llaç tancat més gran entre tots els controladors disponibles que assegurin evitar la saturació.

Acknowledgements

This thesis was carried out at the Research Center for Supervision, Safety and Automatic Control (CS2AC) with the financial support of UPC and AGAUR through the contracts FPI-UPC 2018 and FI-SDUR 2020. These supports are gratefully acknowledged.

First of all, I would like to thank my thesis supervisors and PhD directors: Dr. Bernardo Morcego Seix and Dr. Damiano Rotondo, for their patience, dedication, and support throughout the development of this thesis. For helping me grow both professionally and personally, believing in me, and dedicating some of their time to giving me advice when I needed it. Without them, this work would not have been possible.

Despite the exceptional situation because of COVID-19, I had the opportunity to enjoy a stay in a warm and welcoming country like Norway. I would like to thank all the people in the Department of Electrical and Computer Engineering (IDE) who made me feel like one of them. In this group, I had the opportunity to meet wonderful people. Thank you for everything.

I would like to thank the CS2AC research group for giving me not only the opportunity to conduct this work but also for their dedication to teaching during my university years. I would also like to thank all the wonderful people I have had the privilege to meet over the years. In particular, I would like to thank Tomeu, Julen, Helem, Carlos, Juli, Jaume, Boutrous, Débora, Sergio, and many more.

To my friends, who with their patience, encouragement, and curiosity have helped me carry out this journey.

Last but not least, I want to give special thanks to my parents, Lucio and Carmen, for giving me the opportunity to build my future, for their patience, for instilling in me the example of effort and self-improvement, and for always supporting me. To my sister Laia, who has always been there for me and has brought a smile to my face when I needed it most. I cannot thank you enough.

Adrián Ruiz Royo
Terrassa, June of 2023

Contents

List of Figures

List of Tables

Acronyms

BMI	Bilinear matrix inequality
CoG	Centre of gravity
CT	Continuous-time
DAR	Differential algebraic representation
DoF	Degree of Freedom
FBL	Feedback linearization
GS	Gain-scheduled
GSDR	Guaranteed shifting decay rate
GSWDR	Guaranteed switching decay rate
LMI	Linear matrix inequality
LPV	Linear parameter-varying
LTI	Linear time-invariant
LTV	Linear time-varying
MIMO	Multiple-input multiple-output
MPC	Model predictive control
MVE	Minimum volume ellipsoid
PDQ	Parameter-dependent quadratic
PDQB	Parameter-dependent quadratic boundedness
PDQLF	Parameter-dependent quadratic Lyapunov function
QB	Quadratic boundedness
QLF	Quadratic Lyapunov function
SDP	Semidefinite programming
SOS	Sum of squares
UAV	Unmanned Aerial Vehicle

Notation

Fields and spaces

$\mathbb{N}$	the set of natural numbers
$\mathbb{Z}$	the set of integers
$\mathbb{R}$	the set of real numbers
$\mathbb{R}_+$	the set of non-negative real numbers
$\mathbb{R}^n$	the $n-$dimensional real space
$\mathbb{R}^{n\times m}$	the set of real matrices of dimensions $n \times m$
$\mathbb{S}^n$	the set of symmetric real matrices of dimension n
$\mathcal{I}$	the subset of ordered integers
$\mathcal{D}_A$	domain of attraction of the origin
$\mathcal{D}_x$	domain of $\mathbb{R}^n$ containing the origin
$\mathcal{X}$	subset of $\mathcal{D}_x$
$\mathcal{X}_0$	region of expected initial conditions
$\mathcal{X}_p$	region of expected initial plant conditions
$\mathcal{Z}_0$	region of expected initial transformed state variables
$\mathcal{Z}$	space of the transformed state variables
$\mathcal{W}$	energy bound of w
Φ	domain of variation of φ
Φ_d	domain of variation of $\dot{\varphi}$
Θ	domain of variation of ϑ
Θ_d	domain of variation of $\dot{\vartheta}$

Operators

$\overset{(i)}{y}$	denotes the i^{th} derivative of y
$\bullet^{-1}$	inverse
$\bullet^\top$	transposition
$A_{[i]}$	the i^{th} row of matrix A
$A_{[ij]}$	the element of the i^{th} row and the j^{th} column of matrix A
$\prec$, $(\preceq)$	negative (semi-)definite
$\succ$, $(\succeq)$	positive (semi-)definite
$\mathrm{diag}\{\cdot\}$	builds a diagonal (block-)matrix with the elements of its argument
$\mathrm{He}\{\cdot\}$	denotes the shorthand $(\cdot) + (\cdot)^\top$
I_n	the identity matrix of dimensions $n \times n$
$0_{n\times m}$	the zero matrix of dimensions $n \times m$
$\|x\|_2$	the L_2-norm of x, i.e., $\|x\|_2 = \sqrt{\int_0^\infty x^\top x\, dt}$

$\mathrm{Co}\{\cdot\}$	the convex hull of the elements of its argument
$\mathrm{sign}(x)$	the sign function of $x \in \mathbb{R}$
$\mathrm{card}(\cdot)$	stands for the cardinality of a set
$\mathrm{sat}(\cdot)$	stands for the saturation function
$\bar{(\cdot)}$	largest value of a set
$\underline{(\cdot)}$	smallest value of a set
$\mathrm{vec}(\cdot)$	matrix vectorization
v_i	the i^{th} element of the vector v
$v_{i,j}$	the i^{th} element of the vector v located in the j^{th} vertex/region
$v^{\{i\}}$	the i^{th} vector of a set of vectors
$v^{\{i\}}_j$	the j^{th} element of $v^{\{i\}}$
∇	gradient with respect to x
$L_f h(x)$	the Lie derivative of h along f
$\star$	denotes the block induced by symmetry in a matrix
$\otimes$	Kronecker product

Signals and variables

t	time variable (continuous-time)
x	(augmented) state vector
x_c	controller state vector
x_p	plant state vector
u	input vector
u_c	controller output vector
w	disturbance vector
y	output vector
z_∞	output performance vector
z	transformed state vector
ν	virtual input vector
$n_\bullet$	dimension of an specific element
$\underline{u}, \bar{u}$	the lower and upper saturation limit vectors of u
$\bar{v}_i$	i^{th} saturation limit vector when switching control is used
σ	time-varying saturation limit vector / index of the active controller gain when switching control is used
φ	vector of performance-varying parameters
ϑ	vector of varying parameters

Related to the polytopic representation

Δ^n	unit simplex in $\mathbb{R}^n$
$\mathcal{P}_\bullet$	polytope
α, β, μ, η	polytopic weight vectors
$\underline{\delta\eta}_i, \bar{\delta\eta}_i$	are the i^{th} lower and upper bounds of $\dot{\eta}_i$
$\underline{\delta\mu}_i, \bar{\delta\mu}_i$	are the i^{th} lower and upper bounds of $\dot{\mu}_i$

Related to the feedback linearization

f	a sufficiently smooth vector field on $\mathbb{R}^{n_x}$
h	a sufficiently smooth function on $\mathbb{R}^{n_x}$
b	feedback linearizing law term
r_i	the i^{th} relative degree
r_t	total relative degree
G	mapping matrix whose columns are smooth vector fields in $\mathbb{R}^{n_x}$
M	decoupling matrix function
T	diffeomorphism
$\mathcal{V}$	polyhedral region in which the virtual input ν do not saturate
$\hat{\mathcal{V}}$	symmetric approximation of the region $\mathcal{V}$
$\mathcal{R}_z$	representation of $\hat{\mathcal{V}}$ in the $z-$coordinates

Others

A	state matrix
B	input matrix
C	output matrix
D	feedthrough matrix
B_w	disturbance input matrix
C_z	performance output matrix
D_{zu}	performance feedthrough matrix
D_{zw}	disturbance feedthrough matrix
K	controller matrix
A_c, B_c, C_c, D_c	dynamic output-feedback control matrices
Y	auxiliary variable to convert BMIs into LMIs
P	(parameter-dependent) Lyapunov matrix
V	(parameter-dependent) quadratic Lyapunov function
$\mathbb{A}$	augmented state matrix
$\mathbb{B}$	augmented input matrix
$\mathbb{B}_w$	augmented disturbance input matrix
$\mathbb{C}_z$	augmented performance output matrix
$\mathbb{K}$	augmented controller matrix
$\mathrm{d_R}$	guaranteed decay rate
γ	$\mathcal{H}_\infty$ performance
$\hat{\sigma}_l$	convex representation of $\sigma_l(\cdot)^2$
$\mathcal{E}$	ellipsoidal region
$\mathcal{E}_Z$	minimum volume ellipsoid covering $\mathcal{Z}$
$\mathcal{E}_w$	ellipsoidal region containing w
$\mathcal{L}$	polyhedral region in which the actuators do not saturate
$\mathcal{U}$	maximal ellipsoidal region contained in $\mathcal{L}$ (input-domain)
$\mathcal{U}_x$	state-domain representation of the ellipsoidal region $\mathcal{U}$

Additional notations

Throughout this thesis, $p-$dimensional multi-indexes are denoted by boldface elements such as $\boldsymbol{i} = (i_1, i_2, \ldots, i_p) \in \mathbb{N}^p$, whereas $\mathcal{P}(\boldsymbol{i})$ is the set of permutations with possible repeated elements of $\boldsymbol{i}$. $\mathcal{I}_{[a,b]}$ denotes the set of integers $\{a, a+1, \ldots, b\}$ with $a, b \in \mathbb{Z}$ and $a \leq b$. For $M \in \mathbb{S}^n$, $M \succ 0$ $(M \succeq 0)$ and $M \prec 0$ $(M \preceq 0)$ stand for a positive (semi-)definite matrix and for a negative (semi-)definite matrix, respectively. $M \in \mathbb{S}^n_+$ is used as a shorthand for positive-definite symmetric matrices. The generic arguments of a function are denoted by $(\cdot)$. Given $u \in \mathbb{R}^m$ and the limits $a, b \in \mathbb{R}^m_+ \backslash \{0\}$, the polyhedral region $\mathcal{L}(u, a, b)$ is defined as:

$$\mathcal{L}(u, a, b) \triangleq \left\{ u \in \mathbb{R}^m : -a_l \leq u_l \leq b_l,\ l \in \mathcal{I}_{[1,m]} \right\}.$$

Then, the abbreviated notation $\mathcal{L}(u, a)$ is used when $a = b$, and $\mathcal{L}(K, a, b)$ stands for a representation in $\mathbb{R}^n$, e.g. by the mapping $u = Kx$ with $K \in \mathbb{R}^{m \times n}$ and $x \in \mathbb{R}^n$. Furthermore, $\mathcal{L}_s$ is used to indicate that the region is associated with a switching control strategy.

1 Introduction

1.1 Context of the thesis

The results presented in this thesis have been developed at the Research Center for Supervision, Safety and Automatic Control (CS2AC) of the Universitat Politècnica de Catalunya (UPC) in Terrassa, Spain. The research was jointly supervised by Dr. Bernardo Morcego Seix and Dr. Damiano Rotondo, and was sponsored partly by UPC through an FPI-UPC grant and by the Agència de Gestió d'Ajuts Universitaris i de Recerca (AGAUR) through the contract FI-SDUR. The supports are gratefully acknowledged.

1.2 Motivations

It is well known that for physical, safety, or technological reasons, any real-world system presents constraints. Among all these constraints, actuator saturation is probably the nonlinearity that has been studied the most in the control theory field, owing to the potential performance degradation or destabilizing effects induced on the closed-loop system. Examples of some actuator limitations could be easily found in most common devices in industrial processes, such as the voltage limit in electromechanical actuators, the pneumatic power in pneumatic actuators, or the flow volume or rate limits in hydraulic actuators. Also, the presence of actuator saturation can be found in other fields, such as aerospace applications, through deflection limits, among others. Hence, it is crucial to design controllers that consider this phenomenon to avoid possible accidents such as the meltdown of the Chornobyl nuclear power station or aircraft crashes (see [116]).

Over the last few decades, many studies have focused on developing controller design methodologies based on rigorous theory to guarantee desirable system performance, taking into account the actuator saturation phenomenon. These methods can preserve the overall system stability under saturation avoidance or even the allowance of the actuator to perform in saturation mode for a finite interval of time, under the common consideration of saturation limits being constant in time. Even though many of these approaches have achieved successful performance, an open direction remains central to the design of actuator saturation controllers: the time-variability of the saturation limits. The presence of time-varying saturation limits should be considered a consequence of the existence of time-varying conditions and the actuator's inherent physical limitations, which play a crucial role in the saturation's behaviour. They could arise in control systems due to several reasons, such as the natural wear of actuators, which would provide a progressive lack of actuation signal, or temporary power shortages. In autonomous aerial vehicles, for example, the progressive lack of energy availability or the variations of the aerodynamic coefficients as a consequence of environmental changes can affect the availability of the actuator action [1, 21, 32, 41, 49, 52, 89]. This could happen in hazardous zones when performing different tasks such

as assisting firefighters in extinguishing fires [75], monitoring coastal areas and/or high mountains for rescue teams [124], or measuring the melting ice caps [16]. Additionally, in trajectory tracking problems, the control action is typically calculated as the addition of a feedforward and a feedback action. When a time-varying trajectory is taken into account, the feedforward component changes with time, which is perceived by the feedback controller as a time-varying saturation.

The suitability of the linear parameter-varying (LPV) framework for controlling nonlinear systems has attracted considerable attention due to its elegant way of addressing nonlinearities and uncertainties through an appropriate definition of time-varying parameters [51]. For this reason, the design of LPV controllers could be a viable solution to consider the risk caused by time-varying conditions affecting actuator saturation behaviour and, consequently, the availability of the control action. Furthermore, a recent line of research has presented a new methodology for designing LPV controllers based on the shifting paradigm concept [92], which allows the extension of the scheduling parameter vector for introducing online changes in the desired system performance.

An interesting perspective for tackling the problem of the time-variability of the saturation limits emerges from the combination of the shifting paradigm concept, the LPV framework, and the actuator saturation control. Therefore, the motivation of this PhD dissertation is to exploit the shifting paradigm concept by focusing on developing shifting feedback controllers for LPV systems subject to time-varying saturations, guaranteeing time-varying saturation avoidance, and fulfilling desired performance specifications.

1.3 Thesis objectives

The objectives of this thesis are the following:

- to propose an approach for the design of shifting state-feedback controllers for time-varying saturated LPV systems that can guarantee some desired closed-loop performance according to the saturation limit changes;
- to propose an approach for the design of shifting output-feedback controllers for time-varying saturated LPV systems that can guarantee some desired closed-loop performance according to the saturation limit changes;
- to propose an approach for the design of shifting feedback linearizing controllers for full-feedback linearized systems under state-dependent saturations;
- to consider the presence of asymmetric saturations in linear systems such that the designed controller guarantees convergence to zero with a desired closed-loop performance.

1.4 Outline of the thesis

The content of this thesis is organized as follows:

- **Chapter 2** provides some mathematical background required for understanding the content of this thesis. Particularly, it shows the concept and useful properties of linear matrix inequality (LMI), the definition and polytopic representation of linear parameter-varying

(LPV) systems, as well as the analysis and design of LPV control systems using (parameter-dependent) quadratic Lyapunov functions. A finite-dimensional LMI relaxation procedure along with an introduction to the shifting paradigm concept are also provided. The chapter is concluded by a brief overview of the existing control approaches for addressing actuator saturation and the concept of saturation avoidance. The reader who is familiarized with the above concepts can safely skip this chapter and proceed to Chap. 3.

- **Chapter 3** addresses the problem of designing shifting state-feedback controllers for time-varying saturated LPV systems. In the proposed approach, a possible mapping between the instantaneous saturation limit values and a performance scheduling vector is introduced. The resulting idea is exploited through the shifting paradigm concept, enabling the design of a gain-scheduling controller that adapts the closed-loop system performance in accordance with the saturation limit variations. By means of some considerations, the problem's solution is expressed as an LMI-based design condition that can efficiently be solved via available solvers. It is worth highlighting that saturation avoidance of the control action is ensured. Furthermore, closed-loop convergence speed or disturbance rejection effectiveness is regulated online according to the performance scheduling vector through the shifting paradigm concept. To conclude, numerical examples are used to demonstrate the effectiveness of the proposed approaches.

- **Chapter 4** focuses on designing shifting output-feedback controllers for time-varying saturated LPV systems, extending the LMI-based methodology suggested in Chap. 3. Concretely, the combination of a gain-scheduled dynamic output-feedback controller with the shifting paradigm concept and the formulation of requirements for ensuring time-varying saturation avoidance under shifting performance specifications. Then, an overall LMI-based design approach is presented using parameter-dependent quadratic Lyapunov functions (PDQLFs). The practical implementation of the controller is discussed to provide a finite number of design conditions under certain constraints. Finally, the chapter is concluded by the presentation of some simulation results using a nonlinear quadrotor model to illustrate the effectiveness of the proposed approach.

- **Chapter 5** is devoted to designing shifting state-feedback controllers for full-feedback linearized systems under state-dependent saturations. The presented design conditions are based on integrating the shifting paradigm concept and the feedback linearization (FBL) technique through the framework proposed in Chap. 3. Also, it is shown that an input constraint mapping is required for defining the linear region of the actuators in the domain of the virtual inputs. Therefore, this chapter proposes a shifting control strategy to guarantee the stabilization of the constrained linearized system under saturation avoidance, such that the combination of the linearizing law and the shifting state-feedback control law remains within the limits of the actuator. Furthermore, the designed controller adapts its closed-loop performance in terms of convergence speed according to the instantaneous values of the time-varying system's linearity region. The potential and performance of the proposed approach are demonstrated on the Quanser 3-DoF hover platform.

- **Chapter 6** deals with the development of non-saturating switching state-feedback controllers for linear systems under asymmetric saturations. The proposed methodology is based on transforming an asymmetrically saturated linear system to an analogous switching system with symmetrical saturations. The primary difference between the suggested approach and existing results is that the switching rule is defined with attainable closed-loop performance in mind. Furthermore, a closed-loop performance criterion is established by assigning different decay rate values to the different possible controller modes, allowing the control system to adjust its closed-loop performance in terms of guaranteed convergence speed. Although the discussion is focused on LTI systems for keeping the notation simpler, the extension to the LPV case is also discussed. The chapter is concluded with an illustrative example to validate the approach.

- **Chapter 7** concludes this thesis with a summary of the main conclusions and outlines possible directions for future research.

1.5 List of publications

The research contained in this thesis has been published in several conferences and journals. A list of articles based on the methodology, concepts, and results achieved in the thesis is provided below:

- [95] A. Ruiz, D. Rotondo, and B. Morcego. "Design of state-feedback controllers for linear parameter varying systems subject to time-varying input saturation". *Applied Sciences* 9:17, 2019, p. 3606. ISSN: 2076-3417

- [96] A. Ruiz, D. Rotondo, and B. Morcego. "Shifting $\mathcal{H}_\infty$ linear parameter varying state-feedback controllers subject to time-varying input saturations". *IFAC-PapersOnLine* 53:2, 2020. 21th IFAC World Congress, pp. 7338–7343. ISSN: 2405-8963. DOI: https://doi.org/10.1016/j.ifacol.2020.12.991

- [97] A. Ruiz, D. Rotondo, and B. Morcego. "Design of shifting state-feedback controllers for constrained feedback linearized systems: application to quadrotor attitude control". *International Journal of Robust and Nonlinear Control*, 2023. Under review.

- [98] A. Ruiz, D. Rotondo, and B. Morcego. "Design of switching state-feedback controllers for linear systems subject to asymmetric saturations". *IFAC-PapersOnLine*, 2023. 22nd IFAC World Congress. Accepted.

- [99] A. Ruiz, D. Rotondo, and B. Morcego. "Design of shifting state-feedback controllers for LPV systems subject to time-varying saturations via parameter-dependent Lyapunov functions". *ISA Transactions*, 2021. ISSN: 0019-0578. DOI: https://doi.org/10.1016/j.isatra.2021.07.025

- [100] A. Ruiz, D. Rotondo, and B. Morcego. "Design of shifting output-feedback controllers for LPV systems subject to time-varying saturations". *IFAC-PapersOnLine* 55:35, 2022. 5th IFAC Workshop on Linear Parameter Varying Systems 2022, pp. 13–18. ISSN: 2405-8963. DOI: https://doi.org/10.1016/j.ifacol.2022.11.283

2 Background

For the purpose of the development of this thesis, some well-known mathematical background on control theory will be presented in this chapter. Particularly, the concept and useful properties of linear matrix inequality (LMI), the definition and control of linear parameter-varying (LPV) systems, and current approaches for addressing the control of linear systems subject to actuator saturation are provided. For comprehensive and detailed proofs of the presented results, see [23, 26, 119] and the references therein.

2.1 Linear matrix inequalities

The use of linear matrix inequalities (LMIs) in control theory has its roots in the 1890s with the introduction of what is now known as Lyapunov theory [71]. However, it was not until the 1940s that Lur'e, Postnikov, and other researchers in the Soviet Union applied Lyapunov's theory to practical engineering problems where the LMIs were solved analytically by hand [22]. From the early 1960s to the late 1980s, their importance in control theory was strongly highlighted by the work of Kalman, Yakubovich, Popov, and Willems, as well as the development of optimization algorithms such as the interior-point algorithm [80], which provided an efficient and optimal way to solve LMIs numerically. Over the last few decades, its application in control theory has evolved and expanded as a powerful tool for handling a variety of control problems, including stability analysis, controller design, and optimization (see [23, 31, 107] and references therein). The key to their success lies in formulating control problems as well-defined optimization problems, such as linear and quadratic programming or semi-definite programming (SDP), which are well-established in convex optimization. Another factor contributing to their popularity is the availability of commercial or non-commercial solvers such as SeDuMi [117], SDPT3 [121], or MOSEK [8] together with the use of the YALMIP toolbox [70] or the CVX interface [46] for solving this kind of problems.

Let us now formally define the LMI as [31]:

Definition 2.1.1. An LMI is an expression of the form:

$$F(x) \triangleq F_0 + \sum_{i=1}^{n} x_i F_i \prec 0, \tag{2.1}$$

where $x \in \mathbb{R}^n$ represents the vector of n real decision variables and F_i are known symmetric matrices for $i \in \mathcal{I}_{[0,n]}$. Note that $F(x) \preceq 0$ is a *non-strict* LMI.

On the other hand, certain control design conditions cannot be effectively expressed using an LMI formulation, resulting in a more complex condition known as the bilinear matrix inequality (BMI), which is defined as follows:

Definition 2.1.2. A BMI is an expression of the form:

$$H(x) \triangleq H_0 + \sum_{i=1}^{n} x_i H_i + \sum_{i=1}^{n}\sum_{j=1}^{n} x_i x_j H_{ij} \prec 0, \quad i,j \in \mathcal{I}_{[0,n]}, \tag{2.2}$$

where $x \in \mathbb{R}^n$, H_i and H_{ij} are known symmetric matrices.

2.1.1 Useful properties and tools for LMI formulation

Since BMI conditions will arise for some control design problems treated in this thesis, we present below a recapitulation of some useful properties and existing results from the literature for reformulating LMIs or transforming matrix inequalities into LMIs.

Congruence transformation

If A is a square matrix and Π is a square nonsingular matrix, the product $\Pi^\top A \Pi$ is referred to as a congruence transformation of A. A recognized characteristic of this transformation is that it preserves the definiteness of a symmetric or Hermitian matrix. Thus defining, e.g.,

$$A \succ 0 \iff \Pi^\top A \Pi \succ 0. \tag{2.3}$$

Change of variables

For particular situations, a BMI can be converted into an LMI using a change of variables that is chosen as a one-to-one mapping [31].

Example 2.1.1. Consider the matrices $A \in \mathbb{R}^{n\times n}$ and $B \in \mathbb{R}^{n\times m}$, the decision matrices $K \in \mathbb{R}^{m\times n}$ and $X \in \mathbb{S}^n_+$ and the matrix inequality:

$$AX + XA^\top + BKX + XK^\top B^\top \prec 0, \tag{2.4}$$

which is a BMI due to the product between K and X. Then, the above BMI can be transformed into the following LMI by means of the change of variable $Y = KX$:

$$AX + XA^\top + BY + Y^\top B^\top \prec 0. \tag{2.5}$$

Once the LMI (2.5) is solved, the original BMI (2.4) can be recovered by $K = YX^{-1}$. ▲

Schur's complement lemma

Let us recall the following lemma, known as Schur's complement, which allows us to convert nonlinear convex inequalities into LMIs.

Lemma 2.1.1 (Schur's complement [23])**.** *Consider the matrices $Q \in \mathbb{S}^n$, $R \in \mathbb{S}^m$ and $S \in \mathbb{R}^{n\times m}$. Then, the statements below are equivalent:*

(i) $\begin{bmatrix} Q & S \\ S^\top & R \end{bmatrix} \succ 0.$

(ii) $Q \succ 0, \quad R - S^\top Q^{-1} S \succ 0.$

(iii) $R \succ 0, \quad Q - S R^{-1} S^\top \succ 0.$

S-Procedure

The condition of a quadratic function (or quadratic form) being negative if certain other quadratic functions (or quadratic forms) are all negative appears, e.g., in the robust control literature for some problems. To this end, the S-Procedure is recalled for reformulating such a problem into an LMI, which can be conservative but is often a suitable approximation of the constraint.

Lemma 2.1.2 (S-Procedure [23])**.** *Let us consider the symmetric matrices $M_i \in \mathbb{S}^n$, the known vectors of appropriate dimensions a_i and b_i, and the quadratic functions $F_i(x) : \mathbb{R}^n \to \mathbb{R}$ of the variable $x \in \mathbb{R}^n$ defined as:*

$$F_i(x) \triangleq x^\top M_i x + 2 a_i^\top x + b_i, \quad i \in \mathcal{I}_{[0,p]}. \tag{2.6}$$

If there exist real numbers $\lambda_1 \dots \lambda_p \in \mathbb{R}_+$, such that $\forall x$:

$$F_0(x) - \sum_{i=1}^{p} \lambda_i F_i(x) \geq 0, \tag{2.7}$$

then $F_0(x) \geq 0$ holds $\forall x$ such that $F_i(x) \geq 0$ for $i \in \mathcal{I}_{[1,p]}$. Note that for $p = 1$, the converse holds if there exists x_0 such that $F_1(x_0) > 0$.

2.2 Linear parameter-varying systems

LPV systems were first introduced by Shamma in 1988 as a special case of linear time-varying (LTV) systems, where the system dynamics depend on quantifiable parameters that vary with time [110]. By an appropriate definition of the time-varying parameters, nonlinearities and uncertainties of complex systems can be embedded into the LPV framework, making it a powerful tool for addressing nonlinear control problems. The term quasi-LPV is used to emphasize the fact that the time-varying parameters depend on endogenous signals, such as states and/or inputs. Nevertheless, due to the fact that there is no unique manner to obtain an LPV representation, there exist several approaches in the literature for modelling nonlinear systems as LPV systems, such as Jacobian linearisation [12], function substitution [118] or state transformation [111], which yield different properties in terms of stability analysis and/or control performance.

In recent years, this framework has become increasingly popular due to its remarkable success in handling challenging nonlinear control problems in various fields such as automotive, robotics and aerospace (see monographs [26, 109, 127], surveys [51, 67, 68, 94], and references therein), as well as in several practical applications such as energy production systems [78], wind turbine systems [17] or induced motors [14]. The application of Lyapunov-based approaches also contributes to their popularity by expressing effective conditions for the stability and design of stabilization control LPV systems through the use of LMIs. Furthermore, three different approaches have emerged in the literature as the most popular for representing LPV systems, i.e. linear fractional transformation (LFT) [85], LPV input-output models [3] and the polytopic approach [26].

Among the available LPV representations, the polytopic representation is chosen in this thesis without loss of generality due to its popularity [51] and capacity for transforming other parameter dependencies into polytopic ones [127].

2.2.1 LPV representation

Let us consider the continuous-time (CT) LPV system in its general form:

$$\dot{x}(t) = A(\vartheta(t))x(t) + B(\vartheta(t))u(t), \tag{2.8a}$$
$$y(t) = C(\vartheta(t))x(t) + D(\vartheta(t))u(t), \tag{2.8b}$$

where $x(t) \in \mathbb{R}^{n_x}$, $u(t) \in \mathbb{R}^{n_u}$ and $y(t) \in \mathbb{R}^{n_y}$ are the state, the control input and the system output vector, respectively, and $A(\vartheta(t)) \in \mathbb{R}^{n_x \times n_x}$, $B(\vartheta(t)) \in \mathbb{R}^{n_x \times n_u}$, $C(\vartheta(t)) \in \mathbb{R}^{n_y \times n_x}$ and $D(\vartheta(t)) \in \mathbb{R}^{n_y \times n_u}$ are parameter-dependent matrices. The parameter-varying scheduling vector is denoted by $\vartheta(t) \in \Theta \subset \mathbb{R}^{n_\vartheta}$, whose elements are measured or estimated in real time. Assume that $\vartheta_i(t)$ and its rate of variation $\dot{\vartheta}_i(t)$ are smooth and belong to known, bounded and closed polytopes Θ and Θ_{d}, respectively, defined through the known lower and upper bounds $\underline{\vartheta}_i \le \bar{\vartheta}_i$ and $\underline{\delta\vartheta}_i \le \overline{\delta\vartheta}_i$ for $i \in \mathcal{I}_{[1,n_\vartheta]}$.

By means of the polytopic representation, the parameter-dependent matrices in (2.8) are defined as a convex combination of a finite set of n_μ known vertices:

$$\begin{bmatrix} A(\vartheta(t)) & B(\vartheta(t)) \\ C(\vartheta(t)) & D(\vartheta(t)) \end{bmatrix} = \sum_{i=1}^{n_\mu} \mu_i(\vartheta(t)) \begin{bmatrix} A_i & B_i \\ C_i & D_i \end{bmatrix}, \tag{2.9}$$

where $A_i \in \mathbb{R}^{n_x \times n_x}$, $B_i \in \mathbb{R}^{n_x \times n_u}$, $C_i \in \mathbb{R}^{n_y \times n_x}$ and $D_i \in \mathbb{R}^{n_y \times n_u}$ stand for the given known vertex matrices. $\mu(\vartheta(t)) \in \mathbb{R}^{n_\vartheta}$ corresponds to the polytopic weight vector belonging to the unit simplex:

$$\Delta^{n_\mu} \triangleq \left\{ \mu(\vartheta(t)) \in \mathbb{R}^{n_\mu} : \sum_{i=1}^{n_\mu} \mu_i(\vartheta(t)) = 1,\ \mu_i(\vartheta(t)) \ge 0,\ i \in \mathcal{I}_{[1,n_\mu]} \right\}. \tag{2.10}$$

2.2.2 Stability analysis of LPV systems

This section recalls some of the most popular LMI-based conditions for stability analysis and control synthesis of LPV systems, expressed through the Lyapunov theory.

Let us consider the CT LPV autonomous system [1]:

$$\dot{x} = A(\vartheta)x, \tag{2.11}$$

where $x \in \mathbb{R}^{n_x}$ is the state, $\vartheta \in \Theta \subset \mathbb{R}^{n_\vartheta}$ is the parameter-varying scheduling vector and $A(\vartheta)$ is a parameter-dependent matrix of appropriate dimensions.

[1] To simplify the notation, the time dependence of time-varying variables is now omitted.

Stability analysis of system (2.11) is based on the common approach called quadratic stability, which implies the consideration of a quadratic Lyapunov function (QLF) defined in this case as:

$$V(x) = x^\top P^{-1} x, \quad P \in \mathbb{S}^{n_x}_+. \tag{2.12}$$

Theorem 2.2.1 (Quadratic stability of CT LPV systems)**.** *The autonomous LPV system* (2.11) *is quadratically stable if one of the following statements is satisfied:*

1. *There exists* $P^{-1} \in \mathbb{S}^{n_x}_+$ *such that:*

$$P^{-1} A(\vartheta) + A^\top(\vartheta) P^{-1} \prec 0, \quad \forall \vartheta \in \Theta. \tag{2.13}$$

2. *There exists* $P \in \mathbb{S}^{n_x}_+$ *such that:*

$$A(\vartheta) P + P A^\top(\vartheta) \prec 0, \quad \forall \vartheta \in \Theta. \tag{2.14}$$

Proof. As a result of a direct extension of well-known conclusions for linear time-invariant (LTI) systems [26, Chap. 2], the proof is omitted. ■

Albeit, it is well known that the usage of QLFs involves a degree of conservatism that can lead to suboptimal performance or even make the design problem infeasible for constant or slowly-varying parameters on the polytopic domain. This issue can be alleviated by considering more general classes of Lyapunov functions, such as homogeneous polynomial Lyapunov functions [33, 83], parameter-dependent quadratic Lyapunov functions (PDQLFs) [42, 45], piecewise Lyapunov functions [4, 37], or polyhedral Lyapunov functions [18, 113], at the expense of increased computational complexity. For sake of simplicity, only PDQLFs in the form:

$$V(x, \vartheta) = x^\top P(\vartheta)^{-1} x, \quad P(\vartheta) \in \mathbb{S}^{n_x}_+, \quad \forall \vartheta \in \Theta \tag{2.15}$$

are considered in this chapter. Then, the time-derivative of the Lyapunov function (2.15) is defined as:

$$\dot{V}(x, \vartheta) = \begin{bmatrix} \dot{x} \\ x \end{bmatrix}^\top \begin{bmatrix} 0 & P(\vartheta)^{-1} \\ \star & \frac{\mathrm{d}}{\mathrm{d}t} P(\vartheta)^{-1} \end{bmatrix} \begin{bmatrix} \dot{x} \\ x \end{bmatrix}. \tag{2.16}$$

Hereinafter, we will use $\dot{P}(\vartheta)^{-1}$ as a shorthand for $\frac{\mathrm{d}}{\mathrm{d}t} P(\vartheta)^{-1}$ for sake of clarity and readability. Furthermore, the terminology of parameter-dependent quadratic (PDQ) stability/stabilization will reflect the use of a PDQLF in the development.

Theorem 2.2.2 (PDQ stability of CT LPV systems)**.** *The autonomous LPV system* (2.11) *is parameter-dependent quadratically stable if one of the following statements is satisfied:*

1. *There exists* $P(\vartheta)^{-1} \in \mathbb{S}^{n_x}_+$ *such that:*

$$P(\vartheta)^{-1} A(\vartheta) + A^\top(\vartheta) P(\vartheta)^{-1} + \dot{P}(\vartheta)^{-1} \prec 0, \quad \forall \vartheta \in \Theta. \tag{2.17}$$

2. *There exists* $P(\vartheta) \in \mathbb{S}^{n_x}_+$ *such that:*

$$A(\vartheta) P(\vartheta) + P(\vartheta) A^\top(\vartheta) - \dot{P}(\vartheta) \prec 0, \quad \forall \vartheta \in \Theta. \tag{2.18}$$

Proof. The condition (2.17) is obtained by replacing $\dot{x}$ with (2.11) and enforcing the negative definiteness of the expression (2.16) for all $x \neq 0$ [26, Chap. 2]. Then, condition (2.18) can be obtained by pre- and post-multiplying the constraint (2.17) by $P(\vartheta)$, while keeping in mind the matrix property: $\dot{P}(\vartheta) = -P(\vartheta)\dot{P}(\vartheta)^{-1}P(\vartheta)$ [87, § 2.2]. ∎

2.2.3 External stability analysis of LPV systems

This section summarizes the methods for stabilizing LPV systems susceptible to external bounded signals used in the development of this thesis. In particular, the definitions of the quadratic boundedness (QB) approach and the well-known $\mathcal{H}_\infty$ performance are provided.

Consider the CT LPV system governed by:

$$\dot{x} = A(\vartheta)x + B_w(\vartheta)w, \tag{2.19a}$$
$$z_\infty = C_z(\vartheta)x + D_{zw}(\vartheta)w, \tag{2.19b}$$

where $A(\vartheta)$, $B_w(\vartheta)$, $C_z(\vartheta)$ and $D_{zw}(\vartheta)$ are parameter-varying matrices of appropriate dimensions, $\vartheta \in \Theta \subset \mathbb{R}^{n_\vartheta}$ is the parameter-varying scheduling vector, $x \in \mathbb{R}^{n_x}$ and $z_\infty \in \mathbb{R}^{n_{z_\infty}}$ are the state and the performance output vectors, respectively, and $w \in \mathbb{R}^{n_w}$ is an exogenous signal such that one or both of the following conditions are considered:

- **Amplitude bound:** the exogenous signal $w(t)$ belongs to the following set:

$$\mathcal{E}_w(Q) \triangleq \left\{w \in \mathbb{R}^{n_w} \,:\, w^\top Q^{-1} w \leq 1\right\}, \tag{2.20}$$

  where $Q \in \mathbb{S}_+^{n_w}$ is a given matrix that contains information about the region.

- **Energy bound:** the exogenous signal $w(t)$ belongs to the following set of functions:

$$\mathcal{W} \triangleq \left\{w : [0,\infty) \to \mathbb{R}^{n_w};\ \int_0^\infty w^\top Q^{-1} w\, dt \leq 1\right\}, \tag{2.21}$$

  for some $Q \in \mathbb{S}_+^{n_w}$.

Quadratic boundedness

Let us recall the definition of the QB based on the works [27, 64] and its extension to the case of using a PDQLF for addressing the amplitude bound condition (2.20).

Definition 2.2.1 (Quadratic boundedness [27])**.** Given the set $\mathcal{E}_w(Q)$ defined by (2.20), the LPV system (2.19a) is quadratically bounded with a QLF (2.12) if:

$$\dot{V}(x) \leq 0 \quad \forall (x, w) :\, V(x) \geq 1,\ w \in \mathcal{E}_w(Q). \tag{2.22}$$

Definition 2.2.2 (Parameter-dependent quadratic boundedness (PDQB))**.** Given the set $\mathcal{E}_w(Q)$ defined by (2.20), the LPV system (2.19a) is quadratically bounded with a PDQLF (2.15) if:

$$\dot{V}(x, \vartheta) \leq 0 \quad \forall (x, \vartheta, w) :\, V(x, \vartheta) \geq 1,\ \vartheta \in \Theta,\ w \in \mathcal{E}_w(Q). \tag{2.23}$$

Regardless of the exogenous signal $w(t)$ in (2.19), the main idea of the (PD)QB approach is to force all state trajectories to converge into an ellipsoidal region described by the unit level set of a (PD)QLF for all $w(t) \in \mathcal{E}_w(Q)$.

Theorem 2.2.3 (QB of LPV systems)**.** *Given the set $\mathcal{E}_w(Q)$ defined by (2.20), the LPV system (2.19a) is quadratically bounded with the QLF (2.12) if there exist positive scalars λ_1 and λ_2 such that:*

$$0 < \lambda_2 \leq \lambda_1, \tag{2.24}$$

and one of the following statements is satisfied:

1. *There exists $P^{-1} \in \mathbb{S}_+^{n_x}$ such that:*

$$\begin{bmatrix} \mathrm{He}\{P^{-1}A(\vartheta)\} + \lambda_1 P^{-1} & P^{-1}B_w(\vartheta) \\ \star & -\lambda_2 Q^{-1} \end{bmatrix} \leq 0, \quad \forall \vartheta \in \Theta. \tag{2.25}$$

2. *There exists $P \in \mathbb{S}_+^{n_x}$ such that:*

$$\begin{bmatrix} \mathrm{He}\{A(\vartheta)P\} + \lambda_1 P & B_w(\vartheta) \\ \star & -\lambda_2 Q^{-1} \end{bmatrix} \leq 0, \quad \forall \vartheta \in \Theta. \tag{2.26}$$

Proof. This proof follows the reasoning in [27, 64]. By means of the S-Procedure (Lemma 2.1.2), the conditions (2.22) introduced by Definition 2.2.1 for ensuring that system (2.19a) is quadratically bounded can be expressed as follows:

$$\dot{V}(x) + \lambda_1\left(x^\top P^{-1}x - 1\right) + \lambda_2\left(1 - w^\top Q^{-1}w\right) \leq 0. \tag{2.27}$$

Then, the negative semi-definiteness of the inequality (2.27) can be verified if the following conditions are satisfied:

$$\dot{V}(x) + \lambda_1 x^\top P^{-1}x - \lambda_2 w^\top Q^{-1}w \leq 0, \tag{2.28}$$

$$-\lambda_1 + \lambda_2 \leq 0. \tag{2.29}$$

By setting $\dot{V}(x) = 2x^\top P^{-1}(A(\vartheta)x + B_w(\vartheta)w)$, the condition (2.28) can be formulated as:

$$\begin{bmatrix} x \\ w \end{bmatrix}^\top \begin{bmatrix} \mathrm{He}\{P^{-1}A(\vartheta)\} + \lambda_1 P^{-1} & P^{-1}B_w(\vartheta) \\ \star & -\lambda_2 Q^{-1} \end{bmatrix} \begin{bmatrix} x \\ w \end{bmatrix} \leq 0, \quad \forall \vartheta \in \Theta, \tag{2.30}$$

thus obtaining the LMI (2.25) by ensuring the negative semi-definiteness of (2.30) $\forall (x, w) \neq 0$, and establishing the condition (2.24) directly from (2.29). On the other hand, the LMI (2.26) can be obtained by pre- and post-multiplying (2.25) by $\mathrm{diag}\{P, \mathrm{I}_{n_w}\}$, thus concluding the proof. ■

Theorem 2.2.4 (PDQB of LPV systems)**.** *Given the set $\mathcal{E}_w(Q)$ defined by (2.20), the LPV system (2.19a) is quadratically bounded with the PDQLF (2.15) if there exist positive scalars λ_1 and λ_2 such that:*

$$0 < \lambda_2 \leq \lambda_1, \tag{2.31}$$

and one of the following statements is satisfied:

1. *There exists* $P(\vartheta)^{-1} \in \mathbb{S}_{+}^{n_x}$ *such that:*

$$\begin{bmatrix} \mathrm{He}\{P(\vartheta)^{-1}A(\vartheta)\} + \dot{P}(\vartheta)^{-1} + \lambda_1 P(\vartheta)^{-1} & P(\vartheta)^{-1}B_w(\vartheta) \\ \star & -\lambda_2 Q^{-1} \end{bmatrix} \preceq 0. \quad \forall \vartheta \in \Theta. \tag{2.32}$$

2. *There exists* $P(\vartheta) \in \mathbb{S}_{+}^{n_x}$ *such that:*

$$\begin{bmatrix} \mathrm{He}\{A(\vartheta)P(\vartheta)\} - \dot{P}(\vartheta) + \lambda_1 P(\vartheta) & B_w(\vartheta) \\ \star & -\lambda_2 Q^{-1} \end{bmatrix} \preceq 0. \quad \forall \vartheta \in \Theta. \tag{2.33}$$

Proof. The proof follows a reasoning similar to the one of Theorem 2.2.3, thus is omitted. ■

$\mathcal{H}_\infty$ PERFORMANCE

Assume that the exogenous signal $w(t)$ in system (2.19) is energy bounded such that $w \in \mathcal{W}$. Then, consider that the set $\mathcal{W}$ defined in (2.21) represents the L_2-bounded disturbance if $Q^{-1} = \mathrm{I}_{n_w}$ and the definition of the L_2-norm of w as $\|w\|_2 = \sqrt{\int_0^\infty w^\top w \, dt}$ [23], thus introducing the $\mathcal{H}_\infty$ performance concept:

Definition 2.2.3 ($\mathcal{H}_\infty$ performance of an LPV system)**.** The LPV system (2.19) is said to achieve $\mathcal{H}_\infty$ performance γ if the induced L_2-gain of the input/output map is bounded by $\gamma \in \mathbb{R}_+\backslash\{0\}$ i.e.

$$\sup_{\substack{w \neq 0 \\ w \in \mathrm{L}_2}} \frac{\|z_\infty\|_2}{\|w\|_2} < \gamma \tag{2.34}$$

along all possible trajectories $\vartheta \in \Theta$.

Considering the parameter-independent and the parameter-dependent QLF defined in (2.12) and (2.15), respectively, the following theorems stand for the external stability analysis problem involving an L_2-bounded disturbance, based on the works [6, 23, 44, 131]:

Theorem 2.2.5 (Quadratic $\mathcal{H}_\infty$ performance for LPV systems)**.** *The system* (2.19) *with* $\|w\|_2 \leq 1$ *has a quadratic* $\mathcal{H}_\infty$ *performance* γ *if there exists a scalar* $\gamma \in \mathbb{R}_+\backslash\{0\}$ *and one of the following statements is satisfied:*

1. *There exists* $P^{-1} \in \mathbb{S}_{+}^{n_x}$ *such that:*

$$\begin{bmatrix} \mathrm{He}\{P^{-1}A(\vartheta)\} & P^{-1}B_w(\vartheta) & C_z^\top(\vartheta) \\ \star & -\gamma \mathrm{I}_{n_w} & D_{zw}^\top(\vartheta) \\ \star & \star & -\gamma \mathrm{I}_{n_{z_\infty}} \end{bmatrix} < 0, \quad \forall \vartheta \in \Theta. \tag{2.35}$$

2. *There exists* $P \in \mathbb{S}_{+}^{n_x}$ *such that:*

$$\begin{bmatrix} \mathrm{He}\{A(\vartheta)P\} & B_w(\vartheta) & PC_z^\top(\vartheta) \\ \star & -\gamma \mathrm{I}_{n_w} & D_{zw}^\top(\vartheta) \\ \star & \star & -\gamma \mathrm{I}_{n_{z_\infty}} \end{bmatrix} < 0, \quad \forall \vartheta \in \Theta. \tag{2.36}$$

Proof. The proof follows the reasoning in [23, § 6.3.2]. To prove that the L_2-gain of the system (2.19) between the admissible disturbance signal $w(t)$ and the performance output $z_\infty(t)$ is bounded by γ, assume that the following condition is verified for all t:

$$\dot{V}(x) + \gamma^{-1} z_\infty{}^\top z_\infty - \gamma w^\top w < 0. \tag{2.37}$$

By integrating the condition (2.37), from $t = 0$ to $t = \infty$, one gets:

$$V(x(\infty)) - V(x(0)) + \gamma^{-1} \int_0^\infty z_\infty{}^\top z_\infty \, dt - \gamma \int_0^\infty w^\top w \, dt < 0, \tag{2.38}$$

which is equivalent to:

$$V(x(\infty)) - V(x(0)) + \gamma^{-1} \|z_\infty\|_2^2 - \gamma \|w\|_2^2 < 0. \tag{2.39}$$

Hence, for $x(0) = 0$, it is possible to conclude that:

$$\|z_\infty\|_2^2 < \gamma^2 \|w\|_2^2, \tag{2.40}$$

since $V(x(\infty)) \geq 0$ and $V(x(0)) = 0$ by definition, thus demonstrating the condition (2.34).

Consider the QLF (2.12), $\dot{V}(x) = 2x^\top P^{-1}(A(\vartheta)x + B_w(\vartheta)w)$ and $z_\infty(t)$ in (2.19). Then, by means of appropriate manipulations the inequality (2.37) can be formulated $\forall (x, w) \neq 0$ as the LMI:

$$\begin{bmatrix} \mathrm{He}\{P^{-1}A(\vartheta)\} + \gamma^{-1} C_z^\top(\vartheta) C_z(\vartheta) & P^{-1}B_w(\vartheta) + \gamma^{-1} C_z^\top(\vartheta) D_{zw}(\vartheta) \\ \star & \gamma^{-1} D_{zw}^\top(\vartheta) D_{zw}(\vartheta) - \gamma \mathrm{I}_{n_w} \end{bmatrix} \prec 0. \tag{2.41}$$

Thus, obtaining the LMI (2.35) by applying Schur's complement to (2.41). On the other hand, the LMI (2.36) can be obtained by pre- and post-multiplying (2.35) by $\mathrm{diag}\{P, \mathrm{I}_{n_w}, \mathrm{I}_{n_{z_\infty}}\}$, thus concluding the proof. ■

Theorem 2.2.6 (PDQ $\mathcal{H}_\infty$ performance for LPV systems)**.** *The system* (2.19) *with* $\|w\|_2 \leq 1$ *has a parameter-dependent quadratically* $\mathcal{H}_\infty$ *performance* γ *if there exists a scalar* $\gamma \in \mathbb{R}_+ \backslash \{0\}$ *and one of the following statements is satisfied:*

1. *There exists* $P(\vartheta)^{-1} \in \mathbb{S}_+^{n_x}$ *such that:*

$$\begin{bmatrix} \mathrm{He}\{P(\vartheta)^{-1}A(\vartheta)\} + \dot{P}(\vartheta)^{-1} & P(\vartheta)^{-1}B_w(\vartheta) & C_z^\top(\vartheta) \\ \star & -\gamma \mathrm{I}_{n_w} & D_{zw}^\top(\vartheta) \\ \star & \star & -\gamma \mathrm{I}_{n_{z_\infty}} \end{bmatrix} \prec 0, \quad \forall \vartheta \in \Theta. \tag{2.42}$$

2. *There exists* $P(\vartheta) \in \mathbb{S}_+^{n_x}$ *such that:*

$$\begin{bmatrix} \mathrm{He}\{A(\vartheta)P(\vartheta)\} - \dot{P}(\vartheta) & B_w(\vartheta) & P(\vartheta)C_z^\top(\vartheta) \\ \star & -\gamma \mathrm{I}_{n_w} & D_{zw}^\top(\vartheta) \\ \star & \star & -\gamma \mathrm{I}_{n_{z_\infty}} \end{bmatrix} \prec 0, \quad \forall \vartheta \in \Theta. \tag{2.43}$$

Proof. The proof follows a reasoning similar to the one of Theorem 2.2.5, thus is omitted. ■

2.2.4 Control of LPV systems

The sequel will present the problem of designing a control law while taking the analytical requirements stated in Sections 2.2.2 and 2.2.3 into account, such that the final closed-loop system has certain desired characteristics.

For the sake of simplicity and without loss of generality, the following results are mainly formulated considering the gain-scheduled (GS) static state-feedback control law of the form:

$$u = K(\vartheta)x, \quad \forall \vartheta \in \Theta, \tag{2.44}$$

where the parameter-dependent controller gain $K(\vartheta) \in \mathbb{R}^{n_u \times n_x}$ is to be determined. It is important to keep in mind that this control law requires complete system state information, which may be lacking in real-world systems. In order to solve this problem, an observer-based control scheme is needed to provide the controller with a system's state estimation to be fed with [39, 90]. In cases where this is not possible, the interested reader is directed to alternate control strategies like input-output controller synthesis [3, 122] or output-feedback controller synthesis [38, 81].

Theorem 2.2.7 (Quadratic stabilization of LPV systems via state-feedback control)**.** *The LPV system* (2.8a) *with control law* (2.44) *is quadratically stable if there exist a matrix* $P \in \mathbb{S}^{n_x}_+$ *and a matrix function* $K(\vartheta) \in \mathbb{R}^{n_u \times n_x}$ *such that:*

$$\mathrm{He}\{A(\vartheta)P + B(\vartheta)K(\vartheta)P\} \prec 0, \quad \forall \vartheta \in \Theta. \tag{2.45}$$

Proof. It follows from Theorem 2.2.1, replacing the autonomous state matrix $A(\vartheta)$ with the closed-loop state matrix $A(\vartheta) + B(\vartheta)K(\vartheta)$. ■

Theorem 2.2.8 (PDQ stabilization of LPV systems via state-feedback control)**.** *The LPV system* (2.8a) *with control law* (2.44) *is parameter-dependent quadratically stable if there exist matrix functions* $P(\vartheta) \in \mathbb{S}^{n_x}_+$ *and* $K(\vartheta) \in \mathbb{R}^{n_u \times n_x}$ *such that:*

$$\mathrm{He}\{A(\vartheta)P(\vartheta) + B(\vartheta)K(\vartheta)P(\vartheta)\} - \dot{P}(\vartheta) \prec 0, \quad \forall \left(\vartheta, \dot{\vartheta}\right) \in \Theta \times \Theta_d. \tag{2.46}$$

Proof. The proof follows a reasoning similar to the one of Theorem 2.2.7, thus is omitted. ■

Theorem 2.2.9 (QB for LPV state-feedback control)**.** *Given the set* $\mathcal{E}_w(Q)$ *defined by* (2.20)*, the LPV system:*

$$\dot{x} = A(\vartheta)x + B_w(\vartheta)w + B(\vartheta)u \tag{2.47}$$

with control law (2.44) *is quadratically bounded with the QLF* (2.12) *if there exist positive scalars* λ_1 *and* λ_2*, a matrix* $P \in \mathbb{S}^{n_x}_+$ *and a matrix function* $K(\vartheta) \in \mathbb{R}^{n_u \times n_x}$ *such that:*

$$0 < \lambda_2 \leq \lambda_1, \tag{2.48}$$

$$\begin{bmatrix} \mathrm{He}\{A(\vartheta)P + B(\vartheta)K(\vartheta)P\} + \lambda_1 P & B_w(\vartheta) \\ \star & -\lambda_2 Q^{-1} \end{bmatrix} \leq 0, \quad \forall \vartheta \in \Theta. \tag{2.49}$$

Proof. It follows from Theorem 2.2.3, replacing the autonomous state matrix $A(\vartheta)$ with the closed-loop state matrix $A(\vartheta) + B(\vartheta)K(\vartheta)$. ■

Theorem 2.2.10 (PDQB for LPV state-feedback control)**.** *Given the set $\mathcal{E}_w(Q)$ defined by (2.20), the LPV system (2.47) with control law (2.44) is quadratically bounded with the PDQLF (2.15) if there exist positive scalars λ_1 and λ_2, and matrix functions $P(\vartheta) \in \mathbb{S}^{n_x}_+$ and $K(\vartheta) \in \mathbb{R}^{n_u \times n_x}$ such that:*

$$0 < \lambda_2 \leq \lambda_1, \tag{2.50}$$

$$\begin{bmatrix} \Psi_{[11]}(\vartheta) + \lambda_1 P(\vartheta) & B_w(\vartheta) \\ \star & -\lambda_2 Q^{-1} \end{bmatrix} \leq 0, \quad \forall \left(\vartheta, \dot{\vartheta}\right) \in \Theta \times \Theta_d, \tag{2.51}$$

where $\Psi_{[11]}(\vartheta) \triangleq \mathrm{He}\{A(\vartheta)P(\vartheta) + B(\vartheta)K(\vartheta)P(\vartheta)\} - \dot{P}(\vartheta)$.

Proof. The proof follows a reasoning similar to the one of Theorem 2.2.9, thus is omitted. ■

Theorem 2.2.11 (Quadratic $\mathcal{H}_\infty$ state-feedback control for LPV systems)**.** *The LPV system:*

$$\dot{x} = A(\vartheta)x + B_w(\vartheta)w + B(\vartheta)u, \tag{2.52a}$$

$$z_\infty = C_z(\vartheta)x + D_{zw}(\vartheta)w + D_{zu}(\vartheta)u, \tag{2.52b}$$

with $\|w\|_2 \leq 1$ and control law (2.44) has a quadratic $\mathcal{H}_\infty$ performance γ if there exists a scalar $\gamma \in \mathbb{R}_+ \backslash \{0\}$, a matrix $P \in \mathbb{S}^{n_x}_+$ and a matrix function $K(\vartheta) \in \mathbb{R}^{n_u \times n_x}$ such that:

$$\begin{bmatrix} \mathrm{He}\{A(\vartheta)P + B(\vartheta)K(\vartheta)P\} & B_w(\vartheta) & PC_z^\top(\vartheta) + PK^\top(\vartheta)D_{zu}^\top(\vartheta) \\ \star & -\gamma \mathrm{I}_{n_w} & D_{zw}^\top(\vartheta) \\ \star & \star & -\gamma \mathrm{I}_{n_{z_\infty}} \end{bmatrix} < 0, \quad \forall \vartheta \in \Theta. \tag{2.53}$$

Proof. It follows from Theorem 2.2.5, replacing the autonomous state matrix $A(\vartheta)$ with the closed-loop state matrix $A(\vartheta) + B(\vartheta)K(\vartheta)$, and the closed-loop performance output matrix $C_z(\vartheta)$ with $C_z(\vartheta) + D_{zu}(\vartheta)K(\vartheta)$. ■

Theorem 2.2.12 (Parameter-dependent quadratic $\mathcal{H}_\infty$ state-feedback control for LPV systems)**.** *The LPV system (2.52) with $\|w\|_2 \leq 1$ and control law (2.44) has a parameter-dependent quadratically $\mathcal{H}_\infty$ performance γ if there exists a scalar $\gamma \in \mathbb{R}_+ \backslash \{0\}$ and matrix functions $P(\vartheta) \in \mathbb{S}^{n_x}_+$ and $K(\vartheta) \in \mathbb{R}^{n_u \times n_x}$ such that:*

$$\begin{bmatrix} \Psi_{[11]}(\vartheta) & B_w(\vartheta) & \Psi_{[13]}(\vartheta) \\ \star & -\gamma \mathrm{I}_{n_w} & D_{zw}^\top(\vartheta) \\ \star & \star & -\gamma \mathrm{I}_{n_{z_\infty}} \end{bmatrix} < 0, \quad \forall \left(\vartheta, \dot{\vartheta}\right) \in \Theta \times \Theta_d, \tag{2.54}$$

where:

$$\Psi_{[11]}(\vartheta) \triangleq \mathrm{He}\{A(\vartheta)P(\vartheta) + B(\vartheta)K(\vartheta)P(\vartheta)\} - \dot{P}(\vartheta),$$
$$\Psi_{[13]}(\vartheta) \triangleq P(\vartheta)C_z^\top(\vartheta) + P(\vartheta)K^\top(\vartheta)D_{zu}^\top(\vartheta).$$

Proof. The proof follows a reasoning similar to the one of Theorem 2.2.11, thus is omitted. ■

2.2.5 Finite-dimensional LMI relaxations

Considering the necessity of checking an infinite number of constraints in Theorems 2.2.1-2.2.12 due to the presence of parameter-dependent LMIs, the problem of reducing them to a finite-dimensional representation is illustrated hereinafter through the use of the polytopic representation defined in Section 2.2.1 and the application of the Pólya's relaxation theorem inherited from [102].

Following the work of Sala et. al. [102], a multi-index notation is introduced with the purpose of compactly representing a $p-$dimensional polytopic summation through the definition of the following sets:

$$\mathbb{I}_{(p,n_\mu)} \triangleq \left\{ \boldsymbol{i} \in \mathbb{N}^p \ : \ 1 \leq i_k \leq n_\mu, \ \forall k \in \mathcal{I}_{[1,p]} \right\}, \tag{2.55a}$$

$$\mathbb{I}^+_{(p,n_\mu)} \triangleq \left\{ \boldsymbol{i} \in \mathbb{I}_{(p,n_\mu)} \ : \ i_k \leq i_{k+1}, \ \forall k \in \mathcal{I}_{[1,p-1]} \right\}, \tag{2.55b}$$

where $\boldsymbol{i} = (i_1, \ldots, i_p) \in \mathbb{N}^p$ denotes a p-dimensional multi-index. Furthermore, notation $\mathcal{P}(\boldsymbol{i}) \subset \mathbb{I}_{(p,n_\mu)}$ will denote the set of permutations with possible repeated elements of the multi-index $\boldsymbol{i}$. For example, for $\boldsymbol{i} = (1,1,3)$, the possible permutations are:

$$\mathcal{P}(\boldsymbol{i}) = \{(1,1,3), (1,3,1), (3,1,1)\}.$$

Let us generalize the finite-dimensional formulation of a parameter-dependent LMI that requires negative definiteness of a p-dimensional polytopic summation, thus defining:

$$\Xi(\vartheta) \triangleq \sum_{i_1=1}^{n_\mu} \sum_{i_2=1}^{n_\mu} \cdots \sum_{i_p=1}^{n_\mu} \mu_{i_1}(\vartheta)\mu_{i_2}(\vartheta)\cdots\mu_{i_p}(\vartheta) \ x^\top \Upsilon_{i_1 \ldots i_p} x < 0, \quad \forall x \neq 0, \tag{2.56}$$

where $\Upsilon_{i_1 \ldots i_p}$ corresponds to symmetric matrices that are linear in some decision matrices. By means of the multi-index notation, the expression (2.56) can be compactly formulated as:

$$\Xi(\vartheta) \triangleq \sum_{\boldsymbol{i} \in \mathbb{I}_{(p,n_\mu)}} \mu_{\boldsymbol{i}}(\vartheta) \ x^\top \Upsilon_{\boldsymbol{i}} x < 0, \quad \forall x \neq 0, \tag{2.57}$$

with $\mu_{\boldsymbol{i}}(\vartheta) = \prod_{k=1}^{p} \mu_{i_k}(\vartheta)$ and $\boldsymbol{i} \in \mathbb{I}_{(p,n_\mu)}$. For instance, $\mu_{(1,1,3)}(\vartheta) = \mu_1^2(\vartheta)\mu_3(\vartheta)$ will be the polytopic weight associated to the term Υ_{113} for a 3-dimensional polytopic summation with $n_\mu \geq 3$.

In order to state Pólya's relaxation theorem from [102] (here referred to as Pólya's relaxation lemma), let us recall an essential concept about a set-theoretic relation between multi-indices by the following proposition:

Proposition 2.2.13 ([102, Proposition 1])**.** *Given any index $\boldsymbol{j} \in \mathbb{I}_{(p,n_\mu)}$, there exists a unique permutation of it, denoted as $\boldsymbol{i} \in \mathbb{I}^+_{(p,n_\mu)}$, such that:*

$$\sum_{\boldsymbol{j} \in \mathbb{I}_{(p,n_\mu)}} \mu_{\boldsymbol{j}}(\vartheta)\Upsilon_{\boldsymbol{j}} = \sum_{\boldsymbol{i} \in \mathbb{I}^+_{(p,n_\mu)}} \sum_{\boldsymbol{j} \in \mathcal{P}(\boldsymbol{i})} \mu_{\boldsymbol{j}}(\vartheta)\Upsilon_{\boldsymbol{j}} = \sum_{\boldsymbol{i} \in \mathbb{I}^+_{(p,n_\mu)}} \mu_{\boldsymbol{i}}(\vartheta) \sum_{\boldsymbol{j} \in \mathcal{P}(\boldsymbol{i})} \Upsilon_{\boldsymbol{j}}. \tag{2.58}$$

Proof. For further details, see [9] and [102]. ∎

Then, by considering Proposition 2.2.13 and the fact that:

$$\sum_{i=1}^{n_\mu} \mu_i(\vartheta) = \left(\sum_{i=1}^{n_\mu} \mu_i(\vartheta)\right)^p = \sum_{\boldsymbol{i}\in\mathbb{I}_{(p,n_\mu)}} \mu_{\boldsymbol{i}}(\vartheta) = 1$$

for any positive integer p, the following result holds.

Lemma 2.2.14 (Pólya's relaxation lemma)**.** *Consider the LMI* (2.57) *and a chosen Pólya's relaxation degree $d \in \mathbb{N}$, with $d \geq p$, such that the following set of LMIs is satisfied:*

$$\sum_{\boldsymbol{j}\in\mathcal{P}(\boldsymbol{i})} \Upsilon_{\boldsymbol{j}} \prec 0, \quad \boldsymbol{i} \in \mathbb{I}^{+}_{(d,n_\mu)}, \tag{2.59}$$

Then, the negative-definiteness of (2.57) *is ensured with the necessary conditions for large values of d, thus reducing the overall conservatism at the cost of increasing the computational burden.*

Let us illustrate the application of Lemma 2.2.14 through the following example.

Example 2.2.1. Consider the following 2−dimensional polytopic summation with $n_\mu = 3$:

$$\sum_{i_1=1}^{3}\sum_{i_2=1}^{3} \mu_{i_1}(\vartheta)\mu_{i_2}(\vartheta)\, x^\top \Upsilon_{i_1 i_2} x \prec 0, \quad \forall x \neq 0 \tag{2.60}$$

and a Pólya's relaxation degree $d = 2$, thus defining the sets in (2.55) as:

$$\mathbb{I}_{(2,3)} = \{(1,1),(1,2),(1,3),(2,1),(2,2),(2,3),(3,1),(3,2),(3,3)\},$$
$$\mathbb{I}^{+}_{(2,3)} = \{(1,1),(1,2),(1,3),(2,2),(2,3),(3,3)\}.$$

Then, by applying Lemma 2.2.14 to (2.60), its negative-definiteness is guaranteed if the following conditions are satisfied:

$$\begin{array}{lll} \Upsilon_{11} \prec 0, & \Upsilon_{12} + \Upsilon_{21} \prec 0, & \Upsilon_{13} + \Upsilon_{31} \prec 0, \\ \Upsilon_{22} \prec 0, & \Upsilon_{23} + \Upsilon_{32} \prec 0, & \Upsilon_{33} \prec 0. \end{array} \tag{2.61}$$

▲

2.2.6 Shifting paradigm

The shifting paradigm concept was presented in [92] for polytopic LPV systems as a possible approach that exploits the properties of polytopes and the versatility offered by the LMI approach, enabling the design of gain-scheduling controllers that adapt the system's closed-loop performance online depending on a known performance vector $\varphi(t) \in \Phi \subset \mathbb{R}^{n_\varphi}$ that reflects the variability of some chosen criteria, e.g., guaranteed decay rate, robust bounds as $\mathcal{H}_2\backslash\mathcal{H}_\infty$, or pole clustering.

For the purpose of developing shifting control strategies, it is assumed that the known performance vector $\varphi(t)$ is both smooth and a member of the known polytopic region Φ, which can be defined through the known lower and upper bounds $\underline{\varphi}_j \leq \bar{\varphi}_j$ for $j \in \mathcal{I}_{[1,n_\varphi]}$. Then,

the polytopic representation of generic matrices such as $O(\varphi)$ and $G(\vartheta,\varphi)$ with dependency on $(\vartheta,\varphi) \in \Theta \times \Phi$ are defined as the convex combination of a finite set of n_η and $n_\mu \times n_\eta$ known vertices, respectively:

$$O(\varphi) \triangleq \sum_{j=1}^{n_\eta} \eta_j(\varphi) O_j, \tag{2.62a}$$

$$G(\vartheta,\varphi) \triangleq \sum_{i=1}^{n_\mu} \mu_i(\vartheta) G_i(\varphi) = \sum_{i=1}^{n_\mu} \sum_{j=1}^{n_\eta} \mu_i(\vartheta)\eta_j(\varphi) G_{ij}, \tag{2.62b}$$

where O_j and G_{ij} are generic vertex matrices to be determined, $\mu(\vartheta) \in \Delta^{n_\mu}$ and $\eta(\varphi) \in \Delta^{n_\eta}$ represent the known polytopic weight vectors, the simplex Δ^{n_μ} corresponds to (2.10), and the simplex Δ^{n_η} is:

$$\Delta^{n_\eta} \triangleq \left\{ \eta(\varphi) \in \mathbb{R}^{n_\eta} \ : \ \sum_{j=1}^{n_\eta} \eta_j(\varphi) = 1, \ \eta_j(\varphi) \geq 0, \ j \in \mathcal{I}_{[1,n_\eta]} \right\}. \tag{2.63}$$

Additionally, the rate of variation $\dot{\varphi}(t) \in \Phi_d \subset \mathbb{R}^{n_\varphi}$ is assumed to be smooth, with Φ_d as a known, bounded, and closed set that can be determined through the known lower and upper bounds $\delta\underline{\varphi}_j \leq \delta\bar{\varphi}_j$ for $j \in \mathcal{I}_{[1,n_\varphi]}$. Although the definition of Φ_d is possible, it should be emphasized that in real-world applications, online measurement of $\dot{\varphi}(t)$ may not be accessible due to the possible dependence on endogenous and/or exogenous signals, and its estimation may be hampered by measurement noise. For example, in the case of a quadrotor, the use of $\varphi(t)$ to schedule the availability of the actuator action, i.e. the lack of resulting thrust force for a given command, is affected not only by the current battery voltage but also by other factors such as air density [21, 89]. Consequently, the rate at which the battery voltage discharges must be considered, among other conditions, for the acquisition of $\dot{\varphi}(t)$.

Finally, the shifting specifications under consideration in this thesis are formally stated in the following.

Definition 2.2.4 (Guaranteed shifting decay rate (GSDR))**.** The LPV system (2.52a) is said to have a *guaranteed shifting decay rate* $\mathrm{d_R}(\varphi) : \mathbb{R}^{n_\varphi} \to \mathbb{R}_+$ if the following condition is satisfied:

$$\dot{V}(\cdot) \leq -2\mathrm{d_R}(\varphi) V(\cdot), \tag{2.64}$$

where $\mathrm{d_R}(\varphi)$ is assumed to be a continuous positive function $\forall \varphi \in \Phi \subset \mathbb{R}^{n_\varphi}$ and $V(\cdot)$ corresponds to a candidate Lyapunov function that can be defined by a QLF as (2.12) or by its parameter-dependent version (2.15).

Definition 2.2.5 (Shifting $\mathcal{H}_\infty$ performance)**.** The LPV system (2.52) is said to achieve *shifting $\mathcal{H}_\infty$ performance* $\gamma(\varphi) : \mathbb{R}^{n_\varphi} \to \mathbb{R}_+ \backslash \{0\}$ if the induced L_2-gain of the input/output map is bounded by $\gamma(\varphi)$ i.e.

$$\left\| \gamma(\varphi)^{-\frac{1}{2}} z_\infty \right\|_2 < \left\| \gamma(\varphi)^{\frac{1}{2}} w \right\|_2 \tag{2.65}$$

along all possible trajectories $\vartheta \in \Theta \subset \mathbb{R}^{n_\vartheta}$ and $\varphi \in \Phi \subset \mathbb{R}^{n_\varphi}$.

2.3 Linear systems subject to actuator saturation

Due to the potential performance degradation or even destabilization induced in the closed-loop system, actuator saturation is probably one of the most investigated nonlinearities in control theory (see, for example, monographs [54, 59, 119], and references therein). In general, existing approaches for addressing the actuator saturation problem are classified into two main categories based on how saturation is handled. The first approach involves pairing a pre-designed controller that ignores saturation during the design stage with a compensator that mitigates the negative consequences of saturation [112, 120, 125, 130]. The key concept behind this approach, called anti-windup compensation, is to provide additional feedback so that the actuator remains appropriately within the saturation limits. The second approach, consists of addressing the input restrictions during the controller design stage [30, 55, 60, 129]. This is the design approach that is used in this thesis. Such an approach entails developing feedback laws that are valid throughout the entirety or a major portion of a null controllable region, allowing the saturating actuators to push state trajectories back to the origin.

In the following, we present a brief overview of preliminary concepts concerning nonlinear systems and the context of saturation avoidance performance. Note that the solution to the problem of designing controllers under saturation avoidance is not given in this section, but can be found in the cited references or in the next chapters of this thesis for the situation where a time-varying saturation is present.

2.3.1 Preliminaries

Consider the autonomous nonlinear system:

$$\dot{x} = g(x), \quad x(0) = x_0, \tag{2.66}$$

where $x \in \mathbb{R}^{n_x}$ is the state and $g(x)\colon \mathcal{D}_x \to \mathbb{R}^{n_x}$ denotes a locally Lipschitz map from a domain $\mathcal{D}_x \subset \mathbb{R}^{n_x}$ into $\mathbb{R}^{n_x}$. Then, let us introduce the following concepts [63, Chap. 4]:

Definition 2.3.1 (Domain of attraction of the origin)**.** The *domain of attraction* of the origin, denoted as $\mathcal{D}_A$, is defined as:

$$\mathcal{D}_A \triangleq \left\{ x_0 \in \mathbb{R}^{n_x} \,:\, \lim_{t\to\infty} \zeta(t, x_0) = 0 \right\}, \tag{2.67}$$

where $\zeta(t, x_0)$ denotes the trajectory of the system (2.66) that starts at initial condition x_0 at time $t = 0$.

Definition 2.3.2 (Invariant set)**.** A set $\mathcal{S}$ is said to be an invariant set with respect to (2.66) if:

$$x_0 \in \mathcal{S} \implies x(t) \in \mathcal{S}, \quad \forall t \in \mathbb{R} \tag{2.68}$$

Let $V(x) = x^\top P^{-1} x$ be a candidate Lyapunov function as (2.12). The associated level sets of $V(x)$ are defined as:

$$\mathcal{E}(P, c) \triangleq \left\{ x \in \mathbb{R}^{n_x} \,:\, x^\top P^{-1} x \le c \right\} = \left\{ x \in \mathbb{R}^{n_x} \,:\, V(x) \le c \right\}, \tag{2.69}$$

where $P \in \mathbb{S}_+^{n_x}$ and c is a positive scalar. If $\dot{V}(x) < 0 \ \forall x \in \mathcal{E}(P,c)\backslash\{0\}$, then the ellipsoidal set $\mathcal{E}(P,c)$ is said to be contractively invariant. Clearly, if $\mathcal{E}(P,c)$ is contractive, then it is contained in the domain of attraction $\mathcal{D}_A$ [55, 119].

Remark 2.3.1. It should be noted that there exists a trade-off between the accuracy in approximating the domain of attraction and the simplicity of the representation method used to do so, as discussed in [19]. Nonetheless, among all the shapes considered in the literature for determining contractively invariant regions, ellipsoidal regions are most commonly used due to their simplicity for obtaining LMI conditions. For this reason, ellipsoidal sets have been considered in this thesis.

2.3.2 Saturation avoidance condition

As shown in [119], the concepts related to stabilization of saturated linear systems can be transferred from the linear time-invariant (LTI) framework to the LPV framework. Therefore, for sake of simplicity and clarity, the concepts recalled in this section are shown only for the LTI framework and the case of the state-feedback controller, i.e. $u = Kx$.

Let us consider the following CT system subject to an input saturation:

$$\dot{x} = Ax + B\,\mathrm{sat}(u, \underline{u}, \bar{u}), \tag{2.70a}$$

$$u = Kx, \tag{2.70b}$$

where $x \in \mathbb{R}^{n_x}$ is the state vector and $u \in \mathbb{R}^{n_u}$ denotes the control input vector. $A \in \mathbb{R}^{n_x \times n_x}$, $B \in \mathbb{R}^{n_x \times n_u}$ and $K \in \mathbb{R}^{n_u \times n_x}$ represent the state matrix, the input matrix and the controller gain matrix, respectively, and $\mathrm{sat}(u, \underline{u}, \bar{u}) : \mathbb{R}^{n_u} \to \mathbb{R}^{n_u}$ denotes the standard asymmetric function defined as:

$$\mathrm{sat}(u, \underline{u}, \bar{u}) \triangleq \begin{bmatrix} \mathrm{sat}(u_1, \underline{u}_1, \bar{u}_1) \\ \vdots \\ \mathrm{sat}(u_l, \underline{u}_l, \bar{u}_l) \\ \vdots \\ \mathrm{sat}(u_{n_u}, \underline{u}_{n_u}, \bar{u}_{n_u}) \end{bmatrix}, \quad \mathrm{sat}(u_l, \underline{u}_l, \bar{u}_l) \triangleq \begin{cases} \bar{u}_l, & \text{if } u_l > \bar{u}_l \\ u_l, & \text{if } u_l \in [\underline{u}_l, \bar{u}_l] \\ -\underline{u}_l, & \text{if } u_l < -\underline{u}_l \end{cases} \tag{2.71}$$

for $l \in \mathcal{I}_{[1,n_u]}$, where $\underline{u} = [\underline{u}_1, \ldots, \underline{u}_{n_u}]^\top$ and $\bar{u} = [\bar{u}_1, \ldots, \bar{u}_{n_u}]^\top$ are given vectors with positive entries. Note that the standard symmetric saturation function is recovered if $\underline{u}_l = \bar{u}_l \forall l \in \mathcal{I}_{[1,n_u]}$, which will be denoted by the notation $\mathrm{sat}(u, \bar{u})$.

The closed-loop performance of a saturated system may be categorized into two major groups based on the degree of saturation allowance [119]:

- **Saturation avoidance:** this performance criterion involves the study of the closed-loop system's linear behaviour for designing control laws in order to avoid actuator saturation.
- **Saturation allowance:** this performance criterion addresses the closed-loop system's nonlinear behaviour by seeking the utilization of all the actuator's capacity with the purpose of achieving a good balance between the related estimate of the region of attraction and the closed-loop system's performance or robustness.

Definition 2.3.3 (Region of linearity)**.** The region of linearity of a system subject to a saturation function, denoted as $\mathcal{L}$, is defined as the set of all control inputs $u(t) \in \mathbb{R}^{n_u}$ such that the control signal is not saturated and, hence, $\mathrm{sat}(u, \underline{u}, \bar{u}) = u$.

Definition 2.3.4 (Region of admissible initial conditions)**.** Let $\mathcal{X}_0$ be the region of admissible initial conditions that can be described by one of the following sets:

(a) Ellipsoidal set:

$$\mathcal{X}_0 \triangleq \left\{x \in \mathbb{R}^{n_x} \,:\, x^\top X_0^{-1} x \leq 1\right\}, \tag{2.72}$$

where $X_0^{-1} \in \mathbb{S}_+^{n_x}$ is a known given matrix that contains information about where the initial conditions $x(0)$ are expected to lie.

(b) Polyhedral set:

$$\mathcal{X}_0 \triangleq \mathrm{Co}\{v_1, \ldots, v_{n_v}\}, \quad v_s \in \mathbb{R}^{n_x}, \quad \forall s \in \mathcal{I}_{[1,n_v]}, \tag{2.73}$$

where n_v is the number of vertices and v_s represents each vertex of the polyhedral set.

Then, from the saturation function (2.71), the linearity region of the system (2.70) can be characterized as the following polyhedral set:

$$\mathcal{L}(u, \underline{u}, \bar{u}) = \left\{u \in \mathbb{R}^{n_u} : -\underline{u}_l \leq u_l \leq \bar{u}_l,\ l \in \mathcal{I}_{[1,n_u]}\right\}, \tag{2.74}$$

which can be expressed as a region in the state-space domain through the mapping entailed by the choice of $u = Kx$, thus yielding:

$$\mathcal{L}(K, \underline{u}, \bar{u}) = \left\{x \in \mathbb{R}^{n_x} : -\underline{u}_l \leq K_{[l]} x \leq \bar{u}_l,\ l \in \mathcal{I}_{[1,n_u]}\right\}, \tag{2.75}$$

where $K_{[l]}$ denotes the l^{th} row of the matrix K. Note that polyhedral Lyapunov functions should be considered within the design procedure for an accurate representation of the linearity region (2.75). However, this introduces computational complexity as the resulting design conditions cannot be expressed as LMIs. Therefore, only the use of (PD)QLF, which defines an ellipsoid as a level set, is considered.

The idea behind the saturation avoidance approach relies on forcing the region $\mathcal{E}(P, c)$ in (2.69) to reside within the region of linearity (2.75), thus ensuring that all trajectories initialized in $\mathcal{X}_0$ do not leave $\mathcal{E}(P, c)$. In summary, the conditions for saturation avoidance can be formally stated by Proposition 2.3.1.

Proposition 2.3.1 (Saturation avoidance condition)**.** *Let $\mathcal{L}(K, \underline{u}, \bar{u})$ be a polyhedral set defined as in (2.75). If $\mathcal{E}(P, c)$ is a contractively invariant set satisfying:*

$$\mathcal{X}_0 \subset \mathcal{E}(P, c) \subset \mathcal{L}(K, \underline{u}, \bar{u}), \tag{2.76}$$

then for any initial condition $x_0 \in \mathcal{X}_0$, and hence $x_0 \in \mathcal{E}(P, c)$, the convergence of the corresponding state trajectory $x(t) \to 0$ when $t \to \infty$ is ensured under saturation avoidance.

Proof. See [119]. ∎

3 Shifting state-feedback control

The content of this chapter is based on the following work:

- [95] A. Ruiz, D. Rotondo, and B. Morcego. "Design of state-feedback controllers for linear parameter varying systems subject to time-varying input saturation". *Applied Sciences* 9:17, 2019, p. 3606. ISSN: 2076-3417
- [96] A. Ruiz, D. Rotondo, and B. Morcego. "Shifting $\mathcal{H}_\infty$ linear parameter varying state-feedback controllers subject to time-varying input saturations". *IFAC-PapersOnLine* 53:2, 2020. 21th IFAC World Congress, pp. 7338–7343. ISSN: 2405-8963. DOI: https://doi.org/10.1016/j.ifacol.2020.12.991
- [99] A. Ruiz, D. Rotondo, and B. Morcego. "Design of shifting state-feedback controllers for LPV systems subject to time-varying saturations via parameter-dependent Lyapunov functions". *ISA Transactions*, 2021. ISSN: 0019-0578. DOI: https://doi.org/10.1016/j.isatra.2021.07.025

3.1 Introduction

In the last two decades, works addressing the actuator saturation problem have been an important field of research due to the actuators' inherent physical limitations. However, the controller design has been commonly performed under the assumption of considering that saturation limits are constant in time. For instance, a health-aware controller based on the remaining useful life estimation of a battery has been designed for an autonomous racing vehicle assuming that the input/output limits are constant in time [61]. A similar assumption holds for [28], where a model predictive control (MPC) has been developed for polytopic LPV systems subject to input saturations. On the other hand, some works have proposed using saturation indicator parameters to schedule the input constraints whose limits are still constant in time [36, 128]. Alternatively, a technique based on nested ellipsoids with switching and scheduling policies has been stated in [35], inducing a guaranteed exponential convergence rate by the corresponding saturated feedback.

In addition to the actuation saturation problem, real-world systems can also be affected by unknown disturbances, which can contribute to the saturation of the control input, emphasize actuator deterioration, and potentially make the system unstable. Previous works in the literature have addressed, mostly, the disturbance rejection problem for saturated systems under the same assumption. For example, two GS controllers have been designed using the $\mathcal{H}_\infty$ methodology and the QB concept through a PDQLF [65]. These controllers are subject to saturations with constant limits and provide a guaranteed L_2 gain. Furthermore, the controllers adapt their gains based on the distance from the origin, providing high-gains when the states are close to the origin, thus increasing the system's performance. An extension to the previous work has been presented

in [101] adding an anti-windup to handle the saturation under worst-case disturbance. In [88], the assumption of the input saturation limits being constant in time is maintained with the objective of approximating the region of attraction by means of off-line optimization algorithms. Also, this approach allows to design a saturated dynamic output-feedback controller for an LPV system with bounded disturbances using the QB concept.

In this chapter, the problem of designing a shifting LPV state-feedback controller for time-varying saturated LPV systems is considered. In the proposed approach, a possible mapping between the instantaneous saturation limit values and a performance scheduling vector is introduced. The resulting idea is exploited through the shifting paradigm concept presented in [92], enabling the design of a gain-scheduling controller that adapts the closed-loop system performance in consonance with the saturation limit variations. By means of the LPV framework and the use of the shifting paradigm and the invariant ellipsoidal theory, the problem's solution is expressed as an LMI-based methodology which can efficiently be solved via available solvers. It is worth highlighting that the proposed approach handles the problem establishing a set of region inclusions for ensuring that the control action remains in the linearity region of the system where saturation does not occur. Furthermore, closed-loop converge speed or disturbance rejection effectiveness is regulated online according to the performance scheduling vector through the shifting paradigm concept.

The solution proposed in this chapter differs from the recent work [79], where the importance of considering time-varying saturations as a consequence of an induced actuator fault has been stated without a possible regulation of the closed-loop performance in sense of e.g. convergence speed according to the amount of control action available.

3.2 Problem formulation

Consider the following CT LPV system:

$$\dot{x} = A(\vartheta)x + B_w(\vartheta)w + B(\vartheta)\,\mathrm{sat}(u, \sigma(t)), \quad x(0) = x_0, \tag{3.1a}$$

$$z_\infty = C_z(\vartheta)x + D_{zw}(\vartheta)w + D_{zu}(\vartheta)\,\mathrm{sat}(u, \sigma(t)), \tag{3.1b}$$

where $u \in \mathbb{R}^{n_u}$ is the control input, $w \in \mathbb{R}^{n_w}$ is a vector of exogenous inputs (such as reference signals, disturbance signals or sensor noise), $z_\infty \in \mathbb{R}^{n_{z_\infty}}$ is the output performance signal related with the $\mathcal{H}_\infty$ performance (see Definition 2.2.3), and $\vartheta \in \Theta \subset \mathbb{R}^{n_\vartheta}$ is the time-varying scheduling parameter vector. $\mathrm{sat}(u, \sigma(t)) : \mathbb{R}^{n_u} \to \mathbb{R}^{n_u}$ represents the time-varying symmetric saturation function defined as:

$$\mathrm{sat}(u, \sigma(t)) \triangleq \begin{bmatrix} \mathrm{sat}(u_1, \sigma_1(t)) \\ \vdots \\ \mathrm{sat}(u_l, \sigma_l(t)) \\ \vdots \\ \mathrm{sat}(u_{n_u}, \sigma_{n_u}(t)) \end{bmatrix}, \quad \mathrm{sat}(u_l, \sigma_l(t)) \triangleq \mathrm{sign}(u_l)\min(|u_l|, \sigma_l(t)) \tag{3.2}$$

for $l \in \mathcal{I}_{[1,n_u]}$, where $\sigma(t) = [\sigma_1(t), \ldots, \sigma_{n_u}(t)]^\top$ is a time-varying vector with given known positive time-varying limits $\sigma_l(t)$. The instantaneous value of $\sigma_l(t)$ belongs to the interval $[\underline{\sigma}_l, \bar{\sigma}_l]$

$\forall l \in \mathcal{I}_{[1,n_u]}$, with $\underline{\sigma}_l \in \mathbb{R}_+\backslash\{0\}$ and $\bar{\sigma}_l \in \mathbb{R}_+\backslash\{0\}$ as the lowest and highest possible saturation limits for each u_l, respectively.

Before stating the goal of this chapter, let us define the time-varying region of linearity as a slight modification of Definition 2.3.3:

Definition 3.2.1 (Time-varying region of linearity)**.** The region of linearity of a system subject to a saturation function whose limits are time-varying, denoted as $\mathcal{L}(t)$, is defined as the set of all control inputs $u(t) \in \mathbb{R}^{n_u}$ such that the control signal is not saturated.

For the sake of simplicity, we focus on the scenario in which $\mathcal{L}(t)$ shrinks over time as a consequence of a possible lack of energy availability, thus affecting the actuator action availability of $u(t)$ in (3.1). Then, the time-varying region of linearity of the system (3.1) can be characterized as the following time-varying symmetrical polyhedral set:

$$\mathcal{L}(u(t),\sigma(t)) \triangleq \left\{u(t) \in \mathbb{R}^{n_u} \,:\, -\sigma_l(t) \leq u_l(t) \leq \sigma_l(t),\ \forall l \in \mathcal{I}_{[1,n_u]}\right\}, \tag{3.3}$$

such that the largest control action is available when $\sigma_l(t) \to \bar{\sigma}_l\ \forall l \in \mathcal{I}_{[1,n_u]}$ whereas a more restrictive control action is obtainable when all the instantaneous values $\sigma_l(t)$ are closer to $\underline{\sigma}_l$.

Fig. 3.1 illustrates the possible degradation of the actuator overtime, which would affect the online closed-loop performance of the system (3.1).

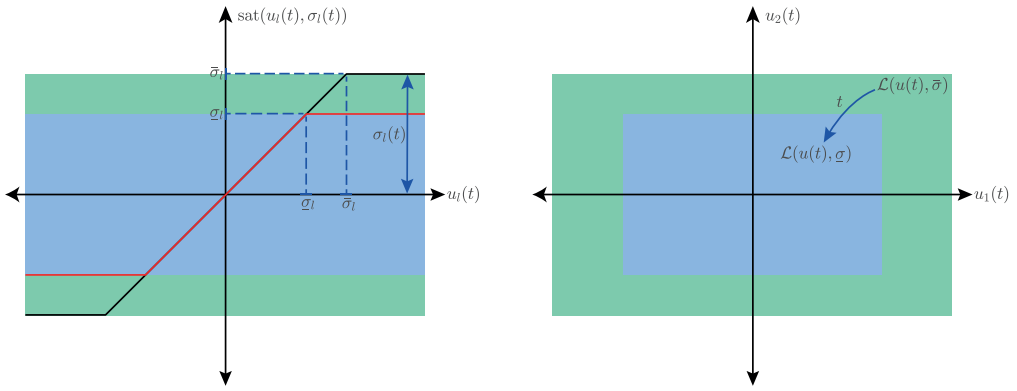

(a) (b)

Figure 3.1: Illustration of a time-varying symmetric saturation function. (a) depicts the time-varying limit variability over a single input u_l. (b) shows the shrinking of the time-varying region of linearity due to the lack of energy availability ($\sigma_l(t) \to \underline{\sigma}_l \forall l \in \mathcal{I}_{[1,2]}$).

The goal of this chapter is the stabilization of the system (3.1) through the definition of the following GS state-feedback control law:

$$u = K(\vartheta,\varphi)x, \quad \forall(\vartheta,\varphi) \in \Theta \times \Phi, \tag{3.4}$$

such that the closed-loop system response of the system (3.1) has one of the shifting performance criteria presented in Definitions 2.2.4 and 2.2.5 in accordance with the variations of $\mathcal{L}(u,\sigma)$. To that purpose, the next sections outline a mapping between possible instantaneous values of $\sigma_l(t)$

and the scheduling vector $\varphi(t)$ under the assumption that $\sigma(t)$ is known for all $t \geq 0$, as well as the LMI-based methodology for designing a shifting state-feedback controller presented in (3.4), with the objective of solving the following control design problems:

Problem 3.2.1. For the LPV system (3.1a) subject to a time-varying saturation function (3.2) and a given set of admissible initial conditions $\mathcal{X}_0$, design a GS state-feedback control law (3.4) such that for any initial state $x_0 \in \mathcal{X}_0$ the closed-loop system response ensures the guaranteed shifting decay rate performance $\mathrm{d_R}(\varphi)\colon \mathbb{R}^{n_\varphi} \to \mathbb{R}_+$, defined as in (2.64):

$$\dot{V}(\cdot) \leq -2\mathrm{d_R}(\varphi)V(\cdot), \tag{3.5}$$

where $V(\cdot)$ is a candidate Lyapunov function that can be defined by a (PD)QLF. □

Problem 3.2.2. For the LPV system (3.1) subject to a time-varying saturation function (3.2) and the given set of admissible initial conditions $\mathcal{X}_0$ and the set $\mathcal{W}$, design a GS state-feedback control law (3.4) such that for $x_0 \in \mathcal{X}_0$ and $\|w\|_2 \leq 1$:

1. the closed-loop system response guarantees the shifting $\mathcal{H}_\infty$ performance $\gamma(\varphi)\colon \mathbb{R}^{n_\varphi} \to \mathbb{R}_+\backslash\{0\}$, defined as in (2.65):

$$\left\|\gamma(\varphi)^{-\frac{1}{2}} z_\infty\right\|_2 < \left\|\gamma(\varphi)^{\frac{1}{2}} w\right\|_2 \tag{3.6}$$

   along all possible trajectories $\vartheta \in \Theta \subset \mathbb{R}^{n_\vartheta}$ and $\varphi \in \Phi \subset \mathbb{R}^{n_\varphi}$.

2. the closed-loop system trajectories $x(t)$ are quadratically bounded by a (PD)QLF.

□

3.3 Time-varying saturation handling

Due to the presence of a nonlinear expression of $u(t)$ in (3.1), the conditions presented in Section 2.2.4 cannot be extended to address the controller design problems stated in Section 3.2 complicating the obtention of computationally applicable design conditions. With the purpose of alleviating this issue, the conditions presented in Section 2.3.2 for dealing with saturated linear systems are extended along this section to the case where the inputs of an LPV system is under a time-varying symmetric saturation as (3.2).

First, in order to describe a time-varying saturation in a polytopic form, let us establish below a mapping between the possible instantaneous values of $\sigma_l(t)$ and the values of the performance scheduling vector $\varphi(t) \in \Phi \subset \mathbb{R}^{n_\varphi}$ with $n_\varphi = n_u$:

$$\varphi_l(t) = \frac{\bar{\sigma}_l^2 - \sigma_l(t)^2}{\bar{\sigma}_l^2 - \underline{\sigma}_l^2}, \quad \varphi_l(t) \in [0, 1], \quad \forall l \in \mathcal{I}_{[1,n_\varphi]}, \tag{3.7}$$

allowing $\sigma_l(t)^2$ to be expressed as a function of $\varphi_l(t)$ from relation (3.7):

$$\hat{\sigma}_l(\varphi_l(t)) \triangleq \sigma_l(t)^2 = \bar{\sigma}_l^2 + \varphi_l(t)\left(\underline{\sigma}_l^2 - \bar{\sigma}_l^2\right), \quad \forall l \in \mathcal{I}_{[1,n_\varphi]}. \tag{3.8}$$

As a result, the closed-loop response of the LPV system (3.1) can be adapted online using the control law (3.4) in terms of convergence speed or disturbance rejection effectiveness in line with the instantaneous value of $\sigma_l(t)$. In this way, a faster response or a better disturbance rejection can be guaranteed when a large control action is available ($\sigma_l(t) \to \bar{\sigma}_l \ \forall l \in \mathcal{I}_{[1,n_\varphi]}$) whereas the controller will provide a more conservative performance when all instantaneous values $\sigma_l(t)$ are closer to their corresponding ϱ_l.

Remark 3.3.1. It should be noted that the necessary number of scheduling parameters for defining the time-varying saturation limits can be $n_\varphi \leq n_u$ in cases where some time-varying saturation limits exhibit some correlation. Furthermore, there exist several potential mappings between $\sigma_l(t)$ and $\varphi_l(t)$ $\forall l \in \mathcal{I}_{[1,n_\varphi]}$ since the representation of the polytopic set Φ is not unique.

Let us now discuss and analyse two alternative propositions based on invariant ellipsoidal set theory [23] and the convex expression (3.8) for extending Proposition 2.3.1 to the time-varying saturation avoidance case and, therefore, obtaining design conditions that ensure $u \in \mathcal{L}(u,\sigma)$ $\forall t \geq 0$. For the purpose of simplicity and clarity, Propositions 3.3.1 and 3.3.2 are formulated for the level sets of a candidate Lyapunov function as in (2.12). Nevertheless, they can be extended to the case when the Lyapunov level sets are associated with a PDQLF, as in (2.15).

Consider a parameter-dependent set as the maximal ellipsoidal region contained in $\mathcal{L}(u,\sigma)$, defined as follows:

$$\mathcal{U}(\varphi) \triangleq \left\{u \in \mathbb{R}^{n_u} \ : \ u^\top U(\varphi)^{-1} u \leq 1\right\}, \tag{3.9}$$

where $U(\varphi)^{-1} \triangleq \mathrm{R}_\mathrm{o}^\top \Lambda(\varphi) \mathrm{R}_\mathrm{o} \in \mathbb{S}^{n_u}$, R_o is a rotation matrix that describes the axes' orientation of the region and $\Lambda(\varphi)$ denotes the parameter-dependent axes' magnitude:

$$\Lambda(\varphi) \triangleq \mathrm{diag}\{\hat{\sigma}_1(\varphi_1), \ldots, \hat{\sigma}_{n_u}(\varphi_{n_u})\}^{-1} = \begin{bmatrix} \frac{1}{\hat{\sigma}_1(\varphi_1)} & & & \\ & \frac{1}{\hat{\sigma}_2(\varphi_2)} & & \\ & & \ddots & \\ & & & \frac{1}{\hat{\sigma}_{n_u}(\varphi_{n_u})} \end{bmatrix}. \tag{3.10}$$

Note that the region $\mathcal{U}(\varphi)$, although defined in the input space, is mapped onto the state-space domain as a parameter-dependent ellipsoidal set by means of the GS state-feedback control law (3.4), thus obtaining the parameter-dependent set in (3.11) for the formulation of Proposition 3.3.1.

Proposition 3.3.1. *Let $\mathcal{U}_x(\vartheta,\varphi)$ be a parameter-dependent ellipsoidal set given by:*

$$\mathcal{U}_x(\vartheta,\varphi) \triangleq \left\{x \in \mathbb{R}^{n_x} \ : \ x^\top K(\vartheta,\varphi)^\top U(\varphi)^{-1} K(\vartheta,\varphi) x \leq 1\right\}. \tag{3.11}$$

If $\mathcal{E}(P,c)$ is a contractively invariant set satisfying $\forall(\vartheta,\varphi) \in \Theta \times \Phi$:

$$\mathcal{X}_0 \subset \mathcal{E}(P,c) \subset \mathcal{U}_x(\vartheta,\varphi), \tag{3.12}$$

then for any initial condition $x_0 \in \mathcal{X}_0$, and hence $x_0 \in \mathcal{E}(P,c)$, the convergence of the corresponding state trajectory $x(t) \to 0$ when $t \to \infty$ is ensured under saturation avoidance.

Proof. The proof follows the reasoning in Proposition 2.3.1. The inclusion $\mathcal{X}_0 \subset \mathcal{E}(P,c)$ ensures for $x_0 \in \mathcal{X}_0$ that any trajectory $x(t) \in \mathcal{E}(P,c)$ $\forall t$ as long as the system works in the region of

linearity (3.3). Furthermore, taking into account the inclusion $\mathcal{E}(P,c) \subset \mathcal{U}_x(\vartheta,\varphi)$ any state trajectory $x(t)$ contained in $\mathcal{E}(P,c)$ will also be located in $\mathcal{U}_x(\vartheta,\varphi)$, so no saturation happens and, therefore, the convergence of $x(t) \to 0$ when $t \to \infty$ is guaranteed for any $x_0 \in \mathcal{E}(P,c)$, and hence for any $x_0 \in \mathcal{X}_0$. ■

Hereinafter, without loss of generality, it can be assumed that $\mathrm{R_o} = \mathrm{I}_{n_u}$ since in most of the cases the axes of the ellipsoidal region $\mathcal{U}(\varphi)$ are aligned with the axes of the input space.

Let us now consider the symmetrical polyhedral set (3.3), which can be mapped onto the state-domain through the relationship (3.4), thus yielding:

$$\mathcal{L}(K(\vartheta,\varphi),\sigma(t)) \triangleq \left\{x \in \mathbb{R}^{n_x} \,:\, |K(\vartheta,\varphi)_{[l]}x| \leq \sigma_l(t),\ l \in \mathcal{I}_{[1,n_u]}\right\}. \tag{3.13}$$

Then, the region $\mathcal{L}(K(\vartheta,\varphi),\sigma(t))$ can be rewritten as:

$$\mathcal{L}(K(\vartheta,\varphi),\sigma(t)) \triangleq \left\{x \in \mathbb{R}^{n_x} \,:\, x^\top \frac{K(\vartheta,\varphi)_{[l]}^\top K(\vartheta,\varphi)_{[l]}}{\sigma_l(t)^2} x \leq 1,\ l \in \mathcal{I}_{[1,n_u]}\right\}, \tag{3.14}$$

which is equivalent to the parameter-dependent set (3.15) through the convex representation (3.8), thus allowing the formulation of Proposition 3.3.2.

Proposition 3.3.2. *Let $\mathcal{L}(K(\vartheta,\varphi),\hat{\sigma}(\varphi))$ be a parameter-dependent set given by:*

$$\mathcal{L}(K(\vartheta,\varphi),\hat{\sigma}_l(\varphi)) \triangleq \left\{x \in \mathbb{R}^{n_x} \,:\, x^\top \frac{K(\vartheta,\varphi)_{[l]}^\top K(\vartheta,\varphi)_{[l]}}{\hat{\sigma}_l(\varphi)} x \leq 1,\ l \in \mathcal{I}_{[1,n_u]}\right\}. \tag{3.15}$$

If $\mathcal{E}(P,c)$ is a contractively invariant set satisfying $\forall(\vartheta,\varphi) \in \Theta \times \Phi$:

$$\mathcal{X}_0 \subset \mathcal{E}(P,c) \subset \mathcal{L}(K(\vartheta,\varphi),\hat{\sigma}(\varphi)), \tag{3.16}$$

then for any initial condition $x_0 \in \mathcal{X}_0$, and hence $x_0 \in \mathcal{E}(P,c)$, the convergence of the corresponding state trajectory $x(t) \to 0$ when $t \to \infty$ is ensured under saturation avoidance.

Proof. The proof follows a reasoning similar to the one of Propositions 2.3.1 and 3.3.1, thus is omitted. ■

While both propositions aim to guarantee that $u \in \mathcal{L}(u,\sigma)\ \forall t \geq 0$ through a set of region inclusions that must be held, they differ in the manner of considering the region $\mathcal{L}(u,\sigma)$ within the design procedure. It should be emphasized that the capacity to consider the size and orientation of the ellipsoidal set (3.11) by Proposition 3.3.1 may yield conservative results when contrasted with Proposition 3.3.2. Nonetheless, it can be useful in some situations where mathematical complexity needs to be kept simple. Proposition 3.3.2, on the other hand, discusses the inclusion of the ellipsoidal set $\mathcal{E}(P,c)$ in the symmetrical polyhedral set (3.15). This inclusion may be extended to the situation in which an asymmetrical polyhedral set is required in the presence of an asymmetric saturation function. However, due to the symmetry of the region $\mathcal{E}(P,c)$, this extension will lead to some apparent conservative results.

3.4 Controller design using a parameter-independent quadratic Lyapunov function

By taking into consideration the conditions in Section 3.3, LMI-based design conditions similar to those described in Section 2.2.4 can be used to address LPV systems subject to time-varying saturations. Let us present an LMI-based methodology for designing a shifting state-feedback controller (3.4) with the objective of solving the different problems formulated in Section 3.2. For this purpose, we will consider throughout this section the use of a parameter-independent QLF, as in (2.12):

$$V(x) = x^\top P^{-1} x, \quad P \in \mathbb{S}^{n_x}_+, \tag{3.17}$$

and its associated unit level set:

$$\mathcal{E}(P,1) \triangleq \{x \in \mathbb{R}^{n_x} : V(x) \leq 1\}. \tag{3.18}$$

Furthermore, if conditions (3.12) or (3.16) hold, the saturated LPV system (3.1) can be reduced to the following non-saturated LPV system for design purposes:

$$\dot{x} = A(\vartheta)x + B_w(\vartheta)w + B(\vartheta)u, \quad x(0) = x_0, \tag{3.19a}$$

$$z_\infty = C_z(\vartheta)x + D_{zw}(\vartheta)w + D_{zu}(\vartheta)u. \tag{3.19b}$$

Let us start by introducing the following theorem which gives a parameter-dependent LMI for designing a GS control law (3.4) that ensures the quadratic stabilization of an LPV system with some desired guaranteed shifting decay rate performance (3.5), thus guaranteeing the online adaptation of the closed-loop system response in sense of convergence speed according to the variations of the scheduling vector $\varphi(t)$.

Theorem 3.4.1 (GSDR performance of LPV systems via shifting state-feedback control)**.** *Consider the LPV system* (3.19a) *with control law* (3.4)*,* $B_w(\vartheta) = 0$*, and a given desired guaranteed shifting decay rate* $\mathrm{d_R}(\varphi) \in \mathbb{R}_+$*. Assume that there exist* $P \in \mathbb{S}^{n_x}_+$ *and* $Y(\vartheta,\varphi) \in \mathbb{R}^{n_u \times n_x}$ *such that* $\forall(\vartheta,\varphi) \in \Theta \times \Phi$ *the following parameter-dependent LMI is satisfied:*

$$\mathrm{He}\{A(\vartheta)P + B(\vartheta)Y(\vartheta,\varphi)\} + 2\mathrm{d_R}(\varphi)P \prec 0. \tag{3.20}$$

Then, the closed-loop response of system (3.19a) *has a guaranteed shifting decay rate performance* (3.5) *if the controller gain is computed as* $K(\vartheta,\varphi) = Y(\vartheta,\varphi)P^{-1}$*.*

Proof. By introducing the GS control law (3.4) into the system's equation (3.19a), the following LPV closed-loop system representation is obtained under the assumption that $B_w(\vartheta) = 0$ and $u(t) \in \mathcal{L}(u,\sigma)$ for all t:

$$\dot{x} = (A(\vartheta) + B(\vartheta)K(\vartheta,\varphi))x. \tag{3.21}$$

Then, let us calculate $\dot{V}(x)$ from the expression described by (3.17), thus obtaining:

$$\dot{V}(x) = 2x^\top P^{-1}\dot{x} = 2x^\top P^{-1}(A(\vartheta) + B(\vartheta)K(\vartheta,\varphi))x, \tag{3.22}$$

which is equivalent to:

$$\dot{V}(x) = x^{\top}\big(\mathrm{He}\big\{P^{-1}A(\vartheta) + P^{-1}B(\vartheta)K(\vartheta,\varphi)\big\}\big)x. \tag{3.23}$$

In order to ensure that the LPV closed-loop system response (3.21) satisfies a shifting guaranteed decay rate $\mathrm{d_R}(\varphi)$, $\dot{V}(x)$ must satisfy the condition (3.5) $\forall x \neq 0$, thus getting:

$$\mathrm{He}\big\{P^{-1}A(\vartheta) + P^{-1}B(\vartheta)K(\vartheta,\varphi)\big\} + 2\mathrm{d_R}(\varphi)P^{-1} \prec 0. \tag{3.24}$$

Then, by pre- and post-multiplying (3.24) by P, one gets the following inequality:

$$\mathrm{He}\{A(\vartheta)P + B(\vartheta)K(\vartheta,\varphi)P\} + 2\mathrm{d_R}(\varphi)P \prec 0, \tag{3.25}$$

which is a BMI due to the product between the decision variables $K(\vartheta,\varphi)$ and P. In order to transform it into parameter-dependent LMI, the change of variable $Y(\vartheta,\varphi) = K(\vartheta,\varphi)P$ is used, thus obtaining (3.20) and concluding the proof. ■

Taking into account the result obtained in Theorem 3.4.1, the following theorem provides a set of LMIs for solving Problem 3.2.1 based on Proposition 3.3.1. Theorem 3.4.2 guarantees that $\mathcal{E}(P,1)$ is an invariant and contractively ellipsoidal set with respect to all closed-loop trajectories of the system (3.1a), forcing x to reside within this region where $u \in \mathcal{U}(\varphi) \subset \mathcal{L}(u,\sigma)$ in absence of external disturbances.

Theorem 3.4.2. *Given the regions* (2.72) *and* (3.11) *with the known matrices* $X_0^{-1} \in \mathbb{S}_+^{n_x}$ *and* $U(\varphi) \in \mathbb{S}_+^{n_u}$*, respectively, and a desired guaranteed shifting decay rate* $\mathrm{d_R}(\varphi) \in \mathbb{R}_+$*, assume that there exist* $P \in \mathbb{S}_+^{n_x}$ *and* $Y(\vartheta,\varphi) \in \mathbb{R}^{n_u \times n_x}$ *such that* $\forall(\vartheta,\varphi) \in \Theta \times \Phi$ *the parameter-dependent LMI* (3.20) *is satisfied together with:*

$$\begin{bmatrix} P & \mathrm{I}_{n_x} \\ \star & X_0^{-1} \end{bmatrix} \succeq 0, \tag{3.26}$$

$$\begin{bmatrix} U(\varphi) & Y(\vartheta,\varphi) \\ \star & P \end{bmatrix} \succeq 0. \tag{3.27}$$

Then, the closed-loop response of the time-varying saturated LPV system (3.1a)*, with* $B_w(\vartheta) = 0$ *and the control law* (3.4) *with the controller gain computed as* $K(\vartheta,\varphi) = Y(\vartheta,\varphi)P^{-1}$ *has a guaranteed shifting decay rate performance* (3.5)*. Furthermore, the convergence of* $x(t) \to 0$ *when* $t \to \infty$ *is ensured for any* $x_0 \in \mathcal{X}_0$ *such that* $x(t) \in \mathcal{U}_x(\vartheta(t),\varphi(t))$*, and hence,* $u(t) \in \mathcal{L}(u(t),\sigma(t))$*.*

Proof. The fact that (3.20) guarantees a desired shifting decay rate $\mathrm{d_R}(\varphi)$ as long as it works in the region of linearity of the actuators, $\mathcal{L}(u,\sigma)$, is a direct consequence of Theorem 3.4.1. Hence, let us demonstrate that if conditions (3.26) and (3.27) hold, then $u(t)$ remains inside the region $\mathcal{U}(\varphi) \subset \mathcal{L}(u,\sigma)$ for all t, as long as $x_0 \in \mathcal{X}_0$.

To this end, let us consider from Proposition 3.3.1 the set of region inclusions (3.12) with $\mathcal{X}_0$ defined as in (2.72) and the given unit level set (3.18). The inclusion $\mathcal{X}_0 \subset \mathcal{E}(P,1)$ may be formulated as:

$$x^{\top}P^{-1}x \leq x^{\top}X_0^{-1}x, \tag{3.28}$$

which is equivalent to:

$$X_0^{-1} - \mathrm{I}_{n_x}^{\top} P^{-1} \mathrm{I}_{n_x} \geq 0 \tag{3.29}$$

and that, by applying Schur's complement, becomes:

$$\begin{bmatrix} P & \mathrm{I}_{n_x} \\ \star & X_0^{-1} \end{bmatrix} \geq 0.$$

Similarly, taking into account (3.11), the inclusion $\mathcal{E}(P,1) \subset \mathcal{U}_x(\vartheta,\varphi)$ can be rewritten as:

$$x^{\top} K(\vartheta,\varphi)^{\top} U(\varphi)^{-1} K(\vartheta,\varphi) x \leq x^{\top} P^{-1} x. \tag{3.30}$$

Then, manipulating the above expression one gets:

$$P^{-1} - K(\vartheta,\varphi)^{\top} U(\varphi)^{-1} K(\vartheta,\varphi) \geq 0. \tag{3.31}$$

Now, let us pre- and post-multiply (3.31) by P, thus obtaining:

$$P - P K(\vartheta,\varphi)^{\top} U(\varphi)^{-1} K(\vartheta,\varphi) P \geq 0. \tag{3.32}$$

By applying the change of variable $Y(\vartheta,\varphi) = K(\vartheta,\varphi)P$, and using Schur's complement, (3.32) becomes:

$$\begin{bmatrix} U(\varphi) & Y(\vartheta,\varphi) \\ \star & P \end{bmatrix} \geq 0.$$

Consequently, $x \in \mathcal{U}_x(\vartheta,\varphi)$ is ensured for any trajectory $x \in \mathcal{E}(P,1)$ and, hence, $u \in \mathcal{U}(\varphi) \subset \mathcal{L}(u,\sigma)$, thus concluding the proof. ■

Remark 3.4.1. Previous knowledge of the plant can be exploited to define regions $\mathcal{X}_0$ and $\mathcal{U}(\varphi)$ in (2.72) and (3.9) through the matrices X_0^{-1} and $U(\varphi)^{-1}$, so that these regions have a physical interpretation. These regions define the initial conditions of interest and the control action space, respectively. As a consequence of this fact, the solution of Theorem 3.4.2 is conditioned by trade-offs related to these regions, e.g., using a smaller region of the expected initial conditions facilitates the feasibility of the LMI-based problem, although it is desirable that the controller operates over a region of possible initial conditions which is as big as possible. However, from a practical point of view, this is constrained by the available range of the control action. For instance, when a wider range of control action is available, a larger region $\mathcal{X}_0$ could be considered while maintaining feasibility of the LMIs.

Similarly to Theorem 3.4.2, Theorem 3.4.3 provides a set of LMIs to address Problem 3.2.1 based on Proposition 3.3.2. The fundamental difference between Theorems 3.4.2 and 3.4.3 lies in how the region $\mathcal{L}(u,\sigma)$ is characterized. Theorem 3.4.2 tackles the issue by considering the maximal ellipsoidal region (3.9) contained in $\mathcal{L}(u,\sigma)$, whereas Theorem 3.4.3 directly considers (3.15) as the state-domain representation of $\mathcal{L}(u,\sigma)$.

Theorem 3.4.3. *Given the region* (2.72) *with the known matrix* $X_0^{-1} \in \mathbb{S}_+^{n_x}$*, the set* (3.15) *and a desired guaranteed shifting decay rate* $\mathrm{d_R}(\varphi) \in \mathbb{R}_+$*, assume that there exist* $P \in \mathbb{S}_+^{n_x}$ *and* $Y(\vartheta,\varphi) \in \mathbb{R}^{n_u \times n_x}$ *such that* $\forall(\vartheta,\varphi) \in \Theta \times \Phi$ *conditions* (3.20) *and* (3.26) *are satisfied together with:*

$$\begin{bmatrix} \hat{\sigma}_l(\varphi) & Y_{[l]}(\vartheta,\varphi) \\ \star & P \end{bmatrix} \geq 0, \quad \forall l \in \mathcal{I}_{[1,n_u]}. \tag{3.33}$$

Then, the closed-loop response of the time-varying saturated LPV system (3.1a)*, with* $B_w(\vartheta) = 0$ *and the control law* (3.4) *with the controller gain computed as* $K(\vartheta,\varphi) = Y(\vartheta,\varphi)P^{-1}$ *has a guaranteed shifting decay rate performance* (3.5)*. Furthermore, the convergence of* $x(t) \to 0$ *when* $t \to \infty$ *is ensured for any* $x_0 \in \mathcal{X}_0$ *such that* $x(t) \in \mathcal{L}(K(\vartheta(t),\varphi(t)),\sigma(t))$*, and hence,* $u(t) \in \mathcal{L}(u(t),\sigma(t))$.

Proof. Let us pre- and post-multiply the parameter-dependent LMI (3.33) by $\mathrm{diag}\{1, P^{-1}\}$, thus obtaining:

$$\begin{bmatrix} \hat{\sigma}_l(\varphi) & K_{[l]}(\vartheta,\varphi) \\ \star & P^{-1} \end{bmatrix} \geq 0, \quad l \in \mathcal{I}_{[1,n_u]},$$

which by applying Schur's complement and pre- and post-multiplying by $x^\top$ and x, respectively, leads to:

$$x^\top \frac{K_{[l]}^\top(\vartheta,\varphi)K_{[l]}(\vartheta,\varphi)}{\hat{\sigma}_l(\varphi)} x \leq x^\top P^{-1} x, \; l \in \mathcal{I}_{[1,n_u]},$$

which yields the inclusion $\mathcal{E}(P,1) \subset \mathcal{L}(K(\vartheta,\varphi),\hat{\sigma})$ in (3.16). Therefore, $x \in \mathcal{L}(K(\vartheta,\varphi),\hat{\sigma})$ is ensured for any trajectory $x \in \mathcal{E}(P,1)$ and, hence, $u \in \mathcal{L}(u,\sigma)$.

The remaining of the proof follows a reasoning similar to the one of Theorem 3.4.2, and thus is omitted. ■

Let us now define the following theorems for designing a GS control law (3.4) based on the QB concept and the shifting $\mathcal{H}_\infty$ performance (see Definitions 2.2.1 and 2.2.5, respectively). Theorem 3.4.4 introduces an LMI-based condition that guarantees QB of an LPV system, thus ensuring that all the closed-loop system trajectories evolve towards the unit level set (3.18), in spite of the external disturbance $w(t)$.

Theorem 3.4.4 (QB of LPV systems via shifting state-feedback control)**.** *Given the set* $\mathcal{E}_w(Q)$ *defined by* (2.20)*, the LPV system* (3.19a) *with control law* (3.4) *is quadratically bounded with the QLF* (3.17) *if there exist positive scalars* λ_1 *and* λ_2*,* $P \in \mathbb{S}_+^{n_x}$ *and* $Y(\vartheta,\varphi) \in \mathbb{R}^{n_u \times n_x}$ *such that* $\forall(\vartheta,\varphi) \in \Theta \times \Phi$ *the following conditions are satisfied:*

$$0 < \lambda_2 \leq \lambda_1, \tag{3.34}$$

$$\begin{bmatrix} \mathrm{He}\{A(\vartheta)P + B(\vartheta)Y(\vartheta,\varphi)\} + \lambda_1 P & B_w(\vartheta) \\ \star & -\lambda_2 Q^{-1} \end{bmatrix} \leq 0. \tag{3.35}$$

Proof. The parameter-dependent LMI (3.35) is obtained from condition (2.49) in Theorem 2.2.9, by considering that K depends on ϑ and φ, and by applying the change of variable $Y(\vartheta,\varphi) = K(\vartheta,\varphi)P$. ■

Thereupon, Theorem 3.4.5 provides the condition to ensure the robustness of an LPV system against $w(t)$ meanwhile the shifting $\mathcal{H}_\infty$ performance (3.6) is guaranteed. The resultant controller will modify online its performance whenever the input saturation limit undergoes variations. Consequently, the controller will exhibit a stronger rejection of the disturbances when larger control actions are available and, conversely, a weaker rejection when the saturation limits are smaller.

Theorem 3.4.5 (Quadratic shifting $\mathcal{H}_\infty$ state-feedback control for LPV systems)**.** *The LPV system* (3.19) *with* $\|w\|_2 \leq 1$ *and control law* (3.4) *has a quadratic shifting* $\mathcal{H}_\infty$ *performance* $\gamma(\varphi)$ *if there exists* $\gamma(\varphi) \in \mathbb{R}_+\backslash\{0\}$, $P \in \mathbb{S}_+^{n_x}$ *and* $Y(\vartheta,\varphi) \in \mathbb{R}^{n_u \times n_x}$ *such that* $\forall(\vartheta,\varphi) \in \Theta \times \Phi$ *the following parameter-dependent LMI is satisfied:*

$$\begin{bmatrix} \mathrm{He}\{A(\vartheta)P + B(\vartheta)Y(\vartheta,\varphi)\} & B_w(\vartheta) & PC_z^\intercal(\vartheta) + Y^\intercal(\vartheta,\varphi)D_{zu}^\intercal(\vartheta) \\ \star & -\gamma(\varphi)\mathrm{I}_{n_w} & D_{zw}^\intercal(\vartheta) \\ \star & \star & -\gamma(\varphi)\mathrm{I}_{n_{z_\infty}} \end{bmatrix} < 0. \quad (3.36)$$

Proof. It follows from condition (2.53) in Theorem 2.2.11, by considering that γ is function of φ, that K depends on ϑ and φ, and $Y(\vartheta,\varphi) = K(\vartheta,\varphi)P$. ■

Combining Theorems 3.4.4 and 3.4.5 with Proposition 3.3.1, Corollary 3.4.1 provides the LMI-based conditions for solving Problem 3.2.2 such that the exogenous signal $w(t)$ satisfies the condition $\|w\|_2 \leq 1$. Furthermore, the resultant shifting state-feedback controller is able to adapt online its rejection performance according to the instantaneous saturation limit values, considering that $u \in \mathcal{U}(\varphi) \subset \mathcal{L}(u,\sigma)$.

Corollary 3.4.1. *Given the known matrices* $X_0^{-1} \in \mathbb{S}_+^{n_x}$ *and* $U(\varphi) \in \mathbb{S}_+^{n_u}$, *let there exist positive scalars* λ_1 *and* λ_2, *matrices* $P \in \mathbb{S}_+^{n_x}$ *and* $Y(\vartheta,\varphi) \in \mathbb{R}^{n_u \times n_x}$, *and a function* $\gamma(\varphi) \in \mathbb{R}_+\backslash\{0\}$ *such that conditions* (3.26), (3.27), (3.34), (3.35) *and* (3.36) *are satisfied* $\forall(\vartheta,\varphi) \in \Theta \times \Phi$ *and* $Q^{-1} = \mathrm{I}_{n_w}$. *If the controller gain* (3.4) *is computed as* $K(\vartheta,\varphi) = Y(\vartheta,\varphi)P^{-1}$ *and* $\|w\|_2 \leq 1$, *then the closed-loop response of the time-varying saturated LPV system* (3.1) *is quadratically bounded with a QLF* (3.17) *against external disturbances with a shifting* $\mathcal{H}_\infty$ *performance* $\gamma(\varphi)$. *Furthermore, if* $x_0 \in \mathcal{X}_0$, *then* $x_0 \in \mathcal{E}(P,1)$ *and the control input* $u(t)$ *is such that* $u(t) \in \mathcal{U}(\varphi(t)) \subset \mathcal{L}(u(t),\sigma(t))$.

Proof. It is a direct consequence of Theorems 3.4.4 and 3.4.5 when $Q^{-1} = \mathrm{I}_{n_w}$, and the stated conditions (3.26) and (3.27) in Theorem 3.4.2. ■

Similarly, Corollary 3.4.2 is formulated below considering Proposition 3.3.2 as an alternative approach for solving Problem 3.2.2.

Corollary 3.4.2. *Given the known matrix* $X_0^{-1} \in \mathbb{S}_+^{n_x}$, *let there exist positive scalars* λ_1 *and* λ_2, *matrices* $P \in \mathbb{S}_+^{n_x}$ *and* $Y(\vartheta,\varphi) \in \mathbb{R}^{n_u \times n_x}$, *and a function* $\gamma(\varphi) \in \mathbb{R}_+\backslash\{0\}$ *such that conditions* (3.26), (3.33), (3.34), (3.35) *and* (3.36) *are satisfied* $\forall(\vartheta,\varphi) \in \Theta \times \Phi$ *and* $Q^{-1} = \mathrm{I}_{n_w}$. *If the controller gain* (3.4) *is computed as* $K(\vartheta,\varphi) = Y(\vartheta,\varphi)P^{-1}$ *and* $\|w\|_2 \leq 1$, *then the closed-loop response of the time-varying saturated LPV system* (3.1) *is quadratically bounded with a QLF* (3.17) *against external disturbances with a shifting* $\mathcal{H}_\infty$ *performance* $\gamma(\varphi)$. *Furthermore, if* $x_0 \in \mathcal{X}_0$, *then* $x_0 \in \mathcal{E}(P,1)$ *and the control input* $u(t)$ *is such that* $u(t) \in \mathcal{L}(u(t),\sigma(t))$.

Proof. It is a direct consequence of Theorems 3.4.4 and 3.4.5 when $Q^{-1} = \mathrm{I}_{n_w}$, the stated condition (3.26) in Theorem 3.4.2, and condition (3.33) in Theorem 3.4.3. ∎

3.4.1 Finite-dimensional LMI design conditions

The conditions provided in Theorems 3.4.1–3.4.5 and Corollaries 3.4.1–3.4.2 cannot be used for design purposes, since the presence of parameter-dependent LMIs imposes an infinite number of constraints. This can be alleviated by considering the following polytopic representation:

$$\begin{bmatrix} A(\vartheta) & B_w(\vartheta) & B(\vartheta) \\ C_z(\vartheta) & D_{zw}(\vartheta) & D_{zu}(\vartheta) \end{bmatrix} = \sum_{i=1}^{n_\mu} \mu_i(\vartheta) \begin{bmatrix} A_i & B_{w,i} & B_i \\ C_{z,i} & D_{zw,i} & D_{zu,i} \end{bmatrix}, \tag{3.37a}$$

$$\begin{bmatrix} U(\varphi) & \hat{\sigma}(\varphi) \\ \mathrm{d_R}(\varphi) & \gamma(\varphi) \end{bmatrix} = \sum_{j=1}^{n_\eta} \eta_j(\varphi) \begin{bmatrix} U_j & \hat{\sigma}_j \\ \mathrm{d_R}_j & \gamma_j \end{bmatrix}, \tag{3.37b}$$

$$Y(\vartheta, \varphi) = \sum_{i=1}^{n_\mu} \sum_{j=1}^{n_\eta} \mu_i(\vartheta) \eta_j(\varphi) Y_{ij}, \tag{3.37c}$$

where $A_i, \ldots, \mathrm{d_R}_j$ stand for the given known vertex terms with appropriate dimensions, $\gamma_j > 0$ and $Y_{ij} \in \mathbb{R}^{n_u \times n_x}$ corresponds to decision vertex terms, and the polytopic weight vectors $\mu(\vartheta) \in \Delta^{n_\mu}$ and $\eta(\varphi) \in \Delta^{n_\eta}$ belong, respectively, to the simplexes defined as in (2.10) and (2.63):

$$\Delta^{n_\mu} \triangleq \left\{ \mu(\vartheta) \in \mathbb{R}^{n_\mu} \ : \ \sum_{i=1}^{n_\mu} \mu_i(\vartheta) = 1, \ \mu_i(\vartheta) \geq 0, \ i \in \mathcal{I}_{[1,n_\mu]} \right\}. \tag{3.38}$$

$$\Delta^{n_\eta} \triangleq \left\{ \eta(\varphi) \in \mathbb{R}^{n_\eta} \ : \ \sum_{j=1}^{n_\eta} \eta_j(\varphi) = 1, \ \eta_j(\varphi) \geq 0, \ j \in \mathcal{I}_{[1,n_\eta]} \right\}. \tag{3.39}$$

Therefore, the conditions provided by Theorems 3.4.1–3.4.5 and Corollaries 3.4.1–3.4.2 are reduced to a finite number of conditions, as stated by Corollaries 3.4.3–3.4.12b. A detailed classification of these corollaries based on their focus and design assumptions is presented in Table 3.1.

Table 3.1: Classification of Corollaries 3.4.3–3.4.12b according to their focus and design assumptions.

	Assumption on $B(\vartheta)$ and $D_{zu}(\vartheta)$	
Corollary focused on	Parameter-independent	Parameter-dependent
Guaranteed shifting decay rate (GSDR)	Corollary 3.4.3	Corollary 3.4.8
Problem 3.2.1	Corollary 3.4.4a / 3.4.4b	Corollary 3.4.9a / 3.4.9b
Quadratic boundedness (QB)	Corollary 3.4.5	Corollary 3.4.10
Shifting $\mathcal{H}_\infty$ performance	Corollary 3.4.6	Corollary 3.4.11
Problem 3.2.2	Corollary 3.4.7a / 3.4.7b	Corollary 3.4.12a / 3.4.12b

Corollary 3.4.3. *Given the desired guaranteed shifting decay rate vertices* $\mathrm{d}_{\mathrm{R}j} \in \mathbb{R}_+$*, let there exist matrices* $P \in \mathbb{S}_+^{n_x}$ *and* $Y_{ij} \in \mathbb{R}^{n_u \times n_x}$ *with* $i \in \mathcal{I}_{[1,n_\mu]}$ *and* $j \in \mathcal{I}_{[1,n_\eta]}$ *such that:*

$$\mathrm{He}\{A_i P + B Y_{ij}\} + 2\,\mathrm{d}_{\mathrm{R}j}\, P \prec 0. \tag{3.40}$$

Then, Theorem 3.4.1 holds for $B(\vartheta) = B$ *and all parameter-dependent terms appearing in* (3.37)*.*

Proof. By means of the polytopic representation (3.37) and the fact that $\mu(\vartheta) \in \Delta^{n_\mu}$ and $\eta(\varphi) \in \Delta^{n_\eta}$, the parameter-dependent LMI (3.20) with $B(\vartheta) = B$ can be rewritten as follows:

$$\sum_{i=1}^{n_\mu} \mu_i(\vartheta)[\mathrm{He}\{A_i P + B Y_i(\varphi)\} + 2\mathrm{d}_{\mathrm{R}}(\varphi) P] \prec 0, \tag{3.41}$$

which is equivalent to:

$$\sum_{i=1}^{n_\mu} \sum_{j=1}^{n_\eta} \mu_i(\vartheta)\eta_j(\varphi)\big[\mathrm{He}\{A_i P + B Y_{ij}\} + 2\mathrm{d}_{\mathrm{R}j} P\big] \prec 0. \tag{3.42}$$

Then, due to a basic property of matrices [53], (3.42) is guaranteed to be negative-definite if:

$$\mathrm{He}\{A_i P + B Y_{ij}\} + 2\mathrm{d}_{\mathrm{R}j} P \prec 0, \quad i \in \mathcal{I}_{[1,n_\mu]}, \quad j \in \mathcal{I}_{[1,n_\eta]}, \tag{3.43}$$

thus obtaining the LMI (3.40) and concluding the proof. ■

Corollaries 3.4.4a and 3.4.4b state alternate design conditions to solve Problem 3.2.1, considering the results of Theorems 3.4.2 and 3.4.3, respectively, together with the LMI (3.40).

Corollary 3.4.4a. *Given the known matrix* $X_0^{-1} \in \mathbb{S}_+^{n_x}$*, the known vertex matrices* $U_j \in \mathbb{S}_+^{n_u}$ *and the desired guaranteed shifting decay rate vertices* $\mathrm{d}_{\mathrm{R}j} \in \mathbb{R}_+$*, let there exist matrices* $P \in \mathbb{S}_+^{n_x}$ *and* $Y_{ij} \in \mathbb{R}^{n_u \times n_x}$ *with* $i \in \mathcal{I}_{[1,n_\mu]}$ *and* $j \in \mathcal{I}_{[1,n_\eta]}$ *such that conditions* (3.26) *and* (3.40) *are satisfied together with:*

$$\begin{bmatrix} U_j & Y_{ij} \\ \star & P \end{bmatrix} \succeq 0, \tag{3.44}$$

Then, Theorem 3.4.2 holds for $B(\vartheta) = B$ *and all parameter-dependent terms appearing in* (3.37)*.*

Proof. Similar to that of Corollary 3.4.3, thus omitted. ■

Corollary 3.4.4b. *Given the known matrix* $X_0^{-1} \in \mathbb{S}_+^{n_x}$ *and the desired guaranteed shifting decay rate vertices* $\mathrm{d}_{\mathrm{R}j} \in \mathbb{R}_+$*, let there exist matrices* $P \in \mathbb{S}_+^{n_x}$ *and* $Y_{ij} \in \mathbb{R}^{n_u \times n_x}$ *with* $i \in \mathcal{I}_{[1,n_\mu]}$ *and* $j \in \mathcal{I}_{[1,n_\eta]}$ *such that conditions* (3.26) *and* (3.40) *are satisfied together with:*

$$\begin{bmatrix} \hat{\sigma}_{l,j} & Y_{[l],ij} \\ \star & P \end{bmatrix} \succeq 0, \quad \forall l \in \mathcal{I}_{[1,n_u]}. \tag{3.45}$$

Then, Theorem 3.4.3 holds for $B(\vartheta) = B$ *and all parameter-dependent terms appearing in* (3.37)*.*

Proof. Similar to that of Corollary 3.4.3, thus omitted. ■

From the respective Theorems 3.4.4 and 3.4.5, one gets:

Corollary 3.4.5. *For fixed positive scalars $\lambda_1 \geq \lambda_2$ and a given known matrix $Q^{-1} \in \mathbb{S}_+^{n_w}$, let there exist matrices $P \in \mathbb{S}_+^{n_x}$ and $Y_{ij} \in \mathbb{R}^{n_u \times n_x}$ with $i \in \mathcal{I}_{[1,n_\mu]}$ and $j \in \mathcal{I}_{[1,n_\eta]}$ such that the following set of LMIs is satisfied:*

$$\begin{bmatrix} \mathrm{He}\{A_i P + B Y_{ij}\} + \lambda_1 P & B_{w,i} \\ \star & -\lambda_2 Q^{-1} \end{bmatrix} \preceq 0. \tag{3.46}$$

Then, Theorem 3.4.4 holds for $B(\vartheta) = B$ and all parameter-dependent terms appearing in (3.37).

Proof. Similar to that of Corollary 3.4.3, thus omitted. ∎

Corollary 3.4.6. *Let there exist $P \in \mathbb{S}_+^{n_x}$, $Y_{ij} \in \mathbb{R}^{n_u \times n_x}$ and vertex terms $\gamma_j > 0$ with $i \in \mathcal{I}_{[1,n_\mu]}$ and $j \in \mathcal{I}_{[1,n_\eta]}$ such that the following set of LMIs is satisfied:*

$$\begin{bmatrix} \mathrm{He}\{A_i P + B Y_{ij}\} & B_{w,i} & P C_{z,i}^\top + Y_{ij}^\top D_{zu}^\top \\ \star & -\gamma_j \mathrm{I}_{n_w} & D_{zw,i}^\top \\ \star & \star & -\gamma_j \mathrm{I}_{n_{z_\infty}} \end{bmatrix} \prec 0. \tag{3.47}$$

Then, Theorem 3.4.5 holds for $B(\vartheta) = B$, $D_{zu}(\vartheta) = D_{zu}$ and all parameter-dependent terms appearing in (3.37).

Proof. Similar to that of Corollary 3.4.3, thus omitted. ∎

Combining the results of Corollaries 3.4.5 and 3.4.6 with condition (3.44) in Corollary 3.4.4a, we can then state the following design conditions to solve Problem 3.2.2:

Corollary 3.4.7a. *For fixed positive scalars $\lambda_1 \geq \lambda_2$, the given known matrix $X_0^{-1} \in \mathbb{S}_+^{n_x}$ and the known vertex matrices $U_j \in \mathbb{S}_+^{n_u}$, let there exist $P \in \mathbb{S}_+^{n_x}$, $Y_{ij} \in \mathbb{R}^{n_u \times n_x}$ and vertex terms $\gamma_j > 0$ with $i \in \mathcal{I}_{[1,n_\mu]}$ and $j \in \mathcal{I}_{[1,n_\eta]}$ such that conditions (3.26),(3.44), (3.46) and (3.47) are satisfied for $Q^{-1} = \mathrm{I}_{n_w}$. Then, Corollary 3.4.1 holds for $B(\vartheta) = B$, $D_{zu}(\vartheta) = D_{zu}$ and all parameter-dependent terms appearing in (3.37).*

Proof. It is a direct consequence of Corollaries 3.4.5 and 3.4.6 when $Q^{-1} = \mathrm{I}_{n_w}$, the stated condition (3.26) in Theorem 3.4.2, and condition (3.44) in Corollary 3.4.4a. ∎

Similarly, Corollary 3.4.7b is given as an alternative to Corollary 3.4.7a in light of the condition (3.45) in Corollary 3.4.4b.

Corollary 3.4.7b. *For fixed positive scalars $\lambda_1 \geq \lambda_2$ and a given matrix $X_0^{-1} \in \mathbb{S}_+^{n_x}$, let there exist $P \in \mathbb{S}_+^{n_x}$, $Y_{ij} \in \mathbb{R}^{n_u \times n_x}$ and vertex terms $\gamma_j > 0$ with $i \in \mathcal{I}_{[1,n_\mu]}$ and $j \in \mathcal{I}_{[1,n_\eta]}$ such that conditions (3.26),(3.45), (3.46) and (3.47) are satisfied for $Q^{-1} = \mathrm{I}_{n_w}$. Then, Corollary 3.4.2 holds for $B(\vartheta) = B$, $D_{zu}(\vartheta) = D_{zu}$ and all parameter-dependent terms appearing in (3.37).*

Proof. It is a direct consequence of Corollaries 3.4.5 and 3.4.6 when $Q^{-1} = \mathrm{I}_{n_w}$, the stated condition (3.26) in Theorem 3.4.2, and condition (3.45) in Corollary 3.4.4b. ∎

Unfortunately, it is not always possible to assume the parameter independence of matrices $B(\vartheta)$ and $D_{zu}(\vartheta)$ (see, e.g., the quasi-LPV model of a two-link planar robot [66]). In order to handle this case, Corollaries 3.4.8–3.4.12b provide appropriate design conditions for Theorems 3.4.1–3.4.5 and Corollaries 3.4.1–3.4.2 by considering the polytopic representation (3.37) together with the application of the Pólya's relaxation theorem (Lemma 2.2.14).

Corollary 3.4.8. *Given a chosen relaxation degree $d \in \mathbb{N}$ with $d \geq 2$ and the desired guaranteed shifting decay rate vertices $\mathrm{d}_{\mathrm{R}j} \in \mathbb{R}_+$, let there exist matrices $P \in \mathbb{S}_+^{n_x}$ and $Y_{ij} \in \mathbb{R}^{n_u \times n_x}$ with $i \in \mathcal{I}_{[1,n_\mu]}$ and $j \in \mathcal{I}_{[1,n_\eta]}$ such that:*

$$\sum_{\boldsymbol{p} \in \mathcal{P}(\boldsymbol{i})} \left[\mathrm{He}\{A_{p_1} P + B_{p_1} Y_{p_2 j}\} + 2\,\mathrm{d}_{\mathrm{R}j} P \right] \prec 0, \quad \forall \boldsymbol{i} \in \mathbb{I}^{+}_{(d,n_\mu)}. \tag{3.48}$$

Then, Theorem 3.4.1 holds for all parameter-dependent terms appearing in (3.37).

Proof. The proof follows a reasoning similar to the one of Corollary 3.4.3. By means of (3.37), the parameter-dependent LMI (3.20) can be expressed as follows:

$$\sum_{i_1=1}^{n_\mu} \sum_{i_2=1}^{n_\mu} \mu_{i_1}(\vartheta)\mu_{i_2}(\vartheta)[\mathrm{He}\{A_{i_1} P + B_{i_1} Y_{i_2}(\varphi)\} + 2\mathrm{d}_{\mathrm{R}}(\varphi) P] \prec 0, \tag{3.49}$$

which is equivalent to:

$$\sum_{i_1=1}^{n_\mu} \sum_{i_2=1}^{n_\mu} \sum_{j=1}^{n_\eta} \mu_{i_1}(\vartheta)\mu_{i_2}(\vartheta)\eta_j(\varphi)\left[\mathrm{He}\{A_{i_1} P + B_{i_1} Y_{i_2 j}\} + 2\mathrm{d}_{\mathrm{R}j} P\right] \prec 0. \tag{3.50}$$

Since the negative-definiteness of the expression (3.50) involves multiple polytopic summations, the use of Lemma 2.2.14 is required to obtain the LMI (3.48) from (3.50). ■

Using the result obtained in Corollary 3.4.8, we can now introduce the following corollaries, which provide alternative design conditions to those proposed in Corollaries 3.4.4a and 3.4.4b:

Corollary 3.4.9a. *Given a chosen relaxation degree $d \in \mathbb{N}$ with $d \geq 2$, the known matrix $X_0^{-1} \in \mathbb{S}_+^{n_x}$, the known vertex matrices $U_j \in \mathbb{S}_+^{n_u}$ and the desired guaranteed shifting decay rate vertices $\mathrm{d}_{\mathrm{R}j} \in \mathbb{R}_+$, let there exist matrices $P \in \mathbb{S}_+^{n_x}$ and $Y_{ij} \in \mathbb{R}^{n_u \times n_x}$ with $i \in \mathcal{I}_{[1,n_\mu]}$ and $j \in \mathcal{I}_{[1,n_\eta]}$ such that conditions* (3.26), (3.44) *and* (3.48) *are satisfied. Then, Theorem 3.4.2 holds for all parameter-dependent terms appearing in* (3.37).

Proof. It is a direct consequence of Corollaries 3.4.4a and 3.4.8 when a parameter-dependent matrix $B(\vartheta)$ is considered. ■

Corollary 3.4.9b. *Given a chosen relaxation degree $d \in \mathbb{N}$ with $d \geq 2$, the known matrix $X_0^{-1} \in \mathbb{S}_+^{n_x}$ and the desired guaranteed shifting decay rate vertices $\mathrm{d}_{\mathrm{R}j} \in \mathbb{R}_+$, let there exist matrices $P \in \mathbb{S}_+^{n_x}$ and $Y_{ij} \in \mathbb{R}^{n_u \times n_x}$ with $i \in \mathcal{I}_{[1,n_\mu]}$ and $j \in \mathcal{I}_{[1,n_\eta]}$ such that conditions* (3.26), (3.45) *and* (3.48) *are satisfied. Then, Theorem 3.4.3 holds for all parameter-dependent terms appearing in* (3.37).

Proof. It is a direct consequence of Corollaries 3.4.4b and 3.4.8 when a parameter-dependent matrix $B(\vartheta)$ is considered. ■

Corollaries 3.4.10 and 3.4.11, on the other hand, are provided as alternatives to Corollaries 3.4.5 and 3.4.6 when dealing with parameter-dependent matrices $B(\vartheta)$ and $D_{zu}(\vartheta)$.

Corollary 3.4.10. *For fixed positive scalars $\lambda_1 \geq \lambda_2$, a given known matrix $Q^{-1} \in \mathbb{S}_+^{n_w}$ and a chosen relaxation degree $d \in \mathbb{N}$ with $d \geq 2$, let there exist $P \in \mathbb{S}_+^{n_x}$ and $Y_{ij} \in \mathbb{R}^{n_u \times n_x}$ with $i \in \mathcal{I}_{[1,n_\mu]}$ and $j \in \mathcal{I}_{[1,n_\eta]}$ such that the following set of LMIs is satisfied:*

$$\sum_{\boldsymbol{p} \in \mathcal{P}(\boldsymbol{i})} \begin{bmatrix} \mathrm{He}\{A_{p_1} P + B_{p_1} Y_{p_2 j}\} + \lambda_1 P & B_{w,p_1} \\ \star & -\lambda_2 Q^{-1} \end{bmatrix} \preceq 0, \quad \forall \boldsymbol{i} \in \mathbb{I}_{(d,n_\mu)}^{+}. \tag{3.51}$$

Then, Theorem 3.4.4 holds for all parameter-dependent terms appearing in (3.37).

Proof. Similar to that of Corollary 3.4.8, thus omitted. ■

Corollary 3.4.11. *Given a chosen relaxation degree $d \in \mathbb{N}$ with $d \geq 2$, let there exist $P \in \mathbb{S}_+^{n_x}$, $Y_{ij} \in \mathbb{R}^{n_u \times n_x}$ and vertex terms $\gamma_j > 0$ with $i \in \mathcal{I}_{[1,n_\mu]}$ and $j \in \mathcal{I}_{[1,n_\eta]}$ such that the following set of LMIs is satisfied:*

$$\sum_{\boldsymbol{p} \in \mathcal{P}(\boldsymbol{i})} \begin{bmatrix} \mathrm{He}\{A_{p_1} P + B_{p_1} Y_{p_2 j}\} & B_{w,p_1} & P C_{z,p_1}^{\top} + Y_{p_1 j}^{\top} D_{zu,p_2}^{\top} \\ \star & -\gamma_j \mathrm{I}_{n_w} & D_{zw,p_1}^{\top} \\ \star & \star & -\gamma_j \mathrm{I}_{n_{z_\infty}} \end{bmatrix} \prec 0, \quad \forall \boldsymbol{i} \in \mathbb{I}_{(d,n_\mu)}^{+}. \tag{3.52}$$

Then, Theorem 3.4.5 holds for all parameter-dependent terms appearing in (3.37).

Proof. Similar to that of Corollary 3.4.8, thus omitted. ■

Similarly, the following corollaries state alternative design options to Corollaries 3.4.7a and 3.4.7b, respectively:

Corollary 3.4.12a. *For fixed positive scalars $\lambda_1 \geq \lambda_2$, a given known matrix $X_0^{-1} \in \mathbb{S}_+^{n_x}$, the known vertex matrices $U_j \in \mathbb{S}_+^{n_u}$ and a chosen relaxation degree $d \in \mathbb{N}$ with $d \geq 2$, let there exist $P \in \mathbb{S}_+^{n_x}$, $Y_{ij} \in \mathbb{R}^{n_u \times n_x}$ and vertex terms $\gamma_j > 0$ with $i \in \mathcal{I}_{[1,n_\mu]}$ and $j \in \mathcal{I}_{[1,n_\eta]}$ such that conditions (3.26), (3.44), (3.51) and (3.52) are satisfied for $Q^{-1} = \mathrm{I}_{n_w}$. Then, Corollary 3.4.1 holds for all parameter-dependent terms appearing in (3.37).*

Proof. It is a direct result of Corollaries 3.4.7a, 3.4.10 and 3.4.11 when parameter-dependent matrices $B(\vartheta)$ and $D_{zu}(\vartheta)$ are considered. ■

Corollary 3.4.12b. *For fixed positive scalars $\lambda_1 \geq \lambda_2$, a given known matrix $X_0^{-1} \in \mathbb{S}_+^{n_x}$ and a chosen relaxation degree $d \in \mathbb{N}$ with $d \geq 2$, let there exist $P \in \mathbb{S}_+^{n_x}$, $Y_{ij} \in \mathbb{R}^{n_u \times n_x}$ and vertex terms $\gamma_j > 0$ with $i \in \mathcal{I}_{[1,n_\mu]}$ and $j \in \mathcal{I}_{[1,n_\eta]}$ such that conditions (3.26), (3.45), (3.51) and (3.52) are satisfied for $Q^{-1} = \mathrm{I}_{n_w}$. Then, Corollary 3.4.2 holds for all parameter-dependent terms appearing in (3.37).*

Proof. It is a direct result of Corollaries 3.4.7b, 3.4.10 and 3.4.11 when parameter-dependent matrices $B(\vartheta)$ and $D_{zu}(\vartheta)$ are considered. ■

Note that in some circumstances, we can be interested in conditions involving a polyhedral set of admissible initial conditions $\mathcal{X}_0$ defined as (2.73) instead of an ellipsoidal one (2.72). Therefore, in order to take it into account within the design procedure, we can replace the condition (3.26) appearing in Theorems 3.4.2–3.4.3 and corollaries presented throughout this section by the following LMI, as demonstrated in [54, Chap. 7]:

$$\begin{bmatrix} P & v_s \\ \star & 1 \end{bmatrix} \geq 0, \ \forall s \in \mathcal{I}_{[1,n_v]}. \tag{3.53}$$

3.5 Controller design using a parameter-dependent quadratic Lyapunov function

Despite its simplicity, the approach presented in Section 3.4 has the disadvantage of conservatism owing to the use of the parameter-independent candidate Lyapunov function (3.17). A way to alleviate this source of conservatism is to use a PDQLF as:

$$V(x,\vartheta,\varphi) = x^{\mathsf{T}} P(\vartheta,\varphi)^{-1} x, \quad P(\vartheta,\varphi) \in \mathbb{S}^{n_x}_{+}, \quad \forall (\vartheta,\varphi) \in \Theta \times \Phi \tag{3.54}$$

and its associated unit level set:

$$\mathcal{E}(P(\vartheta,\varphi),1) \triangleq \{x \in \mathbb{R}^{n_x} \, : \, V(x,\vartheta,\varphi) \leq 1\}. \tag{3.55}$$

Hereafter, the results presented in Section 3.4 are extended to the case where the PDQLF (3.54) is used in order to solve the problems formulated in Section 3.2.

Theorem 3.5.1 (GSDR performance of LPV systems via shifting state-feedback control)**.** *Consider the LPV system* (3.19a) *with control law* (3.4)*,* $B_w(\vartheta) = 0$*, and a given desired guaranteed shifting decay rate* $\mathrm{d_R}(\varphi) \in \mathbb{R}_+$*. Assume that there exist* $P(\vartheta,\varphi) \in \mathbb{S}^{n_x}_{+}$ *and* $Y(\vartheta,\varphi) \in \mathbb{R}^{n_u \times n_x}$ *such that* $\forall \left(\vartheta, \dot{\vartheta}\right) \in \Theta \times \Theta_d$ *and* $\forall (\varphi, \dot{\varphi}) \in \Phi \times \Phi_d$ *the following parameter-dependent LMI is satisfied:*

$$\mathrm{He}\{A(\vartheta)P(\vartheta,\varphi) + B(\vartheta)Y(\vartheta,\varphi)\} + 2\mathrm{d_R}(\varphi)P(\vartheta,\varphi) - \dot{P}(\vartheta,\varphi) \prec 0. \tag{3.56}$$

Then, the closed-loop response of system (3.19a) *has the guaranteed shifting decay rate performance* (3.5) *if the controller gain is computed as* $K(\vartheta,\varphi) = Y(\vartheta,\varphi)P(\vartheta,\varphi)^{-1}$.

Proof. The proof follows a reasoning similar to the one of Theorem 3.4.1. Let us prove that $\dot{V}(x,\vartheta,\varphi) < -2\mathrm{d_R}(\varphi)V(x,\vartheta,\varphi)$ is satisfied $\forall x \neq 0$ with $V(x,\vartheta,\varphi)$ defined as in (3.54), thus obtaining:

$$\mathrm{He}\left\{P(\vartheta,\varphi)^{-1}A_{cl}(\vartheta,\varphi)\right\} + \dot{P}(\vartheta,\varphi)^{-1} + 2\mathrm{d_R}(\varphi)P(\vartheta,\varphi)^{-1} \prec 0, \tag{3.57}$$

where $A_{cl}(\vartheta,\varphi) = A(\vartheta) + B(\vartheta)K(\vartheta,\varphi)$.

Then, by pre- and post-multiplying (3.57) by $P(\vartheta,\varphi)$, one gets the following inequality:

$$\mathrm{He}\{A_{cl}(\vartheta,\varphi)P(\vartheta,\varphi)\} + P(\vartheta,\varphi)\dot{P}(\vartheta,\varphi)^{-1}P(\vartheta,\varphi) + 2\mathrm{d_R}(\varphi)P(\vartheta,\varphi) \prec 0, \tag{3.58}$$

which is equivalent to:

$$\mathrm{He}\{A(\vartheta,\varphi)P(\vartheta,\varphi) + B(\vartheta)K(\vartheta,\varphi)P(\vartheta,\varphi)\} + 2\mathrm{d_R}(\varphi)P(\vartheta,\varphi) - \dot{P}(\vartheta,\varphi) \prec 0, \tag{3.59}$$

where the property $\dot{P}(\vartheta,\varphi) = -P(\vartheta,\varphi)\dot{P}(\vartheta,\varphi)^{-1}P(\vartheta,\varphi)$ is used.

By using the change of variable $Y(\vartheta,\varphi) = K(\vartheta,\varphi)P(\vartheta,\varphi)$, the parameter-dependent LMI (3.56) is obtained from the BMI (3.59) thus concluding the proof. ■

Theorem 3.5.2. *Given the regions* (2.72) *and* (3.11) *with the known matrices* $X_0^{-1} \in \mathbb{S}_+^{n_x}$ *and* $U(\varphi) \in \mathbb{S}_+^{n_u}$*, respectively, and a desired guaranteed shifting decay rate* $\mathrm{d_R}(\varphi) \in \mathbb{R}_+$*, assume that there exist* $P(\vartheta,\varphi) \in \mathbb{S}_+^{n_x}$ *and* $Y(\vartheta,\varphi) \in \mathbb{R}^{n_u\times n_x}$ *such that* $\forall\left(\vartheta,\dot{\vartheta}\right) \in \Theta\times\Theta_d$ *and* $\forall(\varphi,\dot{\varphi}) \in \Phi\times\Phi_d$ *the parameter-dependent LMI* (3.56) *is satisfied together with:*

$$\begin{bmatrix} P(\vartheta,\varphi) & \mathrm{I}_{n_x} \\ \star & X_0^{-1} \end{bmatrix} \succeq 0, \tag{3.60}$$

$$\begin{bmatrix} U(\varphi) & Y(\vartheta,\varphi) \\ \star & P(\vartheta,\varphi) \end{bmatrix} \succeq 0. \tag{3.61}$$

Then, the closed-loop response of the time-varying saturated LPV system (3.1a)*, with* $B_w(\vartheta) = 0$ *and the control law* (3.4) *with the controller gain computed as* $K(\vartheta,\varphi) = Y(\vartheta,\varphi)P(\vartheta,\varphi)^{-1}$ *has the guaranteed shifting decay rate performance* (3.5)*. Furthermore, the convergence of* $x(t) \to 0$ *when* $t \to \infty$ *is ensured for any* $x_0 \in \mathcal{X}_0$ *such that* $x(t) \in \mathcal{U}_x(\vartheta(t),\varphi(t))$*, and hence,* $u(t) \in \mathcal{L}(u(t),\sigma(t))$*.*

Proof. It is a direct consequence of Theorems 3.4.2 and 3.5.1 when the PDQLF (3.54) is considered. ■

Theorem 3.5.3. *Given the region* (2.72) *with the known matrix* $X_0^{-1} \in \mathbb{S}_+^{n_x}$*, the set* (3.15) *and a desired guaranteed shifting decay rate* $\mathrm{d_R}(\varphi) \in \mathbb{R}_+$*, assume that there exist* $P \in \mathbb{S}_+^{n_x}$ *and* $Y(\vartheta,\varphi) \in \mathbb{R}^{n_u\times n_x}$ *such that* $\forall\left(\vartheta,\dot{\vartheta}\right) \in \Theta\times\Theta_d$ *and* $\forall(\varphi,\dot{\varphi}) \in \Phi\times\Phi_d$ *conditions* (3.56) *and* (3.60) *are satisfied together with:*

$$\begin{bmatrix} \hat{\sigma}_l(\varphi) & Y_{[l]}(\vartheta,\varphi) \\ \star & P(\vartheta,\varphi) \end{bmatrix} \succeq 0, \quad \forall l \in \mathcal{I}_{[1,n_u]}. \tag{3.62}$$

Then, the closed-loop response of the time-varying saturated LPV system (3.1a)*, with* $B_w(\vartheta) = 0$ *and the control law* (3.4) *with the controller gain computed as* $K(\vartheta,\varphi) = Y(\vartheta,\varphi)P(\vartheta,\varphi)^{-1}$ *has the guaranteed shifting decay rate performance* (3.5)*. Furthermore, the convergence of* $x(t) \to 0$ *when* $t \to \infty$ *is ensured for any* $x_0 \in \mathcal{X}_0$ *such that* $x(t) \in \mathcal{L}(K(\vartheta(t),\varphi(t)),\sigma(t))$*, and hence,* $u(t) \in \mathcal{L}(u(t),\sigma(t))$*.*

Proof. It is a direct consequence of Theorems 3.4.3 and 3.5.1 when the PDQLF (3.54) is considered. ■

Theorem 3.5.4 (PDQB of LPV systems via shifting state-feedback control)**.** *Given the set* $\mathcal{E}_w(Q)$ *defined by* (2.20)*, the LPV system* (3.19a) *with control law* (3.4) *is quadratically bounded with the PDQLF* (3.54) *if there exist positive scalars* λ_1 *and* λ_2*,* $P(\vartheta,\varphi) \in \mathbb{S}^{n_x}_+$ *and* $Y(\vartheta,\varphi) \in \mathbb{R}^{n_u\times n_x}$ *such that:*

$$0 < \lambda_2 \leq \lambda_1, \tag{3.63}$$

and $\forall\left(\vartheta,\dot{\vartheta}\right) \in \Theta\times\Theta_d$ *and* $\forall(\varphi,\dot{\varphi}) \in \Phi\times\Phi_d$ *the following condition is satisfied:*

$$\begin{bmatrix} \mathrm{He}\{A(\vartheta)P(\vartheta,\varphi) + B(\vartheta)Y(\vartheta,\varphi)\} + \lambda_1 P(\vartheta,\varphi) - \dot{P}(\vartheta,\varphi) & B_w(\vartheta) \\ \star & -\lambda_2 Q^{-1} \end{bmatrix} \leq 0. \tag{3.64}$$

Proof. The inequality (3.64) is obtained from condition (2.51) in Theorem 2.2.10, by considering that K and P depend on ϑ and φ, and by applying the change of variable $Y(\vartheta,\varphi) = K(\vartheta,\varphi)P(\vartheta,\varphi)$. ■

Theorem 3.5.5 (PDQ shifting $\mathcal{H}_\infty$ state-feedback control for LPV systems)**.** *The LPV system* (3.19) *with* $\|w\|_2 \leq 1$ *and control law* (3.4) *has a shifting* $\mathcal{H}_\infty$ *performance* $\gamma(\varphi)$ *if there exists* $\gamma(\varphi) \in \mathbb{R}_+\backslash\{0\}$*,* $P(\vartheta,\varphi) \in \mathbb{S}^{n_x}_+$ *and* $Y(\vartheta,\varphi) \in \mathbb{R}^{n_u\times n_x}$ *such that* $\forall\left(\vartheta,\dot{\vartheta}\right) \in \Theta\times\Theta_d$ *and* $\forall(\varphi,\dot{\varphi}) \in \Phi\times\Phi_d$ *the following parameter-dependent LMI is satisfied:*

$$\begin{bmatrix} \Psi_{[11]}(\vartheta,\varphi) & B_w(\vartheta) & \Psi_{[13]}(\vartheta,\varphi) \\ \star & -\gamma(\varphi)\mathrm{I}_{n_w} & D^\top_{zw}(\vartheta) \\ \star & \star & -\gamma(\varphi)\mathrm{I}_{n_{z_\infty}} \end{bmatrix} \prec 0, \tag{3.65}$$

where:

$$\Psi_{[11]}(\vartheta,\varphi) \triangleq \mathrm{He}\{A(\vartheta)P(\vartheta,\varphi) + B(\vartheta)Y(\vartheta,\varphi)\} - \dot{P}(\vartheta,\varphi),$$
$$\Psi_{[13]}(\vartheta,\varphi) \triangleq P(\vartheta,\varphi)C^\top_z(\vartheta) + Y^\top(\vartheta,\varphi)D^\top_{zu}(\vartheta).$$

Proof. The inequality (3.65) is obtained from condition (2.54) in Theorem 2.2.12, by considering that γ is function of φ, that K and P depend on ϑ and φ, and $Y(\vartheta,\varphi) = K(\vartheta,\varphi)P(\vartheta,\varphi)$. ■

Corollary 3.5.1. *Given the known matrices* $X_0^{-1} \in \mathbb{S}^{n_x}_+$ *and* $U(\varphi) \in \mathbb{S}^{n_u}_+$*, let there exist positive scalars* λ_1 *and* λ_2*, matrices* $P(\vartheta,\varphi) \in \mathbb{S}^{n_x}_+$ *and* $Y(\vartheta,\varphi) \in \mathbb{R}^{n_u\times n_x}$*, and a function* $\gamma(\varphi) \in \mathbb{R}_+\backslash\{0\}$ *such that conditions* (3.60)*,* (3.61)*,* (3.63)*,* (3.64) *and* (3.65) *are satisfied* $\forall\left(\vartheta,\dot{\vartheta}\right) \in \Theta\times\Theta_d$*,* $\forall(\varphi,\dot{\varphi}) \in \Phi\times\Phi_d$ *and* $Q^{-1} = \mathrm{I}_{n_w}$*. If the controller gain* (3.4) *is computed as* $K(\vartheta,\varphi) = Y(\vartheta,\varphi)P(\vartheta,\varphi)^{-1}$ *and* $\|w\|_2 \leq 1$*, then the closed-loop response of the time-varying saturated LPV system* (3.1) *is quadratically bounded with the PDQLF* (3.54) *with a shifting* $\mathcal{H}_\infty$ *performance* $\gamma(\varphi)$*. Furthermore, if* $x_0 \in \mathcal{X}_0$*, then* $x_0 \in \mathcal{E}(P(\vartheta,\varphi),1)$ *and the control input* $u(t)$ *is such that* $u(t) \in \mathcal{U}(\varphi(t)) \subset \mathcal{L}(u(t),\sigma(t))$*.*

Proof. It follows from Theorems 3.5.4 and 3.5.5 when $Q^{-1} = \mathrm{I}_{n_w}$, and the stated conditions (3.60) and (3.61) in Theorem 3.5.2. ■

Corollary 3.5.2. *Given the known matrix* $X_0^{-1} \in \mathbb{S}_+^{n_x}$*, let there exist positive scalars* λ_1 *and* λ_2*, matrices* $P(\vartheta,\varphi) \in \mathbb{S}_+^{n_x}$ *and* $Y(\vartheta,\varphi) \in \mathbb{R}^{n_u \times n_x}$*, and a function* $\gamma(\varphi) \in \mathbb{R}_+ \backslash \{0\}$ *such that conditions* (3.60)*,* (3.62)*,* (3.63)*,* (3.64) *and* (3.65) *are satisfied* $\forall \left(\vartheta, \dot{\vartheta}\right) \in \Theta \times \Theta_d$*,* $\forall (\varphi, \dot{\varphi}) \in \Phi \times \Phi_d$ *and* $Q^{-1} = \mathrm{I}_{n_w}$*. If the controller gain* (3.4) *is computed as* $K(\vartheta,\varphi) = Y(\vartheta,\varphi)P(\vartheta,\varphi)^{-1}$ *and* $\|w\|_2 \leq 1$*, then the closed-loop response of the time-varying saturated LPV system* (3.1) *is quadratically bounded with the PDQLF* (3.54) *with a shifting* $\mathcal{H}_\infty$ *performance* $\gamma(\varphi)$*. Furthermore, if* $x_0 \in \mathcal{X}_0$*, then* $x_0 \in \mathcal{E}(P(\vartheta,\varphi), 1)$ *and the control input* $u(t)$ *is such that* $u(t) \in \mathcal{L}(u(t), \sigma(t))$*.*

Proof. It follows from Theorems 3.5.4 and 3.5.5 when $Q^{-1} = \mathrm{I}_{n_w}$, the stated condition (3.60) in Theorem 3.5.2, and condition (3.62) in Theorem 3.5.3. ∎

3.5.1 Finite-dimensional LMI design conditions

The conditions stated in Theorems 3.5.1–3.5.5 and Corollaries 3.5.1–3.5.2 can be converted into a finite number of LMIs by considering the polytopic representation (3.37). However, the consideration of (3.54) entails the explicit presence of $P(\vartheta,\varphi)$ and $\dot{P}(\vartheta,\varphi)$ implying the necessity of establishing a suitable polytopic representation for these terms. To this end, let us assume the following polytopic representation:

$$P(\vartheta,\varphi) = \sum_{i=1}^{n_\mu} \sum_{j=1}^{n_\eta} \mu_i(\vartheta)\eta_j(\varphi)P_{ij}, \quad \mu(\vartheta) \in \Delta^{n_\mu},\ \eta(\varphi) \in \Delta^{n_\eta}, \tag{3.66}$$

where $P_{ij} \in \mathbb{S}_+^{n_x}$ corresponds to decision variables for the pair (i,j).

Then, by differentiating the expression (3.66), we find out that $\dot{P}(\vartheta,\varphi)$ can be expressed as:

$$\dot{P}(\vartheta,\varphi) = \sum_{i=1}^{n_\mu} \sum_{j=1}^{n_\eta} \dot{\mu}_i(\vartheta)\eta_j(\varphi)P_{ij} + \sum_{i=1}^{n_\mu} \sum_{j=1}^{n_\eta} \mu_i(\vartheta)\dot{\eta}_j(\varphi)P_{ij}. \tag{3.67}$$

Note that $\mu(\vartheta) \in \Delta^{n_\mu}$ and $\eta(\varphi) \in \Delta^{n_\eta}$, implying that $\dot{\mu}(\vartheta)$ and $\dot{\eta}(\varphi)$ in (3.67) must fulfil the following conditions:

$$\frac{\mathrm{d}}{\mathrm{d}t}\left(\sum_{i=1}^{n_\mu} \mu_i(\vartheta)\right) = \sum_{i=1}^{n_\mu} \dot{\mu}_i(\vartheta) = 0, \tag{3.68}$$

$$\frac{\mathrm{d}}{\mathrm{d}t}\left(\sum_{j=1}^{n_\eta} \eta_j(\varphi)\right) = \sum_{j=1}^{n_\eta} \dot{\eta}_j(\varphi) = 0, \tag{3.69}$$

thus emphasizing the importance of knowing the time-varying parameters (ϑ,φ) and their rates of variation $\left(\dot{\vartheta},\dot{\varphi}\right)$ in contrast to the conditions stated in Section 3.4. Since it is assumed that $\left(\vartheta,\dot{\vartheta}\right) \in \Theta \times \Theta_d$ and $(\varphi,\dot{\varphi}) \in \Phi \times \Phi_d$, the bounds of each $\dot{\mu}_i(\vartheta)$ and $\dot{\eta}_j(\varphi)$ can be computed analytically from $\mu(\vartheta)$ and $\eta(\varphi)$, respectively. Thus, establishing:

$$\underline{\delta\mu}_i \leq \dot{\mu}_i(\vartheta) \leq \overline{\delta\mu}_i, \quad 0 \in \left[\underline{\delta\mu}_i, \overline{\delta\mu}_i\right], \quad \forall i \in \mathcal{I}_{[1,n_\mu]}, \tag{3.70}$$

$$\underline{\delta\eta}_j \leq \dot{\eta}_j(\varphi) \leq \overline{\delta\eta}_j, \quad 0 \in \left[\underline{\delta\eta}_j, \overline{\delta\eta}_j\right], \quad \forall j \in \mathcal{I}_{[1,n_\eta]}, \tag{3.71}$$

where $\underline{\delta\mu}_i, \underline{\delta\eta}_j \in \mathbb{R}$ and $\overline{\delta\mu}_i, \overline{\delta\eta}_j \in \mathbb{R}$ denote, respectively, the lower and upper bounds.

Then, according to [33, 45, 77, 84], it is possible to compute the convex combination of a finite number of n_α and n_β vectors that satisfies the conditions imposed by (3.68) and (3.69), respectively, $\forall\left(\vartheta,\dot{\vartheta}\right) \in \Theta \times \Theta_d$ and $\forall(\varphi,\dot{\varphi}) \in \Phi \times \Phi_d$:

$$\delta_\mu \triangleq \sum_{m=1}^{n_\alpha} \alpha_m\left(\vartheta,\dot{\vartheta}\right)\mathrm{e}^{\{m\}}, \quad \forall m \in \mathcal{I}_{[1,n_\alpha]}, \quad \alpha\left(\vartheta,\dot{\vartheta}\right) \in \Delta^{n_\alpha}, \tag{3.72}$$

$$\delta_\eta \triangleq \sum_{n=1}^{n_\beta} \beta_n(\varphi,\dot{\varphi})\mathrm{o}^{\{n\}}, \quad \forall n \in \mathcal{I}_{[1,n_\beta]}, \quad \beta(\varphi,\dot{\varphi}) \in \Delta^{n_\beta}, \tag{3.73}$$

being the vectors $\mathrm{e}^{\{m\}} \in \mathcal{P}_{\dot{\mu}} \subset \mathbb{R}^{n_\mu}$ and $\mathrm{o}^{\{n\}} \in \mathcal{P}_{\dot{\eta}} \subset \mathbb{R}^{n_\eta}$ the vertices of the polytopes obtained as the intersections of the hyper-rectangle defined by the constraints (3.70)–(3.71) and the hyperplanes defined in (3.68)–(3.69), respectively. Then, the regions where $\dot{\mu}(\vartheta)$ and $\dot{\eta}(\varphi)$ lie can be described as follows:

$$\mathcal{P}_{\dot{\mu}} \triangleq \left\{\delta_\mu \in \mathbb{R}^{n_\mu} : \delta_\mu = \sum_{m=1}^{n_\alpha} \alpha_m\left(\vartheta,\dot{\vartheta}\right)\mathrm{e}^{\{m\}}, \sum_{i=1}^{n_\mu} \mathrm{e}_i^{\{m\}} = 0, \begin{array}{c}\forall m \in \mathcal{I}_{[1,n_\alpha]} \\ \alpha\left(\vartheta,\dot{\vartheta}\right) \in \Delta^{n_\alpha}\end{array}\right\}, \tag{3.74}$$

$$\mathcal{P}_{\dot{\eta}} \triangleq \left\{\delta_\eta \in \mathbb{R}^{n_\eta} : \delta_\eta = \sum_{n=1}^{n_\beta} \beta_n(\varphi,\dot{\varphi})\mathrm{o}^{\{n\}}, \sum_{j=1}^{n_\eta} \mathrm{o}_j^{\{n\}} = 0, \begin{array}{c}\forall n \in \mathcal{I}_{[1,n_\beta]} \\ \beta(\varphi,\dot{\varphi}) \in \Delta^{n_\beta}\end{array}\right\}, \tag{3.75}$$

where the polytopic weight vectors $\alpha\left(\vartheta,\dot{\vartheta}\right) \in \Delta^{n_\alpha}$ and $\beta(\varphi,\dot{\varphi}) \in \Delta^{n_\beta}$ belong, respectively, to the simplexes:

$$\Delta^{n_\alpha} \triangleq \left\{\alpha\left(\vartheta,\dot{\vartheta}\right) \in \mathbb{R}^{n_\alpha} \ : \ \sum_{m=1}^{n_\alpha} \alpha_m\left(\vartheta,\dot{\vartheta}\right) = 1, \ \alpha_m\left(\vartheta,\dot{\vartheta}\right) \geq 0, \ m \in \mathcal{I}_{[1,n_\alpha]}\right\}. \tag{3.76}$$

$$\Delta^{n_\beta} \triangleq \left\{\beta(\varphi,\dot{\varphi}) \in \mathbb{R}^{n_\beta} \ : \ \sum_{n=1}^{n_\beta} \beta_n(\varphi,\dot{\varphi}) = 1, \ \beta_n(\varphi,\dot{\varphi}) \geq 0, \ n \in \mathcal{I}_{[1,n_\beta]}\right\}. \tag{3.77}$$

Recalling from [2], the set of n_α vectors $\mathrm{v_e} \triangleq \left\{\mathrm{e}^{\{1\}},\ldots,\mathrm{e}^{\{n_\alpha\}}\right\}$ can be systematically constructed by solving the enumeration vertex problem (Problem 3.5.1) through the expression of conditions (3.68) and (3.70) in the form $A_e x \leq b_e$ and $A_\mu x \leq b_\mu$, and the use of the Multi-Parametric Toolbox 3.0 (MPT3) [50]. Similarly, the set of n_β vectors $\mathrm{v_o} \triangleq \left\{\mathrm{o}^{\{1\}},\ldots,\mathrm{o}^{\{n_\beta\}}\right\}$ can be obtained for constraints (3.69) and (3.71).

Problem 3.5.1 (Enumeration vertex problem [10])**.** For given bounds $\underline{\delta\mu}_i, \overline{\delta\mu}_i \in \mathbb{R}$ and $i \in \mathcal{I}_{[1,n_\mu]}$, find the set of n_α vectors $\mathrm{v_e} \in \mathbb{R}^{n_\mu \times n_\alpha}$ such that the constraints $A_\mu x \leq b_\mu$ and $A_e x \leq b_e$ are satisfied together for:

$$x = \begin{bmatrix}\dot{\mu}_1(\vartheta)\\ \vdots \\ \dot{\mu}_{n_\mu}(\vartheta)\end{bmatrix}, \ A_\mu = \mathrm{I}_{n_\mu} \otimes \begin{bmatrix}1\\-1\end{bmatrix}, \ b_\mu = \begin{bmatrix}\overline{\delta\mu}_i\\ -\underline{\delta\mu}_i\\ \vdots \\ \overline{\delta\mu}_{n_\mu}\\ -\underline{\delta\mu}_{n_\mu}\end{bmatrix}, \ A_e = \underbrace{\begin{bmatrix}1 & \cdots & 1\end{bmatrix}}_{n_\mu \text{ times}}, \ b_e = 0. \tag{3.78}$$

□

Then, the following result holds.

Lemma 3.5.6. *Consider a finite number of vectors* $\mathrm{e}^{\{m\}}$ *and* $\mathrm{o}^{\{n\}}$ *for which* (3.74) *and* (3.75) *hold, the polytopic representation* (3.66) *and its time derivative expression* (3.67)*, then it follows for* $i, a \in \mathcal{I}_{[1,n_\mu]}$, $j, b \in \mathcal{I}_{[1,n_\eta]}$, $m \in \mathcal{I}_{[1,n_\alpha]}$ *and* $n \in \mathcal{I}_{[1,n_\beta]}$*:*

$$\begin{aligned}\dot{P}(\vartheta,\varphi) = &\sum_{i=1}^{n_\mu}\sum_{j=1}^{n_\eta}\sum_{m=1}^{n_\alpha}\sum_{n=1}^{n_\beta}\mu_i(\vartheta)\eta_j(\varphi)\alpha_m\big(\vartheta,\dot{\vartheta}\big)\beta_n(\varphi,\dot{\varphi})\\ &\times\left[\sum_{a=1}^{n_\mu}\mathrm{e}_a^{\{m\}}P_{aj}+\sum_{b=1}^{n_\eta}\mathrm{o}_b^{\{n\}}P_{ib}\right],\end{aligned} \tag{3.79}$$

where $\mu(\vartheta) \in \Delta^{n_\mu}$, $\eta(\varphi) \in \Delta^{n_\eta}$, $\alpha\big(\vartheta,\dot{\vartheta}\big) \in \Delta^{n_\alpha}$ *and* $\beta(\varphi,\dot{\varphi}) \in \Delta^{n_\beta}$ *correspond to some polytopic weight vectors.*

Proof. Let us take into account an equivalent expression of (3.67):

$$\dot{P}(\vartheta,\varphi) = \sum_{j=1}^{n_\eta}\eta_j(\varphi)\sum_{a=1}^{n_\mu}\dot{\mu}_a(\vartheta)P_{aj}+\sum_{i=1}^{n_\mu}\mu_i(\vartheta)\sum_{b=1}^{n_\eta}\dot{\eta}_b(\varphi)P_{ib}, \tag{3.80}$$

which can be rewritten taking into account that coefficients $\mu(\vartheta)$ and $\eta(\varphi)$ appearing in (3.80) sum to one, thus obtaining:

$$\dot{P}(\vartheta,\varphi) = \sum_{i=1}^{n_\mu}\sum_{j=1}^{n_\eta}\mu_i(\vartheta)\eta_j(\varphi)\left[\sum_{a=1}^{n_\mu}\dot{\mu}_a(\vartheta)P_{aj}+\sum_{b=1}^{n_\eta}\dot{\eta}_b(\varphi)P_{ib}\right]. \tag{3.81}$$

Thereupon, let us replace $\dot{\mu}(\vartheta)$ and $\dot{\eta}(\varphi)$ in (3.81) by the convex representations given in (3.74) and (3.75), respectively, as follows:

$$\dot{P}(\vartheta,\varphi) = \sum_{i=1}^{n_\mu}\sum_{j=1}^{n_\eta}\mu_i(\vartheta)\eta_j(\varphi)\left[\sum_{a=1}^{n_\mu}\sum_{m=1}^{n_\alpha}\alpha_m\big(\vartheta,\dot{\vartheta}\big)\mathrm{e}_a^{\{m\}}P_{aj}+\sum_{b=1}^{n_\eta}\sum_{n=1}^{n_\beta}\beta_n(\varphi,\dot{\varphi})\mathrm{o}_b^{\{n\}}P_{ib}\right]. \tag{3.82}$$

Since $\alpha\big(\vartheta,\dot{\vartheta}\big) \in \Delta^{n_\alpha}$ and $\beta(\varphi,\dot{\varphi}) \in \Delta^{n_\beta}$, the expression (3.82) is equivalent to the one given in (3.79) thus concluding the proof. ■

Given the above discussion, we can now introduce the following corollaries, which provide a finite number of LMIs that can be used to assess the conditions in Theorems 3.5.1–3.5.5 and Corollaries 3.5.1–3.5.2.

Corollary 3.5.3. *Given a finite number of vectors* $\mathrm{e}^{\{m\}}$ *and* $\mathrm{o}^{\{n\}}$ *for which* (3.74) *and* (3.75) *hold, the desired guaranteed shifting decay rate vertices* $\mathrm{d}_{\mathrm{R}j} \in \mathbb{R}_+$ *and some previously chosen relaxation degrees* $d_1, d_2 \in \mathbb{N}$ *with* $d_1, d_2 \geq 2$*, let there exist matrices* $P_{ij} \in \mathbb{S}_+^{n_x}$ *and* $Y_{ij} \in \mathbb{R}^{n_u \times n_x}$ *with*

$i \in \mathcal{I}_{[1,n_\mu]}$ and $j \in \mathcal{I}_{[1,n_\eta]}$ such that the following set of LMIs is satisfied $\forall m \in \mathcal{I}_{[1,n_\alpha]}$ and $\forall n \in \mathcal{I}_{[1,n_\beta]}$:

$$\sum_{\boldsymbol{q}\in\mathcal{P}(\boldsymbol{j})}\sum_{\boldsymbol{p}\in\mathcal{P}(\boldsymbol{i})}\Big[\mathrm{He}\{A_{p_1}P_{p_2q_1}+B_{p_1}Y_{p_2q_1}\}+2\,\mathrm{d}_{\mathrm{R}q_1}P_{p_1q_2}-\dot{\Upsilon}^{\{m,n\}}_{p_1q_1}\Big]\prec 0, \tag{3.83}$$

where multi-indexes $\boldsymbol{i}$ and $\boldsymbol{j}$ are associated to the sets $\mathbb{I}^{+}_{(d_1,n_\mu)}$ and $\mathbb{I}^{+}_{(d_2,n_\eta)}$, respectively, and

$$\dot{\Upsilon}^{\{m,n\}}_{p_1q_1}\triangleq\sum_{a=1}^{n_\mu}\mathrm{e}_a^{\{m\}}P_{aq_1}+\sum_{b=1}^{n_\eta}\mathrm{o}_b^{\{n\}}P_{p_1b}. \tag{3.84}$$

Then, Theorem 3.5.1 holds for all parameter-dependent terms appearing in (3.37), (3.66) and (3.79).

Proof. The proof omits, for clarity's sake, the dependence of the polytopic weight vectors on ϑ, $\dot{\vartheta}$, φ and $\dot{\varphi}$. Then, let us consider the fact that $(\mu,\eta)\in\Delta^{n_\mu}\times\Delta^{n_\eta}$, so that the parameter-dependent LMI (3.56) is expressed through the polytopic representations (3.37) and (3.66), as follows:

$$\sum_{i_1=1}^{n_\mu}\sum_{i_2=1}^{n_\mu}\mu_{i_1}\mu_{i_2}[\mathrm{He}\{A_{i_1}P_{i_2}(\varphi)+B_{i_1}Y_{i_2}(\varphi)\}+2\mathrm{d}_{\mathrm{R}}(\varphi)P_{i_1}(\varphi)]-\dot{P}(\vartheta,\varphi)\prec 0, \tag{3.85}$$

which is equivalent to:

$$\sum_{i_1=1}^{n_\mu}\sum_{i_2=1}^{n_\mu}\sum_{j_1=1}^{n_\eta}\sum_{j_2=1}^{n_\eta}\mu_{i_1}\mu_{i_2}\eta_{j_1}\eta_{j_2}\Big[\mathrm{He}\{A_{i_1}P_{i_2j_1}+B_{i_1}Y_{i_2j_1}\}+2\mathrm{d}_{\mathrm{R}j_1}P_{i_1j_2}\Big]-\dot{P}(\vartheta,\varphi)\prec 0. \tag{3.86}$$

Right after, let us replace $\dot{P}(\vartheta,\varphi)$ with the expression given in (3.79), thus obtaining:

$$\begin{aligned}&\sum_{i_1=1}^{n_\mu}\sum_{i_2=1}^{n_\mu}\sum_{j_1=1}^{n_\eta}\sum_{j_2=1}^{n_\eta}\mu_{i_1}\mu_{i_2}\eta_{j_1}\eta_{j_2}\Big[\mathrm{He}\{A_{i_1}P_{i_2j_1}+B_{i_1}Y_{i_2j_1}\}+2\mathrm{d}_{\mathrm{R}j_1}P_{i_1j_2}\Big]\\&-\sum_{i_1=1}^{n_\mu}\sum_{j_1=1}^{n_\eta}\sum_{m=1}^{n_\alpha}\sum_{n=1}^{n_\beta}\mu_{i_1}\eta_{j_1}\alpha_m\beta_n\Big[\sum_{a=1}^{n_\mu}\mathrm{e}_a^{\{m\}}P_{aj_1}+\sum_{b=1}^{n_\eta}\mathrm{o}_b^{\{n\}}P_{i_1b}\Big]\prec 0,\end{aligned} \tag{3.87}$$

Since $(\alpha,\beta)\in\Delta^{n_\alpha}\times\Delta^{n_\beta}$, condition (3.87) can be expressed as:

$$\begin{aligned}&\sum_{i_1=1}^{n_\mu}\sum_{i_2=1}^{n_\mu}\sum_{j_1=1}^{n_\eta}\sum_{j_2=1}^{n_\eta}\sum_{m=1}^{n_\alpha}\sum_{n=1}^{n_\beta}\mu_{i_1}\mu_{i_2}\eta_{j_1}\eta_{j_2}\alpha_m\beta_n\\&\times\Big[\mathrm{He}\{A_{i_1}P_{i_2j_1}+B_{i_1}Y_{i_2j_1}\}+2\mathrm{d}_{\mathrm{R}j_1}P_{i_1j_2}-\Big(\sum_{a=1}^{n_\mu}\mathrm{e}_a^{\{m\}}P_{aj_1}+\sum_{b=1}^{n_\eta}\mathrm{o}_b^{\{n\}}P_{i_1b}\Big)\Big]\prec 0.\end{aligned} \tag{3.88}$$

By means of the multi-index notation presented in Section 2.2.5, (3.88) is rewritten as:

$$\sum_{m=1}^{n_\alpha}\sum_{n=1}^{n_\beta}\alpha_m\beta_n\Big[\sum_{\boldsymbol{i}\in\mathbb{I}_{(2,n_\mu)}}\sum_{\boldsymbol{j}\in\mathbb{I}_{(2,n_\eta)}}\mu_{\boldsymbol{i}}\eta_{\boldsymbol{j}}\Big(\Upsilon_{\boldsymbol{ij}}-\dot{\Upsilon}^{\{m,n\}}_{\boldsymbol{ij}}\Big)\Big]\prec 0, \tag{3.89}$$

where:

$$\Upsilon_{\boldsymbol{ij}} \triangleq \mathrm{He}\{A_{i_1} P_{i_2 j_1} + B_{i_1} Y_{i_2 j_1}\} + 2\mathrm{d}_{\mathrm{R}j_1} P_{i_1 j_2},$$
$$\dot{\Upsilon}_{\boldsymbol{ij}}^{\{m,n\}} \triangleq \sum_{a=1}^{n_\mu} \mathrm{e}_a^{\{m\}} P_{a j_1} + \sum_{b=1}^{n_\eta} \mathrm{o}_b^{\{n\}} P_{i_1 b}.$$

By applying Lemma 2.2.14 on the definiteness of (3.89), the set of LMI in (3.83) is obtained, thus concluding the proof. ■

Remark 3.5.1. Note that possible codependence between the coefficients $\mu_i(\vartheta)$ and $\alpha_m(\vartheta, \dot{\vartheta})$ has been neglected. The same applies to the codependence between $\eta_j(\varphi)$ and $\beta_n(\varphi, \dot{\varphi})$. Albeit introducing some conservativeness, this assumption has enabled the application of Lemma 2.2.14, so that the computational complexity during the design stage has been reduced.

Remark 3.5.2. According to [82], the fact of considering arbitrarily large values for the bounds (3.70) and (3.71) in Corollary 3.5.3 implies that the only possible solution for solving the condition (3.83) is to choose $P_{11} \approx \ldots \approx P_{n_\mu n_\eta}$, thus making the term in (3.84) equal to zero. In this case, the QLF $V(x) = x^T P^{-1} x$ can be recovered by considering $P > 0$ as the common decision variable for all the pairs (i, j) in (3.66).

Corollary 3.5.4. *Given a finite number of vectors* $\mathrm{e}^{\{m\}}$ *and* $\mathrm{o}^{\{n\}}$ *for which* (3.74) *and* (3.75) *hold, the known matrix* $X_0^{-1} \in \mathbb{S}_+^{n_x}$*, the known vertex matrices* $U_j \in \mathbb{S}_+^{n_u}$*, the desired guaranteed shifting decay rate vertices* $\mathrm{d}_{\mathrm{R}j} \in \mathbb{R}_+$ *and some previously chosen relaxation degrees* $d_1, d_2 \in \mathbb{N}$ *with* $d_1, d_2 \geq 2$*, let there exist matrices* $P_{ij} \in \mathbb{S}_+^{n_x}$ *and* $Y_{ij} \in \mathbb{R}^{n_u \times n_x}$ *with* $i \in \mathcal{I}_{[1,n_\mu]}$ *and* $j \in \mathcal{I}_{[1,n_\eta]}$ *such that condition* (3.83) *is satisfied* $\forall m \in \mathcal{I}_{[1,n_\alpha]}$ *and* $\forall n \in \mathcal{I}_{[1,n_\beta]}$ *together with:*

$$\begin{bmatrix} P_{ij} & \mathrm{I}_{n_x} \\ \star & X_0^{-1} \end{bmatrix} \geq 0, \tag{3.90}$$

$$\begin{bmatrix} U_j & Y_{ij} \\ \star & P_{ij} \end{bmatrix} \geq 0. \tag{3.91}$$

Then, Theorem 3.5.2 holds for all parameter-dependent terms appearing in (3.37), (3.66) *and* (3.79).

Proof. Similar to that of Corollary 3.4.9a, thus omitted. ■

Corollary 3.5.5. *Given a finite number of vectors* $\mathrm{e}^{\{m\}}$ *and* $\mathrm{o}^{\{n\}}$ *for which* (3.74) *and* (3.75) *hold, the known matrix* $X_0^{-1} \in \mathbb{S}_+^{n_x}$*, the desired guaranteed shifting decay rate vertices* $\mathrm{d}_{\mathrm{R}j} \in \mathbb{R}_+$ *and some previously chosen relaxation degrees* $d_1, d_2 \in \mathbb{N}$ *with* $d_1, d_2 \geq 2$*, let there exist matrices* $P_{ij} \in \mathbb{S}_+^{n_x}$ *and* $Y_{ij} \in \mathbb{R}^{n_u \times n_x}$ *with* $i \in \mathcal{I}_{[1,n_\mu]}$ *and* $j \in \mathcal{I}_{[1,n_\eta]}$ *such that conditions* (3.83) *and* (3.90) *are satisfied* $\forall m \in \mathcal{I}_{[1,n_\alpha]}$ *and* $\forall n \in \mathcal{I}_{[1,n_\beta]}$ *together with:*

$$\begin{bmatrix} \hat{\sigma}_{l,j} & Y_{[l],ij} \\ \star & P_{ij} \end{bmatrix} \geq 0, \quad \forall l \in \mathcal{I}_{[1,n_u]}. \tag{3.92}$$

Then, Theorem 3.5.3 holds for all parameter-dependent terms appearing in (3.37), (3.66) *and* (3.79).

Proof. Similar to that of Corollary 3.4.9b, thus omitted. ■

Corollary 3.5.6. *For fixed positive scalars $\lambda_1 \geq \lambda_2$, a given finite number of vectors $\mathrm{e}^{\{m\}}$ and $\mathrm{o}^{\{n\}}$ for which (3.74) and (3.75) hold, the known matrix $Q^{-1} \in \mathbb{S}_+^{n_w}$ and a previously chosen relaxation degree $d \in \mathbb{N}$ with $d \geq 2$, let there exist $P_{ij} \in \mathbb{S}_+^{n_x}$ and $Y_{ij} \in \mathbb{R}^{n_u \times n_x}$ with $i \in \mathcal{I}_{[1,n_\mu]}$ and $j \in \mathcal{I}_{[1,n_\eta]}$ such that the following set of LMIs is satisfied $\forall m \in \mathcal{I}_{[1,n_\alpha]}$ and $\forall n \in \mathcal{I}_{[1,n_\beta]}$:*

$$\sum_{\boldsymbol{p} \in \mathcal{P}(\boldsymbol{i})} \begin{bmatrix} \mathrm{He}\{A_{p_1} P_{p_2 j} + B_{p_1} Y_{p_2 j}\} + \lambda_1 P_{p_1 j} - \dot{\Upsilon}_{p_1 j}^{\{m,n\}} & B_{w,p_1} \\ \star & -\lambda_2 Q^{-1} \end{bmatrix} \preceq 0, \ \forall \boldsymbol{i} \in \mathbb{I}_{(d,n_\mu)}^{+}, \quad (3.93)$$

where $\dot{\Upsilon}_{p_1 j}^{\{m,n\}}$ is defined as in (3.84). Then, Theorem 3.5.4 holds for all parameter-dependent terms appearing in (3.37), (3.66) and (3.79).

Proof. Similar to that of Corollary 3.5.3, thus omitted. ∎

Corollary 3.5.7. *Given a finite number of vectors $\mathrm{e}^{\{m\}}$ and $\mathrm{o}^{\{n\}}$ for which (3.74) and (3.75) hold and a previously chosen relaxation degree $d \in \mathbb{N}$ with $d \geq 2$, let there exist $P_{ij} \in \mathbb{S}_+^{n_x}$, $Y_{ij} \in \mathbb{R}^{n_u \times n_x}$ and vertex terms $\gamma_j > 0$ with $i \in \mathcal{I}_{[1,n_\mu]}$ and $j \in \mathcal{I}_{[1,n_\eta]}$ such that the following set of LMIs is satisfied $\forall m \in \mathcal{I}_{[1,n_\alpha]}$ and $\forall n \in \mathcal{I}_{[1,n_\beta]}$:*

$$\sum_{\boldsymbol{p} \in \mathcal{P}(\boldsymbol{i})} \begin{bmatrix} \mathrm{He}\{A_{p_1} P_{p_2 j} + B_{p_1} Y_{p_2 j}\} - \dot{\Upsilon}_{p_1 j}^{\{m,n\}} & B_{w,p_1} & P_{p_1 j} C_{z,p_2}^{\mathsf{T}} + Y_{p_1 j}^{\mathsf{T}} D_{zu,p_2}^{\mathsf{T}} \\ \star & -\gamma_j \mathrm{I}_{n_w} & D_{zw,p_1}^{\mathsf{T}} \\ \star & \star & -\gamma_j \mathrm{I}_{n_{z_\infty}} \end{bmatrix} \prec 0, \quad (3.94)$$

where multi-index $\boldsymbol{i}$ is associated to the set $\mathbb{I}_{(d_1,n_\mu)}^{+}$ and $\dot{\Upsilon}_{p_1 j}^{\{m,n\}}$ is defined as in (3.84). Then, Theorem 3.5.5 holds for all parameter-dependent terms appearing in (3.37), (3.66) and (3.79).

Proof. Similar to that of Corollary 3.5.3, thus omitted. ∎

Corollary 3.5.8. *For fixed positive scalars $\lambda_1 \geq \lambda_2$, a given finite number of vectors $\mathrm{e}^{\{m\}}$ and $\mathrm{o}^{\{n\}}$ for which (3.74) and (3.75) hold, the known matrix $X_0^{-1} \in \mathbb{S}_+^{n_x}$, the known vertex matrices $U_j \in \mathbb{S}_+^{n_u}$ and a previously chosen relaxation degree $d \in \mathbb{N}$ with $d \geq 2$, let there exist $P_{ij} \in \mathbb{S}_+^{n_x}$, $Y_{ij} \in \mathbb{R}^{n_u \times n_x}$ and vertex terms $\gamma_j > 0$ with $i \in \mathcal{I}_{[1,n_\mu]}$ and $j \in \mathcal{I}_{[1,n_\eta]}$ such that conditions (3.90), (3.91), (3.93) and (3.94) are satisfied $\forall m \in \mathcal{I}_{[1,n_\alpha]}$, $\forall n \in \mathcal{I}_{[1,n_\beta]}$ and $Q^{-1} = \mathrm{I}_{n_w}$. Then, Corollary 3.5.1 holds for all parameter-dependent terms appearing in (3.37), (3.66) and (3.79).*

Proof. It is a direct consequence of Corollaries 3.5.6 and 3.5.7 when $Q^{-1} = \mathrm{I}_{n_w}$, and the stated conditions (3.90) and (3.91) in Corollary 3.5.4. ∎

Corollary 3.5.9. *For fixed positive scalars $\lambda_1 \geq \lambda_2$, a given finite number of vectors $\mathrm{e}^{\{m\}}$ and $\mathrm{o}^{\{n\}}$ for which (3.74) and (3.75) hold, the known matrix $X_0^{-1} \in \mathbb{S}_+^{n_x}$ and a previously chosen relaxation degree $d \in \mathbb{N}$ with $d \geq 2$, let there exist $P_{ij} \in \mathbb{S}_+^{n_x}$, $Y_{ij} \in \mathbb{R}^{n_u \times n_x}$ and vertex terms $\gamma_j > 0$ with $i \in \mathcal{I}_{[1,n_\mu]}$ and $j \in \mathcal{I}_{[1,n_\eta]}$ such that conditions (3.90), (3.92), (3.93) and (3.94) are satisfied $\forall m \in \mathcal{I}_{[1,n_\alpha]}$, $\forall n \in \mathcal{I}_{[1,n_\beta]}$ and $Q^{-1} = \mathrm{I}_{n_w}$. Then, Corollary 3.5.2 holds for all parameter-dependent terms appearing in (3.37), (3.66) and (3.79).*

Proof. It is a direct consequence of Corollaries 3.5.6 and 3.5.7 when $Q^{-1} = \mathrm{I}_{n_w}$, the stated condition (3.90) in Corollary 3.5.4, and condition (3.92) in Corollary 3.5.5. ∎

3.6 Selection of desired shifting specification values

The design conditions presented in Sections 3.4 and 3.5 can be formulated as an LMI-based optimization procedure to cope with the selection of the desired GSDR vertex values $\mathrm{d}_{\mathrm{R}j} \in \mathbb{R}_+$ and the vertex decision variables $\gamma_j > 0$ for $j \in \mathcal{I}_{[1,n_\eta]}$. Due to the fact that parameter-dependent terms $\mathrm{d}_{\mathrm{R}}(\varphi)$ and $\gamma(\varphi)$ play a key role in complying with the shifting performance conditions (3.5) and (3.6), respectively, let us recall from (3.37b) their polytopic representation to make the understanding of the vertex value selection easier:

$$\begin{bmatrix}\mathrm{d}_{\mathrm{R}}(\varphi) & \gamma(\varphi)\end{bmatrix} = \sum_{j=1}^{n_\eta} \eta_j(\varphi)\begin{bmatrix}\mathrm{d}_{\mathrm{R}j} & \gamma_j\end{bmatrix}, \quad \eta(\varphi) \in \Delta^{n_\eta}. \tag{3.95}$$

In order to establish a systematic approach to the determination of each expression of $\eta_j(\varphi)$ in (3.95), it is assumed that the performance scheduling vector $\varphi(t)$ belongs to the hypercube:

$$\Phi \triangleq \left\{\varphi \in \mathbb{R}^{n_\varphi} \ : \ \varphi_h \in [0,1], \ h \in \mathcal{I}_{[1,n_\varphi]}\right\}, \tag{3.96}$$

thus allowing the definition of $\eta_j(\varphi)$ for $j \in \mathcal{I}_{[1,n_\eta]}$ and $n_\eta = 2^{n_\varphi}$ as follows:

$$\eta_j(\varphi) = \prod_{h=1}^{n_\varphi} \xi_{jh}(\varphi_h), \tag{3.97}$$

where $\xi_{jh}(\varphi_h)$ represents each potential term of $\eta_j(\varphi)$ to be selected:

$$\xi_{jh}(\varphi_h) = \begin{cases} 1-\varphi_h & \text{if } (j \bmod 2^h) \in \mathcal{I}_{[1,2^{h-1}]} \\ \varphi_h & \text{otherwise} \end{cases}. \tag{3.98}$$

For instance, for $n_\varphi = 2$, the expressions of $\eta_j(\varphi)$ with $j \in \mathcal{I}_{[1,4]}$ are:

$$\begin{aligned}
\eta_1(\varphi) &= \xi_{11}(\varphi_1)\xi_{12}(\varphi_2) = (1-\varphi_1)(1-\varphi_2),\\
\eta_2(\varphi) &= \xi_{21}(\varphi_1)\xi_{22}(\varphi_2) = \varphi_1(1-\varphi_2),\\
\eta_3(\varphi) &= \xi_{31}(\varphi_1)\xi_{32}(\varphi_2) = (1-\varphi_1)\varphi_2,\\
\eta_4(\varphi) &= \xi_{41}(\varphi_1)\xi_{42}(\varphi_2) = \varphi_1\varphi_2.
\end{aligned}$$

The desired GSDR vertex values $\mathrm{d}_{\mathrm{R}j}$ in (3.37b) are defined for $j \in \mathcal{I}_{[1,n_\eta]}$ with the objective of getting the maximum feasible value of $\mathrm{d}_{\mathrm{R}}(\varphi)$ when the largest possible control action is available which involves that the instantaneous saturation limit $\sigma_l(t) \to \bar{\sigma}_l \ \forall l \in \mathcal{I}_{[1,n_u]}$, as follows:

$$\mathrm{d}_{\mathrm{R}j} \triangleq \frac{\bar{\mathrm{d}}_{\mathrm{R}}\mathcal{C}_j + \underline{\mathrm{d}}_{\mathrm{R}}(n_\varphi - \mathcal{C}_j)}{n_\varphi}, \tag{3.99}$$

where $\underline{\mathrm{d}}_{\mathrm{R}} \in \mathbb{R}_+$ and $\bar{\mathrm{d}}_{\mathrm{R}} \in \mathbb{R}_+$ are the given lower and upper limit values of $\mathrm{d}_{\mathrm{R}}(\varphi)$, respectively. $\mathcal{C}_j \triangleq \mathrm{card}\left(\left\{h \in \mathcal{I}_{[1,n_\varphi]} : (j \bmod 2^h) \in \mathcal{I}_{[1,2^{h-1}]}\right\}\right)$ stands for the number of times that condition $\xi_{jh}(\varphi_h) = 1-\varphi_h$ in (3.98) is satisfied. Thus, Corollary 3.4.4a-3.4.4b and Corollar-

ies 3.4.9a–3.4.9b can be cast to the following LMI-based optimization procedure for a fixed value of $\underline{\mathrm{d}}_{\mathrm{R}}$ and a given set of possible values $\mathcal{S}_{\mathrm{d}_{\mathrm{R}}} \subset \mathbb{R}_+$:

$$\mathcal{O}_1 : \begin{cases} \max\limits_{\bar{\mathrm{d}}_{\mathrm{R}} \in \mathcal{S}_{\mathrm{d}_{\mathrm{R}}}} & \bar{\mathrm{d}}_{\mathrm{R}} \\ \text{subject to} & \text{conditions (3.26) or (3.53), (3.40) or (3.48),} \\ & \text{and (3.44) or (3.45)} \end{cases} \tag{3.100}$$

Similarly, Corollaries 3.5.4–3.5.5 can be formulated as follows:

$$\mathcal{O}_2 : \begin{cases} \max\limits_{\bar{\mathrm{d}}_{\mathrm{R}} \in \mathcal{S}_{\mathrm{d}_{\mathrm{R}}}} & \bar{\mathrm{d}}_{\mathrm{R}} \\ \text{subject to} & \text{conditions (3.83), (3.90) and (3.91) or (3.92)} \end{cases} \tag{3.101}$$

Remark 3.6.1. Note that if $\bar{\mathrm{d}}_{\mathrm{R}}$ is considered as a decision variable in (3.99), then conditions (3.40), (3.48) and (3.83) become BMIs. In order to avoid this, the optimization problems (3.100) and (3.101) can be solved by using the bisection algorithm [2].

Let us define each value of γ_j in (3.37b) in order to acquire the highest performance in sense of disturbance rejection when $\sigma_l(t) \to \bar{\sigma}_l \ \forall l \in \mathcal{I}_{[1,n_u]}$, as follows:

$$\gamma_j \triangleq \frac{\underline{\gamma}\mathcal{C}_j + \bar{\gamma}(n_\varphi - \mathcal{C}_j)}{n_\varphi}, \quad j \in \mathcal{I}_{[1,n_\eta]} \tag{3.102}$$

where $\underline{\gamma} > 0$ and $\bar{\gamma} > 0$ are two decision variables that represent the lower and upper limits of $\gamma(\varphi)$, respectively. As a result, Corollaries 3.4.7a–3.4.7b and Corollaries 3.4.12a–3.4.12b are expressed for given positive scalars $\lambda_1 \geq \lambda_2$ as follows [3]:

$$\mathcal{O}_3 : \begin{cases} \min\limits_{\underline{\gamma}>0,\, \bar{\gamma}>0} & \dfrac{\underline{\gamma} + \bar{\gamma}}{2} \\ \text{subject to} & \text{conditions (3.26) or (3.53), (3.44) or (3.45),} \\ & \text{(3.46) and (3.47) or (3.51) and (3.52)} \end{cases} \tag{3.103}$$

In the same way, we can extend Corollaries 3.5.8–3.5.9 to:

$$\mathcal{O}_4 : \begin{cases} \min\limits_{\underline{\gamma}>0,\, \bar{\gamma}>0} & \dfrac{\underline{\gamma} + \bar{\gamma}}{2} \\ \text{subject to} & \text{conditions (3.90), (3.91) or (3.92), (3.93) and (3.94)} \end{cases} \tag{3.104}$$

[2] https://en.wikipedia.org/wiki/Bisection_method

[3] Note that the objective function is similar to the one proposed in [65].

3.7 Illustrative examples

This section looks at five illustrative examples to assess the LMI-based methodology developed in this chapter. The content is organized as follows: First, Section 3.7.1 illustrates the trade-off between the choice of the desired GSDR values and the feasibility of the problem, as well as the flexibility of the approach. In Section 3.7.2, a performance evaluation is given between the use of a QLF and a PDQLF for the GSDR specification (3.5). In Sections 3.7.3 and 3.7.4, academic examples are given to demonstrate the effectiveness of the designed controllers under the GSDR specification (3.5) and the shifting $\mathcal{H}_\infty$ performance (3.6), respectively. Finally, an example based on the attitude control of a quadrotor is given in Section 3.7.5.

3.7.1 Illustrative example 1: GSDR vertex selection

Consider the following simple system (balancing pointer) which is affected by a time-varying saturation as (3.2) with $\sigma(t) \in [5, 10]$:

$$\dot{x} = \begin{bmatrix} 0 & 1 \\ 1 & 0 \end{bmatrix} x + \begin{bmatrix} 0 \\ -1 \end{bmatrix} \mathrm{sat}(u, \sigma(t))$$

Note that this system is open-loop unstable since the eigenvalues of the state matrix are 1 and -1.

For illustrative purposes, consider that $n_\eta = 2$ and the vertex matrices appearing in (3.37a) for matrices $A(\vartheta)$, $B(\vartheta)$ and $B_w(\vartheta)$ are: $A_1 = A_2 = A$, $B_1 = B_2 = B$ and $B_{w,1} = B_{w,2} = 0$, respectively. Let us establish the region of expected initial conditions (2.72), as follows:

$$\mathcal{X}_0 = \left\{ x \in \mathbb{R}^2 \,:\, x^\top \left(\mathrm{r_o}^{-2} \, \mathrm{I}_2 \right) x \leq 1, \; \mathrm{r_o} > 0 \right\}.$$

By solving the optimization procedure (3.100) subject to constraints (3.26), (3.40), (3.45) and $\mathrm{r_o} \in \{0.25, 0.5, 0.75, 1, 1.25, 1.5\}$, one gets the feasible GSDR vertex values in Fig. 3.2. It should be noted that the problem's feasibility is conditioned by an obvious trade-off between the size of region $\mathcal{X}_0$ and the pair of feasible values $(\mathrm{d_{R1}}, \mathrm{d_{R2}})$. Nonetheless, shifting GSDR performance (3.5) demonstrates design flexibility. For instance, if $\mathrm{r_o} = 0.25$ and the pair of values $(\mathrm{d_{R1}}, \mathrm{d_{R2}}) = (3.896, 0)$ are chosen as design specifications, then the designed controller will guarantee the fastest closed-loop convergence speed when $\sigma(t) \to \bar{\sigma}$ whereas the most conservative response is provided when $\sigma(t)$ is closer to $\underline{\sigma}$. On the other hand, if $(\mathrm{d_{R1}}, \mathrm{d_{R2}}) = (3, 1)$, then the designed controller will provide a less aggressive speed convergence at the cost of increasing the speed when $\sigma(t) \to \underline{\sigma}$. Finally, a constant decay rate is recovered when $\mathrm{d_{R1}} = \mathrm{d_{R2}}$.

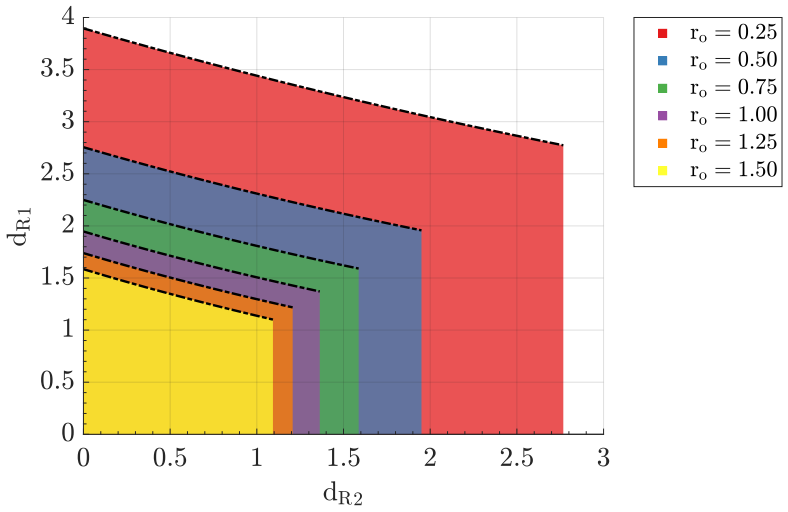

Figure 3.2: Illustration of feasible GSDR vertex values.

3.7.2 Illustrative example 2: feasible GSDR comparison

Consider an open-loop unstable LPV system modelled as in (3.1a), $\vartheta \in [0, 1]$, $B_w(\vartheta) = 0$ and the following state-space matrices:

$$A(\vartheta) = \begin{bmatrix} 4.25 + 3.5\vartheta & 3.8971 \\ 3.8971 & 8.75 - 5.5\vartheta \end{bmatrix} \quad B = \begin{bmatrix} 1 & 0 \\ 0 & 0.5 \end{bmatrix},$$

where matrices $A(\vartheta)$ and B can be written in polytopic form by means of (3.37a), assuming that B has the same value for all the $n_\mu = 2$ vertices:

$$A_1 = \begin{bmatrix} 4.25 & 3.8971 \\ 3.8971 & 8.75 \end{bmatrix}, \quad A_2 = \begin{bmatrix} 7.75 & 3.8971 \\ 3.8971 & 3.25 \end{bmatrix}.$$

Let us define the time-varying saturation for the inputs $u_1(t)$ and $u_2(t)$ as follows:

$$\mathrm{sat}(u_l(t), \sigma_l(t)) \triangleq \mathrm{sign}(u_l(t)) \min(|u_l(t)|, \sigma_l(t)), \quad l = 1, 2,$$

where $\sigma_1(t)$ varies within the interval $[5, \bar{\sigma}_1]$ and, with the purpose of reducing the complexity of the example, $\sigma_2(t) = \sigma_2 = 5$. Thereupon, let us introduce the scheduling parameter $\varphi(t)$, which is linked to $\sigma_1(t)$ as follows:

$$\varphi(t) = \frac{\bar{\sigma}_1^2 - \sigma_1(t)^2}{\bar{\sigma}_1^2 - 25},$$

so that $\varphi(t) \in [0, 1]$. Moreover, note that the above formulation allows us expressing $\sigma_1(t)^2$ as a function of $\varphi(t)$:

$$\sigma_1(\varphi(t))^2 = \bar{\sigma}_1^2 + \varphi(t)(25 - \bar{\sigma}_1^2).$$

Then, the axis magnitudes of the ellipsoidal region $\mathcal{U}(\varphi)$ (3.9) are described by the matrix function $U(\varphi)$ as follows:

$$U(\varphi) = \operatorname{diag}\{\sigma_1(\varphi)^2, 25\}$$

and the corresponding vertex matrices are:

$$U_1 = \begin{bmatrix} \bar{\sigma}_1^2 & 0 \\ 0 & 25 \end{bmatrix}, \quad U_2 = \begin{bmatrix} 25 & 0 \\ 0 & 25 \end{bmatrix}.$$

Let us establish the following set of conditions with the purpose of evaluating the advantage of using the PDQLF (3.54) instead of a QLF. To this end, $\bar{\sigma}_1 \in \mathcal{S}_{\sigma_1}$ and the maximum desired decay rate value $\bar{\mathrm{d}}_{\mathrm{R}} \in \mathcal{S}_{\mathrm{d_R}}$ are generated as follows:

$$\mathcal{S}_{\sigma_1} \triangleq \{\bar{\sigma}_1 \in \mathbb{R}_+ : 5 < \bar{\sigma}_1 \leq 105\}, \quad \mathcal{S}_{\mathrm{d_R}} \triangleq \{\bar{\mathrm{d}}_{\mathrm{R}} \in \mathbb{R}_+ : 0 \leq \bar{\mathrm{d}}_{\mathrm{R}} \leq 100\}.$$

Furthermore, the desired vertex values of $\mathrm{d_R}(\varphi)$ in (3.95) are fixed to:

$$\mathrm{d_{R1}} = \bar{\mathrm{d}}_{\mathrm{R}}, \ \mathrm{d_{R2}} = 0,$$

where $\mathrm{d_{R1}}$ will be evaluated for each combination of the selected values of $\bar{\sigma}_1$ and $\bar{\mathrm{d}}_{\mathrm{R}}$.

Table 3.2 shows the specifications for the different established scenarios. Scenario **A** corresponds to use the QLF defined in (3.17), whereas Scenarios **B**-**D** correspond to use the PDQLF defined in (3.54) and the polytopic representations (3.66) and (3.79).

Table 3.2: Experiment specifications for the feasible GSDR comparison example. (Relaxation degrees d_1, d_2; X_0^{-1} magnitudes of (2.72); $\langle \dot{\mu}_i \rangle$, $\langle \dot{\eta}_j \rangle$ time-derivative polytopic weights limits (3.70) and (3.71)), for $i, j = 1, 2$

Scenario	d_1	d_2	X_0^{-1}	$\langle \dot{\mu}_i \rangle$	$\langle \dot{\eta}_j \rangle$
A	2	-	$\operatorname{diag}\{100, 100\}$	-	-
B	2	2	$\operatorname{diag}\{100, 100\}$	[-1, 1]	[-1, 1]
C	2	2	$\operatorname{diag}\{100, 100\}$	[-1, 1]	[-5, 5]
D	2	2	$\operatorname{diag}\{100, 100\}$	[-1, 1]	[-10, 10]

Finally, Corollary 3.5.4 is evaluated for each element of $\bar{\sigma}_1$ and $\bar{\mathrm{d}}_{\mathrm{R}}$ under the different scenarios described in Table 3.2 and the use of the optimization procedure $\mathcal{O}_2$ in (3.101). To this end, the SeDuMi solver [117] and the YALMIP toolbox [70] were used. Additionally, the Multi-Parametric Toolbox 3.0 [50] was employed to obtain a finite number of vectors in (3.72) and (3.73) by the vertex enumeration problem (Problem 3.5.1). Fig. 3.3 shows, for each fixed value of $\bar{\sigma}_1$, the maximum value obtained for $\bar{\mathrm{d}}_{\mathrm{R}}$ so that the set of LMIs described in Corollary 3.5.4 is feasible. The benefits of using a PDQLF instead of using a QLF can be observed, in that a larger feasible guaranteed decay rate is obtained when a larger range of variation of $\sigma_1(t)$ is considered. However, note that for small variations of $\sigma_1(t)$, the maximum feasible values of $\bar{\mathrm{d}}_{\mathrm{R}}$ are practically the same

for both cases. Furthermore, note that for big values of $\bar{\sigma}_1$, the proposed PDQLF approach tends to perform similarly to the QLF approach when considering large constraints on $\dot{\eta}_j(\varphi)$.

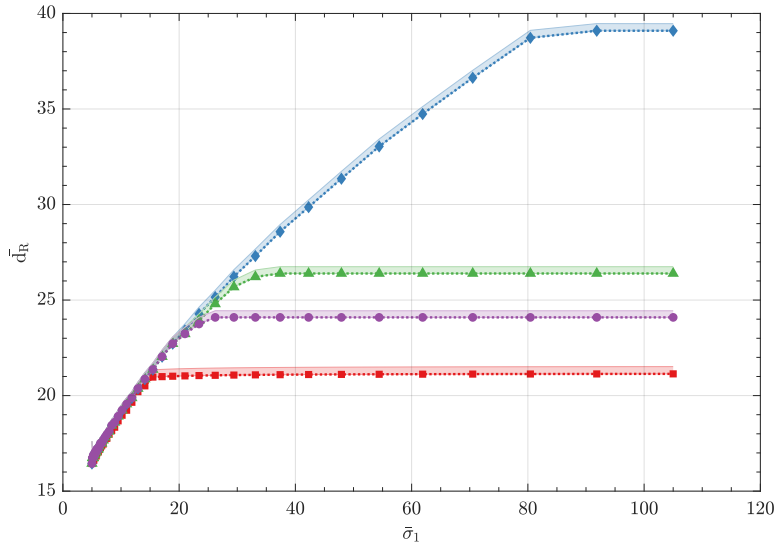

Figure 3.3: Results of applying Corollary 3.5.4 in the feasible GSDR comparison example. (The following symbols denote the selected scenarios: ··· ■ ··· **A**; ··· ♦ ··· **B**; ··· ▲ ··· **C**; and ··· ● ··· **D**.)

3.7.3 Illustrative example 3: GSDR performance

Consider a saturated LPV system (3.1a) that has two inputs with time-varying saturation limits as follows:

$$\sigma_1(t) \in [10, 15], \quad \sigma_2(t) \in [5, 7.5],$$

and the following state-space matrices:

$$A(\vartheta) = \begin{bmatrix} 10 - 5\vartheta & \vartheta \\ 9\vartheta - 9 & \vartheta + 1 \end{bmatrix}, \quad B(\vartheta) = B = \begin{bmatrix} 1 & 0 \\ 0 & 0.5 \end{bmatrix}, \quad B_w(\vartheta) = 0,$$

where $\vartheta \in [0, 1]$ and the matrix $A(\vartheta(t))$ can be written in the polytopic form (3.37a) with $n_\mu = 2$ and vertex matrices (note that the system is open-loop unstable for every frozen value of ϑ):

$$A_1 = \begin{bmatrix} 10 & 0 \\ -9 & 1 \end{bmatrix}, \quad A_2 = \begin{bmatrix} 5 & 1 \\ 0 & 2 \end{bmatrix}.$$

By means of the proposed mapping (3.7) in Section 3.3, the shifting LPV state-feedback controller (3.4) is scheduled by ϑ and the following performance parameters:

$$\varphi_1(t) = \frac{\bar{\sigma}_1^2 - \sigma_1(t)^2}{\bar{\sigma}_1^2 - \underline{\sigma}_1^2}, \quad \varphi_2(t) = \frac{\bar{\sigma}_2^2 - \sigma_2(t)^2}{\bar{\sigma}_2^2 - \underline{\sigma}_2^2}, \quad \varphi_1(t), \varphi_2(t) \in [0, 1].$$

The controller's design is obtained solving Corollary 3.4.4a, which is particularized as follows:

$$\begin{cases} \begin{bmatrix} P & I \\ \star & X_0^{-1} \end{bmatrix} \geq 0 \\ \mathrm{He}\{A_i P + B Y_{ij}\} + 2\,\mathrm{d}_{\mathrm{R}j}\, P \prec 0\,, \\ \begin{bmatrix} U_j & Y_{ij} \\ \star & P \end{bmatrix} \geq 0 \end{cases}$$

where $P \in \mathbb{S}^2_+$, $i = 1, 2$, $j \in \mathcal{I}_{[1,4]}$ and X_0^{-1} has been chosen as:

$$X_0^{-1} = \begin{bmatrix} 100 & 0 \\ 0 & 100 \end{bmatrix},$$

so that the expected initial condition for the system lies in a circle centred in the origin of the state space, with radius 0.1. On the other hand, considering $n_\eta = 4$ and (3.95)–(3.98), the polytopic expression of $\mathrm{d}_{\mathrm{R}}(\varphi)$ can be defined as follows:

$$\mathrm{d}_{\mathrm{R}}(\varphi) \triangleq (1-\varphi_1)(1-\varphi_2)\mathrm{d}_{\mathrm{R}1} + \varphi_1(1-\varphi_2)\mathrm{d}_{\mathrm{R}2} + (1-\varphi_1)\varphi_2\mathrm{d}_{\mathrm{R}3} + \varphi_1\varphi_2\mathrm{d}_{\mathrm{R}4},$$

and it is chosen to vary within the interval $[1, 10]$, giving the following coefficients through (3.99):

$$\mathrm{d}_{\mathrm{R}1} = 10,\ \mathrm{d}_{\mathrm{R}2} = \mathrm{d}_{\mathrm{R}3} = 5.5,\ \mathrm{d}_{\mathrm{R}1} = 1.$$

Finally, taking into account the variability of $\sigma_1(t)$ and $\sigma_2(t)$, the matrices U_j are given by:

$$U_1 = \begin{bmatrix} 15^2 & 0 \\ 0 & 7.5^2 \end{bmatrix},\quad U_2 = \begin{bmatrix} 10^2 & 0 \\ 0 & 7.5^2 \end{bmatrix},\quad U_3 = \begin{bmatrix} 15^2 & 0 \\ 0 & 5^2 \end{bmatrix},\quad U_4 = \begin{bmatrix} 10^2 & 0 \\ 0 & 5^2 \end{bmatrix}.$$

By using the SeDuMi solver [117] and the YALMIP [70] toolbox, we find a solution of Problem 3.2.1 that, through $K_{ij} = Y_{ij} P^{-1}$, allows us to calculate the eight controller vertex gains:

$$K_{11} = \begin{bmatrix} -32.3324 & 16.4314 \\ 3.6128 & -22.7568 \end{bmatrix},\quad K_{12} = \begin{bmatrix} -22.8601 & 12.0997 \\ 4.1199 & -21.2087 \end{bmatrix},$$
$$K_{13} = \begin{bmatrix} -31.2651 & 18.2873 \\ 1.9555 & -12.9664 \end{bmatrix},\quad K_{14} = \begin{bmatrix} -21.7977 & 13.8038 \\ 2.2048 & -10.6816 \end{bmatrix},$$
$$K_{21} = \begin{bmatrix} -28.9436 & 9.0140 \\ 3.1265 & -27.9253 \end{bmatrix},\quad K_{22} = \begin{bmatrix} -19.7186 & 5.3862 \\ 3.4018 & -24.7843 \end{bmatrix},$$
$$K_{23} = \begin{bmatrix} -28.0168 & 11.5395 \\ 1.6600 & -18.0466 \end{bmatrix},\quad K_{24} = \begin{bmatrix} -19.1225 & 7.6903 \\ 1.7932 & -15.0194 \end{bmatrix},$$

with:

$$P = \begin{bmatrix} 0.196 & 0.053 \\ 0.053 & 0.074 \end{bmatrix}.$$

It is worth noting that the designed controller gain matrices K_{ij} result in reduced gain values when the saturation limit tends to be the most restrictive available control action ($j = 4$).

Hereafter, two different scenarios are used to show that the designed LPV state-feedback controller is able to guarantee the closed-loop system stability and the capacity to adapt its performance online taking into account the time-varying limits of the input saturation.

Scenario I: frozen φ values

Let us evaluate the closed-loop system stability and its closed-loop performance for a given initial condition with three different constant values of the control input saturation. To do this, we simulate the closed-loop response from an initial state $x_0 = [0.42, 0.04]^\top$ and $\vartheta(t) = 1 - \mathrm{e}^{-t}$. Finally, fixing the frozen values of $\varphi_1 = \varphi_2 = 0$, $\varphi_1 = \varphi_2 = 0.5$ and $\varphi_1 = \varphi_2 = 1$, thus obtaining instantaneous saturation limits values $\sigma_1 = 15$ and $\sigma_2 = 7.5$, $\sigma_1 = 12.75$ and $\sigma_2 = 6.37$ and $\sigma_1 = 10$ and $\sigma_2 = 5$, respectively.

As shown in Fig. 3.4, the closed-loop system stability is guaranteed for all the values of σ_1 and σ_2 that were mentioned. Moreover, note that the system's response that was evaluated with the scheduling parameters $\varphi_1 = \varphi_2 = 0$, corresponds to the maximum allowed limit values of σ_1 and σ_2, obtaining the fastest system response and showing that the designed LPV state-feedback controller is able to adjust the system's performance depending on the different values taken by σ.

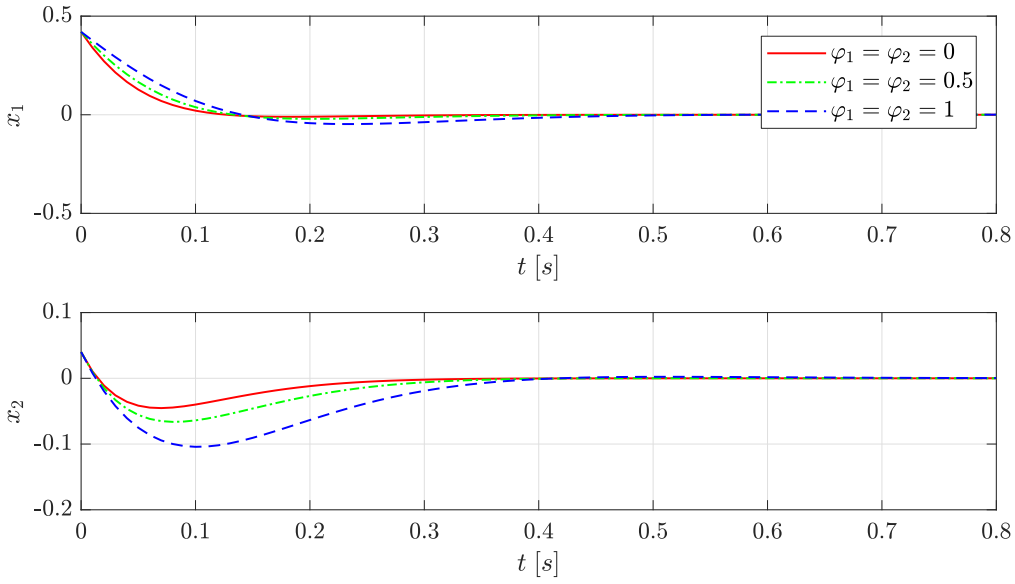

Figure 3.4: Scenario I: closed-loop system response.

Fig. 3.5 shows the instantaneous values of the saturation limit of u_1 and u_2 for the three frozen values of φ_1 and φ_2 and the response of the control signals. For illustrative purposes, since the signal u_1 takes only negative values during the system's response, only the lower bound of the saturation is plotted. As a variation of the saturation limit occurs, the input signal changes as a result of the adaptability of the designed controller. For example, the interval of linearity of the

control signal u_1 corresponds to $[-15, 15]$ when $\varphi_1 = \varphi_2 = 0$ and to $[-10, 10]$ when $\varphi_1 = \varphi_2 = 1$. Note that if the controller gain corresponding to $\varphi_1 = \varphi_2 = 0$ had been used for the case in which $\varphi_1 = \varphi_2 = 1$, then saturation would have occurred.

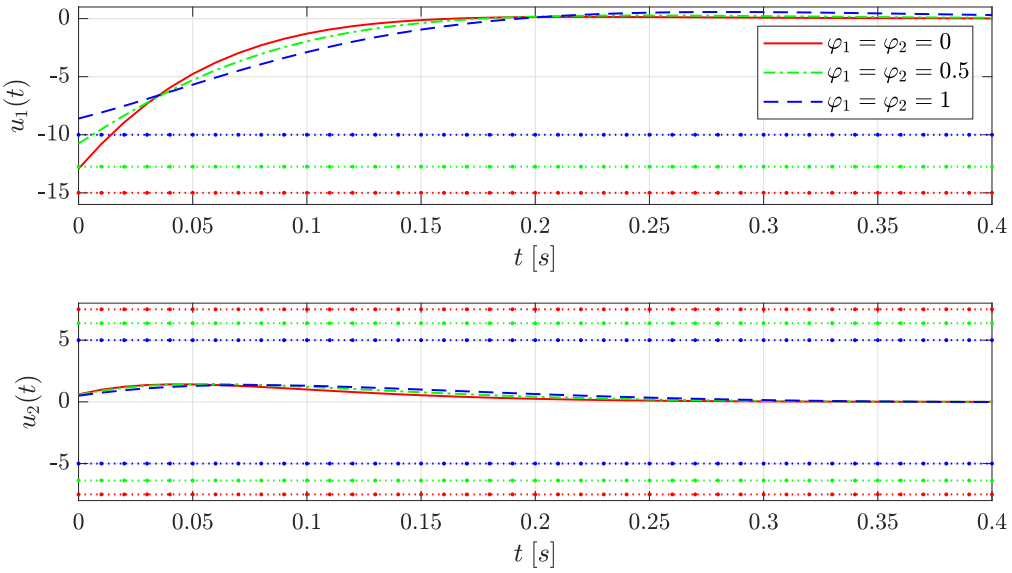

Figure 3.5: Scenario I: control input responses. (The saturation limits are shown as dotted lines.)

Fig. 3.6 shows the behaviour of the Lyapunov function $V(x)$ for the three frozen values of φ_1 and φ_2, which correspond to guaranteed decay rates of 10, 5.5 and 1 respectively. It can be seen that the largest decay rate corresponds to the fastest closed-loop system response, whose saturation scheduling parameters are $\varphi_1 = \varphi_2 = 0$ and $\mathrm{d_R}(\varphi) = 10$. Also, all the functions are under the unit value, hence it is guaranteed by design that none of the control inputs saturates, as already shown in Fig. 3.5.

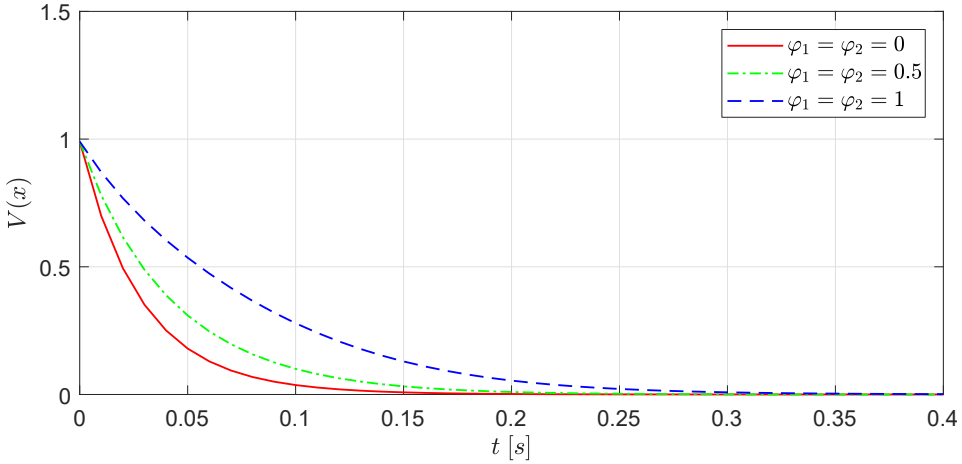

Figure 3.6: Scenario I: Lyapunov functions.

Scenario II: adaptability

Let us shows the adaptability of the designed controller to changes in σ along the transient response of the closed-loop. We consider $x_0 = [0.42, 0.04]^\top$ and $\vartheta(t) = 1 - \mathrm{e}^{-t}$. Also, we fix $\sigma_2(t) = \bar{\sigma}_2$, and we vary $\sigma_1(t)$ such that it switches between its known limits $\bar{\sigma}_1$ and $\underline{\sigma}_1$.

Fig. 3.7 shows that the designed LPV state-feedback controller is able to adapt the generated control signal u_1 taking into account the changes in $\mathrm{sat}(u_1, \sigma_1(t))$.

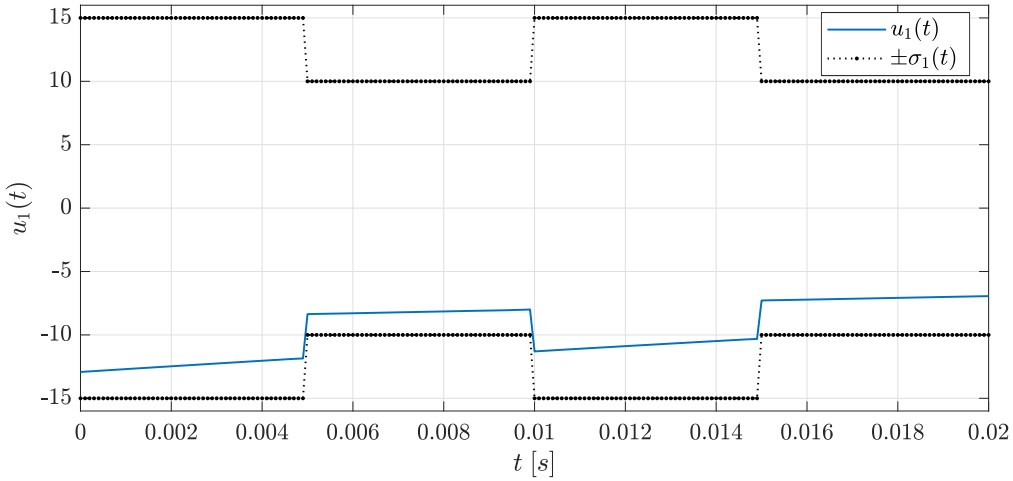

Figure 3.7: Scenario II: adaptability of control signal u_1.

Fig. 3.8 shows the behaviour of the Lyapunov function $V(x)$, which decreases slower when the guaranteed decay rate $\mathrm{d_R}(\varphi) = 5.5$, as a result of fixing $\varphi_2 = 0$ and faster when $\mathrm{d_R}(\varphi) = \bar{\mathrm{d}}_\mathrm{R}$. As a consequence, the closed-loop system performance is modified online according to changes in the saturation limits.

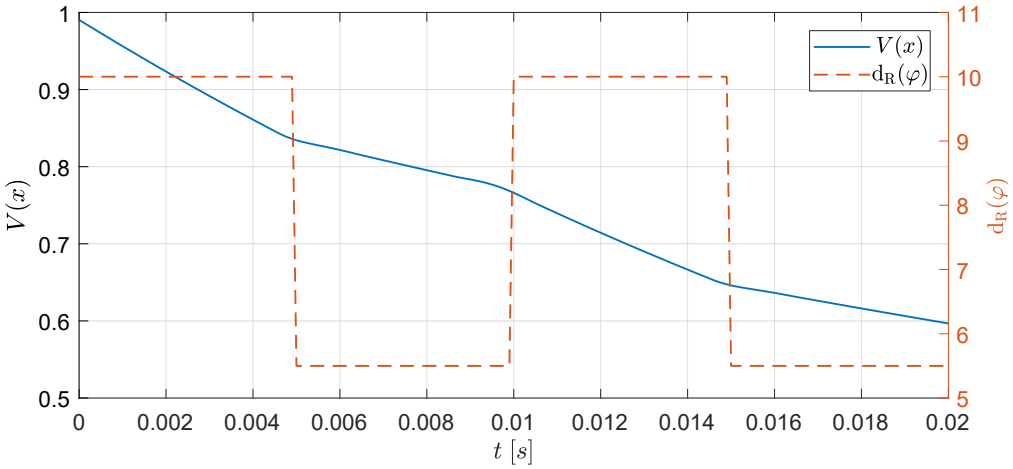

Figure 3.8: Scenario II: Lyapunov function and guaranteed decay rate.

3.7.4 Illustrative example 4: shifting $\mathcal{H}_\infty$ performance

Consider a saturated LPV system (3.1) is perturbed by an exogenous signal $\|w\|_2 \leq 1$, and has two control inputs with time-varying saturation limits as follows:

$$\sigma_1(t) \in [5, 10], \quad \sigma_2(t) \in [5, 10],$$

and matrices:

$$A(\vartheta) = \begin{bmatrix} 4.25 + 3.5\vartheta & 3.8971 \\ 3.8971 & 8.75 - 5.5\vartheta \end{bmatrix}, \quad B(\vartheta) = B = \begin{bmatrix} 1 & 0 \\ 0 & 0.5 \end{bmatrix},$$

$$B_w(\vartheta) = B_w = \begin{bmatrix} 1 \\ 0 \end{bmatrix}, \quad C_z(\vartheta) = C_z = \begin{bmatrix} 1 & 0 \end{bmatrix}, \quad D_{zu}(\vartheta) = D_{zw}(\vartheta) = 0,$$

where $\vartheta \in [0, 1]$. Note that the system is open-loop unstable for every frozen value of ϑ.

Let us introduce the performance scheduling parameter vector $\varphi(t)$, which is linked to the time-varying input saturation limits of $u_1(t)$ and $u_2(t)$ as follows:

$$\varphi_1(t) = \frac{\bar{\sigma}_1^2 - \sigma_1(t)^2}{\bar{\sigma}_1^2 - \underline{\sigma}_1^2}, \quad \varphi_2(t) = \frac{\bar{\sigma}_2^2 - \sigma_2(t)^2}{\bar{\sigma}_2^2 - \underline{\sigma}_2^2},$$

where $\varphi_1(t)$ and $\varphi_2(t)$ vary within the interval $[0, 1]$ for the inputs $u_1(t)$ and $u_2(t)$, respectively.

The controller is obtained applying the optimization procedure (3.103). In this case, the resulting optimization procedure $\mathcal{O}_3$ is as follows:

$$\mathcal{O}_3 : \begin{cases} \min\limits_{\substack{\underline{\gamma}>0,\, \bar{\gamma}>0 \\ Y_{ij},\, P>0}} & \dfrac{\underline{\gamma} + \bar{\gamma}}{2} \\ \text{s.t.} & \begin{cases} \begin{bmatrix} P & I \\ \star & X_0^{-1} \end{bmatrix} \succeq 0 \\ \begin{bmatrix} U_j & Y_{ij} \\ \star & P \end{bmatrix} \succeq 0 \\ \begin{bmatrix} \mathrm{He}\{A_i P + B Y_{ij}\} + \lambda_1 P & B_w \\ \star & -\lambda_2 \mathrm{I}_{n_w} \end{bmatrix} \preceq 0 \\ \begin{bmatrix} \mathrm{He}\{A_i P + B Y_{ij}\} & B_w & P C_z^\intercal \\ \star & -\gamma_j \mathrm{I}_{n_w} & 0 \\ \star & \star & -\gamma_j \mathrm{I}_{n_z} \end{bmatrix} \prec 0 \end{cases} \end{cases}$$

where $i = 1, 2$ and $j \in \mathcal{I}_{[1,4]}$. The parameter $\lambda \triangleq \lambda_1 = \lambda_2$ and the matrix X_0^{-1} have been chosen as:

$$\lambda = 1.2975, \quad X_0^{-1} = \mathrm{diag}\{100, 100\},$$

which means that the expected initial conditions for the system lie in a 0.1 radius circle centred in the origin of the state-space. By considering (3.95)–(3.98), the polytopic expression of $\gamma(\varphi)$ for $n_\eta = 4$ is:

$$\gamma(\varphi) \triangleq (1-\varphi_1)(1-\varphi_2)\,\gamma_1 + \varphi_1(1-\varphi_2)\gamma_2 + (1-\varphi_1)\varphi_2\gamma_3 + \varphi_1\varphi_2\gamma_4,$$

and $\gamma_1, \ldots, \gamma_4$ are obtained by means of (3.102) as follows:

$$\gamma_1 = \underline{\gamma},\ \gamma_2 = \gamma_3 = \frac{\bar{\gamma} + \underline{\gamma}}{2}, \gamma_4 = \bar{\gamma},$$

which are introduced in the LMI-based optimization problem as symbolic decision variables.

Finally, the vertex matrices of U_j are as follows:

$$U_1 = \begin{bmatrix} 10^2 & 0 \\ 0 & 10^2 \end{bmatrix},\quad U_2 = \begin{bmatrix} 5^2 & 0 \\ 0 & 10^2 \end{bmatrix},\quad U_3 = \begin{bmatrix} 10^2 & 0 \\ 0 & 5^2 \end{bmatrix},\quad U_4 = \begin{bmatrix} 5^2 & 0 \\ 0 & 5^2 \end{bmatrix},$$

taking into account the extreme values of $\sigma_1(t)$ and $\sigma_2(t)$.

The solution to Problem 3.2.2 through $\mathcal{O}_3$, was found using the SeDuMi solver [117] and the YALMIP toolbox [70]. The resulting interval of $\gamma(\varphi)$ is $[0.2410, 1.0623]$. Accordingly, the eight controller vertex gains are calculated as $K_{ij} = Y_{ij}P^{-1}$:

$$K_{11} = \begin{bmatrix} -33.3794 & -14.4915 \\ -11.3827 & -33.9409 \end{bmatrix},\quad K_{12} = \begin{bmatrix} -15.4868 & -4.9576 \\ -13.4635 & -35.3024 \end{bmatrix},$$
$$K_{13} = \begin{bmatrix} -29.4655 & -13.4938 \\ -5.4196 & -19.3670 \end{bmatrix},\quad K_{14} = \begin{bmatrix} -10.2462 & -6.0803 \\ -9.4186 & -20.0022 \end{bmatrix},$$
$$K_{21} = \begin{bmatrix} -35.1080 & -11.4615 \\ -11.4611 & -40.5934 \end{bmatrix},\quad K_{22} = \begin{bmatrix} -16.9073 & -3.7123 \\ -14.8493 & -41.5224 \end{bmatrix},$$
$$K_{23} = \begin{bmatrix} -30.0258 & -14.9333 \\ -4.0774 & -14.9120 \end{bmatrix},\quad K_{24} = \begin{bmatrix} -16.8222 & -7.3928 \\ -4.9860 & -15.4252 \end{bmatrix},$$

with:

$$P = \begin{bmatrix} 0.1063 & -0.0518 \\ -0.0518 & 0.0815 \end{bmatrix}$$

Scenario I: constant saturation limits

The controller is tested in a scenario with an external disturbance, $w(t) = \sin(4t)$, subject to three different saturation limit values kept constant throughout the simulation, $\sigma_1 = \sigma_2 = \{10, 7.5, 5\}$ that lead to $\varphi_1 = \varphi_2 = \{0, 0.5, 1\}$ by means of (3.7). The controlled system is simulated with an initial state $x_0 = [0, 0]^\top$ and $\vartheta(t) = 1 - e^{-t}$.

Fig. 3.9 shows the disturbance rejection for the three values of σ_1 and σ_2. Note the controller rejects the disturbance the most when $\varphi_1 = \varphi_2 = 0$, which corresponds to the largest saturation limit and to the obtained value $\underline{\gamma} = 0.2410$. Conversely, the disturbance is less rejected when

$\varphi_1 = \varphi_2 = 1$, showing that the performance of the controller depends on the instantaneous saturation limits.

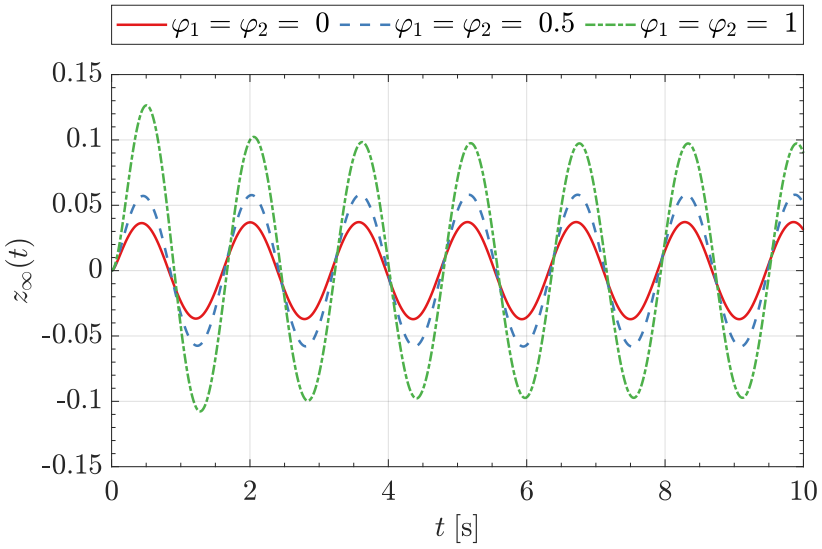

Figure 3.9: Scenario I: plot of $z_\infty(t)$ with different frozen values of $\varphi(t)$.

Fig. 3.10 shows the behaviour of $u_1(t)$ and $u_2(t)$, where it can be seen that they both remain inside the boundaries determined by all the values of $\sigma_1(t)$ and $\sigma_2(t)$ that were mentioned. For the sake of illustration, just the most strict saturation limit for each input, corresponding to $\sigma_1 = \sigma_2 = 5$ and $\varphi_1 = \varphi_2 = 1$, is displayed.

Fig. 3.11 shows the phase portrait with the established ellipsoidal regions $\mathcal{X}_0$ and $\mathcal{E}(P, 1)$ denoted by the solid lines (—) and (—), respectively, and $\mathcal{U}_x(\vartheta, \varphi)$. For illustrative purposes, the region $\mathcal{U}_x(\vartheta, \varphi)$ is drawn only on the vertex values of (ϑ, φ): (•) $\left(\vartheta, [0, 0]^\mathsf{T}\right)$, (•) $\left(\vartheta, [1, 0]^\mathsf{T}\right)$, (•) $\left(\vartheta, [0, 1]^\mathsf{T}\right)$ and (•) $\left(\vartheta, [1, 1]^\mathsf{T}\right)$. It can be seen that the state trajectories (- -) in the worst case scenario, which corresponds to $\varphi_1 = \varphi_2 = 1$ and $\bar{\gamma} = 1.0623$, remain inside $\mathcal{E}(P, 1)$, demonstrating the effectiveness of the QB approach. Moreover, it is guaranteed that the control inputs do not saturate because the states do not exceed the boundaries that are established by the parameter-dependent region $\mathcal{U}_x(\vartheta, \varphi)$.

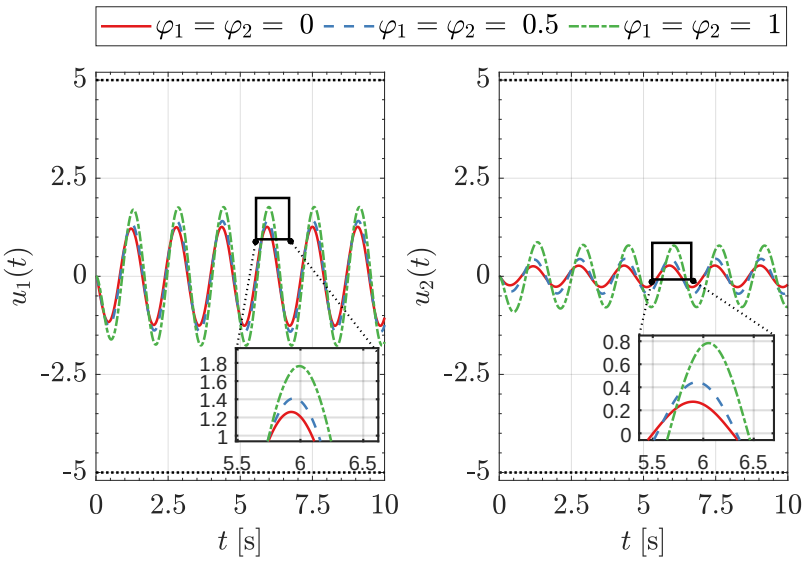

Figure 3.10: Scenario I: plot of $u(t)$ with different frozen values of $\varphi(t)$. (The most restrictive saturation limit for each input, corresponding to $\sigma_1 = \sigma_2 = 5$ and $\varphi_1 = \varphi_2 = 1$, is shown as the dotted black line.)

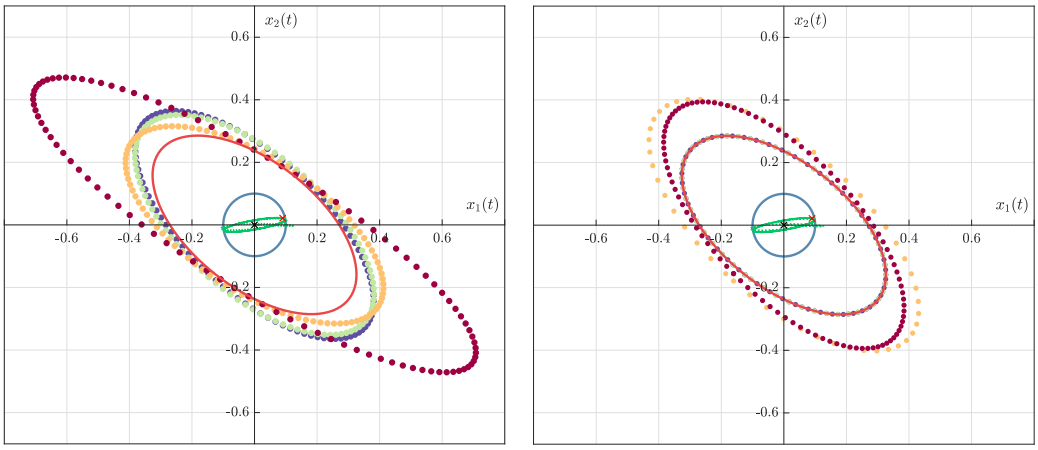

(a) Plot of ellipsoidal regions for $\vartheta(t) = 0$

(b) Plot of ellipsoidal regions for $\vartheta(t) = 1$.

Figure 3.11: Scenario I: plot of ellipsoidal region inclusions. ($\mathcal{X}_0$ and $\mathcal{E}(P, 1)$ are denoted by the solid lines (—) and (—), respectively. $\mathcal{U}_x(\vartheta, \varphi)$ for frozen values (ϑ, φ): • $\left(\vartheta, [0, 0]^\top\right)$, • $\left(\vartheta, [1, 0]^\top\right)$, • $\left(\vartheta, [0, 1]^\top\right)$ and • $\left(\vartheta, [1, 1]^\top\right)$. $x(t)$, x_0 and x_{end} are represented by the dashed line (- -) and the symbols **x** and **x**, respectively.)

Scenario II: time-varying saturation limit

Let us show the adaptability of the designed controller to time variations of the saturation limit of $u_1(t)$. The controller is tested in the same conditions as in the previous scenario, except for the limit of $u_2(t)$, which is fixed to $\sigma_2(t) = 10$, while $\sigma_1(t)$ varies within the interval $[5, 10]$ depending on $\varphi_1(t)$.

Fig. 3.12 shows the adaptability of the control performance output signal $z_\infty(t)$, for the different values of $\sigma_1(t)$. It can be seen that $z_\infty(t)$ is less affected by the external disturbance when $\sigma_1(t) = 10$, which corresponds to $\varphi_1(t) = 0$ and, conversely, it is more affected when $\sigma_1(t) = 5$ ($\varphi_1(t) = 1$). Therefore, it is shown that the controller is able to adapt when the limits of $u_1(t)$ change.

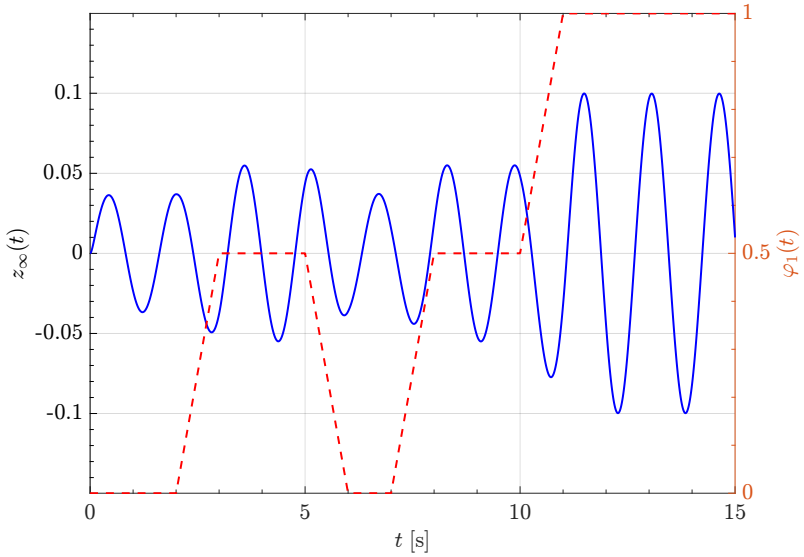

Figure 3.12: Scenario II: behaviour of $z_\infty(t)$ vs $\varphi_1(t)$.

3.7.5 Illustrative example 5: Attitude control of a quadrotor

Consider the quasi-LPV attitude model of a quadrotor taken from [123] with parameters as described in [93], and under the assumption of neglectable external disturbances. Then, the system (3.1a) with $B_w(\vartheta) = 0$ is characterized by the parameters in Table 3.3, $x = \left[\dot{\phi}, \dot{\theta}, \dot{\psi}, \phi, \theta, \psi\right]^\top$ and the moments produced by the rotors $u(t)$, as follows:

$$u = \begin{bmatrix} u_1 \\ u_2 \\ u_3 \end{bmatrix} = \begin{bmatrix} \mathrm{l_a k_T}(\Omega_4^2 - \Omega_2^2) \\ \mathrm{l_a k_T}(\Omega_3^2 - \Omega_1^2) \\ \mathrm{k_Q} \sum_{i=1}^{4} (-1)^i \Omega_i^2 \end{bmatrix}.$$

Table 3.3: Quadrotor model parameters

Symbol	Description	Value	Unit
ϕ, θ, ψ	Roll, Pitch and Yaw angles		rad
$\dot{\phi}, \dot{\theta}, \dot{\psi}$	Roll, Pitch and Yaw angle rates		rad/s
$\mathrm{k_T}$	Thrust coefficient	7.1103×10^{-8}	$\mathrm{N/rpm^2}$
$\mathrm{k_Q}$	Torque coefficient	1.0088×10^{9}	$\mathrm{N\,m/rpm^2}$
$\mathrm{l_a}$	Distance from rotor to CoG	0.171	m
I_{xx}	Moment of inertia $x-$axis	3.4313×10^{-3}	$\mathrm{kg\,m^2}$
I_{yy}	Moment of inertia $y-$axis	3.4313×10^{-3}	$\mathrm{kg\,m^2}$
I_{zz}	Moment of inertia $z-$axis	6.002×10^{-3}	$\mathrm{kg\,m^2}$
J_{tp}	Inertia moment of the rotor	1.302×10^{-3}	$\mathrm{kg\,m^2}$
Ω_i	Angular speed of the i-th propeller		rpm
$\Omega_{\max}$	Maximum propeller speed	8600	rpm
Ω_0	Minimum propeller speed	1075	rpm

Thereupon, the parameter scheduling vector $\vartheta = \left[\dot{\phi}, \dot{\theta}, \Omega_r\right]^\top$ is constructed by the Euler angle rates $\dot{\phi} \in [-1, 1]$ and $\dot{\theta} \in [-1, 1]$, as well as the term $\Omega_r \in [-105, 105]$ (rad/s) that describes in the gyroscopic effect, which is defined as follows:

$$\Omega_r = \frac{\pi}{30}(\Omega_2 + \Omega_4 - \Omega_1 - \Omega_3).$$

In this way, the polytope Θ is a cube with $n_\mu = 8$ vertices that contains the following parameter-dependent system matrices (3.1a):

$$A(\vartheta) = \left[\begin{array}{ccc|c} 0 & -\vartheta_3 \frac{J_{\mathrm{tp}}}{I_{xx}} & \vartheta_2 \frac{I_{yy}-I_{zz}}{I_{xx}} & \\ \vartheta_3 \frac{J_{\mathrm{tp}}}{I_{yy}} & 0 & \vartheta_1 \frac{I_{zz}-I_{xx}}{I_{yy}} & 0_{3\times3} \\ \vartheta_2 \frac{I_{xx}-I_{yy}}{2\,I_{zz}} & \vartheta_1 \frac{I_{xx}-I_{yy}}{2\,I_{zz}} & 0 & \\ \hline \multicolumn{3}{c|}{\mathrm{I_3}} & 0_{3\times3} \end{array}\right], \quad B(\vartheta) = B = \begin{bmatrix} J^{-1} \\ 0_{3\times3} \end{bmatrix},$$

where $J \triangleq \mathrm{diag}\{I_{xx}, I_{yy}, I_{zz}\}$.

Time-varying saturation limits definition

Under the assumption that all rotors share the same behaviour regarding saturation, let us consider $\forall i \in \mathcal{I}_{[1,4]}$ that $\Omega_i \in [\Omega_0,\ \Delta_\Omega(t)]$ where Ω_0 is fixed to 1075 (rpm) and $\Delta_\Omega(t)$ is a known function that describes the instantaneous maximum propeller speed, which varies due to the discharge of the battery. Then, it is also assumed that $\Delta_\Omega(t)$ varies within the interval $[\Delta_{\underline{\Omega}},\ \Delta_{\bar{\Omega}}]$ with $\Omega_0 < \Delta_{\underline{\Omega}} < \Delta_{\bar{\Omega}}$, $\Delta_{\underline{\Omega}} = 4907$ (rpm) and $\Delta_{\bar{\Omega}} = 8600$ (rpm), respectively.

In order to handle the propeller speed limitation, let us define the largest available positive control action, thus defining the time-varying saturation limits in (3.2) as follows:

$$\sigma_1(t) = \sigma_2(t) = \mathrm{l_a k_T}\left(\Delta_\Omega(t)^2 - \Omega_0^2\right), \quad \sigma_3(t) = 2\mathrm{k_Q}\left(\Delta_\Omega(t)^2 - \Omega_0^2\right).$$

Let us assume that the axes of $u(t)$ are aligned with the axes of the ellipsoidal region $\mathcal{U}(\varphi)$ (3.9). Then, let us define the squared expression of $\sigma_1(t)$, $\sigma_2(t)$ and $\sigma_3(t)$ as follows:

$$\sigma_1(t)^2 = \sigma_2(t)^2 = \mathrm{l_a^2 k_T^2}\big(\Delta_\Omega(t)^4 - 2\Omega_0^2\Delta_\Omega(t)^2 + \Omega_0^4\big),$$
$$\sigma_3(t)^2 = 4\mathrm{k_Q^2}\big(\Delta_\Omega(t)^4 - 2\Omega_0^2\Delta_\Omega(t)^2 + \Omega_0^4\big).$$

Thereupon, let us introduce the following scheduling parameters $\varphi_1(t)$ and $\varphi_2(t)$ which are linked to $\Delta_\Omega(t)^2$ and $\Delta_\Omega(t)^4$, respectively, thus obtaining expressions of $\sigma_1(t)^2$, $\sigma_2(t)^2$ and $\sigma_3(t)^2$ as a function of $\varphi(t) = [\varphi_1(t), \varphi_2(t)]^\top$:

$$\sigma_1(\varphi(t))^2 = \sigma_2(\varphi(t))^2 = \mathrm{l_a^2 k_T^2}\big(\varphi_2(t) - 2\Omega_0^2\varphi_1(t) + \Omega_0^4\big),$$
$$\sigma_3(\varphi(t))^2 = 4\mathrm{k_Q^2}\big(\varphi_2(t) - 2\Omega_0^2\varphi_1(t) + \Omega_0^4\big).$$

Once $\sigma_1(\varphi)^2$, $\sigma_2(\varphi)^2$ and $\sigma_3(\varphi)^2$ are obtained, the axis magnitudes of $\mathcal{U}(\varphi)$ are established through the matrix function $U(\varphi)^{-1}$ as follows:

$$U(\varphi)^{-1} = \mathrm{diag}\big\{\sigma_1(\varphi)^2, \sigma_2(\varphi)^2, \sigma_3(\varphi)^2\big\}^{-1}.$$

For the purpose of solving Problem 3.2.1, let us define the polytope Φ (where the scheduling parameters $\varphi_1(t)$ and $\varphi_2(t)$ lie) generating a set of possible values for both parameters taking into account the bounds of $\Delta_\Omega(t)$. Note that these sets reach large values due to $\varphi_1(t)$ and $\varphi_2(t)$ being linked to square and fourth power of $\Delta_\Omega(t)$, respectively. Hence, it is necessary to normalize both parameters in the range $[0, 1]$ in order to avoid numerical issues when computing $\eta_j(\varphi(t))$.

Fig. 3.13 shows the generated values for the normalized parameters $\varphi_{\mathrm{n},1}(t)$ and $\varphi_{\mathrm{n},2}(t)$ as well as the selected $n_\eta = 3$ vertices $\mathrm{v}_\Phi^{\{1\}} = [0, 0]^\top$, $\mathrm{v}_\Phi^{\{2\}} = [0.5, 0.2456]^\top$ and $\mathrm{v}_\Phi^{\{3\}} = [1, 1]^\top$ that define the polytope Φ.

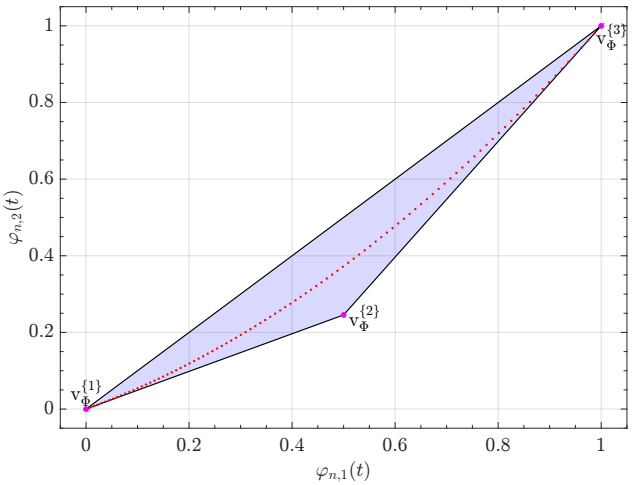

Figure 3.13: Polytope Φ. (• denotes the normalized values of $\varphi_{\mathrm{n},1}(t)$ and $\varphi_{\mathrm{n},2}(t)$; • denotes the polytope vertices.)

Then, taking into account the bounds of the polytope Φ, it is possible to compute $\eta_j(\varphi(t))$ $\forall j \in \mathcal{I}_{[1,3]}$ as the solution of the following equation:

$$\begin{bmatrix} \varphi_{\mathrm{n},1}(t) \\ \varphi_{\mathrm{n},2}(t) \\ 1 \end{bmatrix} = \begin{bmatrix} \mathrm{v}_{1,\Phi}^{\{1\}} & \mathrm{v}_{1,\Phi}^{\{2\}} & \mathrm{v}_{1,\Phi}^{\{3\}} \\ \mathrm{v}_{2,\Phi}^{\{1\}} & \mathrm{v}_{2,\Phi}^{\{2\}} & \mathrm{v}_{2,\Phi}^{\{3\}} \\ 1 & 1 & 1 \end{bmatrix} \begin{bmatrix} \eta_1(\varphi(t)) \\ \eta_2(\varphi(t)) \\ \eta_3(\varphi(t)) \end{bmatrix},$$

where $\mathrm{v}_{k,\Phi}^{\{j\}}$ denotes the k^{th} component of $\mathrm{v}_{\Phi}^{\{j\}}$.

Let us now describe the performance specifications for the controller design considering that the initial state of the quadrotor is around the hover attitude point $(\phi(t) = 0,\ \theta(t) = 0)$ with the purpose of evaluating the LMI methodology described in Corollary 3.5.4 versus the procedure proposed in Corollary 3.4.9a under the scenarios indicated in Table 3.4.

Table 3.4: Expected initial conditions for Euler angles. (ξ_κ and $\bar{\xi}_\kappa$ denote the lower and upper bound value expressed in (rad), respectively.)

κ	$[\xi_\kappa,\ \bar{\xi}_\kappa]$
1	$[-0.0087,\ 0.0087]$
2	$[-0.0436,\ 0.0436]$
3	$[-0.0873,\ 0.0873]$
4	$[-0.1309,\ 0.1309]$
5	$[-0.1745,\ 0.1745]$

To this end, let us define the shape of the region (2.72) considering that the initial attitude of the vehicle $\phi(0)$, $\theta(0)$ and $\psi(0)$ belongs to the interval $[\xi_\kappa,\ \bar{\xi}_\kappa]$ expressed in (rad) for each scenario κ. Furthermore, each initial value of the Euler angle rates $\dot{\phi}(0)$, $\dot{\theta}(0)$ and $\dot{\psi}(0)$ is expected to be inside the interval $[-0.3491, 0.3491]$ $(\mathrm{rad/s})$, thus specifying:

$$X_0^{-1} = \mathrm{diag}\left\{\bar{\xi}_\kappa,\ 0.3491,\ \bar{\xi}_\kappa,\ 0.3491,\ \bar{\xi}_\kappa,\ 0.3491\right\}^{-2},$$

where $\bar{\xi}_\kappa$ denotes the corresponding κ upper bound value of the interval.

Then, with the aim of controlling online the convergence speed of the closed-loop system, let us define the desired decay rate values in (3.95) as follows:

$$\mathrm{d_{R1}} = 0,\ \mathrm{d_{R2}} = 0,\ \mathrm{d_{R3}} = \bar{\mathrm{d}}_\mathrm{R},$$

thus specifying the fastest closed-loop system response when the largest saturation limit of $u(t)$ is available.

Once the performance specifications are defined, let us proceed to compare Corollary 3.5.4 against Corollary 3.4.9a by evaluating $\bar{\mathrm{d}}_\mathrm{R}$ for each value of the set $\left\{\bar{\mathrm{d}}_\mathrm{R} \in \mathbb{R}_+ \ :\ 0 \leq \bar{\mathrm{d}}_\mathrm{R} \leq 100\right\}$. Thus, obtaining the maximum feasible decay rate $\bar{\mathrm{d}}_\mathrm{R}$ shown in Table 3.5 for each scenario κ under the consideration of choosing the Pólya's relaxation degrees $d_1 = d_2 = 2$, the bounds of (3.70) $\forall i \in \mathcal{I}_{[1,8]}$ as $[-0.8, 0.8]$ and, similarly, the bounds in (3.71) are established $\forall j \in \mathcal{I}_{[1,3]}$ as $[-0.05, 0.05]$.

Table 3.5: Maximum feasible values of $\mathrm{d}_{\mathrm{R}3}$. ($\langle\%\rangle$ denotes the improvement in percentage with respect to the value obtained through the Corollary 3.4.9a.)

κ	Corollary 3.4.9a	Corollary 3.5.4	$\langle\%\rangle$
1	19.27	26.46	37.31
2	10.70	14.13	32.06
3	7.67	10.03	30.77
4	6.15	7.56	22.93
5	5.65	7.07	25.13

Table 3.6: Off-line computational cost. (*4 cores 2.80GHz CPU with 16GB RAM)

	Corollary 3.4.9a	Corollary 3.5.4
Number of LMIs	134	90792
Computation time* [s]	0.7126	19134

The benefits of using Corollary 3.5.4 instead of using the Corollary 3.4.9a can be observed in Table 3.5, as an improvement of $20-30\%$ with respect to the largest feasible guaranteed decay rate obtained when QLF is used for the above defined conditions. However, this improvement comes at the cost of increasing significantly the computational cost, as shown in Table 3.6. Note that the increase in computational burden affects only the off-line computation due to the growth of the number of LMIs that must be satisfied. On the other hand, the online computation is not affected, since the total number of vertices does not depend on which of the methodologies is used.

Closed-loop response

Let us show how the performance varies online according to the value of the instantaneous saturation limits given by $\Delta_\Omega(t)$ through the results shown in Figs. 3.14–3.18 which correspond to the controller designed under the initial conditions of scenario $\kappa = 3$ and guaranteed decay rates:

$$\mathrm{d}_{\mathrm{R}1} = 0,\ \mathrm{d}_{\mathrm{R}2} = 0,\ \mathrm{d}_{\mathrm{R}3} = 10.0$$

As shown in Fig. 3.14, the closed-loop system stability is guaranteed $\forall t \geq 0$. Moreover, note that jumps in the values of $\phi(t)$ and $\psi(t)$ were introduced every 10 seconds in order to show the effectiveness of the controller. It can be seen that the slowest system response corresponds to when $\Delta_\Omega(t) \to \Omega_0$ at $t \geq 30$, as shown in Fig. 3.15. Conversely, the fastest closed-loop response corresponds to when the maximum angular speed of each propeller is available. This demonstrates that the designed shifting LPV state-feedback controller adapts online the closed-loop system response in the sense of convergence speed according to the available control action.

Fig. 3.15 shows the behaviour of the maximum available propeller angular speed, which decreases its value over time reproducing an incipient discharge of the battery, which limits the instantaneous value of $u(t)$ according to $\sigma(t)$. This fact is exemplified in Fig. 3.16, where smaller

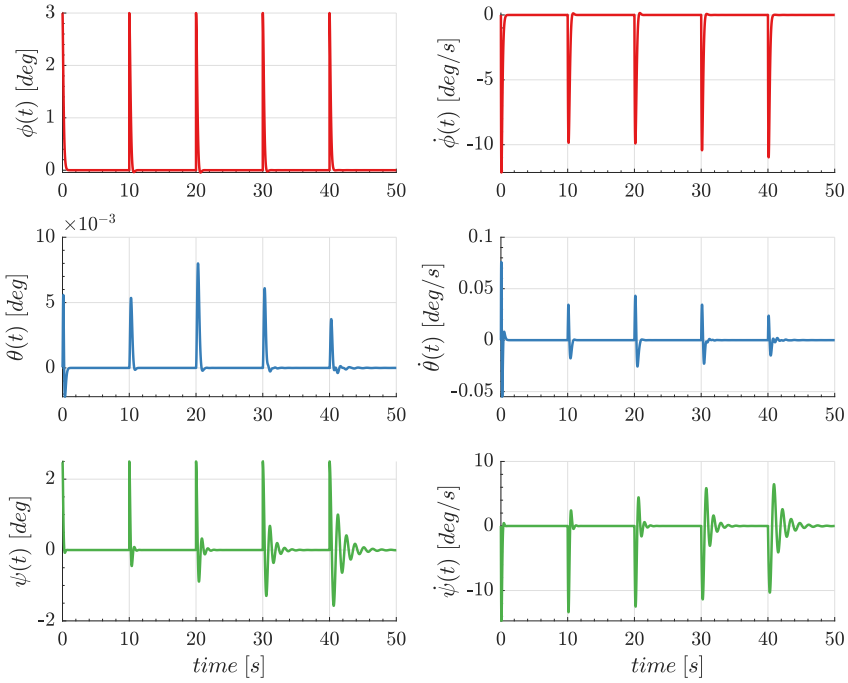

Figure 3.14: Quadrotor's attitude closed-loop response.

values of $u(t)$ were obtained over time preventing saturation to occur. Similarly, Fig. 3.17 shows the behaviour of the angular speed for each propeller under the scenario described above.

Finally, Fig. 3.18 shows the adaptability of the control performance through the behaviour of the PDQLF (3.54). Note that the largest value of $\mathrm{d_R}(\varphi)$ stands for the fastest closed-loop response showed in Fig. 3.14, whose instantaneous saturation limits corresponded to the largest possible ones. Furthermore, $V(x(t), \vartheta(t), \varphi(t))$ is under the unit value $\forall t \geq 0$, which provides theoretical guarantees that none of the control actions saturates during the transient response, as already shown in Fig. 3.16.

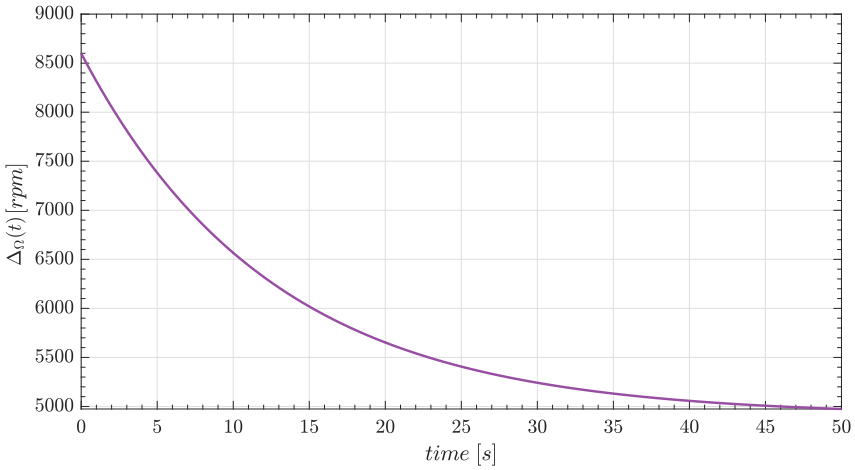

Figure 3.15: Maximum propeller speed due to the battery discharge.

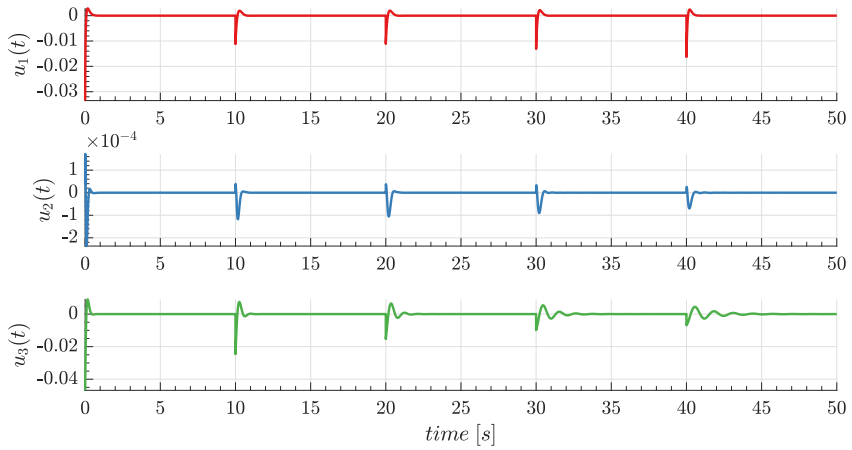

Figure 3.16: Quadrotor's attitude control actions

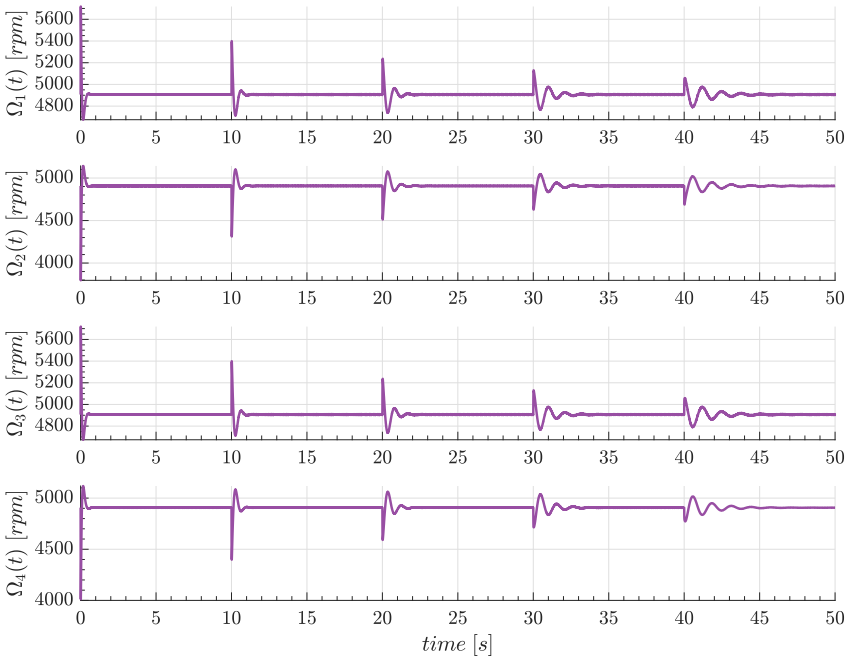

Figure 3.17: Propellers' angular speed.

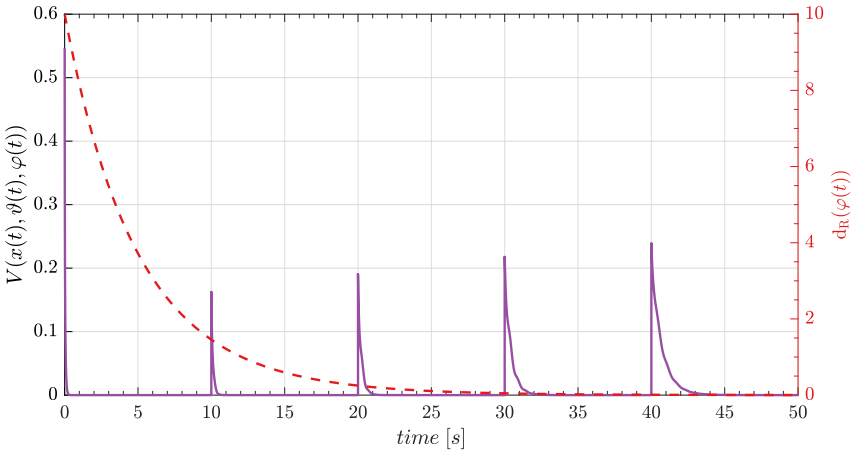

Figure 3.18: PDQLF and guaranteed shifting decay rate. ((—) denotes $V(x(t), \vartheta(t), \varphi(t))$; (- -) represents $d_R(\varphi)$).

3.8 Conclusions

In this chapter, the problem of designing a shifting state-feedback controller for LPV systems subject to time-varying symmetric saturations has been considered. The controller has been designed such that some desired performance is achieved considering the amount of available control action.

In order to generate LMI-based conditions that may be utilized to solve this problem, some well-known results in the control of linear systems subject to saturation functions have been expanded. The provided solution relies on a convex representation of the changes in the saturation limit, allowing the characterization of a parameter-dependent region in which the saturation of the control action does not occur.

The problem has been tackled using both a parameter-independent and a parameter-dependent QLF. Under certain assumptions, it is possible to generate a finite number of LMIs in both scenarios that can be successfully solved by the current solvers. Furthermore, a finite-dimensional LMI relaxation, based on Pólya's relaxation theorem, has been used to deal with multiple polytopic summations during the design stage, allowing the consideration of, e.g., parameter-dependent input matrices.

The results obtained in the illustrative examples have shown the effectiveness of the proposed design conditions. In particular, the designed controller has shown its ability to regulate the closed-loop convergence speed or disturbance rejection according to the instantaneous saturation limit values of the actuator. The results obtained for the case when PDQLF is used appear to be less conservative in contrast with the QLF case, although at the cost of increasing the computational burden and mathematical complexity, which could hinder the implementation of the proposed design approach in higher-order plants due to the large number of required LMIs.

An open issue that requires further investigation is reducing the conservativeness and computational complexity by focusing on the design of saturating controllers and the application of hybrid techniques (for example, MPC with LPV or feedback linearization with LPV) or more advanced LPV frameworks that incorporate switching elements in order to reduce the number of LMIs to be handled.

4 Shifting output-feedback control

The content of this chapter is based on the following work:

- [100] A. Ruiz, D. Rotondo, and B. Morcego. "Design of shifting output-feedback controllers for LPV systems subject to time-varying saturations". *IFAC-PapersOnLine* 55:35, 2022. 5th IFAC Workshop on Linear Parameter Varying Systems 2022, pp. 13–18. ISSN: 2405-8963. DOI: https://doi.org/10.1016/j.ifacol.2022.11.283

4.1 Introduction

In Chap. 3, the problem of designing shifting state-feedback controllers for time-varying saturated LPV systems has been introduced. The resulting approach exploits the shifting paradigm concept [92], the invariant ellipsoidal theory [23] and the LPV framework, enabling the obtention of an LMI-based methodology to design a gain-scheduling controller that adapts the closed-loop system performance in consonance with the saturation limit variations. However, the state-feedback control requires state information, which may not be available in some real-world situations [76]. When the system is observable, an estimated state-feedback law can be considered utilizing an observer-based control approach, such that the observer provides the essential information to perform the control [39, 133]. Since there is a coupling between the dynamics of the plant state and those of the observer state, it is important to note that the simultaneous design of controller gain and observer gain may not allow for a convex formulation [26, 119]. Nonetheless, it is generally known that by tackling the design problem separately, LMI-based design conditions can be obtained. Alternatively, dynamic output-feedback control can also be used to overcome this limitation, due to the observer case being a particular case of a dynamic controller.

Designing shifting output-feedback controllers for time-varying saturated LPV systems is the focus of this chapter, extending the LMI-based methodology suggested in Chap. 3. Particularly, Sections 4.2 and 4.3 outline the problem formulation and the prerequisites for guaranteeing time-varying saturation avoidance. The overall design approach is defined in Section 4.4, taking into account a full-order dynamic output-feedback control structure and the use of a PDQLF. A finite-dimensional LMI-based methodology is also provided under certain design restrictions, and the practical implementation is discussed. Finally, the simulation results utilizing a nonlinear quadrotor model are used to demonstrate the efficacy of the proposed approach.

4.2 Problem formulation

Consider the following slight modification of the time-varying saturated LPV system (3.1):

$$\dot{x}_p = A(\vartheta)x_p + B_w(\vartheta)w + B(\vartheta)\,\mathrm{sat}(u,\sigma(t)), \quad x_p(0) = x_{0p}, \tag{4.1a}$$
$$z_\infty = C_z(\vartheta)x_p + D_{zw}(\vartheta)w + D_{zu}(\vartheta)\,\mathrm{sat}(u,\sigma(t)), \tag{4.1b}$$
$$y = C(\vartheta)x_p, \tag{4.1c}$$

where $x_p \in \mathbb{R}^{n_x}$ is the plant state, $y \in \mathbb{R}^{n_y}$ is the measured output and $\mathrm{sat}(u,\sigma(t)) : \mathbb{R}^{n_u} \to \mathbb{R}^{n_u}$ represents the time-varying symmetric saturation function, defined for $l \in \mathcal{I}_{[1,n_u]}$ as in (3.2):

$$\mathrm{sat}(u,\sigma(t)) \triangleq \begin{bmatrix} \mathrm{sat}(u_1,\sigma_1(t)) \\ \vdots \\ \mathrm{sat}(u_l,\sigma_l(t)) \\ \vdots \\ \mathrm{sat}(u_{n_u},\sigma_{n_u}(t)) \end{bmatrix}, \quad \mathrm{sat}(u_l,\sigma_l(t)) \triangleq \mathrm{sign}(u_l)\min(|u_l|,\sigma_l(t)). \tag{4.2}$$

In order to analogously adapt the procedure stated in Chap. 3 for the output-feedback case, a GS dynamic output-feedback control law has been combined with the shifting paradigm concept presented in Section 2.2.6, thus defining $\forall(\vartheta,\varphi) \in \Theta \times \Phi$ the structure of a full-order shifting output-feedback controller, as follows[4]:

$$\dot{x}_c = A_c(\vartheta,\varphi)x_c + B_c(\vartheta,\varphi)y, \; x_c(0) = x_{0c}, \tag{4.3a}$$
$$u_c = C_c(\vartheta,\varphi)x_c + D_c(\vartheta,\varphi)y, \tag{4.3b}$$

where $x_c \in \mathbb{R}^{n_x}$ is the control state, $u_c \in \mathbb{R}^{n_u}$ denotes the controller's output and $A_c(\vartheta,\varphi)$, $B_c(\vartheta,\varphi)$, $C_c(\vartheta,\varphi)$ and $D_c(\vartheta,\varphi)$ correspond to the parameter-dependent controller matrices, with appropriate dimensions, to be designed[5]. For the sake of controller design, it is further assumed that the pairs $(A(\vartheta),B(\vartheta))$ and $(A(\vartheta),C(\vartheta))$ stated by the LPV system (4.1) are, respectively, stabilizable and detectable w.r.t. $\vartheta \in \Theta$.

Then, assuming the interconnection of (4.1) and (4.3) with $u = u_c$, the closed-loop LPV system dynamics are defined as follows:

$$\dot{x} = \mathbb{A}(\vartheta,\varphi)x + \mathbb{B}_w(\vartheta)w + \mathbb{B}(\vartheta)\,\mathrm{sat}(\mathbb{K}(\vartheta,\varphi)x,\sigma(t)), \tag{4.4a}$$
$$z_\infty = \mathbb{C}_z(\vartheta)x + D_{zw}(\vartheta)w + D_{zu}(\vartheta)\,\mathrm{sat}(\mathbb{K}(\vartheta,\varphi)x,\sigma(t)), \tag{4.4b}$$

where $x = \left[x_p^\top, x_c^\top\right]^\top \in \mathbb{R}^{2n_x}$ is the augmented state vector, $x_0 = \left[x_{0p}^\top, x_{0c}^\top\right]^\top \in \mathbb{R}^{2n_x}$ is the initial state and matrices $\mathbb{A}(\vartheta,\varphi)$, $\mathbb{B}(\vartheta)$, etc. are given as:

$$\mathbb{A}(\vartheta,\varphi) \triangleq \begin{bmatrix} A(\vartheta) & 0 \\ B_c(\vartheta,\varphi)C(\vartheta) & A_c(\vartheta,\varphi) \end{bmatrix}, \quad \mathbb{B}_w(\vartheta) \triangleq \begin{bmatrix} B_w(\vartheta) \\ 0 \end{bmatrix}, \quad \mathbb{B}(\vartheta) \triangleq \begin{bmatrix} B(\vartheta) \\ 0 \end{bmatrix},$$
$$\mathbb{K}(\vartheta,\varphi) \triangleq \begin{bmatrix} D_c(\vartheta,\varphi)C(\vartheta) & C_c(\vartheta,\varphi) \end{bmatrix}, \quad \text{and} \quad \mathbb{C}_z(\vartheta) \triangleq \begin{bmatrix} C_z(\vartheta) & 0 \end{bmatrix}.$$

[4] Note that in order not to limit the controller's dynamics, all controller matrices are considered to depend on (ϑ,φ).
[5] For details on structuring the controller matrices to define a full-order observer-based control law, see [119, § 3.4.3].

In this chapter, the goal is to stabilize the closed-loop dynamics (4.4) such that the closed-loop system regulation fulfils one (or more) of the performance criteria listed below:

- Guaranteed shifting decay rate.
- Quadratic boundedness together with the shifting $\mathcal{H}_\infty$ performance.

To this end, the following sections outline an LMI-based methodology for designing a shifting output-feedback controller (4.3) with the objective of solving the following control design problems:

Problem 4.2.1. For the LPV system (4.1a) subject to a time-varying saturation function (4.2) and a given set of admissible initial conditions $\mathcal{X}_0$, design a GS dynamic output-feedback control law (4.3) such that for any initial state $x_0 \in \mathcal{X}_0$ the closed-loop system dynamics (4.4a) satisfies the guaranteed shifting decay rate performance $\mathrm{d_R}(\varphi)\colon \mathbb{R}^{n_\varphi} \to \mathbb{R}_+$, defined as in (2.64):

$$\dot{V}(\cdot) \leq -2\mathrm{d_R}(\varphi)V(\cdot), \tag{4.5}$$

where $V(\cdot)$ is a candidate Lyapunov function that can be defined by a (PD)QLF. □

Problem 4.2.2. For the LPV system (4.1) subject to a time-varying saturation function (4.2) and the given set of admissible initial conditions $\mathcal{X}_0$ and the set $\mathcal{W}$, design a GS output-feedback control law (4.3) such that for $x_0 \in \mathcal{X}_0$ and $\|w\|_2 \leq 1$:

1. the closed-loop system dynamics (4.4) satisfies the shifting $\mathcal{H}_\infty$ performance $\gamma(\varphi)\colon \mathbb{R}^{n_\varphi} \to \mathbb{R}_+\backslash\{0\}$, defined as in (2.65):

$$\left\|\gamma(\varphi)^{-\frac{1}{2}} z_\infty\right\|_2 < \left\|\gamma(\varphi)^{\frac{1}{2}} w\right\|_2 \tag{4.6}$$

   along all possible trajectories $\vartheta \in \Theta \subset \mathbb{R}^{n_\vartheta}$ and $\varphi \in \Phi \subset \mathbb{R}^{n_\varphi}$.

2. the closed-loop system trajectories $x(t)$ are quadratically bounded by a (PD)QLF.

□

4.3 Time-varying saturation handling

Similarly to Chap. 3, the presence of the nonlinear saturation function (4.2) affects the closed-loop LPV system dynamics (4.4), so it is necessary to ensure that the control input $u(t)$ is within the time-varying region $\mathcal{L}(u(t), \sigma(t))$, defined as in (3.3):

$$\mathcal{L}(u(t), \sigma(t)) \triangleq \left\{u(t) \in \mathbb{R}^{n_u} \,:\, -\sigma_l(t) \leq u_l(t) \leq \sigma_l(t),\ \forall l \in \mathcal{I}_{[1,n_u]}\right\}, \tag{4.7}$$

in order to achieve computable design conditions. For this reason, by considering the convex representation defined as in (3.8):

$$\hat{\sigma}_l(\varphi_l(t)) \triangleq \sigma_l(t)^2 = \bar{\sigma}_l^2 + \varphi_l(t)\left(\underline{\sigma}_l^2 - \bar{\sigma}_l^2\right), \quad \varphi_l(t) \in [0,1],\ \forall l \in \mathcal{I}_{[1,n_\varphi]}, \tag{4.8}$$

and the parameter-dependent matrices in (4.4), this section extends Proposition 3.3.2 to the output-feedback case.

Let us represent the region of the state-space domain which contains the initial condition of interest x_0 as follows:

$$\mathcal{X}_0 \triangleq \left\{x \in \mathbb{R}^{2n_x} : x^\top X_0^{-1} x \leq 1\right\}, \tag{4.9}$$

where $X_0^{-1} \in \mathbb{S}_+^{2n_x}$ is a chosen matrix that contains the information about where the initial states x_0 of the closed-loop LPV dynamic (4.4) are expected to lie. Then, let us consider the relationship:

$$u_l = \mathbb{K}_{[l]}(\vartheta,\varphi)x = \begin{bmatrix} D_{c[l]}(\vartheta,\varphi)C(\vartheta) & C_{c[l]}(\vartheta,\varphi)\end{bmatrix} x, \quad l \in \mathcal{I}_{[1,n_u]},$$

which yields to the obtention of the symmetrical polyhedral set (4.10) and the formulation of Proposition 4.3.1 using a procedure similar to the one stated in Section 3.3.

Proposition 4.3.1. *Let $\mathcal{L}(\mathbb{K}(\vartheta,\varphi),\hat{\sigma}(\varphi))$ be a parameter-dependent set given by:*

$$\mathcal{L}(\mathbb{K}(\vartheta,\varphi),\hat{\sigma}(\varphi)) \triangleq \left\{ x \in \mathbb{R}^{2n_x} : x^\top \frac{\mathbb{K}_{[l]}^\top(\vartheta,\varphi)\mathbb{K}_{[l]}(\vartheta,\varphi)}{\hat{\sigma}_l(\varphi)} x \leq 1,\ l \in \mathcal{I}_{[1,n_u]} \right\} \tag{4.10}$$

If $\mathcal{E}(P(\vartheta,\varphi),c) \subset \mathbb{R}^{2n_x}$ is a contractively invariant set satisfying $\forall(\vartheta,\varphi) \in \Theta \times \Phi$:

$$\mathcal{X}_0 \subset \mathcal{E}(P(\vartheta,\varphi),c) \subset \mathcal{L}(\mathbb{K}(\vartheta,\varphi),\hat{\sigma}(\varphi)), \tag{4.11}$$

then for any initial condition $x_0 \in \mathcal{X}_0$, and hence $x_0 \in \mathcal{E}(P(\vartheta,\varphi),c)$, the convergence of the corresponding state trajectory $x(t) \to 0$ when $t \to \infty$ is ensured under saturation avoidance.

Proof. The proof follows a reasoning similar to the one of Proposition 3.3.2, thus is omitted. ■

Hence, if condition (4.11) is satisfied, the closed-loop LPV dynamics (4.4) can be simplified to the following for design purposes:

$$\dot{x} = \underbrace{\left(\mathbb{A}(\vartheta,\varphi) + \mathbb{B}(\vartheta)\mathbb{K}(\vartheta,\varphi)\right)}_{\mathbb{A}_{cl}(\vartheta,\varphi)} x + \mathbb{B}_w(\vartheta)w, \tag{4.12a}$$

$$z_\infty = \underbrace{\left(\mathbb{C}_z(\vartheta) + D_{zu}(\vartheta)\mathbb{K}(\vartheta,\varphi)\right)}_{\mathbb{C}_{z,cl}(\vartheta,\varphi)} x + D_{zw}(\vartheta)w. \tag{4.12b}$$

4.4 Controller design using a parameter-dependent quadratic Lyapunov function

The design conditions stated in Section 3.5 can be extended to the shifting output-feedback case and solve the problems formulated in Section 4.2 with the use of a parameter-dependent quadratic Lyapunov function as:

$$V(x,\vartheta,\varphi) = x^\top P(\vartheta,\varphi)^{-1} x, \quad P(\vartheta,\varphi) \in \mathbb{S}_+^{2n_x}, \quad \forall(\vartheta,\varphi) \in \Theta \times \Phi \tag{4.13}$$

and its associated unit level set:

$$\mathcal{E}(P(\vartheta,\varphi),1) \triangleq \left\{x \in \mathbb{R}^{2n_x} \,:\, V(x,\vartheta,\varphi) \leq 1\right\}. \tag{4.14}$$

Let us recall below some useful properties from the literature that address the problem of designing dynamic output-feedback controllers. According to [7, 34, 106], a change of control variables is needed, which is achieved by partitioning the Lyapunov matrices $P(\vartheta,\varphi)$ and $P(\vartheta,\varphi)^{-1}$, as follows:

$$P(\vartheta,\varphi) = \begin{bmatrix} R(\vartheta,\varphi) & M(\vartheta,\varphi) \\ M(\vartheta,\varphi)^{\mathsf{T}} & \bullet \end{bmatrix}, \quad P(\vartheta,\varphi)^{-1} = \begin{bmatrix} S(\vartheta,\varphi) & N(\vartheta,\varphi) \\ N(\vartheta,\varphi)^{\mathsf{T}} & \bullet \end{bmatrix}, \tag{4.15}$$

where $\bullet$ represents an element that does not influence further developments and $R(\vartheta,\varphi) \in \mathbb{S}_+^{n_x}$, $S(\vartheta,\varphi) \in \mathbb{S}_+^{n_x}$, $N(\vartheta,\varphi) \in \mathbb{R}^{n_x \times n_x}$ and $M(\vartheta,\varphi) \in \mathbb{R}^{n_x \times n_x}$ are parameter-dependent matrices to be determined. From the identity $P(\vartheta,\varphi)P(\vartheta,\varphi)^{-1} = \mathrm{I}_{n_x}$, the following relationship can be established:

$$P(\vartheta,\varphi)\underbrace{\begin{bmatrix} \mathrm{I}_{n_x} & S(\vartheta,\varphi) \\ 0 & N(\vartheta,\varphi)^{\mathsf{T}} \end{bmatrix}}_{\Pi_S(\vartheta,\varphi)} = \underbrace{\begin{bmatrix} R(\vartheta,\varphi) & \mathrm{I}_{n_x} \\ M(\vartheta,\varphi)^{\mathsf{T}} & 0 \end{bmatrix}}_{\Pi_R(\vartheta,\varphi)} \tag{4.16}$$

with $\Pi_S(\vartheta,\varphi)$ and $\Pi_R(\vartheta,\varphi)$ nonsingular matrices. Then, it follows that:

$$\mathrm{I}_{n_x} - S(\vartheta,\varphi)R(\vartheta,\varphi) = N(\vartheta,\varphi)M(\vartheta,\varphi)^{\mathsf{T}},$$

from which the following identity may be deduced:

$$-\left(\dot{S}(\vartheta,\varphi)R(\vartheta,\varphi) + \dot{N}(\vartheta,\varphi)M(\vartheta,\varphi)^{\mathsf{T}}\right) = S(\vartheta,\varphi)\dot{R}(\vartheta,\varphi) + N(\vartheta,\varphi)\dot{M}(\vartheta,\varphi)^{\mathsf{T}}. \tag{4.17}$$

By considering $\dot{P}(\vartheta,\varphi) = -P(\vartheta,\varphi)\dot{P}(\vartheta,\varphi)^{-1}P(\vartheta,\varphi)$, the relationship (4.16), and the identity (4.17), the following result can be obtained:

$$\Pi_S(\vartheta,\varphi)^{\mathsf{T}}\dot{P}(\vartheta,\varphi)\Pi_S(\vartheta,\varphi) = \underbrace{\begin{bmatrix} \dot{R}(\vartheta,\varphi) & \dot{R}(\vartheta,\varphi)S(\vartheta,\varphi) + \dot{M}(\vartheta,\varphi)N(\vartheta,\varphi)^{\mathsf{T}} \\ \star & -\dot{S}(\vartheta,\varphi) \end{bmatrix}}_{-\Pi_R(\vartheta,\varphi)^{\mathsf{T}}\dot{P}(\vartheta,\varphi)^{-1}\Pi_R(\vartheta,\varphi)}. \tag{4.18}$$

The extension of Theorems 3.5.1, 3.5.3, 3.5.4 and 3.5.5, and Corollary 3.5.2 to the shifting output-feedback case is presented in the next results, where the shorthand notation $\varrho = [\vartheta^{\mathsf{T}}, \varphi^{\mathsf{T}}]^{\mathsf{T}}$ has been used for simplicity and readability.

Theorem 4.4.1 (GSDR performance of LPV systems via shifting output-feedback control)**.** *Consider the closed-loop LPV system* (4.12a) *with* $\mathbb{B}_w(\vartheta) = 0$ *and a given desired guaranteed shifting decay rate* $\mathrm{d_R}(\varphi) \in \mathbb{R}_+$. *Suppose that there exist continuously differentiable matrices* $R(\varrho) \in \mathbb{S}_+^{n_x}$ *and* $S(\varrho) \in \mathbb{S}_+^{n_x}$, *and matrices* $\hat{A}_c(\varrho) \in \mathbb{R}^{n_x \times n_x}$, $\hat{B}_c(\varrho) \in \mathbb{R}^{n_x \times n_y}$, $\hat{C}_c(\varrho) \in \mathbb{R}^{n_u \times n_x}$ *and*

$\hat{D}_c(\varrho) \in \mathbb{R}^{n_u \times n_y}$ such that $\forall(\vartheta, \dot{\vartheta}) \in \Theta \times \Theta_d$ and $\forall(\varphi, \dot{\varphi}) \in \Phi \times \Phi_d$ the following conditions are satisfied:

$$\begin{bmatrix} R(\varrho) & \mathrm{I}_{n_x} \\ \mathrm{I}_{n_x} & S(\varrho) \end{bmatrix} \succ 0, \tag{4.19}$$

$$\begin{bmatrix} \Psi^{\varrho}_{[11]} & \Psi^{\varrho}_{[12]} \\ \star & \Psi^{\varrho}_{[22]} \end{bmatrix} + 2\mathrm{d}_{\mathrm{R}}(\varphi) \begin{bmatrix} R(\varrho) & \mathrm{I}_{n_x} \\ \mathrm{I}_{n_x} & S(\varrho) \end{bmatrix} \prec 0, \tag{4.20}$$

where the block elements of $\Psi(\varrho)$ are defined as:

$$\begin{aligned} \Psi^{\varrho}_{[11]} &\triangleq \mathrm{He}\big\{A(\vartheta)R(\varrho) + B(\vartheta)\hat{C}_c(\varrho)\big\} - \dot{R}(\varrho), \\ \Psi^{\varrho}_{[12]} &\triangleq A(\vartheta) + B(\vartheta)\hat{D}_c(\varrho)C(\vartheta) + \hat{A}_c^{\mathsf{T}}(\varrho), \\ \Psi^{\varrho}_{[22]} &\triangleq \mathrm{He}\big\{S(\varrho)A(\vartheta) + \hat{B}_c(\varrho)C(\vartheta)\big\} + \dot{S}(\varrho). \end{aligned} \tag{4.21}$$

Then, the closed-loop LPV response (4.12a) with $\mathbb{B}_w(\vartheta) = 0$ satisfies (4.5) if the parameter-dependent controller matrices in (4.3) are computed as:

$$\begin{cases} D_c(\varrho) = \hat{D}_c(\varrho), \\ C_c(\varrho) = \big(\hat{C}_c(\varrho) - \hat{D}_c(\varrho)C(\vartheta)R(\varrho)\big)M(\varrho)^{-\mathsf{T}}, \\ B_c(\varrho) = N(\varrho)^{-1}\big(\hat{B}_c(\varrho) - S(\varrho)B(\vartheta)\hat{D}_c(\varrho)\big), \\ A_c(\varrho) = N(\varrho)^{-1}\big[S(\varrho)\dot{R}(\varrho) + N(\varrho)\dot{M}(\varrho)^{\mathsf{T}} + \hat{A}_c(\varrho) \\ \qquad\quad - S(\varrho)\big(A(\vartheta) - B(\vartheta)\hat{D}_c(\varrho)C(\vartheta)\big)R(\varrho) \\ \qquad\quad - \hat{B}_c(\varrho)C(\vartheta)R(\varrho) - S(\varrho)B(\vartheta)\hat{C}_c(\varrho)\big]M(\varrho)^{-\mathsf{T}}, \end{cases} \tag{4.22}$$

where the nonsingular square matrices $N(\varrho) \in \mathbb{R}^{n_x \times n_x}$ and $M(\varrho) \in \mathbb{R}^{n_x \times n_x}$ satisfy the factorization problem: $\mathrm{I}_{n_x} - S(\varrho)R(\varrho) = N(\varrho)M(\varrho)^{\mathsf{T}}$.

Proof. The proof follows the reasoning in Theorem 3.5.1. The condition (4.5) can be defined $\forall x \neq 0$ as a parameter-dependent BMI by means of the closed-loop LPV dynamics (4.12a) with $\mathbb{B}_w(\vartheta) = 0$ and the PDQLF (4.13), thus obtaining:

$$\mathrm{He}\big\{P(\varrho)^{-1}\mathbb{A}_{cl}(\varrho)\big\} + \dot{P}(\varrho)^{-1} + 2\mathrm{d}_{\mathrm{R}}(\varphi)P(\varrho)^{-1} \prec 0. \tag{4.23}$$

Then, let us pre- and post-multiply (4.23) by $P(\varrho)$ getting:

$$\mathrm{He}\{\mathbb{A}_{cl}(\varrho)P(\varrho)\} + P(\varrho)\dot{P}(\varrho)^{-1}P(\varrho) + 2\mathrm{d}_{\mathrm{R}}(\varphi)P(\varrho) \prec 0. \tag{4.24}$$

Let us now define the change of controller variables by pre- and post-multiplying (4.24) by $\Pi_S^{\mathsf{T}}(\varrho)$ and $\Pi_S(\varrho)$, respectively, thus obtaining:

$$\Pi_S^{\mathsf{T}}(\varrho)\big(\mathrm{He}\{\mathbb{A}_{cl}(\varrho)P(\varrho)\} + P(\varrho)\dot{P}(\varrho)^{-1}P(\varrho) + 2\mathrm{d}_{\mathrm{R}}(\varphi)P(\varrho)\big)\Pi_S(\varrho) \prec 0. \tag{4.25}$$

Thereupon, (4.25) is rewritten by means of relations (4.16) and (4.18), as follows:

$$\mathrm{He}\left\{\Pi_S^{\mathsf{T}}(\varrho)\mathbb{A}_{cl}(\varrho)\Pi_R(\varrho)\right\} - \Pi_S^{\mathsf{T}}(\varrho)\dot{P}(\varrho)\Pi_S(\varrho) + 2\mathrm{d_R}(\varphi)\Pi_S^{\mathsf{T}}(\varrho)\Pi_R(\varrho) \prec 0, \tag{4.26}$$

thus obtaining the parameter-dependent LMI described in (4.20) with:

$$\Psi(\varrho) = \mathrm{He}\left\{\Pi_S^{\mathsf{T}}(\varrho)\mathbb{A}_{cl}(\varrho)\Pi_R(\varrho)\right\} - \Pi_S^{\mathsf{T}}(\varrho)\dot{P}(\varrho)\Pi_S(\varrho), \quad \Pi_S^{\mathsf{T}}(\varrho)\Pi_R(\varrho) = \begin{bmatrix} R(\varrho) & \mathrm{I}_{n_x} \\ \mathrm{I}_{n_x} & S(\varrho) \end{bmatrix}.$$

Furthermore, the block elements of $\Psi(\varrho)$ defined in (4.21) contains the controller change of variables:

$$\begin{cases} \hat{D}_c(\varrho) = D_c(\varrho), \\ \hat{C}_c(\varrho) = C_c(\varrho)M(\varrho)^{\mathsf{T}} + \hat{D}_c(\varrho)C(\vartheta)R(\varrho), \\ \hat{B}_c(\varrho) = N(\varrho)B_c(\varrho) + S(\varrho)B(\vartheta)\hat{D}_c(\varrho), \\ \hat{A}_c(\varrho) = N(\varrho)A_c(\varrho)M(\varrho)^{\mathsf{T}} - S(\varrho)\dot{R}(\varrho) - N(\varrho)\dot{M}(\varrho)^{\mathsf{T}} \\ \qquad\quad + S(\varrho)\big(A(\vartheta) - B(\vartheta)\hat{D}_c(\varrho)C(\vartheta)\big)R(\varrho) \\ \qquad\quad + \hat{B}_c(\varrho)C(\vartheta)R(\varrho) + S(\varrho)B(\vartheta)\hat{C}_c(\varrho), \end{cases} \tag{4.27}$$

thus allowing the obtention of the parameter-dependent controller matrices in (4.3) through the expression (4.22).

Finally, the positive definiteness of the PDQLF (4.13) $\forall x \neq 0$ is conditioned by $P(\varrho) \succ 0$, which is equivalent to:

$$\Pi_S^{\mathsf{T}}(\varrho)P(\varrho)\Pi_S(\varrho) \succ 0 \Rightarrow \Pi_S^{\mathsf{T}}(\varrho)\Pi_R(\varrho) \succ 0$$

through the relation (4.16), thus obtaining the parameter-dependent LMI described in (4.19) and concluding the proof. ■

Remark 4.4.1. If matrices $M(\varrho)$ and $N(\varrho)$ have full row rank, then the computation of $A_c(\varrho)$, $B_c(\varrho)$, $C_c(\varrho)$ and $D_c(\varrho)$ through the decision variables appearing in (4.22) is always possible [34]. Furthermore, parameter-dependent controller matrices in (4.3) are uniquely determined if n_x is equal to the number of controller states, thus implying that $M(\varrho)$ and $N(\varrho)$ are nonsingular square matrices.

Theorem 4.4.2 (PDQB of LPV systems via shifting output-feedback control)**.** *For a given set $\mathcal{E}_w(Q)$ defined as in (2.20), suppose that there exist positive scalars $\lambda_1 \geq \lambda_2$, continuously differentiable matrices $R(\varrho) \in \mathbb{S}_+^{n_x}$ and $S(\varrho) \in \mathbb{S}_+^{n_x}$, and matrices $\hat{A}_c(\varrho) \in \mathbb{R}^{n_x \times n_x}$, $\hat{B}_c(\varrho) \in \mathbb{R}^{n_x \times n_y}$, $\hat{C}_c(\varrho) \in \mathbb{R}^{n_u \times n_x}$ and $\hat{D}_c(\varrho) \in \mathbb{R}^{n_u \times n_y}$ such that $\forall\left(\vartheta, \dot{\vartheta}\right) \in \Theta \times \Theta_d$ and $\forall(\varphi, \dot{\varphi}) \in \Phi \times \Phi_d$ condition (4.19) is satisfied together with:*

$$\begin{bmatrix} \Psi_{[11]}^{\varrho} & \Psi_{[12]}^{\varrho} & B_w(\vartheta) \\ \star & \Psi_{[22]}^{\varrho} & S(\varrho)B_w(\vartheta) \\ \star & \star & -\lambda_2 Q^{-1} \end{bmatrix} + \lambda_1 \,\mathrm{diag}\left\{\begin{bmatrix} R(\varrho) & \mathrm{I}_{n_x} \\ \mathrm{I}_{n_x} & S(\varrho) \end{bmatrix}, 0\right\} \preceq 0, \tag{4.28}$$

where block elements $\Psi^{\varrho}_{[11]}$, $\Psi^{\varrho}_{[12]}$ *and* $\Psi^{\varrho}_{[22]}$ *have the same definition as in Theorem 4.4.1. Then, the shifting output-feedback controller* (4.3)*, whose parameter-dependent matrices are given as* (4.22)*, guarantees that the closed-loop LPV response* (4.12a) *is quadratically bounded with a PDQLF* (4.13)*.*

Proof. The same procedure as in Section 2.2.3 is used. Let us prove that the closed-loop LPV dynamics (4.12a) are quadratically bounded with a PDQLF (4.13) by ensuring that $\dot{V}(x,\varrho) \leq 0 \ \forall (x,\varrho,w)$ such that $V(x,\varrho) \geq 1$ and $w \in \mathcal{E}_w(Q)$. To this end, the following parameter-dependent LMI is obtained from condition (2.32) in Theorem 2.2.4, by considering the closed-loop matrix $\mathbb{A}_{cl}(\varrho)$ instead of $A(\vartheta)$, the closed-loop matrix $\mathbb{B}_w(\varrho)$ instead of the disturbance matrix $B_w(\vartheta)$, and that $P(\vartheta)^{-1}$ and $\dot{P}(\vartheta)^{-1}$ depend on ϱ instead of ϑ:

$$\begin{bmatrix} \mathrm{He}\{P(\varrho)^{-1}\mathbb{A}_{cl}(\varrho)\} + \dot{P}(\varrho)^{-1} + \lambda_1 P(\varrho)^{-1} & P(\varrho)^{-1}\mathbb{B}_w(\vartheta) \\ \star & -\lambda_2 Q^{-1} \end{bmatrix} \leq 0. \tag{4.29}$$

By pre- and post-multiplying (4.29) by $\mathrm{diag}\{P(\varrho), \mathrm{I}_{n_w}\}$, one gets:

$$\begin{bmatrix} \mathrm{He}\{\mathbb{A}_{cl}(\varrho)P(\varrho)\} + P(\varrho)\dot{P}(\varrho)^{-1}P(\varrho) + \lambda_1 P(\varrho) & \mathbb{B}_w(\vartheta) \\ \star & -\lambda_2 Q^{-1} \end{bmatrix} \leq 0. \tag{4.30}$$

Thereupon, a congruence transformation with $\mathrm{diag}\{\Pi_S(\varrho), \mathrm{I}_{n_w}\}$ is applied to (4.30) using the relationships (4.16) and (4.18), thus obtaining the following inequality:

$$\begin{bmatrix} \Psi(\varrho) + \lambda_1 \Pi_S^{\mathsf{T}}(\varrho)\Pi_R(\varrho) & \Pi_S^{\mathsf{T}}(\varrho)\mathbb{B}_w(\vartheta) \\ \star & -\lambda_2 Q^{-1} \end{bmatrix} \leq 0 \tag{4.31}$$

where $\Pi_S^{\mathsf{T}}(\varrho)\Pi_R(\varrho) = \begin{bmatrix} R(\varrho) & \mathrm{I}_{n_x} \\ \mathrm{I}_{n_x} & S(\varrho) \end{bmatrix}$, $\Pi_S^{\mathsf{T}}(\varrho)\mathbb{B}_w(\vartheta) = \begin{bmatrix} B_w(\vartheta) \\ S(\varrho)B_w(\varrho) \end{bmatrix}$, and $\Psi(\varrho)$ has the same definition as in Theorem 4.4.1. Finally, the parameter-dependent LMI (4.28) is obtained by expanding the condition (4.31), thus concluding the proof. ∎

Theorem 4.4.3 (PDQ shifting $\mathcal{H}_\infty$ output-feedback control for LPV systems)**.** *Suppose that there exist continuously differentiable matrices* $R(\varrho) \in \mathbb{S}^{n_x}_+$ *and* $S(\varrho) \in \mathbb{S}^{n_x}_+$*, matrices* $\hat{A}_c(\varrho) \in \mathbb{R}^{n_x \times n_x}$*,* $\hat{B}_c(\varrho) \in \mathbb{R}^{n_x \times n_y}$*,* $\hat{C}_c(\varrho) \in \mathbb{R}^{n_u \times n_x}$ *and* $\hat{D}_c(\varrho) \in \mathbb{R}^{n_u \times n_y}$*, and a function* $\gamma(\varphi) \in \mathbb{R}_+ \backslash \{0\}$ *such that* $\forall \left(\vartheta, \dot{\vartheta}\right) \in \Theta \times \Theta_d$ *and* $\forall (\varphi, \dot{\varphi}) \in \Phi \times \Phi_d$ *condition* (4.19) *is satisfied together with:*

$$\begin{bmatrix} \Psi^{\varrho}_{[11]} & \Psi^{\varrho}_{[12]} & B_w(\vartheta) & R(\varrho)C_z^{\mathsf{T}}(\vartheta) + \hat{C}_c^{\mathsf{T}}(\varrho)D_{zu}^{\mathsf{T}}(\vartheta) \\ \star & \Psi^{\varrho}_{[22]} & S(\varrho)B_w(\vartheta) & C_z^{\mathsf{T}}(\vartheta) + C^{\mathsf{T}}(\vartheta)\hat{D}_c^{\mathsf{T}}(\varrho)D_{zu}^{\mathsf{T}}(\vartheta) \\ \star & \star & -\gamma(\varphi)\mathrm{I}_{n_w} & D_{zw}^{\mathsf{T}}(\vartheta) \\ \star & \star & \star & -\gamma(\varphi)\mathrm{I}_{n_{z_\infty}} \end{bmatrix} \prec 0, \tag{4.32}$$

where block elements $\Psi^{\varrho}_{[11]}$, $\Psi^{\varrho}_{[12]}$ *and* $\Psi^{\varrho}_{[22]}$ *have the same definition as in Theorem 4.4.1. Then, the shifting output-feedback controller* (4.3)*, whose parameter-dependent matrices are given as* (4.22)*, guarantees that the closed-loop LPV response* (4.12) *with* $\|w\|_2 \leq 1$ *satisfies* (4.6)*.*

Proof. The proof follows a reasoning similar to the one of Theorem 4.4.2 for condition (2.42) in Theorem 2.2.6, thus is omitted. ∎

Let us provide the conditions for solving Problems 4.2.1 and 4.2.2. The set of inclusions (4.11) in Proposition 4.3.1 forces the state trajectory to remain in $\mathcal{L}(\mathbb{K}(\varrho), \hat{\sigma}(\varphi))$ where the function (4.2) behaves linearly. By defining the region:

$$\mathcal{X}_p \triangleq \left\{x_p \in \mathbb{R}^{n_x} : x_p^\top X_p^{-1} x_p \leq 1\right\}, \tag{4.33}$$

where $X_p \in \mathbb{S}_+^{n_x}$ is a chosen matrix that contains the information about where the initial states $x_p(0)$ are expected to lie, then $x_p(0) \in \mathcal{X}_p$ ensures that any state trajectory $x(t) \in \mathcal{E}(P(\varrho), 1)$ $\forall t \geq 0$ under the assumption that $x_c(0) = 0$ [6]. Hence, the inclusion $\mathcal{X}_0 \subset \mathcal{E}(P(\varrho), 1)$ in (4.11) is modified as:

$$\mathcal{X}_p \subset \mathcal{E}(P(\varrho), 1)|_{(x_p(0),0)}. \tag{4.34}$$

Theorem 4.4.4. *Given the known matrix $X_p^{-1} \in \mathbb{S}_+^{n_x}$ and a desired guaranteed shifting decay rate $\mathrm{d_R}(\varphi) \in \mathbb{R}_+$, suppose that the initial controller's state is $x_c(0) = 0$ and that there exist continuously differentiable matrices $R(\varrho) \in \mathbb{S}_+^{n_x}$ and $S(\varrho) \in \mathbb{S}_+^{n_x}$, and matrices $\hat{A}_c(\varrho) \in \mathbb{R}^{n_x \times n_x}$, $\hat{B}_c(\varrho) \in \mathbb{R}^{n_x \times n_y}$, $\hat{C}_c(\varrho) \in \mathbb{R}^{n_u \times n_x}$ and $\hat{D}_c(\varrho) \in \mathbb{R}^{n_u \times n_y}$ such that $\forall\left(\vartheta, \dot{\vartheta}\right) \in \Theta \times \Theta_d$ and $\forall(\varphi, \dot{\varphi}) \in \Phi \times \Phi_d$ conditions (4.19) and (4.20) are satisfied together with:*

$$X_p^{-1} - S(\varrho) \succeq 0, \tag{4.35}$$

$$\begin{bmatrix} \hat{\sigma}_l(\varphi) & \hat{C}_{c[l]}(\varrho) & \hat{D}_{c[l]}(\varrho)C(\vartheta) \\ \star & R(\varrho) & \mathrm{I}_{n_x} \\ \star & \star & S(\varrho) \end{bmatrix} \succeq 0, \quad \forall l \in \mathcal{I}_{[1,n_u]}. \tag{4.36}$$

Then, the shifting output-feedback controller (4.3), whose parameter-dependent matrices are given as (4.22), guarantees that the closed-loop LPV dynamics (4.4a) with $\mathbb{B}_w(\vartheta) = 0$ satisfy (4.5). Furthermore, the convergence of $x(t) \to 0$ when $t \to \infty$ for any $x_0 \in \mathcal{X}_0$ is ensured such that $x(t) \in \mathcal{L}(\mathbb{K}(\varrho(t)), \sigma(t))$, and hence, $u(t) \in \mathcal{L}(u(t), \sigma(t))$.

Proof. The proof of conditions (4.19) and (4.20) are stated in Theorem 4.4.1 and thus are omitted. Then, consider the set of inclusions (4.11) where $\mathcal{X}_0 \subset \mathcal{E}(P(\varrho), 1)$ can be expressed under the assumption that the initial controller state $x_c(0) = 0$, as follows:

$$\begin{bmatrix} x_p(0) \\ 0 \end{bmatrix}^\top P(\varrho)^{-1} \begin{bmatrix} x_p(0) \\ 0 \end{bmatrix} \leq \begin{bmatrix} x_p(0) \\ 0 \end{bmatrix}^\top \mathcal{X}_0^{-1} \begin{bmatrix} x_p(0) \\ 0 \end{bmatrix}, \tag{4.37}$$

which is equivalent to the next expression taking into account the modified inclusion (4.34) and the Lyapunov matrix partitioning (4.15):

$$x_p(0)^\top S(\varrho) x_p(0) \leq x_p(0)^\top X_p^{-1} x_p(0). \tag{4.38}$$

Then, manipulating the above expression one gets:

$$X_p^{-1} - S(\varrho) \succeq 0 \tag{4.39}$$

[6] This assumption is made to avoid that matrices $M(\varrho)$ and $N(\varrho)$ appearing as decision variables in the LMIs [129].

thus obtaining the parameter-dependent LMI (4.35) which ensures that any state $\left[x_p^\top(0), 0\right]^\top \in \mathcal{X}_0$ is also contained in $\mathcal{E}(P(\varrho), 1)$.

Similarly, the inclusion $\mathcal{E}(P(\varrho), 1) \subset \mathcal{L}(\mathbb{K}(\varrho), \hat{\sigma}(\varphi))$ can be formulated as the following inequality $\forall l \in \mathcal{I}_{[1,n_u]}$:

$$x^\top \frac{\mathbb{K}_{[l]}^\top(\varrho)\mathbb{K}_{[l]}(\varrho)}{\hat{\sigma}_l(\varphi)} x \leq x^\top P(\varrho)^{-1} x, \tag{4.40}$$

which is equivalent to:

$$P(\varrho)^{-1} - \frac{\mathbb{K}_{[l]}^\top(\varrho)\mathbb{K}_{[l]}(\varrho)}{\hat{\sigma}_l(\varphi)} \succeq 0. \tag{4.41}$$

Then, by pre- and post-multiplying (4.41) by $P(\varrho)$ and the use of Schur's complement, the expression (4.41) becomes:

$$\begin{bmatrix} \hat{\sigma}_l(\varphi) & \mathbb{K}_{[l]}(\varrho)P(\varrho) \\ \star & P(\varrho) \end{bmatrix} \succeq 0. \tag{4.42}$$

Thereupon, let us apply the congruence transformation $\operatorname{diag}\{1, \Pi_S(\varrho)\}$ to (4.42) obtaining:

$$\begin{bmatrix} 1 & 0 \\ 0 & \Pi_S^\top(\varrho) \end{bmatrix} \begin{bmatrix} \hat{\sigma}_l(\varphi) & \mathbb{K}_{[l]}(\varrho)P(\varrho) \\ \star & P(\varrho) \end{bmatrix} \begin{bmatrix} 1 & 0 \\ 0 & \Pi_S(\varrho) \end{bmatrix} \succeq 0, \tag{4.43}$$

which can be rewritten through the relation (4.16) as:

$$\begin{bmatrix} \hat{\sigma}_l(\varphi) & \mathbb{K}_{[l]}(\varrho)\Pi_R(\varrho) \\ \star & \Pi_S^\top(\varrho)\Pi_R(\varrho) \end{bmatrix} \succeq 0. \tag{4.44}$$

The parameter-dependent LMI (4.36) is obtained by considering:

$$\Pi_S^\top(\varrho)\Pi_R(\varrho) = \begin{bmatrix} R(\varrho) & \mathrm{I}_{n_x} \\ \mathrm{I}_{n_x} & S(\varrho) \end{bmatrix},$$

and that the term $\mathbb{K}_{[l]}(\varrho)\Pi_R(\varrho)$ is defined through the change of variables described in (4.27), as follows:

$$\begin{aligned} \mathbb{K}_{[l]}(\varrho)\Pi_R(\varrho) &= \begin{bmatrix} D_{c[l]}(\varrho)C(\vartheta) & C_{c[l]}(\varrho) \end{bmatrix} \begin{bmatrix} R(\varrho) & \mathrm{I}_{n_x} \\ M(\varrho)^\top & 0 \end{bmatrix} \\ &= \begin{bmatrix} \hat{C}_{c[l]}(\varrho) & \hat{D}_{c[l]}(\varrho)C(\vartheta) \end{bmatrix}. \end{aligned} \tag{4.45}$$

Consequently, $x \in \mathcal{L}(\mathbb{K}(\varrho), \hat{\sigma}(\varphi))$ is ensured $\forall x \in \mathcal{E}(P(\varrho), 1)$, and hence, the control input $u(t)$ remains for all $t \geq 0$ in $\mathcal{L}(u(t), \sigma(t))$ as long as $x_0 \in \mathcal{X}_0$, thus concluding the proof. ■

Corollary 4.4.1. *Given the known matrix $X_p^{-1} \in \mathbb{S}_+^{n_x}$, suppose that the controller's initial state is $x_c(0) = 0$ and that there exist positive scalars $\lambda_1 \geq \lambda_2$, continuously differentiable matrices $R(\varrho) \in \mathbb{S}_+^{n_x}$ and $S(\varrho) \in \mathbb{S}_+^{n_x}$, matrices $\hat{A}_c(\varrho) \in \mathbb{R}^{n_x \times n_x}$, $\hat{B}_c(\varrho) \in \mathbb{R}^{n_x \times n_y}$, $\hat{C}_c(\varrho) \in \mathbb{R}^{n_u \times n_x}$ and $\hat{D}_c(\varrho) \in \mathbb{R}^{n_u \times n_y}$, and a function $\gamma(\varphi) \in \mathbb{R}_+ \backslash \{0\}$ such that conditions (4.19), (4.28), (4.32), (4.35) and (4.36) are satisfied $\forall \left(\vartheta, \dot{\vartheta}\right) \in \Theta \times \Theta_d$, $\forall (\varphi, \dot{\varphi}) \in \Phi \times \Phi_d$ and $Q^{-1} = \mathrm{I}_{n_w}$. Then, the shifting output-feedback controller (4.3), whose parameter-dependent matrices are given as (4.22),*

guarantees that the closed-loop LPV dynamics (4.4) *with* $\|w\|_2 \leq 1$ *are quadratically bounded with a PDQLF* (4.13) *against external disturbances satisfying* (4.6). *Furthermore, if* $x_0 \in \mathcal{X}_0$, *then* $x_0 \in \mathcal{E}(P(\varrho), 1)$ *and the control input* $u(t)$ *is such that* $u(t) \in \mathcal{L}(u(t), \sigma(t))$.

Proof. It is a direct consequence of Theorems 4.4.2 and 4.4.3 when $Q^{-1} = \mathrm{I}_{n_w}$, and the stated conditions (4.35) and (4.36) in Theorem 4.4.4. ■

Theorems 4.4.1–4.4.4 and Corollary 4.4.1 result in a designed GS controller (4.3) that is dependent on the time derivative of scheduling vectors (ϑ, φ). Due to the necessity of measuring the rates $(\dot{\vartheta}, \dot{\varphi})$, which are usually not available and their reconstruction is hindered by the presence of measurement noise, the implementation of the controller (4.3) is impracticable. As indicated in [5, 104, 105], this issue can be alleviated at the expense of adding some degree of conservatism by imposing some conditions on the decision variables $R(\varrho)$, $S(\varrho)$, $N(\varrho)$ and $M(\varrho)$, which are summarized in Table 4.1. For instance, row 2 of the table corresponds to possible conditions on the decision variables for designing a practical controller considering the PDQLF (4.13) and bounding rates $\left(\dot{\vartheta}, \dot{\varphi}\right) \in \Theta_d \times \Phi_d$.

Table 4.1: Decision variable conditions in the GS output-feedback control problem.

	Decision variable			
	$R(\varrho)$ defined as	$S(\varrho)$ defined as	$N(\varrho)$ defined as	$M(\varrho)$ defined as
QLF	R	S	N	M
PDQLF	R	$S(\varrho)$	$\mathrm{I}_{n_x} - S(\varrho)R$	I_{n_x}
	$R(\varrho)$	S	I_{n_x}	$\mathrm{I}_{n_x} - R(\varrho)S$

By considering the identity (4.17) and the definitions in Table 4.1, a practical computation of the controller matrices can be derived using the given formulas in (4.22) and updating the expression of $A_c(\varrho)$ to:

$$\begin{aligned} A_c(\varrho) = N(\varrho)^{-1}\big[&\hat{A}_c(\varrho) - S(\varrho)\big(A(\vartheta) - B(\vartheta)\hat{D}_c(\varrho)C(\vartheta)\big)R(\varrho) \\ &-\hat{B}_c(\varrho)C(\vartheta)R(\varrho) - S(\varrho)B(\vartheta)\hat{C}_c(\varrho)\big]M(\varrho)^{-\mathsf{T}}. \end{aligned}$$

Remark 4.4.2. It should be emphasized that since the options for $R(\varrho)$ and $S(\varrho)$ are not equivalent, the case of evaluating parameter-dependent matrices with restrictions on the rate of variation presents a loss of duality [5]. Consequently, for certain problems, it is preferable to assume a constant matrix R and a parameter-dependent matrix $S(\varrho)$, whereas other problems will require the opposite.

4.4.1 Finite-dimensional LMI design conditions

Even with the definition of the decision variables in Table 4.1, the conditions stated by Theorems 4.4.1–4.4.4 and Corollary 4.4.1 involve infinitely number of constraints to be handled. To this end, let us recall the polytopic representation from (3.37):

$$\begin{bmatrix} A(\vartheta) & B_w(\vartheta) & B(\vartheta) \\ C_z(\vartheta) & D_{zw}(\vartheta) & D_{zu}(\vartheta) \end{bmatrix} = \sum_{i=1}^{n_\mu} \mu_i(\vartheta) \begin{bmatrix} A_i & B_{w,i} & B_i \\ C_{z,i} & D_{zw,i} & D_{zu,i} \end{bmatrix}, \tag{4.46a}$$

$$\begin{bmatrix} \hat{\sigma}(\varphi) & \mathrm{d_R}(\varphi) & \gamma(\varphi) \end{bmatrix} = \sum_{j=1}^{n_\eta} \eta_j(\varphi) \begin{bmatrix} \hat{\sigma}_j & \mathrm{d_R}_j & \gamma_j \end{bmatrix}, \tag{4.46b}$$

together with:

$$\begin{bmatrix} \hat{A}_c(\vartheta,\varphi) & \hat{B}_c(\vartheta,\varphi) & R(\vartheta,\varphi) \\ \hat{C}_c(\vartheta,\varphi) & \hat{D}_c(\vartheta,\varphi) & S(\vartheta,\varphi) \end{bmatrix} = \sum_{i=1}^{n_\mu} \sum_{j=1}^{n_\eta} \mu_i(\vartheta)\eta_j(\varphi) \begin{bmatrix} \hat{A}_{c,ij} & \hat{B}_{c,ij} & R_{ij} \\ \hat{C}_{c,ij} & \hat{D}_{c,ij} & S_{ij} \end{bmatrix}, \tag{4.47}$$

where $\hat{A}_{c,ij}$, $\hat{B}_{c,ij}$, etc. correspond to decision vertex matrices with appropriate dimensions, and $\mu(\vartheta) \in \Delta^{n_\mu}$ and $\eta(\varphi) \in \Delta^{n_\eta}$ are the polytopic weight vectors. The simplexes Δ^{n_μ} and Δ^{n_η} are defined as in (2.10) and (2.63), respectively:

$$\Delta^{n_\mu} \triangleq \left\{ \mu(\vartheta) \in \mathbb{R}^{n_\mu} \ : \ \sum_{i=1}^{n_\mu} \mu_i(\vartheta) = 1, \ \mu_i(\vartheta) \geq 0, \ i \in \mathcal{I}_{[1,n_\mu]} \right\}. \tag{4.48}$$

$$\Delta^{n_\eta} \triangleq \left\{ \eta(\varphi) \in \mathbb{R}^{n_\eta} \ : \ \sum_{j=1}^{n_\eta} \eta_j(\varphi) = 1, \ \eta_j(\varphi) \geq 0, \ j \in \mathcal{I}_{[1,n_\eta]} \right\}. \tag{4.49}$$

The time derivative expression of matrices $R(\vartheta,\varphi)$ and $S(\vartheta,\varphi)$ in (4.47) is obtained using a similar procedure to the one presented in Section 3.5:

$$\begin{bmatrix} \dot{R}(\vartheta,\varphi) \\ \dot{S}(\vartheta,\varphi) \end{bmatrix} = \sum_{i=1}^{n_\mu} \sum_{j=1}^{n_\eta} \dot{\mu}_i(\vartheta)\eta_j(\varphi) \begin{bmatrix} R_{ij} \\ S_{ij} \end{bmatrix} + \sum_{i=1}^{n_\mu} \sum_{j=1}^{n_\eta} \mu_i(\vartheta)\dot{\eta}_j(\varphi) \begin{bmatrix} R_{ij} \\ S_{ij} \end{bmatrix}, \tag{4.50}$$

such that $\dot{\mu}(\vartheta) \in \mathcal{P}_{\dot{\mu}} \subset \mathbb{R}^{n_\mu}$ and $\dot{\eta}(\varphi) \in \mathcal{P}_{\dot{\eta}} \subset \mathbb{R}^{n_\eta}$, where:

$$\mathcal{P}_{\dot{\mu}} \triangleq \left\{ \delta_\mu \in \mathbb{R}^{n_\mu} : \delta_\mu = \sum_{m=1}^{n_\alpha} \alpha_m\big(\vartheta,\dot{\vartheta}\big) \mathrm{e}^{\{m\}}, \ \sum_{i=1}^{n_\mu} \mathrm{e}_i^{\{m\}} = 0, \ \begin{array}{c} \forall m \in \mathcal{I}_{[1,n_\alpha]} \\ \alpha\big(\vartheta,\dot{\vartheta}\big) \in \Delta^{n_\alpha} \end{array} \right\}, \tag{4.51}$$

$$\mathcal{P}_{\dot{\eta}} \triangleq \left\{ \delta_\eta \in \mathbb{R}^{n_\eta} : \delta_\eta = \sum_{n=1}^{n_\beta} \beta_n(\varphi,\dot{\varphi}) \mathrm{o}^{\{n\}}, \ \sum_{j=1}^{n_\eta} \mathrm{o}_j^{\{n\}} = 0, \ \begin{array}{c} \forall n \in \mathcal{I}_{[1,n_\beta]} \\ \beta(\varphi,\dot{\varphi}) \in \Delta^{n_\beta} \end{array} \right\}, \tag{4.52}$$

with $\alpha\big(\vartheta,\dot{\vartheta}\big) \in \Delta^{n_\alpha}$ and $\beta(\varphi,\dot{\varphi}) \in \Delta^{n_\beta}$ being the polytopic weight vectors [7], and vectors $\mathrm{e}^{\{m\}} \in \mathbb{R}^{n_\mu}$ and $\mathrm{o}^{\{n\}} \in \mathbb{R}^{n_\eta}$ as the vertices of the polytopes $\mathcal{P}_{\dot{\mu}}$ and $\mathcal{P}_{\dot{\eta}}$, respectively.

[7] Due to the similarities with (4.48) and (4.49), the definitions of Δ^{n_α} and Δ^{n_β} are omitted. See (3.76) and (3.77) for further details.

Then, the following result holds.

Lemma 4.4.5. *Consider a finite number of vectors* $\mathrm{e}^{\{m\}}$ *and* $\mathrm{o}^{\{n\}}$ *for which* (4.51) *and* (4.52) *hold, the polytopic representation of matrices* $R(\vartheta,\varphi)$ *and* $S(\vartheta,\varphi)$ *described in* (4.47) *and its time derivative expression* (4.50)*, then it follows for* $i,a \in \mathcal{I}_{[1,n_\mu]}$, $j,b \in \mathcal{I}_{[1,n_\eta]}$, $m \in \mathcal{I}_{[1,n_\alpha]}$ *and* $n \in \mathcal{I}_{[1,n_\beta]}$*:*

$$\begin{aligned}\begin{bmatrix}\dot{R}(\vartheta,\varphi)\\ \dot{S}(\vartheta,\varphi)\end{bmatrix} &= \sum_{i=1}^{n_\mu}\sum_{j=1}^{n_\eta}\sum_{m=1}^{n_\alpha}\sum_{n=1}^{n_\beta}\mu_i(\vartheta)\eta_j(\varphi)\alpha_m\big(\vartheta,\dot{\vartheta}\big)\beta_n(\varphi,\dot{\varphi})\\ &\quad\times\begin{bmatrix}\sum_{a=1}^{n_\mu}\mathrm{e}_a^{\{m\}}R_{aj}+\sum_{b=1}^{n_\eta}\mathrm{o}_b^{\{n\}}R_{ib}\\ \sum_{a=1}^{n_\mu}\mathrm{e}_a^{\{m\}}S_{aj}+\sum_{b=1}^{n_\eta}\mathrm{o}_b^{\{n\}}S_{ib}\end{bmatrix},\end{aligned} \tag{4.53}$$

where $\mu(\vartheta) \in \Delta^{n_\mu}$, $\eta(\varphi) \in \Delta^{n_\eta}$, $\alpha\big(\vartheta,\dot{\vartheta}\big) \in \Delta^{n_\alpha}$ *and* $\beta(\varphi,\dot{\varphi}) \in \Delta^{n_\beta}$ *correspond to some polytopic weight vectors.*

Proof. The proof follows a reasoning similar to the one of Lemma 3.5.6, thus is omitted. ■

Taking into account the definition of the decision variables in Table 4.1 for the QLF case, it is possible to reduce the design conditions provided by Theorems 4.4.1–4.4.4 and Corollary 4.4.1 to a finite number of matrix inequalities, as indicated by the following corollaries.

Corollary 4.4.2. *Given the desired guaranteed shifting decay rate vertices* $\mathrm{d}_{\mathrm{R}j} \in \mathbb{R}_+$ *and a previously chosen relaxation degree* $d \in \mathbb{N}$ *with* $d \geq 3$*, let there exist matrices* $R \in \mathbb{S}_+^{n_x}$, $S \in \mathbb{S}_+^{n_x}$, $\hat{A}_{c,ij} \in \mathbb{R}^{n_x\times n_x}$, $\hat{B}_{c,ij} \in \mathbb{R}^{n_x\times n_y}$, $\hat{C}_{c,ij} \in \mathbb{R}^{n_u\times n_x}$ *and* $\hat{D}_{c,ij} \in \mathbb{R}^{n_u\times n_y}$ *with* $i \in \mathcal{I}_{[1,n_\mu]}$ *and* $j \in \mathcal{I}_{[1,n_\eta]}$ *such that the following set of LMIs is satisfied:*

$$\begin{bmatrix}R & \mathrm{I}_{n_x}\\ \mathrm{I}_{n_x} & S\end{bmatrix} \succ 0, \tag{4.54}$$

$$\sum_{\boldsymbol{p}\in\mathcal{P}(\boldsymbol{i})}\left(\Psi_{\boldsymbol{p}j}+2\mathrm{d}_{\mathrm{R}j}\begin{bmatrix}R & \mathrm{I}_{n_x}\\ \mathrm{I}_{n_x} & S\end{bmatrix}\right) \prec 0, \quad \forall \boldsymbol{i} \in \mathbb{I}^+_{(d,n_\mu)}, \tag{4.55}$$

where $\Psi_{\boldsymbol{p}j}$ *is given as:*

$$\Psi_{\boldsymbol{p}j} \triangleq \begin{bmatrix}\mathrm{He}\big\{A_{p_1}R+B_{p_1}\hat{C}_{c,p_2j}\big\} & A_{p_1}+B_{p_1}\hat{D}_{c,p_2j}C_{p_3}+\hat{A}_{c,p_1j}^{\top}\\ \star & \mathrm{He}\big\{SA_{p_1}+\hat{B}_{c,p_1j}C_{p_2}\big\}\end{bmatrix}.$$

Then, Theorem 4.4.1 holds for all parameter-dependent terms appearing in (4.46) *and* (4.47)*.*

Proof. The proof is divided into two parts. Considering the design conditions that correspond to the QLF case in Table 4.1, the first part shows how one obtains the LMI (4.54). Similarly, the second part demonstrates the finite representation of the parameter-dependent LMI (4.20) through the polytopic representations (4.46) and (4.47), and the utilization of Lemma 2.2.14.

Part 1: The LMI (4.54) follows from (4.19) in Theorem 4.4.1 when $R(\varrho) = R$ and $S(\varrho) = S$.

Part 2: Given that $(\mu(\vartheta), \eta(\varphi)) \in \Delta^{n_\mu} \times \Delta^{n_\eta}$, $R(\varrho) = R$ and $S(\varrho) = S$, the parameter-dependent LMI (4.20) can be expressed using (4.46) and (4.47), as follows:

$$\sum_{i_1=1}^{n_\mu}\sum_{i_2=1}^{n_\mu}\sum_{i_3=1}^{n_\mu}\sum_{j=1}^{n_\eta}\mu_{i_1}(\vartheta)\mu_{i_2}(\vartheta)\mu_{i_3}(\vartheta)\eta_j(\varphi)\left(\Psi_{i_1i_2i_3j} + 2\,\mathrm{d}_{\mathrm{R}j}\begin{bmatrix} R & \mathrm{I}_{n_x} \\ \mathrm{I}_{n_x} & S \end{bmatrix}\right) \prec 0, \tag{4.56}$$

where:

$$\Psi_{i_1i_2i_3j} \triangleq \begin{bmatrix} \mathrm{He}\{A_{i_1}R + B_{i_1}\hat{C}_{c,i_2j}\} & A_{i_1} + B_{i_1}\hat{D}_{c,i_2j}C_{i_3} + \hat{A}_{c,i_1j}^{\top} \\ \star & \mathrm{He}\{SA_{i_1} + \hat{B}_{c,i_1j}C_{i_2}\} \end{bmatrix}.$$

Right after, using the multi-index notation presented in Section 2.2.5, the condition (4.56) is rewritten as:

$$\sum_{j=1}^{n_\eta}\eta_j(\varphi)\sum_{\boldsymbol{i}\in\mathbb{I}_{(3,n_\mu)}}\mu_{\boldsymbol{i}}(\vartheta)\left(\Psi_{\boldsymbol{i}j} + 2\,\mathrm{d}_{\mathrm{R}j}\begin{bmatrix} R & \mathrm{I}_{n_x} \\ \mathrm{I}_{n_x} & S \end{bmatrix}\right) \prec 0, \tag{4.57}$$

which, due to a basic property of matrices [53], is equivalent to:

$$\sum_{\boldsymbol{i}\in\mathbb{I}_{(3,n_\mu)}}\mu_{\boldsymbol{i}}(\vartheta)\left(\Psi_{\boldsymbol{i}j} + 2\,\mathrm{d}_{\mathrm{R}j}\begin{bmatrix} R & \mathrm{I}_{n_x} \\ \mathrm{I}_{n_x} & S \end{bmatrix}\right) \prec 0, \quad j \in \mathcal{I}_{[1,n_\eta]}, \tag{4.58}$$

with $\Psi_{\boldsymbol{i}j} = \Psi_{i_1i_2i_3j}$. Then, the set of LMI in (4.55) is derived by applying Lemma 2.2.14 to (4.58), thus ensuring the definiteness of (4.58) and concluding the proof. ■

Corollary 4.4.3. *For fixed positive scalars $\lambda_1 \geq \lambda_2$, a given known matrix $Q^{-1} \in \mathbb{S}_+^{n_w}$ and a previously chosen relaxation degree $d \in \mathbb{N}$ with $d \geq 3$, let there exist matrices $R \in \mathbb{S}_+^{n_x}$, $S \in \mathbb{S}_+^{n_x}$, $\hat{A}_{c,ij} \in \mathbb{R}^{n_x\times n_x}$, $\hat{B}_{c,ij} \in \mathbb{R}^{n_x\times n_y}$, $\hat{C}_{c,ij} \in \mathbb{R}^{n_u\times n_x}$ and $\hat{D}_{c,ij} \in \mathbb{R}^{n_u\times n_y}$ with $i \in \mathcal{I}_{[1,n_\mu]}$ and $j \in \mathcal{I}_{[1,n_\eta]}$ such that condition (4.54) is satisfied together with:*

$$\sum_{\boldsymbol{p}\in\mathcal{P}(\boldsymbol{i})}\left(\Psi_{\boldsymbol{p}j} + \lambda_1\,\mathrm{diag}\left\{\begin{bmatrix} R & \mathrm{I}_{n_x} \\ \mathrm{I}_{n_x} & S \end{bmatrix}, 0\right\}\right) \preceq 0, \quad \forall \boldsymbol{i} \in \mathbb{I}_{(d,n_\mu)}^{+}, \tag{4.59}$$

where $\Psi_{\boldsymbol{p}j}$ is given as:

$$\Psi_{\boldsymbol{p}j} \triangleq \begin{bmatrix} \Psi_{[11]\boldsymbol{p}j} & \Psi_{[12]\boldsymbol{p}j} & B_{w,p_1} \\ \star & \Psi_{[22]\boldsymbol{p}j} & SB_{w,p_1} \\ \star & \star & -\lambda_2 Q^{-1} \end{bmatrix}$$

and block elements $\Psi_{[11]\boldsymbol{p}j}$, $\Psi_{[12]\boldsymbol{p}j}$ and $\Psi_{[22]\boldsymbol{p}j}$ have the same definition as in Corollary 4.4.2. Then, Theorem 4.4.2 holds for all parameter-dependent terms appearing in (4.46) and (4.47).

Proof. Similar to that of Corollary 4.4.2, thus omitted. ■

Corollary 4.4.4. *Given a chosen relaxation degree $d \in \mathbb{N}$ with $d \geq 3$, let there exist matrices $R \in \mathbb{S}_+^{n_x}$, $S \in \mathbb{S}_+^{n_x}$, $\hat{A}_{c,ij} \in \mathbb{R}^{n_x\times n_x}$, $\hat{B}_{c,ij} \in \mathbb{R}^{n_x\times n_y}$, $\hat{C}_{c,ij} \in \mathbb{R}^{n_u\times n_x}$ and $\hat{D}_{c,ij} \in \mathbb{R}^{n_u\times n_y}$, and vertex terms $\gamma_j > 0$ with $i \in \mathcal{I}_{[1,n_\mu]}$ and $j \in \mathcal{I}_{[1,n_\eta]}$ such that condition (4.54) is satisfied together with:*

$$\sum_{\boldsymbol{p}\in\mathcal{P}(\boldsymbol{i})}\Psi_{\boldsymbol{p}j} \prec 0, \quad \forall \boldsymbol{i} \in \mathbb{I}_{(d,n_\mu)}^{+}, \tag{4.60}$$

where $\Psi_{\boldsymbol{p}j}$ is given as:

$$\Psi_{\boldsymbol{p}j} \triangleq \begin{bmatrix} \Psi_{[11]\boldsymbol{p}j} & \Psi_{[12]\boldsymbol{p}j} & B_{w,p_1} & RC_{z,p_1}^{\mathsf{T}} + \hat{C}_{c,p_1j}^{\mathsf{T}} D_{zu,p_2}^{\mathsf{T}} \\ \star & \Psi_{[22]\boldsymbol{p}j} & SB_{w,p_1} & C_{z,p_1}^{\mathsf{T}} + C_{p_1}^{\mathsf{T}} \hat{D}_{c,p_2j}^{\mathsf{T}} D_{zu,p_3}^{\mathsf{T}} \\ \star & \star & -\gamma_j \mathrm{I}_{n_w} & D_{zw,p_1}^{\mathsf{T}} \\ \star & \star & \star & -\gamma_j \mathrm{I}_{n_{z_\infty}} \end{bmatrix}$$

and block elements $\Psi_{[11]\boldsymbol{p}j}$, $\Psi_{[12]\boldsymbol{p}j}$ and $\Psi_{[22]\boldsymbol{p}j}$ have the same definition as in Corollary 4.4.2. Then, Theorem 4.4.3 holds for all parameter-dependent terms appearing in (4.46) and (4.47).

Proof. Similar to that of Corollary 4.4.2, thus omitted. ■

Corollary 4.4.5. *Given a known matrix $X_p^{-1} \in \mathbb{S}_+^{n_x}$, the desired guaranteed shifting decay rate vertices $\mathrm{d}_{\mathrm{R}j} \in \mathbb{R}_+$ and some previously chosen relaxation degrees $d, r \in \mathbb{N}$ with $d \geq 3$ and $r \geq 2$, suppose that the controller's initial state is $x_c(0) = 0$ and that there exist matrices $R \in \mathbb{S}_+^{n_x}$, $S \in \mathbb{S}_+^{n_x}$, $\hat{A}_{c,ij} \in \mathbb{R}^{n_x \times n_x}$, $\hat{B}_{c,ij} \in \mathbb{R}^{n_x \times n_y}$, $\hat{C}_{c,ij} \in \mathbb{R}^{n_u \times n_x}$ and $\hat{D}_{c,ij} \in \mathbb{R}^{n_u \times n_y}$ with $i \in \mathcal{I}_{[1,n_\mu]}$ and $j \in \mathcal{I}_{[1,n_\eta]}$ such that conditions (4.54) and (4.55) are satisfied together with:*

$$X_p^{-1} - S \succeq 0, \tag{4.61}$$

$$\sum_{\boldsymbol{p} \in \mathcal{P}(\boldsymbol{i})} \begin{bmatrix} \hat{\sigma}_{l,j} & \hat{C}_{c[l],p_1j} & \hat{D}_{c[l],p_1j} C_{p_2} \\ \star & R & \mathrm{I}_{n_x} \\ \star & \star & S \end{bmatrix} \succeq 0, \qquad \begin{matrix} \forall \boldsymbol{i} \in \mathbb{I}_{(r,n_\mu)}^{+} \\ l \in \mathcal{I}_{[1,n_u]} \end{matrix} . \tag{4.62}$$

Then, Theorem 4.4.4 holds for all parameter-dependent terms appearing in (4.46) and (4.47).

Proof. Part of the proof follows a reasoning similar to the one of Corollary 4.4.2, and thus is omitted. Then, the LMI (4.61) follows from (4.35) in Theorem 4.4.4 when $S(\varrho) = S$. ■

Corollary 4.4.6. *For fixed positive scalars $\lambda_1 \geq \lambda_2$, a given known matrix $X_p^{-1} \in \mathbb{S}_+^{n_x}$ and some previously chosen relaxation degrees $d, r \in \mathbb{N}$ with $d \geq 3$ and $r \geq 2$, suppose that the controller's initial state is $x_c(0) = 0$ and that there exist matrices $R \in \mathbb{S}_+^{n_x}$, $S \in \mathbb{S}_+^{n_x}$, $\hat{A}_{c,ij} \in \mathbb{R}^{n_x \times n_x}$, $\hat{B}_{c,ij} \in \mathbb{R}^{n_x \times n_y}$, $\hat{C}_{c,ij} \in \mathbb{R}^{n_u \times n_x}$ and $\hat{D}_{c,ij} \in \mathbb{R}^{n_u \times n_y}$, and vertex terms $\gamma_j > 0$ with $i \in \mathcal{I}_{[1,n_\mu]}$ and $j \in \mathcal{I}_{[1,n_\eta]}$ such that conditions (4.54), (4.59), (4.60), (4.61) and (4.62) are satisfied for $Q^{-1} = \mathrm{I}_{n_w}$. Then, Corollary 4.4.1 holds for all parameter-dependent terms appearing in (4.46) and (4.47).*

Proof. It is a direct consequence of Corollaries 4.4.3 and 4.4.4 when $Q^{-1} = \mathrm{I}_{n_w}$, and the stated conditions (4.61) and (4.62) in Corollary 4.4.5. ■

Corollaries 4.4.2–4.4.6 have the drawback of considering the candidate Lyapunov function (4.13) as a parameter-independent QLF, thus introducing some source of conservatism. Notice that the definition of the decision variables that correspond to the rows 2 and 3 in Table 4.1 can be used for alleviating this issue. As a result, for the purpose of simplicity and similarity, the following corollaries are obtained using only the conditions in row 2. Similar corollaries can be obtained for the case in row 3, but they are omitted.

Corollary 4.4.7. *Given a finite number of vectors* $\mathrm{e}^{\{m\}}$ *and* $\mathrm{o}^{\{n\}}$ *for which* (4.51) *and* (4.52) *hold, the desired guaranteed shifting decay rate vertices* $\mathrm{d}_{\mathrm{R}j} \in \mathbb{R}_+$ *and some previously chosen relaxation degrees* $d_1, d_2 \in \mathbb{N}$ *with* $d_1 \geq 3$ *and* $d_2 \geq 2$*, let there exist matrices* $R \in \mathbb{S}_+^{n_x}$*,* $S_{ij} \in \mathbb{S}_+^{n_x}$*,* $\hat{A}_{c,ij} \in \mathbb{R}^{n_x \times n_x}$*,* $\hat{B}_{c,ij} \in \mathbb{R}^{n_x \times n_y}$*,* $\hat{C}_{c,ij} \in \mathbb{R}^{n_u \times n_x}$ *and* $\hat{D}_{c,ij} \in \mathbb{R}^{n_u \times n_y}$ *with* $i \in \mathcal{I}_{[1,n_\mu]}$ *and* $j \in \mathcal{I}_{[1,n_\eta]}$ *such that condition* (4.63) *is satisfied together with* (4.64) $\forall m \in \mathcal{I}_{[1,n_\alpha]}$ *and* $\forall n \in \mathcal{I}_{[1,n_\beta]}$*. Then, Theorem 4.4.1 holds for all parameter-dependent terms appearing in* (4.46)*,* (4.47) *and* (4.53)*.*

$$\begin{bmatrix} R & \mathrm{I}_{n_x} \\ \mathrm{I}_{n_x} & S_{ij} \end{bmatrix} \succ 0, \tag{4.63}$$

$$\sum_{\boldsymbol{q} \in \mathcal{P}(\boldsymbol{j})} \sum_{\boldsymbol{p} \in \mathcal{P}(\boldsymbol{i})} \left(\Psi_{\boldsymbol{p}q_1} + \dot{\Psi}_{p_1 q_1}^{\{m,n\}} + 2\mathrm{d}_{\mathrm{R}q_1} \begin{bmatrix} R & \mathrm{I}_{n_x} \\ \mathrm{I}_{n_x} & S_{p_1 q_2} \end{bmatrix} \right) \prec 0, \qquad \begin{matrix} \forall \boldsymbol{i} \in \mathbb{I}_{(d_1,n_\mu)}^{+} \\ \forall \boldsymbol{j} \in \mathbb{I}_{(d_2,n_\eta)}^{+} \end{matrix} . \tag{4.64}$$

In (4.64)*,* $\Psi_{\boldsymbol{p}q_1}$ *and* $\dot{\Psi}_{p_1 q_1}^{\{m,n\}}$ *are given as:*

$$\Psi_{\boldsymbol{p}q_1} \triangleq \begin{bmatrix} \mathrm{He}\{A_{p_1} R + B_{p_1} \hat{C}_{c,p_2 q_1}\} & A_{p_1} + B_{p_1} \hat{D}_{c,p_2 q_1} C_{p_3} + \hat{A}_{c,p_1 q_1}^{\top} \\ \star & \mathrm{He}\{S_{p_1 q_1} A_{p_2} + \hat{B}_{c,p_1 q_1} C_{p_2}\} \end{bmatrix},$$

$$\dot{\Psi}_{p_1 q_1}^{\{m,n\}} \triangleq \mathrm{diag}\left\{ 0, \sum_{a=1}^{n_\mu} \mathrm{e}_a^{\{m\}} S_{aq_1} + \sum_{b=1}^{n_\eta} \mathrm{o}_b^{\{n\}} S_{p_1 b} \right\}.$$

Proof. The proof is divided into two parts and the polytopic weight vectors' dependency on ϑ, $\dot{\vartheta}$, φ and $\dot{\varphi}$ is omitted from it for clarity's sake. The first part demonstrates how to derive the LMI (4.63) through the polytopic representation (4.47). Similarly, the second part proves the finite representation of the parameter-dependent LMI (4.20) using polytopic representations (4.46), (4.47) and (4.53), as well as Lemma 2.2.14.

Part 1: By means of (4.47), $R(\varrho) = R$ and the fact that $(\mu, \eta) \in \Delta^{n_\mu} \times \Delta^{n_\eta}$, the parameter-dependent LMI (4.19) can be represented as follows:

$$\sum_{i=1}^{n_\mu} \sum_{j=1}^{n_\eta} \mu_i \eta_j \begin{bmatrix} R & \mathrm{I}_{n_x} \\ \mathrm{I}_{n_x} & S_{ij} \end{bmatrix} \succ 0. \tag{4.65}$$

Then, taking into account a property of matrices detailed in [53], (4.65) is guaranteed to be positive-definite if:

$$\begin{bmatrix} R & \mathrm{I}_{n_x} \\ \mathrm{I}_{n_x} & S_{ij} \end{bmatrix} \succ 0, \quad i \in \mathcal{I}_{[1,n_\mu]}, \quad j \in \mathcal{I}_{[1,n_\eta]},$$

thus obtaining the LMI (4.63).

Part 2: Similarly, the parameter-dependent LMI (4.20) can be expressed using (4.46) and (4.47), as follows:

$$\sum_{i_1=1}^{n_\mu} \sum_{i_2=1}^{n_\mu} \sum_{i_3=1}^{n_\mu} \sum_{j_1=1}^{n_\eta} \sum_{j_2=1}^{n_\eta} \mu_{i_1} \mu_{i_2} \mu_{i_3} \eta_{j_1} \eta_{j_2} \left(\Psi_{i_1 i_2 i_3 j_1} + 2\,\mathrm{d}_{\mathrm{R}j_1} \begin{bmatrix} R & \mathrm{I}_{n_x} \\ \mathrm{I}_{n_x} & S_{i_1 j_2} \end{bmatrix} \right) + \dot{\Psi}(\vartheta, \varphi) \prec 0, \tag{4.66}$$

where $\dot{\Psi}(\vartheta,\varphi) \triangleq \operatorname{diag}\{0, \dot{S}(\vartheta,\varphi)\}$ and the term $\Psi_{i_1 i_2 i_3 j_1}$ is defined as:

$$\Psi_{i_1 i_2 i_3 j_1} \triangleq \begin{bmatrix} \operatorname{He}\{A_{i_1} R + B_{i_1} \hat{C}_{c,i_2 j_1}\} & A_{i_1} + B_{i_1} \hat{D}_{c,i_2 j_1} C_{i_3} + \hat{A}_{c,i_1 j_1}^{\top} \\ \star & \operatorname{He}\{S_{i_1 j_1} A_{i_2} + \hat{B}_{c,i_1 j_1} C_{i_2}\} \end{bmatrix}.$$

Let us now replace $\dot{S}(\vartheta,\varphi)$ in (4.66) with the expression provided in (4.53), yielding:

$$\begin{aligned} \sum_{i_1=1}^{n_\mu}\sum_{i_2=1}^{n_\mu}\sum_{i_3=1}^{n_\mu}\sum_{j_1=1}^{n_\eta}\sum_{j_2=1}^{n_\eta} \mu_{i_1}\mu_{i_2}\mu_{i_3}\eta_{j_1}\eta_{j_2}\left(\Psi_{i_1 i_2 i_3 j_1} + 2\,\mathrm{d}_{\mathrm{R}j_1}\begin{bmatrix} R & \mathrm{I}_{n_x} \\ \mathrm{I}_{n_x} & S_{i_1 j_2}\end{bmatrix}\right) \\ + \sum_{i_1=1}^{n_\mu}\sum_{j_1=1}^{n_\eta}\sum_{m=1}^{n_\alpha}\sum_{n=1}^{n_\beta} \mu_{i_1}\eta_{j_1}\alpha_m\beta_n \dot{\Psi}_{i_1 j_1}^{\{m,n\}} \prec 0, \end{aligned} \tag{4.67}$$

which can be rewritten taking into account that the polytopic coefficients appearing in (4.67) sum to one, thus obtaining:

$$\begin{aligned} \sum_{i_1=1}^{n_\mu}\sum_{i_2=1}^{n_\mu}\sum_{i_3=1}^{n_\mu}\sum_{j_1=1}^{n_\eta}\sum_{j_2=1}^{n_\eta}\sum_{m=1}^{n_\alpha}\sum_{n=1}^{n_\beta} \mu_{i_1}\mu_{i_2}\mu_{i_3}\eta_{j_1}\eta_{j_2}\alpha_m\beta_n \\ \times\left(\Psi_{i_1 i_2 i_3 j_1} + \dot{\Psi}_{i_1 j_1}^{\{m,n\}} + 2\,\mathrm{d}_{\mathrm{R}j_1}\begin{bmatrix} R & \mathrm{I}_{n_x} \\ \mathrm{I}_{n_x} & S_{i_1 j_2}\end{bmatrix}\right) \prec 0, \end{aligned} \tag{4.68}$$

where:

$$\dot{\Psi}_{i_1 j_1}^{\{m,n\}} \triangleq \operatorname{diag}\left\{0, \sum_{a=1}^{n_\mu} \mathrm{e}_a^{\{m\}} S_{a j_1} + \sum_{b=1}^{n_\eta} \mathrm{o}_b^{\{n\}} S_{i_1 b}\right\}.$$

By applying the multi-index notation (Section 2.2.5) to (4.68), one gets:

$$\sum_{m=1}^{n_\alpha}\sum_{n=1}^{n_\beta} \alpha_m\beta_n \sum_{\boldsymbol{i}\in\mathbb{I}_{(3,n_\mu)}}\sum_{\boldsymbol{j}\in\mathbb{I}_{(2,n_\eta)}} \mu_{\boldsymbol{i}}\eta_{\boldsymbol{j}}\left(\Psi_{\boldsymbol{i}j_1} + \dot{\Psi}_{i_1 j_1}^{\{m,n\}} + 2\,\mathrm{d}_{\mathrm{R}j_1}\begin{bmatrix} R & \mathrm{I}_{n_x} \\ \mathrm{I}_{n_x} & S_{i_1 j_2}\end{bmatrix}\right) \prec 0, \tag{4.69}$$

which is equivalent to:

$$\sum_{\boldsymbol{i}\in\mathbb{I}_{(3,n_\mu)}}\sum_{\boldsymbol{j}\in\mathbb{I}_{(2,n_\eta)}} \mu_{\boldsymbol{i}}\eta_{\boldsymbol{j}}\left(\Psi_{\boldsymbol{i}j_1} + \dot{\Psi}_{i_1 j_1}^{\{m,n\}} + 2\,\mathrm{d}_{\mathrm{R}j_1}\begin{bmatrix} R & \mathrm{I}_{n_x} \\ \mathrm{I}_{n_x} & S_{i_1 j_2}\end{bmatrix}\right) \prec 0, \quad \begin{matrix} m \in \mathcal{I}_{[1,n_\alpha]} \\ n \in \mathcal{I}_{[1,n_\beta]} \end{matrix}, \tag{4.70}$$

with $\Psi_{\boldsymbol{i}j_1} = \Psi_{i_1 i_2 i_3 j_1}$. Finally, the proof is completed by using Lemma 2.2.14 to ensure the definiteness of (4.70), thus obtaining the set of LMI in (4.64). ■

Corollary 4.4.8. *For fixed positive scalars $\lambda_1 \geq \lambda_2$, a given finite number of vectors $\mathrm{e}^{\{m\}}$ and $\mathrm{o}^{\{n\}}$ for which (4.51) and (4.52) hold, the known matrix $Q^{-1} \in \mathbb{S}_+^{n_w}$ and a previously chosen relaxation degree $d \in \mathbb{N}$ with $d \geq 3$, let there exist matrices $R \in \mathbb{S}_+^{n_x}$, $S_{ij} \in \mathbb{S}_+^{n_x}$, $\hat{A}_{c,ij} \in \mathbb{R}^{n_x \times n_x}$, $\hat{B}_{c,ij} \in \mathbb{R}^{n_x \times n_y}$, $\hat{C}_{c,ij} \in \mathbb{R}^{n_u \times n_x}$ and $\hat{D}_{c,ij} \in \mathbb{R}^{n_u \times n_y}$ with $i \in \mathcal{I}_{[1,n_\mu]}$ and $j \in \mathcal{I}_{[1,n_\eta]}$ such*

that condition (4.63) *is satisfied together with* (4.71) $\forall m \in \mathcal{I}_{[1,n_\alpha]}$ *and* $\forall n \in \mathcal{I}_{[1,n_\beta]}$. *Then, Theorem* 4.4.2 *holds for all parameter-dependent terms appearing in* (4.46), (4.47) *and* (4.53).

$$\sum_{\boldsymbol{p}\in\mathcal{P}(\boldsymbol{i})}\left(\Psi_{\boldsymbol{p}j}+\dot{\Psi}_{p_1j}^{\{m,n\}}+\lambda_1\operatorname{diag}\left\{\begin{bmatrix}R & \mathrm{I}_{n_x}\\ \mathrm{I}_{n_x} & S_{p_1j}\end{bmatrix},0\right\}\right)\preceq 0,\quad \forall \boldsymbol{i}\in\mathbb{I}_{(d,n_\mu)}^{+},\tag{4.71}$$

In (4.71), $\Psi_{\boldsymbol{p}j}$ *and* $\dot{\Psi}_{p_1j}^{\{m,n\}}$ *are given as:*

$$\Psi_{\boldsymbol{p}j}\triangleq\begin{bmatrix}\Psi_{[11]\boldsymbol{p}j} & \Psi_{[12]\boldsymbol{p}j} & B_{w,p_1}\\ \star & \Psi_{[22]\boldsymbol{p}j} & S_{p_1}B_{w,p_2}\\ \star & \star & -\lambda_2 Q^{-1}\end{bmatrix},$$

$$\dot{\Psi}_{p_1j}^{\{m,n\}}\triangleq\operatorname{diag}\left\{0,\sum_{a=1}^{n_\mu}\mathrm{e}_a^{\{m\}}S_{aj}+\sum_{b=1}^{n_\eta}\mathrm{o}_b^{\{n\}}S_{p_1b},0\right\},$$

where block elements $\Psi_{[11]\boldsymbol{p}j}$, $\Psi_{[12]\boldsymbol{p}j}$ *and* $\Psi_{[22]\boldsymbol{p}j}$ *have the same definition as in Corollary* 4.4.7 *with* $q_1 = j$.

Proof. Similar to that of Corollary 4.4.7, thus omitted. ∎

Corollary 4.4.9. *Given a finite number of vectors* $\mathrm{e}^{\{m\}}$ *and* $\mathrm{o}^{\{n\}}$ *for which* (4.51) *and* (4.52) *hold and a previously chosen relaxation degree* $d \in \mathbb{N}$ *with* $d \geq 3$, *let there exist matrices* $R \in \mathbb{S}_+^{n_x}$, $S_{ij} \in \mathbb{S}_+^{n_x}$, $\hat{A}_{c,ij} \in \mathbb{R}^{n_x\times n_x}$, $\hat{B}_{c,ij} \in \mathbb{R}^{n_x\times n_y}$, $\hat{C}_{c,ij} \in \mathbb{R}^{n_u\times n_x}$ *and* $\hat{D}_{c,ij} \in \mathbb{R}^{n_u\times n_y}$, *and vertex terms* $\gamma_j > 0$ *with* $i \in \mathcal{I}_{[1,n_\mu]}$ *and* $j \in \mathcal{I}_{[1,n_\eta]}$ *such that condition* (4.63) *is satisfied together with* (4.72) $\forall m \in \mathcal{I}_{[1,n_\alpha]}$ *and* $\forall n \in \mathcal{I}_{[1,n_\beta]}$. *Then, Theorem* 4.4.3 *holds for all parameter-dependent terms appearing in* (4.46), (4.47) *and* (4.53).

$$\sum_{\boldsymbol{p}\in\mathcal{P}(\boldsymbol{i})}\left(\Psi_{\boldsymbol{p}j}+\dot{\Psi}_{p_1j}^{\{m,n\}}\right)\prec 0,\quad \forall \boldsymbol{i}\in\mathbb{I}_{(d,n_\mu)}^{+}.\tag{4.72}$$

In (4.72), $\Psi_{\boldsymbol{p}j}$ *and* $\dot{\Psi}_{p_1j}^{\{m,n\}}$ *are given as:*

$$\Psi_{\boldsymbol{p}j}\triangleq\begin{bmatrix}\Psi_{[11]\boldsymbol{p}j} & \Psi_{[12]\boldsymbol{p}j} & B_{w,p_1} & RC_{z,p_1}^{\mathsf{T}}+\hat{C}_{c,p_1j}^{\mathsf{T}}D_{zu,p_2}^{\mathsf{T}}\\ \star & \Psi_{[22]\boldsymbol{p}j} & S_{p_1j}B_{w,p_2} & C_{z,p_1}^{\mathsf{T}}+C_{p_1}^{\mathsf{T}}\hat{D}_{c,p_2j}^{\mathsf{T}}D_{zu,p_3}^{\mathsf{T}}\\ \star & \star & -\gamma_j\mathrm{I}_{n_w} & D_{zw,p_1}^{\mathsf{T}}\\ \star & \star & \star & -\gamma_j\mathrm{I}_{n_{z_\infty}}\end{bmatrix}$$

$$\dot{\Psi}_{p_1j}^{\{m,n\}}\triangleq\operatorname{diag}\left\{0,\sum_{a=1}^{n_\mu}\mathrm{e}_a^{\{m\}}S_{aj}+\sum_{b=1}^{n_\eta}\mathrm{o}_b^{\{n\}}S_{p_1b},0,0\right\},$$

where block elements $\Psi_{[11]\boldsymbol{p}j}$, $\Psi_{[12]\boldsymbol{p}j}$ *and* $\Psi_{[22]\boldsymbol{p}j}$ *have the same definition as in Corollary* 4.4.7 *with* $q_1 = j$.

Proof. Similar to that of Corollary 4.4.7, thus omitted. ∎

Corollary 4.4.10. *Given a finite number of vectors* $\mathrm{e}^{\{m\}}$ *and* $\mathrm{o}^{\{n\}}$ *for which* (4.51) *and* (4.52) *hold, the known matrix* $X_p^{-1} \in \mathbb{S}_+^{n_x}$*, the desired guaranteed shifting decay rate vertices* $\mathrm{d}_{\mathrm{R}j} \in \mathbb{R}_+$ *and some previously chosen relaxation degrees* $d_1, d_2, r \in \mathbb{N}$ *with* $d_1 \geq 3$*,* $d_2 \geq 2$ *and* $r \geq 2$*, suppose that the controller's initial state is* $x_c(0) = 0$ *and that there exist matrices* $R \in \mathbb{S}_+^{n_x}$*,* $S_{ij} \in \mathbb{S}_+^{n_x}$*,* $\hat{A}_{c,ij} \in \mathbb{R}^{n_x \times n_x}$*,* $\hat{B}_{c,ij} \in \mathbb{R}^{n_x \times n_y}$*,* $\hat{C}_{c,ij} \in \mathbb{R}^{n_u \times n_x}$ *and* $\hat{D}_{c,ij} \in \mathbb{R}^{n_u \times n_y}$ *with* $i \in \mathcal{I}_{[1,n_\mu]}$ *and* $j \in \mathcal{I}_{[1,n_\eta]}$ *such that conditions* (4.63) *and* (4.64) *are satisfied* $\forall m \in \mathcal{I}_{[1,n_\alpha]}$ *and* $\forall n \in \mathcal{I}_{[1,n_\beta]}$ *together with:*

$$X_p^{-1} - S_{ij} \geq 0, \tag{4.73}$$

$$\sum_{\boldsymbol{p} \in \mathcal{P}(\boldsymbol{i})} \begin{bmatrix} \hat{\sigma}_{l,j} & \hat{C}_{c[l],p_1 j} & \hat{D}_{c[l],p_1 j} C_{p_2} \\ \star & R & \mathrm{I}_{n_x} \\ \star & \star & S_{p_1 j} \end{bmatrix} \geq 0, \qquad \begin{matrix} \forall \boldsymbol{i} \in \mathbb{I}^+_{(r,n_\mu)} \\ l \in \mathcal{I}_{[1,n_u]} \end{matrix} . \tag{4.74}$$

Then, Theorem 4.4.4 holds for all parameter-dependent terms appearing in (4.46)*,* (4.47) *and* (4.53)*.*

Proof. Similar to that of Corollary 4.4.7, thus omitted. ∎

Corollary 4.4.11. *For fixed positive scalars* $\lambda_1 \geq \lambda_2$*, a given finite number of vectors* $\mathrm{e}^{\{m\}}$ *and* $\mathrm{o}^{\{n\}}$ *for which* (4.51) *and* (4.52) *hold, the known matrix* $X_p^{-1} \in \mathbb{S}_+^{n_x}$ *and some previously chosen relaxation degrees* $d, r \in \mathbb{N}$ *with* $d \geq 3$ *and* $r \geq 2$*, suppose that the controller's initial state is* $x_c(0) = 0$ *and that there exist matrices* $R \in \mathbb{S}_+^{n_x}$*,* $S_{ij} \in \mathbb{S}_+^{n_x}$*,* $\hat{A}_{c,ij} \in \mathbb{R}^{n_x \times n_x}$*,* $\hat{B}_{c,ij} \in \mathbb{R}^{n_x \times n_y}$*,* $\hat{C}_{c,ij} \in \mathbb{R}^{n_u \times n_x}$ *and* $\hat{D}_{c,ij} \in \mathbb{R}^{n_u \times n_y}$*, and vertex terms* $\gamma_j > 0$ *with* $i \in \mathcal{I}_{[1,n_\mu]}$ *and* $j \in \mathcal{I}_{[1,n_\eta]}$ *such that conditions* (4.63)*,* (4.71)*,* (4.72)*,* (4.73) *and* (4.74) *are satisfied* $\forall m \in \mathcal{I}_{[1,n_\alpha]}$*,* $\forall n \in \mathcal{I}_{[1,n_\beta]}$ *and* $Q^{-1} = \mathrm{I}_{n_w}$*. Then, Corollary 4.4.1 holds for all parameter-dependent terms appearing in* (4.46)*,* (4.47) *and* (4.53)*.*

Proof. It is a direct consequence of Corollaries 4.4.8 and 4.4.9 when $Q^{-1} = \mathrm{I}_{n_w}$, and the stated conditions (4.73) and (4.74) in Corollary 4.4.10. ∎

Remark 4.4.3. It should be noted that the corollaries stated in this section can be recast into an optimization strategy using the procedure described in Section 3.6.

4.5 Illustrative examples

In this section, an illustrative example is considered in order to show the extension of the results obtained in Chap. 3 to the shifting output-feedback case. Specifically, the example presents simulation results using a nonlinear quadrotor model whose closed-loop response is adapted in terms of convergence speed according to the instantaneous saturation limit values.

4.5.1 GSDR performance: Attitude control of a quadrotor

Consider the quasi-LPV model of a quadrotor presented in Section 3.7.5 under the assumption of neglectable gyroscopic effect and the absence of external disturbances. Then, the system (4.1a)

and (4.1c) with $B_w(\vartheta) = 0$ is characterized by $x_p = \left[\dot{\phi}, \dot{\theta}, \dot{\psi}, \phi, \theta, \psi\right]^\top$ and the moments produced by the rotors $u(t)$, as follows:

$$u = \begin{bmatrix} u_1 \\ u_2 \\ u_3 \end{bmatrix} = \begin{bmatrix} \mathrm{l_a k_T}(\Omega_4^2 - \Omega_2^2) \\ \mathrm{l_a k_T}(\Omega_3^2 - \Omega_1^2) \\ \mathrm{k_Q} \sum_{i=1}^{4} (-1)^i \Omega_i^2 \end{bmatrix}.$$

The selected scheduling vector is $\vartheta = \left[\dot{\phi}, \dot{\theta}\right]^\top$ with $\dot{\phi}, \dot{\theta} \in [-1, 1]$ (rad/s), thus defining the polytope Θ with $n_\mu = 4$ vertices that contains the following parameter-dependent system matrices (4.1a) and (4.1c):

$$A(\vartheta) = \left[\begin{array}{ccc|c} 0 & 0 & \vartheta_2 \frac{I_{yy} - I_{zz}}{I_{xx}} & \\ 0 & 0 & \vartheta_1 \frac{I_{zz} - I_{xx}}{I_{yy}} & 0_{3\times3} \\ \vartheta_2 \frac{I_{xx} - I_{yy}}{2\, I_{zz}} & \vartheta_1 \frac{I_{xx} - I_{yy}}{2\, I_{zz}} & 0 & \\ \hline \multicolumn{3}{c|}{\mathrm{I_3}} & 0_{3\times3} \end{array}\right], \quad \begin{aligned} B(\vartheta) = B &= \begin{bmatrix} J^{-1} \\ 0_{3\times3} \end{bmatrix}, \\ C(\vartheta) = C &= \begin{bmatrix} 0_{3\times3} & \mathrm{I_3} \end{bmatrix}, \end{aligned}$$

where $J \triangleq \mathrm{diag}\{I_{xx}, I_{yy}, I_{zz}\}$.

As in Section 3.7.5, let assume that all rotors $\Omega_k \in [\Omega_0, \Delta_\Omega(t)]$, $k \in \mathcal{I}_{[1,4]}$, exhibit the identical saturation behaviour, such that the largest possible positive control action is specified as follows:

$$\sigma_1(t) = \sigma_2(t) = \mathrm{l_a k_T}\big(\Delta_\Omega(t)^2 - \Omega_0^2\big), \quad \sigma_3(t) = 2\mathrm{k_Q}\big(\Delta_\Omega(t)^2 - \Omega_0^2\big),$$

where the minimum propeller speed $\Omega_0 = 1075$ (rpm) and $\Delta_\Omega(t)$ represents a known function describing the instantaneous maximum propeller speed, which varies within the interval $[\Delta_{\underline{\Omega}}, \Delta_{\bar{\Omega}}]$ as a result of battery exhaustion with $\Omega_0 < \Delta_{\underline{\Omega}} < \Delta_{\bar{\Omega}}$, $\Delta_{\underline{\Omega}} = 5000$ (rpm) and $\Delta_{\bar{\Omega}} = 8600$ (rpm), respectively.

Then, let us introduce the performance scheduling parameter $\varphi(t) \in [0, 1]$, which is linked to the time-varying saturation function (4.2) and the limits:

$$\begin{aligned} \mathrm{l_a k_T}\big(\Delta_{\underline{\Omega}}^2 - \Omega_0^2\big) \le \sigma_1(t) \le \mathrm{l_a k_T}\big(\Delta_{\bar{\Omega}}^2 - \Omega_0^2\big), \\ \mathrm{l_a k_T}\big(\Delta_{\underline{\Omega}}^2 - \Omega_0^2\big) \le \sigma_2(t) \le \mathrm{l_a k_T}\big(\Delta_{\bar{\Omega}}^2 - \Omega_0^2\big), \\ 2\mathrm{k_Q}\big(\Delta_{\underline{\Omega}}^2 - \Omega_0^2\big) \le \sigma_3(t) \le 2\mathrm{k_Q}\big(\Delta_{\bar{\Omega}}^2 - \Omega_0^2\big) \end{aligned}$$

for the inputs $u_1(t)$, $u_2(t)$ and $u_3(t)$, respectively, as follows:

$$\varphi(t) = \frac{\bar{\sigma}_1^2 - \sigma_1(t)^2}{\bar{\sigma}_1^2 - \underline{\sigma}_1^2} = \frac{\bar{\sigma}_2^2 - \sigma_2(t)^2}{\bar{\sigma}_2^2 - \underline{\sigma}_2^2} = \frac{\bar{\sigma}_3^2 - \sigma_3(t)^2}{\bar{\sigma}_3^2 - \underline{\sigma}_3^2}.$$

Note that $\varphi(t)$ is a unique scheduling parameter due to the fact that $\sigma_l(t) \to \underline{\sigma}_l$ and $\sigma_l(t) \to \bar{\sigma}_l$ $\forall l \in \mathcal{I}_{[1,3]}$ when the function $\Delta_\Omega(t) \to \Delta_{\underline{\Omega}}$ and $\Delta_\Omega(t) \to \Delta_{\bar{\Omega}}$, respectively. Thus, allowing to establish the following mapping:

$$\hat{\sigma}_l(\varphi(t)) \triangleq \sigma_l(t)^2 = \bar{\sigma}_l^2 + \varphi(t)\big(\underline{\sigma}_l^2 - \bar{\sigma}_l^2\big),$$

and, hence, $n_\eta = 2$ and the corresponding vertices of $\hat{\sigma}(\varphi)$:

$$\hat{\sigma}_1 = \left[\bar{\sigma}_1^2, \quad \bar{\sigma}_2^2, \quad \bar{\sigma}_3^2\right]^\top, \quad \hat{\sigma}_2 = \left[\underline{\sigma}_1^2, \quad \underline{\sigma}_2^2, \quad \underline{\sigma}_3^2\right]^\top.$$

Performance illustration

Consider that the initial attitude of the vehicle $\phi(0)$, $\theta(0)$ and $\psi(0)$ belongs to the interval $[-0.0873, 0.0873]$ (rad) and each Euler angle rate $\dot{\phi}(0)$, $\dot{\theta}(0)$ and $\dot{\psi}(0)$ is expected to lie in $[-0.0017, 0.0017]$ (rad/s), thus determining:

$$X_p^{-1} \triangleq \frac{1}{6}\frac{\pi}{180}\,\mathrm{diag}\{0.1, 0.1, 0.1, 5, 5, 5\}^{-2}.$$

Then, let us define the desired decay rate values of $\mathrm{d_R}(\varphi)$ taking into account the polytopic representation (4.46b) with the purpose of regulating the convergence speed of (4.4a) online:

$$\mathrm{d_{R1}} = 3.18, \ \mathrm{d_{R2}} = 0.$$

Remark 4.5.1. Note that the largest feasible value of $\mathrm{d_{R1}}$ that makes Problem 4.2.1 feasible can be obtained by using, e.g., linear search techniques or the bisection algorithm.

Once the design specifications are defined, two Pólya's relaxation degree $d = 4$ and $r = 4$ are chosen and Problem 4.2.1 is solved through Corollary 4.4.5 using the SeDuMi solver [117] and the YALMIP toolbox [70].

The closed-loop performance of the designed controller is tested in a scenario without the presence of external disturbances and under three different saturation limits that remain constant during the simulation for illustrative purposes. To this end, each instantaneous saturation limit is fixed to $\sigma_l(t)^2 = \left\{\bar{\sigma}_l^2, 0.5(\bar{\sigma}_l^2 + \underline{\sigma}_l^2), \underline{\sigma}_l^2\right\}$ $\forall l \in \mathcal{I}_{[1,3]}$ leading to the frozen values of $\varphi = \{0, 0.5, 1\}$ through the established mapping. Furthermore, the controlled system is simulated with $x_p(0) = [0, 0, 0, 0.0524, -0.0349, 0.0175]^\top$ and $x_c(0) = 0$.

Figs. 4.1-4.2 show the closed-loop response of the Euler angles and the controller states, respectively. Note that in both cases the fastest closed-loop convergence speed, denoted by a red line, corresponds to $\sigma_l(t) = \bar{\sigma}_l$ implying $\varphi = 0$. Conversely, it can be seen that the slowest closed-loop response occurs when $\sigma_l(t) \to \underline{\sigma}_l$, which corresponds to $\varphi = 1$. This demonstrates the adaptability of the designed shifting output-feedback controller regarding the closed-loop convergence speed. Furthermore, it is also shown that the controller achieves the closed-loop system stabilization.

Finally, Fig. 4.3 shows the behaviour of the obtained control actions over time for the three frozen values of φ where, for illustrative purposes, the instantaneous saturation limits of each control signal $u_l(t)$ $\forall l \in \mathcal{I}_{[1,3]}$ are not plotted. Furthermore, it can be seen that $u(t)$ remains inside the boundaries established by all the mentioned values of $\sigma(t)$, whose instantaneous values for $\varphi = \{0, 0.5, 1\}$ are, respectively, $\sigma_1 = \sigma_2 = \{0.885, 0.659, 0.29\}$ (N m) and $\sigma_3 = \{0.147, 0.109, 0.048\}$ (N m).

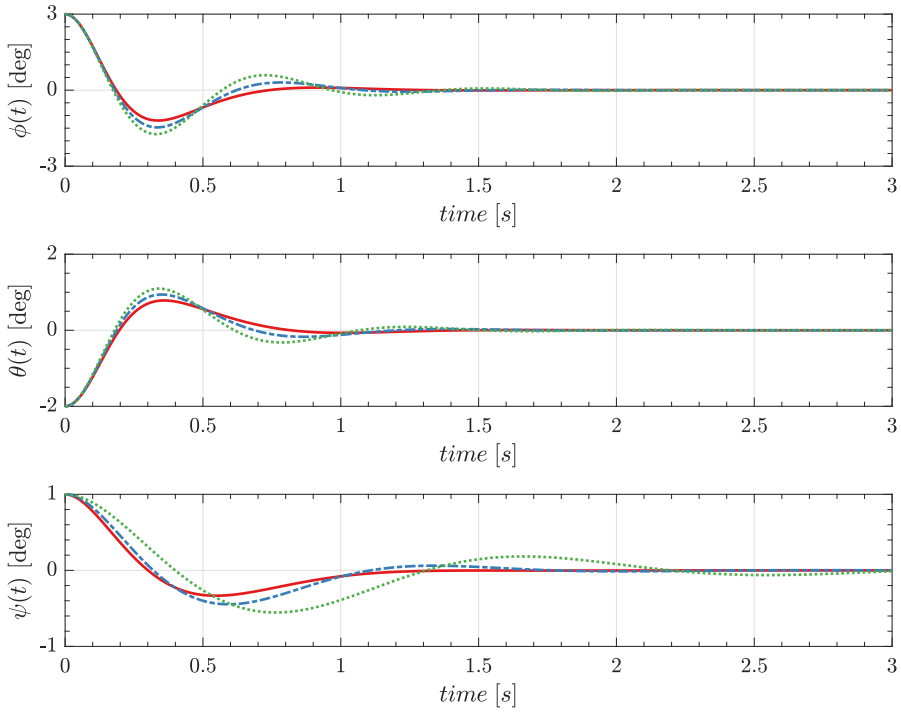

Figure 4.1: Closed-loop Euler angle responses. ((—)$\varphi = 0$, (- - -) $\varphi = 0.5$, and (···) $\varphi = 1$.)

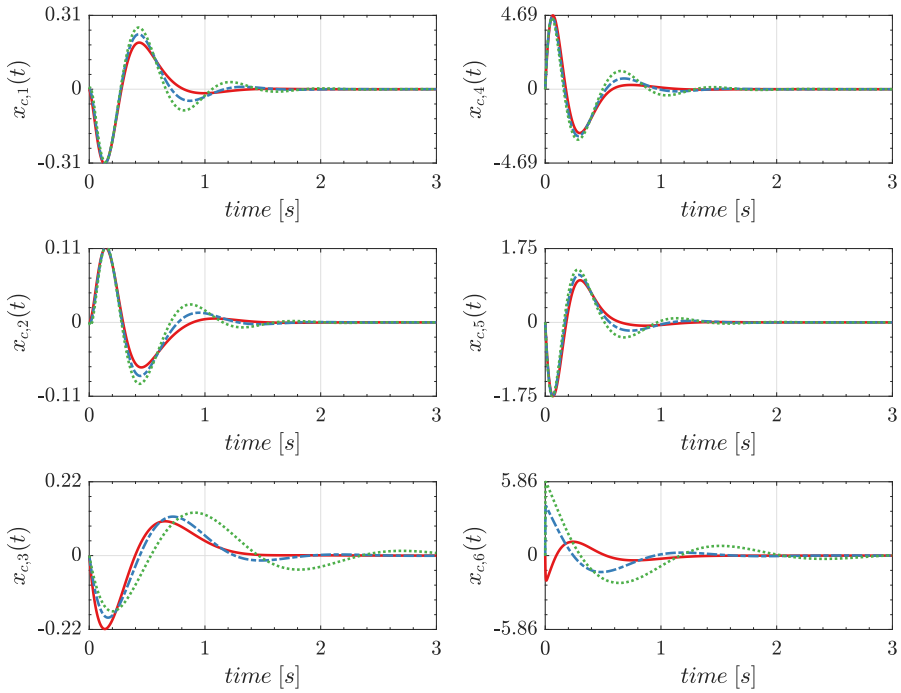

Figure 4.2: Controller states. ((—) $\varphi = 0$, (- - -) $\varphi = 0.5$, and (···) $\varphi = 1$.)

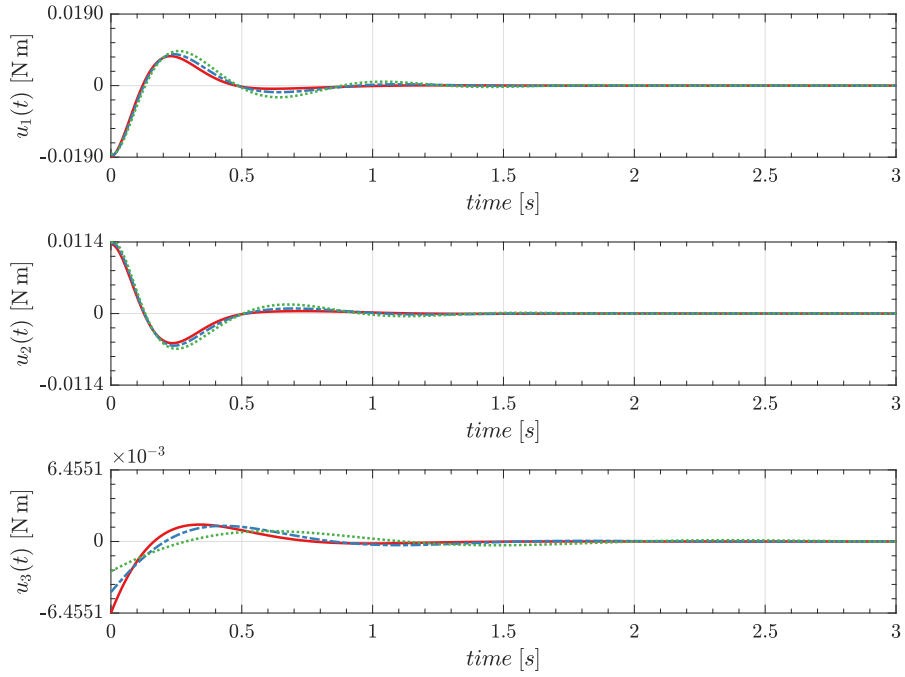

Figure 4.3: Control inputs. ((—) $\varphi = 0$, (- - -) $\varphi = 0.5$, (···) $\varphi = 1$, and the corresponding instantaneous saturation limit values $\sigma_1 = \sigma_2 = \{0.885, 0.659, 0.29\}$ (N m) and $\sigma_3 = \{0.147, 0.109, 0.048\}$ (N m).)

4.6 Conclusions

In this chapter, the problem of designing a shifting output-feedback controller for polytopic LPV systems subject to time-varying saturations has been investigated. Through the use of a (PD)QLF, the invariant ellipsoidal theory and the shifting paradigm concept, the procedure from Chap. 3 has been adapted for the output-feedback case, yielding LMI-based design conditions that can be solved using the available solvers. Additionally, Pólya's relaxation lemma has been used in the design stage to get a finite number of conditions due to the appearance of products between multiple polytopic summations, thus obtaining less conservative solutions at the expense of increasing the computational burden.

The illustrative example has shown that the designed controller satisfies the shifting decay rate performance criterion. The controller adjusts online the closed-loop response in sense of convergence speed based on the actuator saturation limit values. Future studies on this subject will look into saturation allowance and asymmetric saturations in an effort to lessen how conservative the suggested technique is.

5 Shifting feedback linearization control

The content of this chapter is based on the following work:

- [97] A. Ruiz, D. Rotondo, and B. Morcego. "Design of shifting state-feedback controllers for constrained feedback linearized systems: application to quadrotor attitude control". *International Journal of Robust and Nonlinear Control*, 2023. Under review.

5.1 Introduction

Feedback linearization (FBL) is a nonlinear control technique that is commonly used for the stabilization and tracking of nonlinear systems, such as unmanned aerial vehicles (UAVs) or robots (see [13, 40, 62, 74] and references therein). This technique involves the use of a nonlinear transformation of the states, through a diffeomorphism, to perform a system coordinate transformation. The goal is to obtain a fully or partially linear system representation which can be controlled with linear techniques.

The literature on the application of FBL to nonlinear systems subject to input constraints has attracted the interest of researchers, due to the fact that the input constraints that affect the obtained linearized system become time-varying as a consequence of the state nonlinear transformation. For instance, an analysis of the problem of stabilization and trajectory tracking of feedback linearizable systems in the presence of input constraints has been made in [86]. In [58], the combination of model predictive control (MPC) and FBL has been employed to design an effective control allocation in fault-tolerant flight control. In [108], an accurate trajectory tracking control has been developed for underactuated multibody systems in which the constraints are handled through an optimization problem under the same control combination. Similarly, a constraint mapping algorithm has been developed to guarantee the tracking performance of the entry flight control of an aerial vehicle in [126], whereas in [114], a methodology for reducing the computational burden of nonlinear MPC has been proposed for dealing with the nonlinear constraints originated by the combination of the MPC and FBL through the use of a set of dynamically generated local inner polytopic approximations. On the other hand, the works [48] and [11] have both established a linear matrix inequality (LMI)-based methodology that accounts for the state-dependent input saturations using the sum of squares (SOS) method and the differential algebraic representation (DAR), respectively.

Although the discussed works deal with the state dependency of the input restrictions, they do not account for varying closed-loop performance in terms of convergence speed or disturbance rejection due to a potential lack of input availability. For this reason, this chapter is devoted to

integrate the shifting paradigm concept and the FBL technique to regulate the closed-loop performance of a full linearized system subject to state-dependent input saturation. To that aim, an LMI-based methodology via a parameter-independent quadratic Lyapunov function (QLF) has been developed for designing a shifting state-feedback controller, extending the methodology presented in Chap. 3 to the case where an input-output FBL technique is used on multiple-input multiple-output (MIMO) nonlinear systems with input saturation. Specifically, the shifting paradigm is applied in the same way as in Section 3.4, and a set of region inclusions is defined with the goal of ensuring that the control action remains inside the linearity region of the actuators. Finally, the developed approach is demonstrated through an experimental application to the Quanser 3-DoF hover [91].

This chapter is organized as follows: First, in Section 5.2 some mathematical background regarding the FBL technique is reviewed. In Section 5.3, the strategy for solving the stabilization problem of constrained feedback linearized systems is defined. The LMI-based methodology for the controller design is given in Section 5.4. Finally, the design implementation procedure is summarized in Section 5.5, and the experimental results are presented in Section 5.6.

5.2 Feedback linearization

In order to formalize and generalize some mathematical background appearing in this chapter, the following sections recap some concepts presented in [57, 63, 103, 115] involving the FBL technique. Particularly, the concepts of Lie derivative, diffeomorphism, and the input-output FBL of a class of MIMO nonlinear systems are stated.

5.2.1 Lie derivative and diffeomorphism

The emphasis in this chapter is on the use of *sufficiently smooth* vector fields and real functions so that all existing partial derivatives are continuous and defined in a domain $\mathcal{D}_x \subset \mathbb{R}^{n_x}$. Then, the definition of a differential operation called Lie derivative is introduced.

Definition 5.2.1 (Lie derivative operator [63, Chap. 13])**.** The Lie derivative of a *smooth* real-valued function $h(x)\colon \mathcal{D}_x \to \mathbb{R}$ w.r.t. the *sufficiently smooth* vector field $f(x)$ in $\mathbb{R}^{n_x}$ at any point $x \in \mathcal{D}_x \subset \mathbb{R}^{n_x}$ is defined as:

$$L_f h(x) \triangleq \sum_{i=1}^{n_x} \frac{\partial h}{\partial x_i} f_i(x) = \nabla h(x) f(x).$$

For nonlinear systems, the diffeomorphism represents a nonlinear generalization of the well-known concept of changing coordinates, and it is formally defined as follows:

Definition 5.2.2 (Diffeomorphism [115, Chap. 6])**.** A mapping $T(x)\colon \mathcal{D}_x \to \mathbb{R}^{n_x}$ is called a diffeomorphism on a domain $\mathcal{D}_x \subset \mathbb{R}^{n_x}$ if it is a bijective function, and its inverse $T(x)^{-1}$ is differentiable as well. If the region $\mathcal{D}_x$ represents the whole space $\mathbb{R}^{n_x}$, then $T(x)$ is a *global diffeomorphism*. Conversely, if these qualities are only locally valid in the neighbourhood of a given point $x_0 \in \mathcal{D}_x$, then $T(x)$ is referred to as a *local diffeomorphism*.

5.2.2 Input-Output Feedback linearization

Consider a class of nonlinear systems of the form:

$$\dot{x} = f(x) + G(x)u, \tag{5.1a}$$
$$y = h(x), \tag{5.1b}$$

where $x \in \mathcal{D}_x \subset \mathbb{R}^{n_x}$, $u \in \mathbb{R}^m$ and $y \in \mathbb{R}^m$ denote the state, the control input and output vector, respectively, and $\mathcal{D}_x$ represents a domain of $\mathbb{R}^{n_x}$ containing the origin. The mappings $f(x)\colon \mathcal{D}_x \to \mathbb{R}^{n_x}$ and $h(x)\colon \mathcal{D}_x \to \mathbb{R}^m$ are a *sufficiently smooth* vector field and a *sufficiently smooth* function on $\mathbb{R}^{n_x}$, respectively, and $G(x)\colon \mathcal{D}_x \to \mathbb{R}^{n_x \times m}$ corresponds to a mapping matrix whose columns g_j are *smooth* vector fields in $\mathbb{R}^{n_x}$.

Then, the time derivative expression of the i^{th} output y_i of system (5.1) can be defined $\forall i \in \mathcal{I}_{[1,m]}$ by using the Lie derivative operator as:

$$\dot{y}_i = L_f h_i(x) + \sum_{j=1}^{m} \big(L_{g_j} h_i(x)\big) u_j. \tag{5.2}$$

Note that u_j does not appear in (5.2) when the terms $L_{g_j} h_i(x) = 0 \ \forall j \in \mathcal{I}_{[1,m]}$, thus implying that u_j is not directly related to $\dot{y}_i$. Hence, the r_i^{th} time derivative expression of y_i can be obtained under the assumption that y_i is differentiable r_i times before at least one of the terms $L_{g_j} L_f^{r_i - 1} h_i(x) \neq 0$, $\forall j \in \mathcal{I}_{[1,m]}$, as follows:

$$y_i^{(r_i)} = L_f^{r_i} h_i(x) + \sum_{j=1}^{m} L_{g_j}\Big(L_f^{r_i - 1} h_i(x)\Big) u_j, \tag{5.3}$$

where the relative degree $r_i \in \mathbb{N}\backslash\{0\}$ is the smallest integer such that the following condition is satisfied for $i \in \mathcal{I}_{[1,m]}$ and $j \in \mathcal{I}_{[1,m]}$:

$$L_{g_j} L_f^k h_i(x) = 0, \quad k \in \mathcal{I}_{[0, r_i - 2]}, \tag{5.4a}$$
$$L_{g_j} L_f^{r_i - 1} h_i(x) \neq 0, \quad \text{for at least one } j \in \mathcal{I}_{[1,m]}. \tag{5.4b}$$

Let us define the decoupling matrix $M(x) \in \mathbb{R}^{m \times m}$ as:

$$M(x) \triangleq \begin{bmatrix} L_{g_1} L_f^{r_1 - 1} h_1(x) & \dots & L_{g_m} L_f^{r_1 - 1} h_1(x) \\ \vdots & \ddots & \vdots \\ L_{g_1} L_f^{r_m - 1} h_m(x) & \dots & L_{g_m} L_f^{r_m - 1} h_m(x) \end{bmatrix} \tag{5.5}$$

Then, by means of the expressions (5.3) and (5.5), the concept of the relative degree is extended to the case of MIMO nonlinear systems through the following definition:

Definition 5.2.3 (Vector relative degree [103, Chap. 9])**.** The system (5.1) is said to have a vector relative degree $r = [r_1, \dots, r_m]^\top$ at x_0 if:

1. $L_{g_j} L_f^k h_i(x) = 0 \quad \forall i, j \in \mathcal{I}_{[1,m]}$, $\forall k < r_i - 1$ and $\forall x$ in a neighbourhood of x_0.
2. $M(x)$ is nonsingular at x_0.

Due to the assumption of $M(x)$ being nonsingular, the system (5.1) has a well-defined vector relative degree at x_0 allowing the description of (5.3) as follows:

$$\begin{bmatrix} y_1^{(r_1)} \\ \vdots \\ y_m^{(r_m)} \end{bmatrix} = b(x) + M(x)u = \begin{bmatrix} L_f^{r_1} h_1(x) \\ \vdots \\ L_f^{r_m} h_m(x) \end{bmatrix} + M(x)u, \tag{5.6}$$

with $b(x) \in \mathbb{R}^m$. Then, the input-output FBL is achieved through the feedback linearizing law:

$$u = M(x)^{-1}(\nu - b(x)), \tag{5.7}$$

where $\nu = [\nu_1, \ldots, \nu_m]^\top \in \mathbb{R}^m$ corresponds to the vector of transformed input variables, which leads to a decoupled and linear system:

$$\begin{bmatrix} y_1^{(r_1)} \\ \vdots \\ y_m^{(r_m)} \end{bmatrix} = \begin{bmatrix} \nu_1 \\ \vdots \\ \nu_m \end{bmatrix}. \tag{5.8}$$

Furthermore, if the total relative degree $r_t = \sum_{i=1}^{m} r_i$ is equal to n_x, the nonlinear system (5.1) is said to be full-feedback linearizable and the *local diffeomorphism* $T(x)\colon \mathcal{D}_x \to \mathbb{R}^{n_x}$ is completely defined $\forall x \in \mathcal{D}_x$ such that $T(0) = 0$, and the change of coordinates $z = T(x)$ is constructed by:

$$T(x) = \left[T_1^{[1]}(x), \ldots, T_{r_1}^{[1]}(x), \ldots, T_1^{[m]}(x), \ldots, T_{r_m}^{[m]}(x)\right]^\top \tag{5.9}$$

where:

$$T_k^{[i]}(x) = z_k^{[i]} = L_f^{k-1} h_i(x), \quad \forall i \in \mathcal{I}_{[1,m]}, \quad \forall k \in \mathcal{I}_{[1,r_i]}, \tag{5.10}$$

and the superscript $[i]$ indicates the corresponding output index.

By means of the change of coordinates $z = T(x)$, the nonlinear system (5.1) is transformed into the following feedback linearized system:

$$\dot{z} = Az + B\nu, \tag{5.11a}$$

$$y = Cz, \tag{5.11b}$$

where $z \in \mathbb{R}^{n_x}$ is the vector of transformed state variables in the new z-coordinates, and the state-space matrices $A \triangleq \operatorname{diag}\{A_1, \ldots, A_m\} \in \mathbb{R}^{n_x \times n_x}$, $B \triangleq \operatorname{diag}\{B_1, \ldots, B_m\} \in \mathbb{R}^{n_x \times m}$ and $C \triangleq \operatorname{diag}\{C_1, \ldots, C_m\} \in \mathbb{R}^{m \times n_x}$ have a simple canonical structure whose block matrices $A_i \in \mathbb{R}^{r_i \times r_i}$, $B_i \in \mathbb{R}^{r_i}$ and $C_i \in \mathbb{R}^{1 \times r_i}$ are defined $\forall i \in \mathcal{I}_{[1,m]}$ as:

$$A_i \triangleq \begin{bmatrix} 0 & 1 & 0 & \ldots & 0 \\ 0 & 0 & 1 & \ldots & 0 \\ \vdots & \vdots & \vdots & \ddots & \vdots \\ 0 & 0 & 0 & \ldots & 1 \\ 0 & 0 & 0 & \ldots & 0 \end{bmatrix}, \quad B_i \triangleq \begin{bmatrix} 0 \\ 0 \\ \vdots \\ 0 \\ 1 \end{bmatrix}, \quad C_i \triangleq \begin{bmatrix} 1 & 0 & \ldots & 0 & 0 \end{bmatrix}.$$

5.3 Stabilization of constrained feedback linearized systems

The purpose of this chapter is to compute a full linearizing control law for a nonlinear system of the form (5.1) with the presence of actuator saturation:

$$\dot{x} = f(x) + G(x)\,\mathrm{sat}(u, \underline{u}, \bar{u}), \tag{5.12a}$$
$$y = h(x), \tag{5.12b}$$

where $\mathrm{sat}(u, \underline{u}, \bar{u}) \colon \mathbb{R}^m \to \mathbb{R}^m$ represents the standard saturation function, defined as in (2.71):

$$\mathrm{sat}(u, \underline{u}, \bar{u}) \triangleq \begin{bmatrix} \mathrm{sat}(u_1, \underline{u}_1, \bar{u}_1) \\ \vdots \\ \mathrm{sat}(u_l, \underline{u}_l, \bar{u}_l) \\ \vdots \\ \mathrm{sat}(u_m, \underline{u}_m, \bar{u}_m) \end{bmatrix}, \quad \mathrm{sat}(u_l, \underline{u}_l, \bar{u}_l) \triangleq \begin{cases} \bar{u}_l, & \text{if } u_l > \bar{u}_l \\ u_l, & \text{if } u_l \in [\underline{u}_l, \bar{u}_l] \\ -\underline{u}_l, & \text{if } u_l < -\underline{u}_l \end{cases} \tag{5.13}$$

for $l \in \mathcal{I}_{[1,m]}$ with known saturation limits $\underline{u}_l, \bar{u}_l \in \mathbb{R}_+ \backslash \{0\}$. Hence, the actuator's region of linearity of system (5.12), denoted as $\mathcal{U}_a$, is such that $\mathrm{sat}(u, \underline{u}, \bar{u}) = u$ is defined by the following polyhedral set:

$$\mathcal{U}_a \triangleq \left\{ u \in \mathbb{R}^m \ : \ -\underline{u}_l \leq u_l \leq \bar{u}_l, \ l \in \mathcal{I}_{[1,m]} \right\}. \tag{5.14}$$

Let us consider that the total relative degree of the nonlinear system (5.12) is well-defined and equal to n_x for all $u \in \mathcal{U}_a$ and $x \in \mathcal{D}_x \subset \mathbb{R}^{n_x}$. Therefore, the system (5.12) is fully linearizable by the feedback linearizing law (5.7), obtaining the following constrained feedback linearized system:

$$\dot{z} = Az + B\,\mathrm{sat}(\nu, \underline{\nu}(x), \bar{\nu}(x)), \tag{5.15a}$$
$$y = Cz, \tag{5.15b}$$

where the canonical matrices $A \in \mathbb{R}^{n_x \times n_x}$, $B \in \mathbb{R}^{n_x \times m}$ and $C \in \mathbb{R}^{m \times n_x}$ have the same definition as in (5.11), $z \in \mathbb{R}^{n_x}$ is the vector of transformed state variables obtained through the local diffeomorphism (5.9) and, without loss of generality, the virtual input $\nu \in \mathbb{R}^m$ in (5.15a) can be considered affected by a saturation function $\mathrm{sat}(\nu, \underline{\nu}(x), \bar{\nu}(x)) \colon \mathbb{R}^m \to \mathbb{R}^m$ defined for each input element as:

$$\mathrm{sat}(\nu_l, \underline{\nu}_l(x), \bar{\nu}_l(x)) \triangleq \begin{cases} \bar{\nu}_l(x), & \text{if } \nu_l > \bar{\nu}_l(x) \\ \nu_l, & \text{if } \nu_l \in [\underline{\nu}_l(x), \bar{\nu}_l(x)], \\ \underline{\nu}_l(x), & \text{if } \nu_l < \underline{\nu}_l(x) \end{cases} \quad l \in \mathcal{I}_{[1,m]}, \tag{5.16}$$

whose limits $\underline{\nu}_l(x) \in \mathbb{R}$ and $\bar{\nu}_l(x) \in \mathbb{R}$ are state-dependent:

$$\bar{\nu}_l(x) = \max_{\substack{u\in\mathcal{U}_a \\ x\in\mathcal{D}_x}} \Big(b_l(x) + M(x)_{[l]} u \Big), \tag{5.17a}$$

$$\underline{\nu}_l(x) = \min_{\substack{u\in\mathcal{U}_a \\ x\in\mathcal{D}_x}} \Big(b_l(x) + M(x)_{[l]} u \Big). \tag{5.17b}$$

However, the presence of a state-dependent saturation function in (5.15) makes the design of linear controllers that provide system stability without saturating a challenging task. To that aim, the sections that follow address the problem of developing a GS state-feedback controller using some results presented in Chap. 3. In particular, we explore an input constraint mapping, a shifting control strategy, and a set of region inclusions to assure the saturation avoidance of the linearized system (5.15), such that the combination of the linearizing law (5.7) and a shifting state-feedback control law does not saturate.

5.3.1 Input constraint handling

As shown in (5.16) and (5.17), the constraints on the virtual input ν in (5.15) are time-varying due to dependence on $M(x)$ and $b(x)$, thus leading to an expression non-suitable to be handled by optimization approaches. Therefore, a so-called constraint mapping has been proposed in the literature in order to apply optimization approaches, see e.g. [108] and [126], thus transforming the constraints appearing in (5.14) into inequalities that define the linear region of the actuators $\mathcal{V}(x) \subset \mathbb{R}^m \ \forall t \geq 0$ in the ν–domain where ν corresponds to values that do not trigger the saturation in (5.13).

By substituting the feedback linearizing law (5.7) into (5.14), the following expression is obtained:

$$-\underline{u}_l \leq M(x)^{-1}_{[l]}(\nu - b(x)) \leq \bar{u}_l, \quad \forall l \in \mathcal{I}_{[1,m]} \tag{5.18}$$

which is equivalent to the following expression:

$$\underbrace{-\underline{u}_l + M(x)^{-1}_{[l]} b(x)}_{\underline{\varsigma}_l(x)} \leq M(x)^{-1}_{[l]}\nu \leq \underbrace{\bar{u}_l + M(x)^{-1}_{[l]} b(x)}_{\bar{\varsigma}_l(x)}, \tag{5.19}$$

thus leading to $\mathcal{V}(x)$ as:

$$\mathcal{V}(x) \triangleq \Big\{ \nu \in \mathbb{R}^m : \underline{\varsigma}_l(x) \leq M(x)^{-1}_{[l]}\nu \leq \bar{\varsigma}_l(x),\, l \in \mathcal{I}_{[1,m]} \Big\}. \tag{5.20}$$

Note that the region $\mathcal{V}(x)$ is an asymmetric region, even if constraint limits in (5.14) are symmetric, and that the region bounds may potentially have the same sign, owing to the appearance of terms $M(x)^{-1}_{[l]} b(x)$ on both sides of the inequality (5.20).

According to [86], the cost of cancelling the nonlinearities can be large enough to saturate the system. Therefore, it is assumed for further developments that the linearization cost is not signif-

icant enough to saturate the control input, restricting the state x to lie in the set $\mathcal{X} \subset \mathcal{D}_x \subset \mathbb{R}^{n_x}$ containing the origin, defined by:

$$\mathcal{X} \triangleq \left\{ x \in \mathbb{R}^{n_x} : -\underline{x}_i \leq x_i \leq \bar{x}_i,\ |M(x)^{-1}_{[l]} b(x)| \leq \epsilon_l, \quad \begin{matrix} i \in \mathcal{I}_{[1,n_x]} \\ l \in \mathcal{I}_{[1,m]} \end{matrix} \right\}, \tag{5.21}$$

where $\underline{x}_i,\ \bar{x}_i \in \mathbb{R}_+ \backslash \{0\}$ correspond to the given limitation values of the i^{th} state and ϵ_l expresses an upper limit for the control effort required to feedback linearize the system such that $0 < \epsilon_l < \min(\underline{u}_l, \bar{u}_l)$ for $l \in \mathcal{I}_{[1,m]}$. Consequently, the vector of transformed state variables z belongs to the set:

$$\mathcal{Z} = T(\mathcal{X}), \tag{5.22}$$

with $T(x)$ defined as in (5.9), and $0 \in \mathcal{V}(x)$ for all $x \in \mathcal{X} \subset \mathcal{D}_x$.

In addition to the restriction on x, a symmetric approximation of the region $\mathcal{V}(x)$ with the following definition is considered:

$$\hat{\mathcal{V}}(x) \triangleq \left\{ \nu \in \mathbb{R}^m : |M(x)^{-1}_{[l]} \nu| \leq \sigma_l(x),\ l \in \mathcal{I}_{[1,m]} \right\}, \tag{5.23}$$

where $\sigma_l(x) \triangleq \min(|\underline{\sigma}_l(x)|, \bar{\sigma}_l(x))$ and $\sigma_l(x) \in \mathbb{R}_+ \backslash \{0\}$ for all $x \in \mathcal{X} \subset \mathcal{D}_x$ is assumed. The instantaneous value of $\sigma_l(x)$ belongs to the interval $[\underline{\sigma}_l, \bar{\sigma}_l]\ \forall l \in \mathcal{I}_{[1,m]}$ and $\forall x \in \mathcal{X}$, with $\underline{\sigma}_l$ and $\bar{\sigma}_l$ as the lowest and highest possible saturation limit for each input ν_l, respectively. Then, similarly to [119, § C.8], $\hat{\mathcal{V}}(x)$ can be rewritten as:

$$\hat{\mathcal{V}}(x) \triangleq \left\{ \nu \in \mathbb{R}^m : \nu^\top \frac{M(x)^{-\top}_{[l]} M(x)^{-1}_{[l]}}{\sigma_l(x)^2} \nu \leq 1,\ l \in \mathcal{I}_{[1,m]} \right\}. \tag{5.24}$$

Due to its dependence on x, the region $\hat{\mathcal{V}}(x)$ in (5.24) represents an infinite number of constraints on the input ν, making it impossible to establish conditions that are computationally tractable for the controller's design. Then, with the purpose of finding a finite representation of the region $\hat{\mathcal{V}}(x)$, let us consider a set of grid points on each dimension of $\mathcal{X}$ to obtain the set $\mathcal{X}_g \triangleq \{\hat{x}^{\{1\}}, \ldots, \hat{x}^{\{n_p\}}\}$ with a sufficiently large number of n_p state vectors $\hat{x}^{\{n_p\}} \in \mathcal{X}_g \subset \mathcal{X}$.

Thereupon, to account for the variability of $M(x)^{-1}$ for all $x \in \mathcal{X}$, let us consider a scheduling vector $\vartheta \in \Theta \subset \mathbb{R}^{n_\vartheta}$ such that $\vartheta = \varpi_M(x)$, with the mapping $\varpi_M(x) \colon \mathbb{R}^{m \times m} \to \mathbb{R}^{n_\vartheta}$ defined as follows:

$$\varpi_M(x) \triangleq W_\Theta \mathrm{vec}\big(M(x)^{-1}\big), \tag{5.25}$$

where $\mathrm{vec}(\cdot)$ denotes the vectorization operator for a given matrix, and W_Θ represents a linear transformation for, e.g., avoiding the selection of known constant terms of the vectorized matrix. By evaluating $\varpi_M(x)$ for each $\hat{x} \in \mathcal{X}_g$, Θ is then constructed as the convex set defined by the convex hull, the bounding box, or other convex representations of the obtained points. As a result, the parameter-dependent matrix $\hat{M}(\vartheta) \in \mathbb{R}^{m \times m}$ will vary within a polytope of matrices:

$$\hat{M}(\vartheta) \in \mathrm{Co}\big\{\hat{M}_1, \hat{M}_2, \ldots, \hat{M}_{n_\mu}\big\}, \tag{5.26}$$

where the vertex terms correspond to the vertices of Θ.

Considering a mapping as the one proposed in (3.7), the relationship that links $\varphi \in \Phi \subset \mathbb{R}^{n_\varphi}$ with the possible instantaneous values of $\sigma_l(x)^2$ is defined as follows:

$$\varphi_l \triangleq \frac{\bar{\sigma}_l^2 - \sigma_l(x)^2}{\bar{\sigma}_l^2 - \underline{\sigma}_l^2}, \quad \varphi_l \in [0,1], \quad \forall l \in \mathcal{I}_{[1,m]}, \tag{5.27}$$

allowing the definition of Φ as a hypercube with 2^{n_φ} vertices. Additionally, the time-variability of $\sigma_l(x)^2$ in (5.24) can be described as a function of φ_l by the following expression:

$$\hat{\sigma}_l(\varphi) \triangleq \sigma_l(x)^2 = \bar{\sigma}_l^2 + \varphi_l\left(\underline{\sigma}_l^2 - \bar{\sigma}_l^2\right), \ \forall l \in \mathcal{I}_{[1,m]}. \tag{5.28}$$

To illustrate how to obtain $\hat{M}(\vartheta)$ in (5.26) and $\hat{\sigma}(\varphi)$ in (5.28), respectively, let us present Example 5.3.1.

Example 5.3.1. Consider the following nonlinear system:

$$\dot{x} \triangleq \begin{bmatrix} \dot{x}_1 \\ \dot{x}_2 \\ \dot{x}_3 \\ \dot{x}_4 \end{bmatrix} = \underbrace{\begin{bmatrix} x_3 \\ x_4 \\ f_3(x) \\ f_4(x) \end{bmatrix}}_{f(x)} + \underbrace{\begin{bmatrix} 0 & 0 \\ 0 & 0 \\ g_{31}(x) & 0 \\ 0 & g_{42}(x) \end{bmatrix}}_{[g_1(x),\, g_2(x)]} \mathrm{sat}(u, \underline{u}, \bar{u}), \tag{5.29a}$$

$$y = \begin{bmatrix} x_1 & x_2 \end{bmatrix}^\top, \tag{5.29b}$$

where $x \in \mathcal{D}_x \subset \mathbb{R}^4$, $\bar{u} = \underline{u} = [\bar{u}_1, \bar{u}_2]^\top$ is a given vector with positive real entries, and $f_3(x)$, $f_4(x)$, $g_{31}(x)$ and $g_{42}(x)$ are known nonlinear terms.

Now consider $u \in \mathcal{U}_a$ for linearizing the system (5.29) through the procedure detailed in Section 5.2.2, thus obtaining:

$$\begin{gathered} L_f h_1(x) = x_3, \quad L_f^2 h_1(x) = f_3(x), \quad L_{g_1} L_f h_1(x) = g_{31}(x), \\ L_f h_2(x) = x_4, \quad L_f^2 h_2(x) = f_4(x), \quad L_{g_2} L_f h_2(x) = g_{42}(x), \\ L_{g_j} h_i(x) = 0 \ \forall i, j \in \mathcal{I}_{[1,2]}, \quad L_{g_j} L_f h_i(x) = 0 \ \forall i, j \in \mathcal{I}_{[1,2]} \text{ and } i \neq j. \end{gathered}$$

Let us assume that $g_{31}(x)$ and $g_{42}(x)$ take non-zero values $\forall x \in \mathcal{D}_x$ and, hence, the system (5.29) has a relative degree vector $r = [2,2]^\top$ and a total relative degree $r_t = n_x = 4$ such that no zero dynamics exists. Then, $M(x) \in \mathbb{R}^{2\times 2}$ and $b(x) \in \mathbb{R}^2$ in (5.6) can be defined as follows:

$$M(x) = \begin{bmatrix} g_{31}(x) & 0 \\ 0 & g_{42}(x) \end{bmatrix}, \quad b(x) = \begin{bmatrix} f_3(x) \\ f_4(x) \end{bmatrix}.$$

By following Section 5.3.1, the constraint mapping in (5.19) is determined $\forall x \in \mathcal{D}_x$ by:

$$-\bar{u}_l + M(x)_{[l]}^{-1} b(x) \leq M(x)_{[l]}^{-1} \nu \leq \bar{u}_l + M(x)_{[l]}^{-1} b(x), \ l \in \mathcal{I}_{[1,2]},$$

where:

$$M(x)^{-1} = \begin{bmatrix} \frac{1}{g_{31}(x)} & 0 \\ 0 & \frac{1}{g_{42}(x)} \end{bmatrix}, \quad M(x)^{-1} b(x) = \begin{bmatrix} \frac{f_3(x)}{g_{31}(x)} \\ \frac{f_4(x)}{g_{42}(x)} \end{bmatrix}.$$

As a result, the region $\mathcal{V}(x)$ in (5.20) is defined as follows:

$$\mathcal{V}(x) \triangleq \left\{ \nu \in \mathbb{R}^2 : \underline{\varsigma}_l(x) \leq M(x)^{-1}_{[l]} \nu \leq \bar{\varsigma}_l(x),\ l \in \mathcal{I}_{[1,2]} \right\},$$

where:

$$\begin{aligned} \underline{\varsigma}_1(x) &\triangleq -\bar{u}_1 + \frac{f_3(x)}{g_{31}(x)}, \quad \bar{\varsigma}_1(x) \triangleq \bar{u}_1 + \frac{f_3(x)}{g_{31}(x)}, \\ \underline{\varsigma}_2(x) &\triangleq -\bar{u}_2 + \frac{f_4(x)}{g_{42}(x)}, \quad \bar{\varsigma}_2(x) \triangleq \bar{u}_2 + \frac{f_4(x)}{g_{42}(x)}. \end{aligned}$$

Then, let us restrict the state x to lie in a polyhedral set $\mathcal{X} \subset \mathcal{D}_x \subset \mathbb{R}^4$, defined as in (5.21), such that the state-dependent matrix $M(x)$ is nonsingular $\forall x \in \mathcal{X}$ and the linearization cost satisfies:

$$|M(x)^{-1}_{[l]} b(x)| \leq \epsilon_l$$

for $l \in \mathcal{I}_{[1,2]}$, with $0 < \epsilon_l < \bar{u}_l$ as given control effort limits to feedback linearize the system.

Thereupon, let us consider the state-dependent vector $\sigma(x) \in \mathbb{R}^2_+$ whose instantaneous element values are defined $\forall x \in \mathcal{X}$ as:

$$\sigma_1(x) \triangleq \min(|\underline{\varsigma}_1(x)|, \bar{\varsigma}_1(x)), \quad \sigma_2(x) \triangleq \min(|\underline{\varsigma}_2(x)|, \bar{\varsigma}_2(x)),$$

thus defining the region $\hat{\mathcal{V}}(x)$ in (5.24) $\forall x \in \mathcal{X}$ and $l \in \mathcal{I}_{[1,2]}$.

Once the region $\hat{\mathcal{V}}(x)$ is defined, a set of grid points $\hat{x} \in \mathcal{X}_g \subset \mathcal{X}$ with $\mathcal{X}_g = \left\{ \hat{x}^{\{1\}}, \ldots, \hat{x}^{\{n_p\}} \right\}$ and $n_p \in \mathbb{N}$ must be considered to obtain a finite representation of the region $\hat{\mathcal{V}}(x)$.

Let us state the mapping $\varpi_M(x)$ in (5.25), as follows:

$$\varpi_M(x) = \begin{bmatrix} 1 & 0 & 0 & 0 \\ 0 & 0 & 0 & 1 \end{bmatrix} \mathrm{vec}\left(M(x)^{-1} \right).$$

By doing so, we obtain the main diagonal elements of $M(x)^{-1}$ as parameters of the scheduling vector $\vartheta \in \Theta \subset \mathbb{R}^2$, which depicts the state dependence of the matrix. The set Θ is defined as the convex hull of the points obtained by evaluating $\varpi_M(x)$ for each state $\hat{x} \in \mathcal{X}_g$. As a result, the vertices of Θ allow the acquisition of $\hat{M}(\vartheta) \in \mathbb{R}^{2\times 2}$ in (5.26).

Considering $\hat{x} \in \mathcal{X}_g$, the bounds of $\sigma_l(x)^2$ in (5.24) are given, respectively, by:

$$\underline{\sigma}_l^2 = \min_{\hat{x} \in \mathcal{X}_g} \sigma_l(\hat{x})^2, \quad \bar{\sigma}_l^2 = \max_{\hat{x} \in \mathcal{X}_g} \sigma_l(\hat{x})^2, \quad l \in \mathcal{I}_{[1,2]}.$$

Then, the convex set $\Phi \subset \mathbb{R}^2$ is defined using the relationship (5.27), and hence, the expression of $\hat{\sigma}_l(\varphi)$ in (5.28) can be derived. ▲

Finally, a convex representation of the values taken by $M(x)^{-1}$ and $\sigma_l(x)^2$ when x varies in $\mathcal{X}$ is obtained and expressed through parameter-dependent terms $\hat{M}(\vartheta) \in \mathbb{R}^{m\times m}$ and $\hat{\sigma}(\varphi) \in \mathbb{R}^m$, respectively, so that $\hat{\mathcal{V}}(x)$ in (5.24) can be reformulated as follows:

$$\hat{\mathcal{V}}(\vartheta,\varphi) \triangleq \left\{ \nu \in \mathbb{R}^m : \nu^\top \frac{\hat{M}(\vartheta)_{[l]}^\top \hat{M}(\vartheta)_{[l]}}{\hat{\sigma}_l(\varphi)} \nu \leq 1,\ l \in \mathcal{I}_{[1,m]} \right\}, \tag{5.30}$$

where $\vartheta \in \Theta \subset \mathbb{R}^{n_\vartheta}$ and $\varphi \in \Phi \subset \mathbb{R}^{n_\varphi}$ are the scheduling parameter vectors, with Θ and Φ known, bounded and closed polytopic sets.

5.3.2 Shifting control strategy

On the basis of the concepts presented in Chap. 3, a shifting state-feedback control strategy is proposed with the objective of handling the variability of region $\hat{\mathcal{V}}(\vartheta,\varphi)$ and the stabilization of the constrained feedback linearized system (5.15). An overall view of the control strategy is shown in Fig. 5.1.

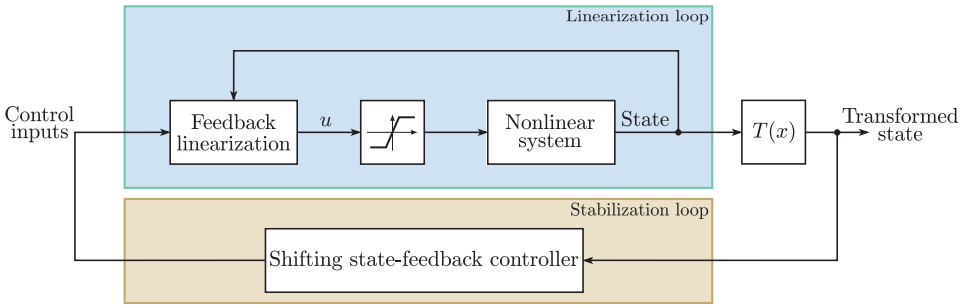

Figure 5.1: Shifting feedback linearization control strategy.

To this end, the following GS control law is defined:

$$\nu = K(\vartheta,\varphi)z, \tag{5.31}$$

where $K(\vartheta,\varphi) \in \mathbb{R}^{m\times n_x}$ is the parameter-dependent controller gain matrix. Then, the closed-loop system (5.15) subject to the control law (5.31) is said to have a guaranteed shifting decay rate $\mathrm{d_R}(\varphi)\colon \mathbb{R}^{n_\varphi} \to \mathbb{R}_+$ if:

$$\dot{V}(z) \leq -2\mathrm{d_R}(\varphi)V(z), \tag{5.32}$$

where $V(z)$ is the QLF:

$$V(z) \triangleq z^\top P^{-1} z,\ P \in \mathbb{S}_+^{n_x}. \tag{5.33}$$

As a result, the control law (5.31) modifies the closed-loop performance of the system (5.15) online in response to changes in $\hat{\mathcal{V}}(\vartheta,\varphi)$. In particular, (5.31) uses the scheduling parameter vector ϑ to account for the variability of $M(x)^{-1}$, whereas the closed-loop convergence speed is adjusted through a mapping that links φ with the possible instantaneous values of $\sigma_l(x)^2$ for $l \in \mathcal{I}_{[1,m]}$.

In this way, a faster response can be guaranteed when $\sigma_l(x)^2 \to \bar{\sigma}_l^2$ while a slower response is obtained when $\sigma_l(x)^2 \to \underline{\sigma}_l^2$, respectively, for all $l \in \mathcal{I}_{[1,m]}$.

5.3.3 Saturation avoidance condition and problem definition

By means of the inequality (5.32), the online closed-loop performance regulation and exponential stability of the closed-loop system are ensured as long as $\mathrm{d_R}(\varphi) > 0 \; \forall \varphi \in \Phi$. Then, with the purpose of guaranteeing $\forall t \geq 0$ that $\nu(t) \in \hat{\mathcal{V}}(\vartheta(t), \varphi(t))$ and, as a consequence $u(t) \in \mathcal{U}_a$ $\forall t \geq 0$, let us define the following regions in the $z-$coordinates:

- The region $\mathcal{R}_z(\vartheta, \varphi)$ as the mapping of (5.30) into the $z-$coordinates through the control law (5.31):

$$\mathcal{R}_z(\vartheta, \varphi) \triangleq \left\{ z \in \mathbb{R}^{n_x} : z^\top \frac{H(\vartheta, \varphi)_{[l]}^\top H(\vartheta, \varphi)_{[l]}}{\hat{\sigma}_l(\varphi)} z \leq 1, \; l \in \mathcal{I}_{[1,m]} \right\}, \tag{5.34}$$

  where $H(\vartheta, \varphi)_{[l]} \triangleq \hat{M}(\vartheta)_{[l]} K(\vartheta, \varphi)$.

- Polyhedral region of expected initial conditions $z_0 = T(x_0)$:

$$\mathcal{Z}_0 \triangleq \mathrm{Co}\{v_1, \ldots, v_{n_v}\} = T(\mathcal{X}_0), \quad v_s \in \mathbb{R}^{n_x}, \quad s \in \mathcal{I}_{[1,n_v]}, \tag{5.35}$$

  where n_v represents the number of vertex values v_s, $\mathcal{X}_0$ corresponds to a polyhedral set that contains the initial conditions of interest x_0, and $T(x)$ is the diffeomorphism (5.9).

- The minimum volume ellipsoid (MVE) covering the set $\mathcal{Z}$ in (5.22):

$$\mathcal{E}_Z \triangleq \left\{ z \in \mathbb{R}^{n_x} : z^\top Z^{-1} z \leq 1 \right\}, \tag{5.36}$$

  where $Z \in \mathbb{S}_+^{n_x}$ is a known given matrix that can be obtained through the approach detailed in [24, § 8.4].

- The associated unit level set of the QLF defined in (5.33):

$$\mathcal{E}(P, 1) \triangleq \{ z \in \mathbb{R}^{n_x} : V(z) \leq 1 \}. \tag{5.37}$$

Then, Proposition 5.3.1 is formulated by following a similar process to that described in Section 3.3:

Proposition 5.3.1. *Let $\mathcal{R}_z(\vartheta, \varphi)$ be a parameter-dependent set defined as in (5.34). If $\mathcal{E}(P, 1)$ is a contractively invariant set satisfying $\forall (\vartheta, \varphi) \in \Theta \times \Phi$:*

$$\mathcal{Z}_0 \subset \mathcal{E}(P, 1) \subset \mathcal{R}_z(\vartheta, \varphi), \tag{5.38a}$$

$$\mathcal{E}(P, 1) \subset \mathcal{E}_Z, \tag{5.38b}$$

then for any initial condition $T(x_0) \in \mathcal{Z}_0$, and hence $T(x_0) \in \mathcal{E}(P, 1)$, the convergence of the corresponding transformed state trajectory $z(t) \to 0$ when $t \to \infty$ is ensured under saturation avoidance and, as a consequence $u(t) \in \mathcal{U}_a$.

Proof. The proof uses same logic as Proposition 2.3.1. The inclusion $\mathcal{E}(P,1) \subset \mathcal{R}_z(\vartheta,\varphi)$ in (5.38) ensures that $\nu(t) \in \hat{\mathcal{V}}(\vartheta(t),\varphi(t)) \ \forall t > 0$ and, hence $u(t) \in \mathcal{U}_a$, during the transient response of $z(t)$ as long as the initial condition x_0 is such that $T(x_0) \in \mathcal{Z}_0$. On the other hand, the inclusion $\mathcal{E}(P,1) \subset \mathcal{E}_Z$ ensures for any $z(t) \in \mathcal{E}(P,1)$ that the trajectory $x(t) = T(z(t))^{-1}$ belongs to the set $\mathcal{X}$ described by (5.21). ■

On the basis of the inequality (5.32) and Proposition 5.3.1, the control design problem considered in this chapter can be formulated formally as follows:

Problem 5.3.1. Given the linearized system (5.15) subject to the state-dependent saturation function (5.16) and the regions (5.34)–(5.37), design a shifting state-feedback controller (5.31) such that for any $T(x_0) \in \mathcal{Z}_0$:

1. The closed-loop system dynamics satisfy the performance specification (5.32) with a QLF given by (5.33).
2. The feedback linearizing law (5.7) belongs to the set $\mathcal{U}_a$ defined in (5.14).

□

5.4 Shifting controller design

Considering the control strategy stated in Section 5.3, let us introduce Theorem 5.4.1 which provides an LMI-based methodology for solving Problem 5.3.1 based on Proposition 5.3.1. Particularly, this theorem ensures $\nu \in \hat{\mathcal{V}}(\vartheta,\varphi)$ and the convergence to zero of any state trajectory $z(t) \in \mathcal{E}(P,1)$ for some desired $\mathrm{d_R}(\varphi)$ and, hence, the trajectory $z(t) \to 0$ for $t \geq 0$ and any $T(x_0) \in \mathcal{Z}_0$.

Theorem 5.4.1. *Given the regions* (5.34)–(5.37) *with the known matrices* $\hat{M}(\vartheta) \in \mathbb{R}^{m\times m}$ *and* $Z \in \mathbb{S}^{n_x}_+$*, the known vertices* v_s*, and a desired guaranteed decay rate* $\mathrm{d_R}(\varphi) \in \mathbb{R}_+$*, let there exist* $P \in \mathbb{S}^{n_x}_+$ *and* $Y(\vartheta,\varphi) \in \mathbb{R}^{m\times n_x}$ *such that* $\forall(\vartheta,\varphi) \in \Theta \times \Phi$ *the following conditions are satisfied:*

$$\mathrm{He}\{AP + BY(\vartheta,\varphi)\} + 2\mathrm{d_R}(\varphi)P \prec 0, \tag{5.39}$$

$$\begin{bmatrix} P & v_s \\ \star & 1 \end{bmatrix} \succeq 0, \quad s \in \mathcal{I}_{[1,n_v]}, \tag{5.40}$$

$$\begin{bmatrix} Z & P \\ \star & P \end{bmatrix} \succeq 0, \tag{5.41}$$

$$\begin{bmatrix} \hat{\sigma}_l(\varphi) & \hat{M}(\vartheta)_{[l]}Y(\vartheta,\varphi) \\ \star & P \end{bmatrix} \succeq 0, \quad l \in \mathcal{I}_{[1,m]}. \tag{5.42}$$

Then, the closed-loop response of the linearized system (5.15) *with the control law* (5.31) *satisfies* (5.32) *if the parameter-dependent controller gain is computed as* $K(\vartheta,\varphi) = Y(\vartheta,\varphi)P^{-1}$*. Furthermore, the convergence of* $z(t) \to 0$ *when* $t \to \infty$ *is ensured for any* x_0 *such that* $T(x_0) \in \mathcal{Z}_0$ *and* $\nu(t) \in \hat{\mathcal{V}}(x(t))$.

Proof. By introducing the control law (5.31) into (5.15), the following closed-loop representation is obtained under the assumption that $\nu(t)$ works in the linearity region of the actuators:

$$\dot{z} = Az + B\nu = (A + BK(\vartheta, \varphi))z. \tag{5.43}$$

Then, the following parameter-dependent BMI can be obtained by taking into account (5.32):

$$\mathrm{He}\{P^{-1}A + P^{-1}BK(\vartheta, \varphi)\} + 2\mathrm{d_R}(\varphi)P^{-1} \prec 0. \tag{5.44}$$

By pre- and post-multiplying (5.44) by P, we get:

$$\mathrm{He}\{AP + BK(\vartheta, \varphi)P\} + 2\mathrm{d_R}(\varphi)P \prec 0, \tag{5.45}$$

which is still a BMI due to the product between the decision variables $K(\vartheta, \varphi)$ and P. Then, in order to transform (5.45) into a parameter-dependent LMI, the change of variable $Y(\vartheta, \varphi) = K(\vartheta, \varphi)P$ is applied to (5.45), thus obtaining (5.39).

Let us demonstrate that (5.40) leads the inclusion $\mathcal{Z}_0 \subset \mathcal{E}(P, 1)$, thus ensuring that any trajectory evolution of $z(t) \to 0$ for any $T(x_0) \in \mathcal{E}(P, 1)$ and, also, for any $T(x_0) \in \mathcal{Z}_0$. Recall from [54, Chap. 7], the inclusion $\mathcal{Z}_0 \subset \mathcal{E}(P, 1)$ is formulated as:

$$v_s^\top P^{-1} v_s \leq 1, \quad s \in \mathcal{I}_{[1,n_v]},$$

which is equivalent to (5.40) through the application of the Schur's complement.

Similarly, the constraint (5.41) enforces the inclusion $\mathcal{E}(P, 1) \subset \mathcal{E}_Z$. This inclusion guarantees that any trajectory $x(t) = T(z(t))^{-1}$ belongs to the set $\mathcal{X}$ described in (5.21) for any $z(t) \in \mathcal{E}(P, 1)$. In fact, the above-mentioned inclusion corresponds to:

$$z^\top Z^{-1} z \leq z^\top P^{-1} z. \tag{5.46}$$

Then, manipulating the above expression one gets:

$$P^{-1} - Z^{-1} \succeq 0, \tag{5.47}$$

and, by pre- and post-multiplying (5.47) by P, we get:

$$P - PZ^{-1}P \succeq 0, \tag{5.48}$$

thus obtaining the LMI (5.41) after applying Schur's complement to (5.48).

Finally, condition (5.42) is obtained from the inclusion $\mathcal{E}(P, 1) \subset \mathcal{R}_z(\vartheta, \varphi)$, thus ensuring that while moving along decreasing values of the Lyapunov function $V(z)$, the input signal ν remains in the region of linearity. The inclusion $\mathcal{E}(P, 1) \subset \mathcal{R}_z(\vartheta, \varphi)$ is expressed as:

$$z^\top \frac{H(\vartheta, \varphi)_{[l]}^\top H(\vartheta, \varphi)_{[l]}}{\hat{\sigma}_l(\varphi)} z \leq z^\top P^{-1} z, \quad l \in \mathcal{I}_{[1,m]}, \tag{5.49}$$

where $H(\vartheta,\varphi)_{[l]} \triangleq \hat{M}(\vartheta)_{[l]}K(\vartheta,\varphi)$. By manipulating the above expression one gets:

$$P^{-1} - \frac{K(\vartheta,\varphi)^{\top}\hat{M}(\vartheta)_{[l]}^{\top}\hat{M}(\vartheta)_{[l]}K(\vartheta,\varphi)}{\hat{\sigma}_l(\varphi)} \succeq 0. \tag{5.50}$$

Then, by pre- and post-multiplying (5.50) by P we obtain:

$$P - \frac{Y(\vartheta,\varphi)^{\top}\hat{M}(\vartheta)_{[l]}^{\top}\hat{M}(\vartheta)_{[l]}Y(\vartheta,\varphi)}{\hat{\sigma}_l(\varphi)} \succeq 0, \tag{5.51}$$

and by means of the Schur's complement in (5.51) the parameter-dependent LMI (5.42) is obtained, thus concluding the proof. ■

5.4.1 Finite-dimensional LMI design conditions

Note that Theorem 5.4.1 is not suitable for design purposes due to the presence of parameter-dependent LMIs (5.39) and (5.42), hence the need of reducing them to a finite number. To this end, a polytopic representation for the parameter-dependent terms appearing in Theorem 5.4.1 is defined by a convex combination of a finite set of n_μ, n_η and $n_\mu \times n_\eta$ known vertices, respectively:

$$\hat{M}(\vartheta) = \sum_{i=1}^{n_\mu} \mu_i(\vartheta)\hat{M}_i, \tag{5.52a}$$

$$\begin{bmatrix}\hat{\sigma}(\varphi) & \mathrm{d_R}(\varphi)\end{bmatrix} = \sum_{j=1}^{n_\eta} \eta_j(\varphi)\begin{bmatrix}\hat{\sigma}_j & \mathrm{d_R}_j\end{bmatrix} \tag{5.52b}$$

$$Y(\vartheta,\varphi) = \sum_{i=1}^{n_\mu}\sum_{j=1}^{n_\eta} \mu_i(\vartheta)\eta_j(\varphi)Y_{ij}, \tag{5.52c}$$

where $\hat{M}_i \in \mathbb{R}^{m\times m}$, $\hat{\sigma}_j \in \mathbb{R}^m$ and $\mathrm{d_R}_j \in \mathbb{R}_+$ stand for the given known vertex terms and $Y_{ij} \in \mathbb{R}^{m\times n_x}$ denotes the decision control gain vertex matrices. $\mu(\vartheta) \in \mathbb{R}^{n_\mu}$ and $\eta(\varphi) \in \mathbb{R}^{n_\eta}$ correspond to the polytopic weight vectors belonging to the unit simplexes, defined as in (2.10) and (2.63), respectively:

$$\Delta^{n_\mu} \triangleq \left\{\mu(\vartheta) \in \mathbb{R}^{n_\mu} \ : \ \sum_{i=1}^{n_\mu}\mu_i(\vartheta) = 1,\ \mu_i(\vartheta) \geq 0,\ i \in \mathcal{I}_{[1,n_\mu]}\right\}, \tag{5.53a}$$

$$\Delta^{n_\eta} \triangleq \left\{\eta(\varphi) \in \mathbb{R}^{n_\eta} \ : \ \sum_{j=1}^{n_\eta}\eta_j(\varphi) = 1,\ \eta_j(\varphi) \geq 0,\ j \in \mathcal{I}_{[1,n_\eta]}\right\}. \tag{5.53b}$$

Based on the above representation (5.52) and (5.53), Corollary 5.4.1 is derived.

Corollary 5.4.1. *Given the known matrices $\hat{M}_i \in \mathbb{R}^{m\times m}$ and $Z \in \mathbb{S}_+^{n_x}$, the known vertices v_s, the desired guaranteed shifting decay rate vertices $\mathrm{d_R}_j \in \mathbb{R}_+$, and a previously chosen relaxation*

degree $d \in \mathbb{N}$ *with* $d \geq 2$, *suppose that there exist* $P \in \mathbb{S}^{n_x}_{+}$ *and* $Y_{ij} \in \mathbb{R}^{m \times n_x}$ *with* $i \in \mathcal{I}_{[1,n_\mu]}$ *and* $j \in \mathcal{I}_{[1,n_\eta]}$ *such that conditions* (5.40) *and* (5.41) *are satisfied together with:*

$$\mathrm{He}\{AP + BY_{ij}\} + 2\,\mathrm{d}_{\mathrm{R}j}\,P \prec 0, \tag{5.54}$$

$$\sum_{\boldsymbol{p} \in \mathcal{P}(\boldsymbol{i})} \begin{bmatrix} \hat{\sigma}_{l,j} & \hat{M}_{[l],p_1} Y_{p_2 j} \\ \star & P \end{bmatrix} \succeq 0, \quad l \in \mathcal{I}_{[1,m]}, \quad \forall \boldsymbol{i} \in \mathbb{I}^{+}_{(d,n_\mu)}. \tag{5.55}$$

Then, Theorem 5.4.1 holds for all parameter-dependent terms appearing in (5.52).

Proof. The proof is divided into two parts. The first part demonstrates the finite representation of the parameter-dependent LMI (5.39) through the application of the polytopic representation (5.52). The second part shows how one obtains the LMI (5.55) using (5.52) and Lemma 2.2.14.

Part 1: By means of (5.52), the parameter-dependent LMI (5.39) can be expressed as follows:

$$\mathrm{He}\left\{ AP + B \sum_{i=1}^{n_\mu} \sum_{j=1}^{n_\eta} \mu_i(\vartheta)\eta_j(\varphi) Y_{ij} \right\} + 2 \sum_{j=1}^{n_\eta} \eta_j(\varphi)\,\mathrm{d}_{\mathrm{R}j}\,P \prec 0, \tag{5.56}$$

which can be rewritten taking into account the fact that $\mu(\vartheta) \in \Delta^{n_\mu}$ and $\eta(\varphi) \in \Delta^{n_\eta}$, thus obtaining:

$$\sum_{i=1}^{n_\mu} \sum_{j=1}^{n_\eta} \mu_i(\vartheta)\eta_j(\varphi)\big[\mathrm{He}\{AP + BY_{ij}\} + 2\,\mathrm{d}_{\mathrm{R}j}\,P\big] \prec 0. \tag{5.57}$$

Then, the negative-definiteness of (5.57) can be guaranteed if:

$$\mathrm{He}\{AP + BY_{ij}\} + 2\,\mathrm{d}_{\mathrm{R}j}\,P \prec 0, \quad i \in \mathcal{I}_{[1,n_\mu]}, \quad j \in \mathcal{I}_{[1,n_\eta]} \tag{5.58}$$

is satisfied, thus obtaining the LMI (5.54).

Part 2: Similarly, the parameter-dependent LMI (5.42) can be expressed as follows:

$$\sum_{i_1=1}^{n_\mu} \sum_{i_2=1}^{n_\mu} \sum_{j=1}^{n_\eta} \mu_{i_1}(\vartheta)\mu_{i_2}(\vartheta)\eta_j(\varphi) \begin{bmatrix} \hat{\sigma}_{l,j} & \hat{M}_{[l],i_1} Y_{i_2 j} \\ \star & P \end{bmatrix} \succeq 0, \quad l \in \mathcal{I}_{[1,m]}. \tag{5.59}$$

Since the positive-definiteness of expression (5.59) includes multiple polytopic summations, the application of Lemma 2.2.14 is required, thus obtaining the LMI (5.55) and concluding the proof. ∎

5.5 Implementation considerations

Based on the results stated in Chap. 3, this section presents some implementation considerations for the control strategy described in Section 5.3.2 with the purpose of getting the maximum feasible value of $\mathrm{d}_{\mathrm{R}}(\varphi)$ when $\sigma(x) \to \bar{\sigma}$.

Let us recall from (3.97) the definition of the polytopic weights $\eta_j(\varphi)$ in (5.52):

$$\eta_j(\varphi) = \prod_{h=1}^{n_\varphi} \xi_{jh}(\varphi_h), \quad j \in \mathcal{I}_{[1,2^{n_\varphi}]} \tag{5.60}$$

where:

$$\xi_{jh}(\varphi_h) = \begin{cases} 1-\varphi_h & \text{if } (j \bmod 2^h) \in \mathcal{I}_{[1,2^{h-1}]} \\ \varphi_h & \text{otherwise} \end{cases}. \tag{5.61}$$

Then, with the consideration of $\mathrm{d_R}(\varphi) \in \left[\underline{\mathrm{d}}_\mathrm{R}, \bar{\mathrm{d}}_\mathrm{R}\right]$ and the use of the procedure stated in Section 3.6, Corollary 5.4.1 can be reformulated into an LMI-based optimization procedure expressed as $\mathcal{O}_5$ in (5.62) for a fixed value $\underline{\mathrm{d}}_\mathrm{R} \geq 0$ and a given set of possible values $\mathcal{S}_{\mathrm{d_R}} \subset \mathbb{R}_+$:

$$\mathcal{O}_5 : \begin{cases} \max\limits_{\bar{\mathrm{d}}_\mathrm{R} \in \mathcal{S}_{\mathrm{d_R}}} & \bar{\mathrm{d}}_\mathrm{R} \\ \text{subject to} & \text{conditions (5.40), (5.41), (5.54) and (5.55)} \end{cases}, \tag{5.62}$$

thus obtaining the desired GSDR vertex values $\mathrm{d}_{\mathrm{R}j} \in \mathbb{R}_+$ in (5.52b) such that the upper limit of $\mathrm{d_R}(\varphi)$ is maximized. Note that the selection of GSDR vertex values in (5.62) is subject to the condition defined in (3.99):

$$\mathrm{d}_{\mathrm{R}j} = \frac{\bar{\mathrm{d}}_\mathrm{R}\mathcal{C}_j + \underline{\mathrm{d}}_\mathrm{R}(n_\varphi - \mathcal{C}_j)}{n_\varphi}, \quad j \in \mathcal{I}_{[1,2^{n_\varphi}]} \tag{5.63}$$

where $\mathcal{C}_j$ is the number of times condition $\xi_{jh}(\varphi_h) = 1 - \varphi_h$ in (5.61) holds.

Finally, the optimization procedure (5.62) is used to solve Problem 5.3.1, which corresponds to an LMI-based feasibility problem subject to the performance criterion (5.32) and the desired vertex decay rate values (5.63). The design and implementation process is outlined below:

Offline procedure:

(i) Find the expressions of the decoupling matrix $M(x)$, the vector $b(x)$ and the diffeomorphism $T(x)$ through (5.5), (5.6) and (5.9), respectively.

(ii) Define the set $\mathcal{X}$ in (5.21).

(iii) Define a set of grid points $\hat{x} \in \mathcal{X}_g \subset \mathcal{X}$ with $\mathcal{X}_g \triangleq \{\hat{x}^{\{1\}}, \ldots, \hat{x}^{\{n_p\}}\}$ and $n_p \in \mathbb{N}$.

(iv) Obtain $\hat{M}(\vartheta)$ and $\hat{\sigma}_l(\varphi)$ through a convex representation of terms $M(x)^{-1}$ and $\sigma_l(x)^2$, as shown in Example 5.3.1.

(v) Define the regions $\mathcal{Z}_0$ and $\mathcal{E}_Z$ in (5.35) and (5.36), respectively.

Online procedure:

(i) Compute the current values of $M(x)$, $b(x)$ and $T(x)$ using (5.5), (5.6) and (5.9), respectively.

(ii) Compute the current value of the polytopic weights $\mu_i(\vartheta)$ and $\eta_j(\varphi)$, for $i \in \mathcal{I}_{[1,n_\mu]}$ and $j \in \mathcal{I}_{[1,n_\eta]}$, respectively.

(iii) Obtain the current value of $Y(\vartheta, \varphi)$ from the expression (5.52c).

(iv) Compute $K(\vartheta, \varphi) = Y(\vartheta, \varphi)P^{-1}$.

(v) Compute the control law (5.31) and the feedback linearizing law (5.7).

5.6 Experimental results

In this section, the three degrees of freedom (3-DoF) hover platform from Quanser™ [91] serves as an experimental validation of the approach developed in this chapter. First, a brief description and the model of the platform are provided in Section 5.6.1. In Section 5.6.2, the experimental closed-loop configuration for the feedback linearization is detailed. In Section 5.6.3, the design specifications are given. Finally, the simulation results and the experimental validation are presented in Sections 5.6.4 and 5.6.5, respectively.

5.6.1 Quanser 3-DoF hover platform

The 3-DoF hover platform consists of a quadrotor positioned over a 3-DoF pivot joint enabling the rotational motion about the body frame $\{\mathbf{B}\}$. Three high-resolution encoders are available for measuring the Euler angles ϕ, θ and ψ, thus allowing the estimation of the Euler angle rates $\dot{\phi}$, $\dot{\theta}$ and $\dot{\psi}$ through a filtering process. Furthermore, the frame $\{\mathbf{B}\}$ is fixed to the platform's centre of gravity (CoG) and the axes (x_B, y_B, z_B) point to the platform's front, right and upper sides, respectively, as shown in Fig. 5.2.

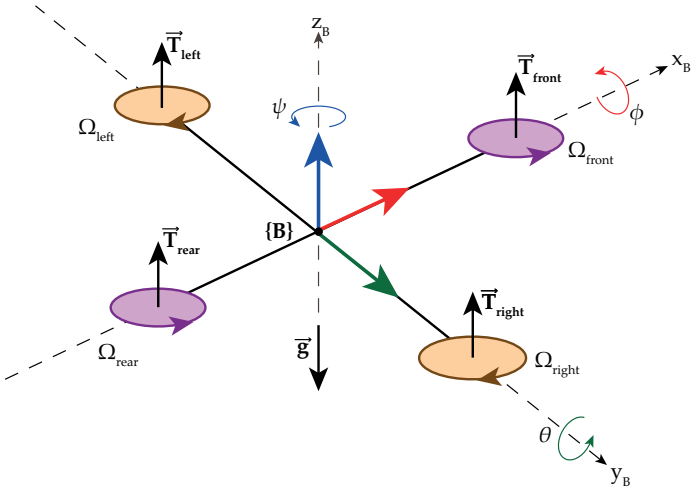

Figure 5.2: Quanser 3-DoF hover system scheme.

The platform's rotational motion is achieved by four propellers located at the extremes in a cross configuration. The rear and front propellers rotate in counter-clockwise direction, while the left and right propellers rotate in a clockwise direction. Due to the actuator actions, the roll,

Table 5.1: Quanser 3-DoF parameters

Symbol	Description	Value / Type	Unit
ϕ, θ, ψ	Roll, Pitch and Yaw angles	Measured	rad
$\dot{\phi}, \dot{\theta}, \dot{\psi}$	Roll, Pitch and Yaw angle rates	Estimated	rad/s
$\mathrm{k_T}$	Thrust coefficient	0.1188	N/V
$\mathrm{k_Q}$	Drag coefficient	0.0036	N m/V
$\mathrm{l_a}$	Distance CoG - rotor	0.1968	m
I_{xx}	Moment of inertia $x-$axis	0.0522	$\mathrm{kg\,m^2}$
I_{yy}	Moment of inertia $y-$axis	0.0522	$\mathrm{kg\,m^2}$
I_{zz}	Moment of inertia $z-$axis	0.1104	$\mathrm{kg\,m^2}$
$\bar{V}_\mathrm{m}$	Maximum motor voltage	24	V
V_bias	Bias motor voltage	12	V
$\mathrm{k}_\mathrm{fr}^{\phi}$	Roll friction coefficient	Estimated	$\mathrm{Nm/rad\,s^{-1}}$
$\mathrm{k}_\mathrm{fr}^{\theta}$	Pitch friction coefficient	Estimated	$\mathrm{Nm/rad\,s^{-1}}$
$\mathrm{k}_\mathrm{fr}^{\psi}$	Yaw friction coefficient	Estimated	$\mathrm{Nm/rad\,s^{-1}}$

pitch and yaw moments $\left(\tau_\phi, \tau_\theta, \tau_\psi\right)$ can be obtained under the assumption that the thrust and drag forces are proportional to the motor's voltage as follows:

$$\begin{bmatrix} \tau_\phi \\ \tau_\theta \\ \tau_\psi \end{bmatrix} = \begin{bmatrix} 0 & -\mathrm{l_a k_T} & 0 & \mathrm{l_a k_T} \\ \mathrm{l_a k_T} & 0 & -\mathrm{l_a k_T} & 0 \\ -\mathrm{k_Q} & \mathrm{k_Q} & -\mathrm{k_Q} & \mathrm{k_Q} \end{bmatrix} \begin{bmatrix} V_{\mathrm{m},1} \\ V_{\mathrm{m},2} \\ V_{\mathrm{m},3} \\ V_{\mathrm{m},4} \end{bmatrix}, \tag{5.64}$$

where $V_{\mathrm{m},1}, \ldots, V_{\mathrm{m},4}$ denote the input voltage of the front, left, rear and right motors in (V), respectively, and the rest of parameters are listed in Table 5.1. Furthermore, the motors' voltages $V_{\mathrm{m},i} = V_i^{\mathrm{fb}} + V_\mathrm{bias}$ are supposed to have the same behaviour regarding the voltage limits considering $V_{\mathrm{m},i} \in \left[0, \bar{V}_\mathrm{m}\right]$ and $V_i^{\mathrm{fb}} \in \left[-V_\mathrm{bias}, \bar{V}_\mathrm{m} - V_\mathrm{bias}\right]$ for $i \in \mathcal{I}_{[1,4]}$, and as a consequence, the torque limits $\bar{u} = \underline{u} \in \mathbb{R}^3_+$ are:

$$|\tau_\phi| \leq \underbrace{\mathrm{l_a k_T} \bar{V}_\mathrm{m}}_{\bar{u}_1}, \quad |\tau_\phi| \leq \underbrace{\mathrm{l_a k_T} \bar{V}_\mathrm{m}}_{\bar{u}_2}, \quad |\tau_\psi| \leq \underbrace{2\mathrm{k_Q} \bar{V}_\mathrm{m}}_{\bar{u}_3}. \tag{5.65}$$

Remark 5.6.1. It should be noted that including a bias voltage avoids the motor voltage from reaching negative values and being cut off, hence preventing potential permanent damage to the power amplifier.

Recall from [20], the nonlinear dynamics of the 3-DoF hover platform are characterized by $x = \left[\phi, \theta, \psi, \dot{\phi}, \dot{\theta}, \dot{\psi}\right]^\top$ and $u = \left[\tau_\phi, \tau_\theta, \tau_\psi\right]^\top$ under the assumptions that the platform's body is rigid

and symmetrical, that the entire state is known and that the gyroscopic effects and disturbances can be neglected:

$$\dot{x} \triangleq \begin{bmatrix} \dot{x}_1 \\ \dot{x}_2 \\ \dot{x}_3 \\ \dot{x}_4 \\ \dot{x}_5 \\ \dot{x}_6 \end{bmatrix} = \begin{bmatrix} x_4 \\ x_5 \\ x_6 \\ \frac{I_{yy}-I_{zz}}{I_{xx}} x_5 x_6 \\ \frac{I_{zz}-I_{xx}}{I_{yy}} x_4 x_6 \\ \frac{I_{xx}-I_{yy}}{I_{zz}} x_4 x_5 \end{bmatrix} + \begin{bmatrix} 0_{3\times 3} \\ J^{-1} \end{bmatrix} \mathrm{sat}(u, \underline{u}, \bar{u}), \tag{5.66}$$
$$y \triangleq h(x) = \begin{bmatrix} x_1 & x_2 & x_3 \end{bmatrix}^\top,$$

where $J \triangleq \mathrm{diag}\{I_{xx}, I_{yy}, I_{zz}\}$.

5.6.2 Experimental configuration for FBL

By implementing the proposed strategy on toy numerical examples, it has been observed that the effect of the proposed shifting controller design is more impactful in situations where a big amount of the control signal is used to feedback linearize the plant. For a multirotor vehicle, this corresponds to operating conditions usually encountered in high friction environments, such as those experienced underwater (see, for example, [72]). In order to emulate such conditions using the available laboratory setup, the existence of higher friction is taken into consideration by generating it using a part of the control law, thus leading to the control-loop configuration shown in Fig. 5.3, which is employed for all the experiments described in this section.

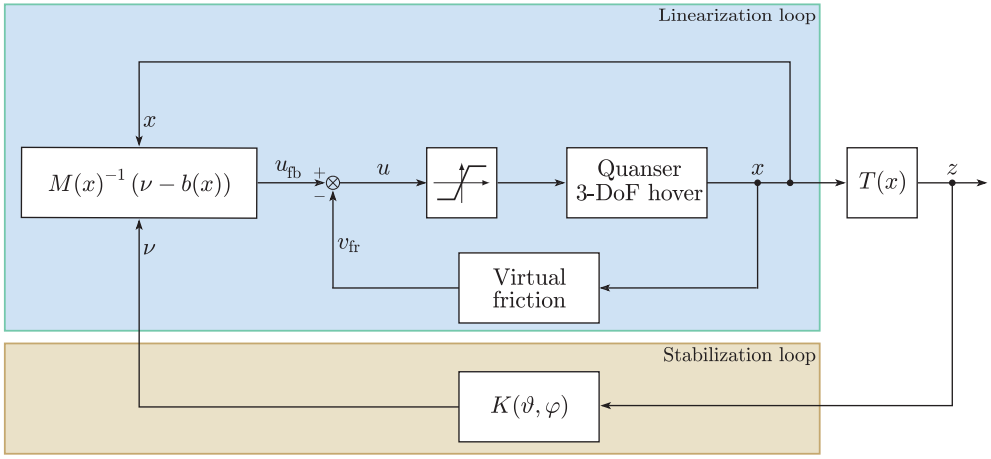

Figure 5.3: Experimental closed-loop configuration. (u_{fb} denotes the limited feedback linearizing law (5.7) due to the presence of the motion's virtual friction.)

Considering the experimental closed-loop configuration in Fig. 5.3, the total control input signal in (5.66) can be defined as follows:

$$u \triangleq u_{\mathrm{fb}} - v_{\mathrm{fr}},$$

where $u_{\text{fb}} \in \mathbb{R}^3$ is the feedback linearizing law (5.7) and $v_{\text{fr}} \in \mathbb{R}^3$ represents the motion's virtual friction:

$$v_{\text{fr}} \triangleq \underbrace{\text{diag}\left\{\text{k}_{\text{fr}}^{\phi}, \text{k}_{\text{fr}}^{\theta}, \text{k}_{\text{fr}}^{\psi}\right\}}_{K_{\text{fr}}} \underbrace{\begin{bmatrix} 0_{3\times 3} & \text{I}_3 \end{bmatrix}}_{F} x,$$

with $K_{\text{fr}} \in \mathbb{R}^{3\times 3}$ as a diagonal matrix containing the given positive friction coefficients $\text{k}_{\text{fr}}^{\phi}$, $\text{k}_{\text{fr}}^{\theta}$ and $\text{k}_{\text{fr}}^{\psi}$, and $F \in \mathbb{R}^{3\times 6}$ as a matrix with appropriate rows of the identity for selecting, in this case, the states x_4, x_5 and x_6.

For the sake of the controller's design, the feedback linearizing law (5.7) is considered to vary within 60% of the torque limit values in (5.65). Hence, the coefficients $\text{k}_{\text{fr}}^{\phi}$, $\text{k}_{\text{fr}}^{\theta}$, and $\text{k}_{\text{fr}}^{\psi}$ have to be chosen to define v_{fr} from the input to vary within 40% of $\bar{u}$ in order to avoid saturation. To this end, a definition of the friction coefficient is proposed below under the assumption that each limit of the states x_4, x_5 and x_6 in (5.21) is symmetric:

$$\text{k}_{\text{fr}}^{\phi} \triangleq \frac{0.4\bar{u}_1}{\bar{x}_4}, \quad \text{k}_{\text{fr}}^{\theta} \triangleq \frac{0.4\bar{u}_2}{\bar{x}_5}, \quad \text{k}_{\text{fr}}^{\psi} \triangleq \frac{0.4\bar{u}_3}{\bar{x}_6},$$

where $\bar{x}_4 = \underline{x}_4$, $\bar{x}_5 = \underline{x}_5$ and $\bar{x}_6 = \underline{x}_6$ are the given symmetric state limits.

Given the above discussion, the following design model is obtained from (5.66):

$$\begin{aligned} \dot{x} \triangleq \begin{bmatrix} \dot{x}_1 \\ \dot{x}_2 \\ \dot{x}_3 \\ \dot{x}_4 \\ \dot{x}_5 \\ \dot{x}_6 \end{bmatrix} &= \begin{bmatrix} x_4 \\ x_5 \\ x_6 \\ \frac{I_{yy}-I_{zz}}{I_{xx}} x_5 x_6 - \frac{\text{k}_{\text{fr}}^{\phi}}{I_{xx}} x_4 \\ \frac{I_{zz}-I_{xx}}{I_{yy}} x_4 x_6 - \frac{\text{k}_{\text{fr}}^{\theta}}{I_{yy}} x_5 \\ \frac{I_{xx}-I_{yy}}{I_{zz}} x_4 x_5 - \frac{\text{k}_{\text{fr}}^{\psi}}{I_{zz}} x_6 \end{bmatrix} + \begin{bmatrix} 0_{3\times 3} \\ J^{-1} \end{bmatrix} \text{sat}(u_{\text{fb}}, \underline{u}_{\text{fb}}, \bar{u}_{\text{fb}}) \\ y \triangleq h(x) &= \begin{bmatrix} x_1 & x_2 & x_3 \end{bmatrix}^{\mathsf{T}}, \end{aligned} \tag{5.67}$$

with the known limits $\bar{u}_{\text{fb}} = \underline{u}_{\text{fb}} = 0.6\ \bar{u}$.

Then, by means of the procedure described in Section 5.2.2, the feedback linearizing law (5.7) can be characterized by the following terms (the details are omitted due to similarities with Example 5.3.1):

$$M(x)^{-1} = J,\ b(x) = \begin{bmatrix} \frac{I_{yy}-I_{zz}}{I_{xx}} x_5 x_6 - \frac{\text{k}_{\text{fr}}^{\phi}}{I_{xx}} x_4 \\ \frac{I_{zz}-I_{xx}}{I_{yy}} x_4 x_6 - \frac{\text{k}_{\text{fr}}^{\theta}}{I_{yy}} x_5 \\ \frac{I_{xx}-I_{yy}}{I_{zz}} x_4 x_5 - \frac{\text{k}_{\text{fr}}^{\psi}}{I_{zz}} x_6 \end{bmatrix}, \tag{5.68}$$

thus obtaining the vector of transformed state variables:

$$z \triangleq T(x) = \begin{bmatrix} \phi, \dot{\phi}, \theta, \dot{\theta}, \psi, \dot{\psi} \end{bmatrix}^{\mathsf{T}}$$

and the following full linearized version of the system (5.67):

$$\dot{z} = \underbrace{\begin{bmatrix} 0 & 1 & 0 & 0 & 0 & 0 \\ 0 & 0 & 0 & 0 & 0 & 0 \\ 0 & 0 & 0 & 1 & 0 & 0 \\ 0 & 0 & 0 & 0 & 0 & 0 \\ 0 & 0 & 0 & 0 & 0 & 1 \\ 0 & 0 & 0 & 0 & 0 & 0 \end{bmatrix}}_{A} z + \underbrace{\begin{bmatrix} 0 & 0 & 0 \\ 1 & 0 & 0 \\ 0 & 0 & 0 \\ 0 & 1 & 0 \\ 0 & 0 & 0 \\ 0 & 0 & 1 \end{bmatrix}}_{B} \mathrm{sat}(\nu, \underline{\nu}(x), \bar{\nu}(x)). \tag{5.69}$$

Note that the terms $\frac{\mathrm{k}_{\mathrm{fr}}^{\phi}}{I_{xx}} x_4$, $\frac{\mathrm{k}_{\mathrm{fr}}^{\theta}}{I_{yy}} x_5$ and $\frac{\mathrm{k}_{\mathrm{fr}}^{\psi}}{I_{zz}} x_6$ in (5.67) and (5.68) hinder platform motion. As a result, the state-dependent input constraints of the linearized plant (5.69) are affected and, consequently, the variability of the region $\hat{\mathcal{V}}(x)$ in (5.24) is also affected.

5.6.3 Design specifications

Let us establish the lower and upper limits of each state as:

$$\begin{aligned} \bar{x}_1 = \underline{x}_1 \triangleq \tfrac{25\pi}{180}, \quad \bar{x}_2 = \underline{x}_2 \triangleq \tfrac{25\pi}{180}, \quad \bar{x}_3 = \underline{x}_3 \triangleq \tfrac{\pi}{2}, \\ \bar{x}_4 = \underline{x}_4 \triangleq \tfrac{\pi}{4}, \quad \bar{x}_5 = \underline{x}_5 \triangleq \tfrac{\pi}{4}, \quad \bar{x}_6 = \underline{x}_6 \triangleq \tfrac{\pi}{4}, \end{aligned}$$

thus defining the set $\mathcal{X}$ in (5.21), and the coefficients $\mathrm{k}_{\mathrm{fr}}^{\phi} = \mathrm{k}_{\mathrm{fr}}^{\theta} = 0.2858$ and $\mathrm{k}_{\mathrm{fr}}^{\psi} = 0.0880$. Similarly, let us consider that the expected initial condition x_0 belongs to the following polyhedral set:

$$\mathcal{X}_0 = \left\{ x \in \mathbb{R}^6 : -\underline{x}_0 \leq x_0 \leq \bar{x}_0 \right\},$$

where $\bar{x}_0 \triangleq \underline{x}_0 = \frac{\pi}{180}[10, 10, 10, 0.1, 0.1, 0.1]^{\top}$. The transformation of sets $\mathcal{X}$ and $\mathcal{X}_0$ into the $z-$coordinates, denoted by $\mathcal{Z}$ and $\mathcal{Z}_0$, respectively, is obtained by using the diffeomorphism $T(x)$. As a result, the MVE that covers $\mathcal{Z}$ is characterized by the following matrix:

$$Z = \mathrm{diag}\{1.1423, 3.7011, 1.1423, 3.7011, 14.8038, 3.7011\},$$

thus defining the region $\mathcal{E}_Z$ in (5.36).

By considering the offline procedure in Section 5.5 and the terms in (5.68), the vertex elements of the convex representation of $\hat{\sigma}(\varphi)$ in (5.52b) are obtained for $j \in \mathcal{I}_{[1,8]}$:

$$\begin{aligned} \hat{\sigma}_1 \triangleq \left[\bar{\sigma}_1^2, \bar{\sigma}_2^2, \bar{\sigma}_3^2\right]^{\top}, \quad \hat{\sigma}_5 \triangleq \left[\bar{\sigma}_1^2, \bar{\sigma}_2^2, \underline{\sigma}_3^2\right]^{\top}, \\ \hat{\sigma}_2 \triangleq \left[\underline{\sigma}_1^2, \bar{\sigma}_2^2, \bar{\sigma}_3^2\right]^{\top}, \quad \hat{\sigma}_6 \triangleq \left[\underline{\sigma}_1^2, \bar{\sigma}_2^2, \underline{\sigma}_3^2\right]^{\top}, \\ \hat{\sigma}_3 \triangleq \left[\bar{\sigma}_1^2, \underline{\sigma}_2^2, \bar{\sigma}_3^2\right]^{\top}, \quad \hat{\sigma}_7 \triangleq \left[\bar{\sigma}_1^2, \underline{\sigma}_2^2, \underline{\sigma}_3^2\right]^{\top}, \\ \hat{\sigma}_4 \triangleq \left[\underline{\sigma}_1^2, \underline{\sigma}_2^2, \bar{\sigma}_3^2\right]^{\top}, \quad \hat{\sigma}_8 \triangleq \left[\underline{\sigma}_1^2, \underline{\sigma}_2^2, \underline{\sigma}_3^2\right]^{\top}, \end{aligned}$$

where $\underline{\sigma}_1^2 = \underline{\sigma}_2^2 = 0.0061$, $\underline{\sigma}_3^2 = 0.0012$, $\bar{\sigma}_1^2 = \bar{\sigma}_2^2 = 0.1134$ and $\bar{\sigma}_3^2 = 0.0105$. Furthermore, in this case, it should be noted that matrix $\hat{M}(\vartheta)$ in (5.52a) is considered parameter-independent, without loss of generality, due to the fact that $M(x)$ is constant for all $x \in \mathcal{X}$.

Finally, Problem 5.3.1 is solved through the LMI-based optimization problem (5.62), which is implemented in MATLAB by using the YALMIP toolbox [70] and the SeDuMi solver [117]. As a result, the following guaranteed shifting decay rate vertices of $\mathrm{d_R}(\varphi)$ in (5.52b) are obtained for the established design specifications, a fixed $\underline{\mathrm{d}}_{\mathrm{R}} = 0$ and a chosen relaxation degree $d = 2$:

$$\begin{aligned}
&\mathrm{d_{R1}} = 0.8337,\\
&\mathrm{d_{R2}} = \mathrm{d_{R3}} = \mathrm{d_{R5}} = 0.5558,\\
&\mathrm{d_{R4}} = \mathrm{d_{R6}} = \mathrm{d_{R7}} = 0.2779,\\
&\mathrm{d_{R8}} = 0.
\end{aligned}$$

5.6.4 Simulation results

This section illustrates the performance of the designed controller under simulation conditions without the presence of disturbances. To this end, the nonlinear system is evaluated for a time simulation of 6 s with $x_0 = \frac{\pi}{180}[-10, -10, 10, 0.1, 0.1, -0.1]^\top \in \mathcal{X}_0$.

Fig. 5.4 shows how the closed-loop state response of the 3-DoF hover platform converges to the origin, thus proving the closed-loop stabilization of the nonlinear system for a non-zero initial condition.

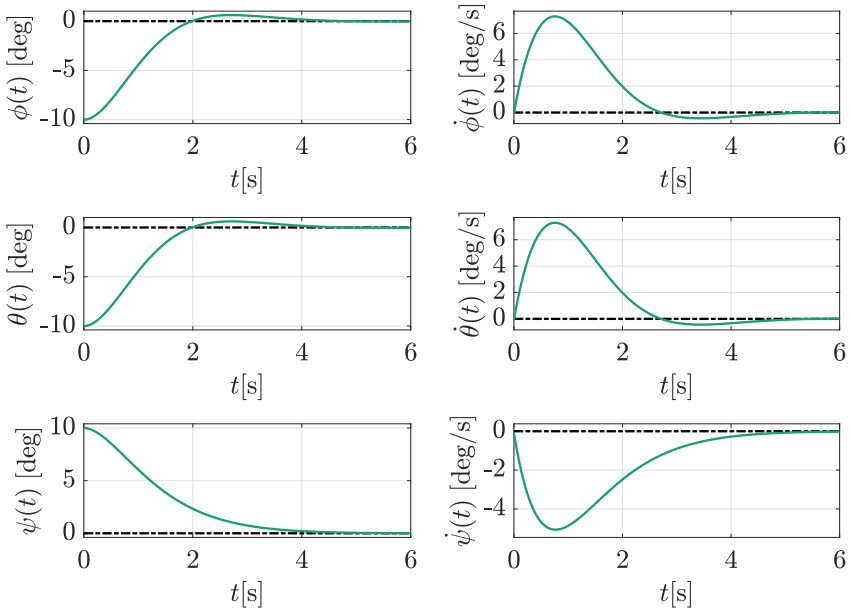

Figure 5.4: Closed-loop state responses (Simulation).

Fig. 5.5 illustrates the time variability of the region $\hat{\mathcal{V}}(x)$ in (5.23) due to its dependence on x. The transient response of the closed-loop system as depicted in Fig. 5.4 corresponds to the time window between $t = 0$ and $t = 2\,\mathrm{s}$, during which the most restrictive constraints are present in $\hat{\mathcal{V}}(x)$. Nevertheless, the calculated value of $M(x)^{-1}_{[l]}\nu$ for $l = 1, 2, 3$ is ensured to lie between the limits $\pm\sigma_l(x)$ for all $t \geq 0$. As a result, the control input (5.7) stays within the input limits, as seen in Fig. 5.6.

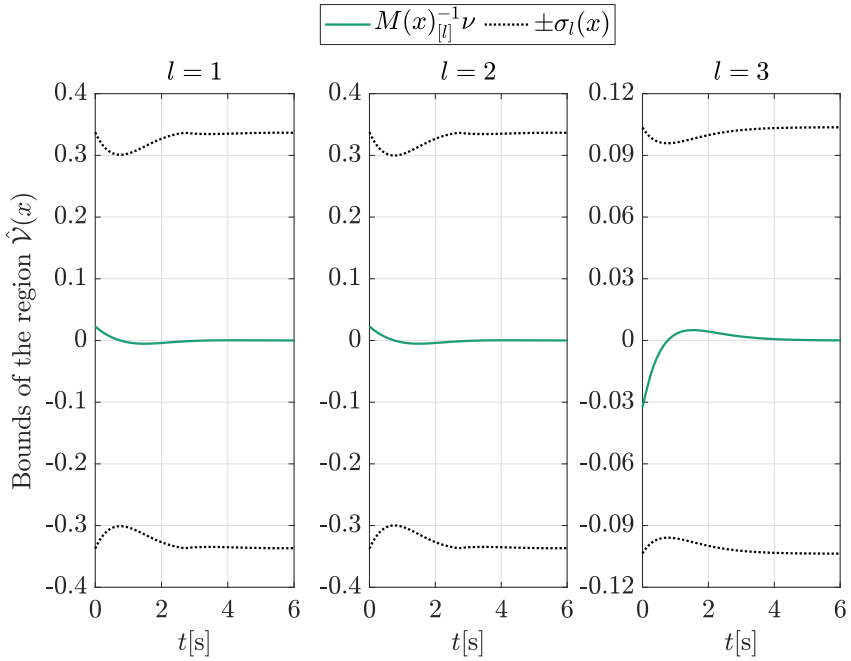

Figure 5.5: Bounds' variation of the region $\hat{\mathcal{V}}(x)$ in (5.23) (Simulation).

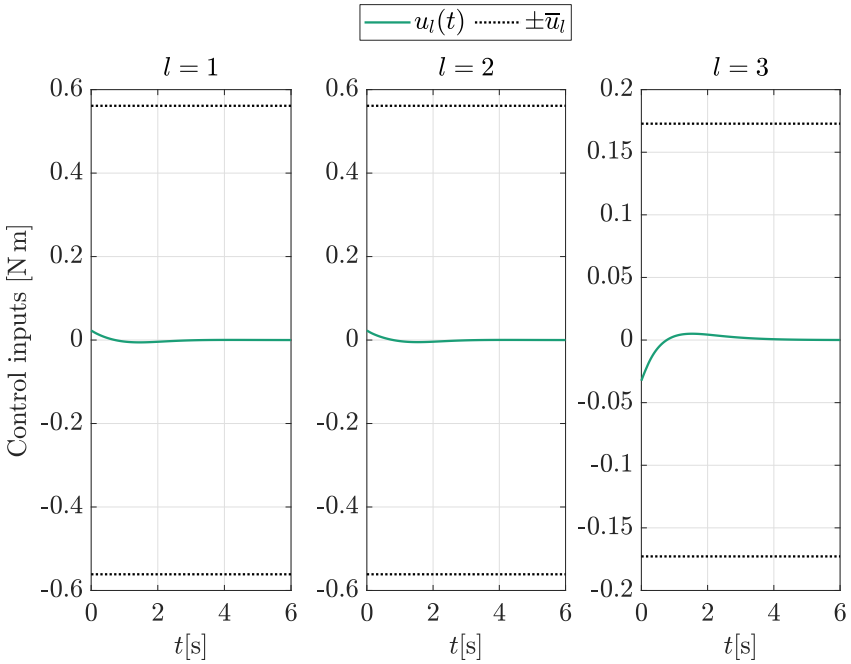

Figure 5.6: Control inputs (Simulation).

Finally, Fig. 5.7 shows that the Lyapunov function $V(z)$ is strictly decreasing for the entire simulation and illustrates the adaptability of the guaranteed shifting decay rate $\mathrm{d_R}(\varphi)$ according to the instantaneous values of $\sigma_l(x)$.

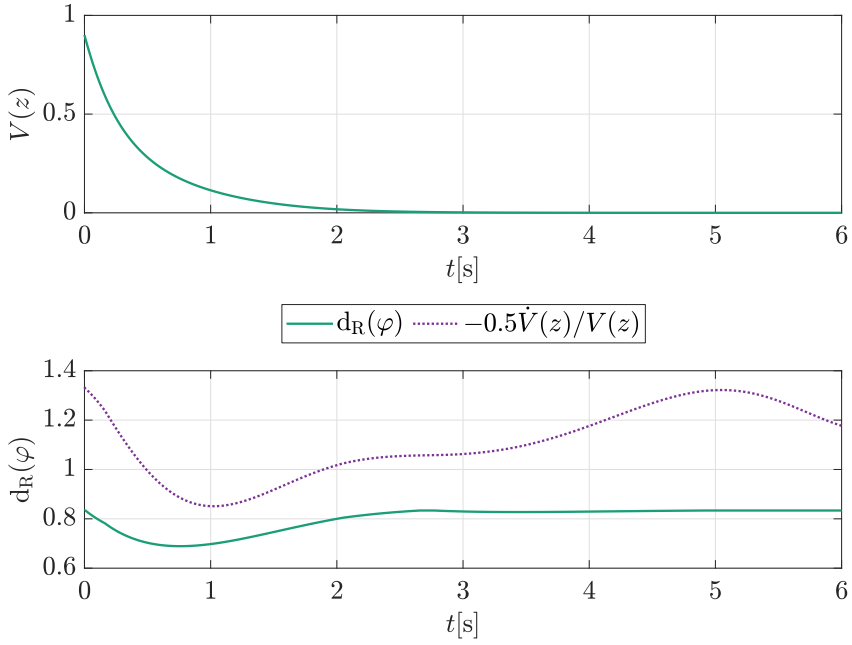

Figure 5.7: Lyapunov function and guaranteed shifting decay rate (Simulation).

5.6.5 Experimental validation

This section describes the experimental evaluation of the closed-loop stability and the closed-loop performance of the 3-DoF hover platform. To do this, we evaluate the closed-loop system response from the hovering point thus implying an initial state value of the Euler angles and rates close to zero. During the experiment, the platform is disturbed for a time interval of 1 s with three independent impulses whose values of $0.125\,\mathrm{N\,m}$, $-0.125\,\mathrm{N\,m}$ and $-0.08\,\mathrm{N\,m}$ are added to the actual τ_ϕ, τ_θ and τ_ψ at instants $t = 10\,\mathrm{s}$, $t = 20\,\mathrm{s}$ and $t = 30\,\mathrm{s}$, respectively, to illustrate the closed-loop transients for different values of the initial state. The disturbance time window between $t = 10\,\mathrm{s}$ and $t = 30\,\mathrm{s}$ is highlighted in Figs. 5.8-5.12 with a grey background ■, and the time intervals when the Lyapunov function $V(z)$ is such that $V(z) > 1$ are highlighted with the red background ■.

Fig. 5.8 shows that the closed-loop stability is guaranteed for all $t \geq 0$, even when the aforementioned disturbances are present. The absence of an integral action and the potential existence of unmodeled terms both contribute to the presence of a steady state error for the pitch angle $\theta(t)$. Note that an integral action can be added to the proposed control law, following the idea of state augmentation presented, e.g., in [43]. However, considering the state augmentation implies the presence of internal dynamics that must be considered and, hence, the partial linearization of the nonlinear system [63], which goes beyond the scope of this chapter.

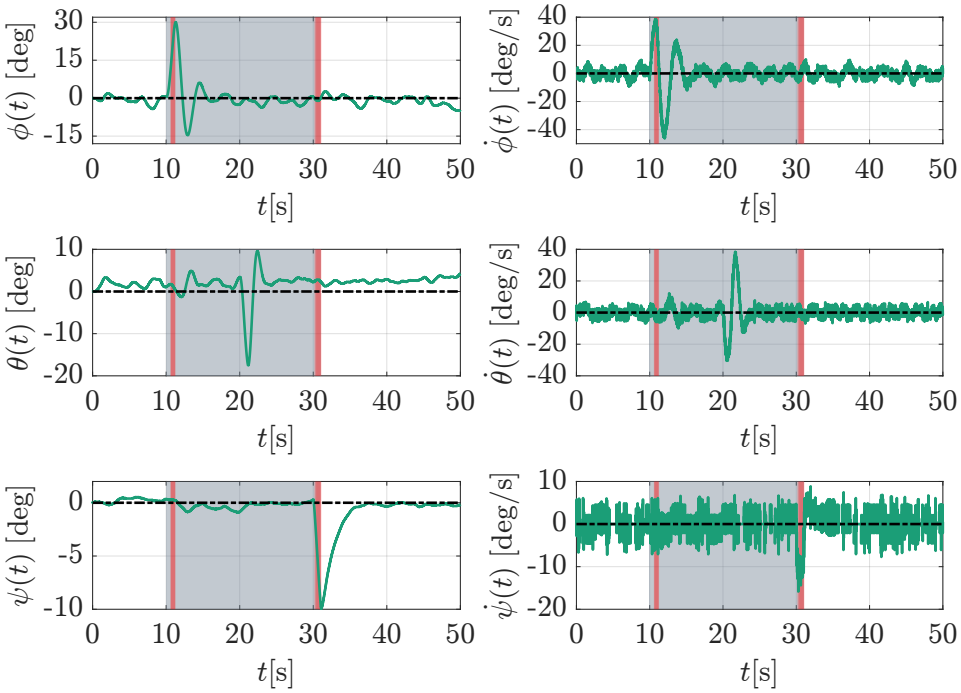

Figure 5.8: Closed-loop state responses (Experimental). (The grey background ■ denotes the disturbance time window. The red background ■ represents the time interval where $V(z) > 1$.)

Fig. 5.9 illustrates how the bounds of the region $\hat{\mathcal{V}}(x)$ in (5.23) vary over time. Due to the lack of robustness against the presence of disturbances, there exists the possibility of ν leaving $\hat{\mathcal{V}}(x)$ for time instants where $V(z) > 1$ (see Fig. 5.12). However, the control input (5.7) can be guaranteed to lie between the input limits as long as the region limits in (5.23) are satisfied, as shown in Fig. 5.10. Furthermore, it is shown in Fig. 5.11 that the applied motor voltages, obtained from the relationship (5.64), remain within the actuator's limits.

Finally, Fig. 5.12 shows the Lyapunov function $V(z)$ and the guaranteed shifting decay rate $\mathrm{d_R}(\varphi)$. Note that after the disturbances have been applied, the bounds of the region $\hat{\mathcal{V}}(x)$ are more restrictive (see Fig. 5.9) and, as a consequence, the actual value of $\mathrm{d_R}(\varphi)$ is reduced. Furthermore, it is also shown that despite $V(z) > 1$ for some instants after the applied disturbances in τ_ϕ and τ_ψ, respectively, the proposed control design approach has some robustness so that it can cope with more extensive operating conditions than those certified by the theoretical proofs of stability and non-saturation.

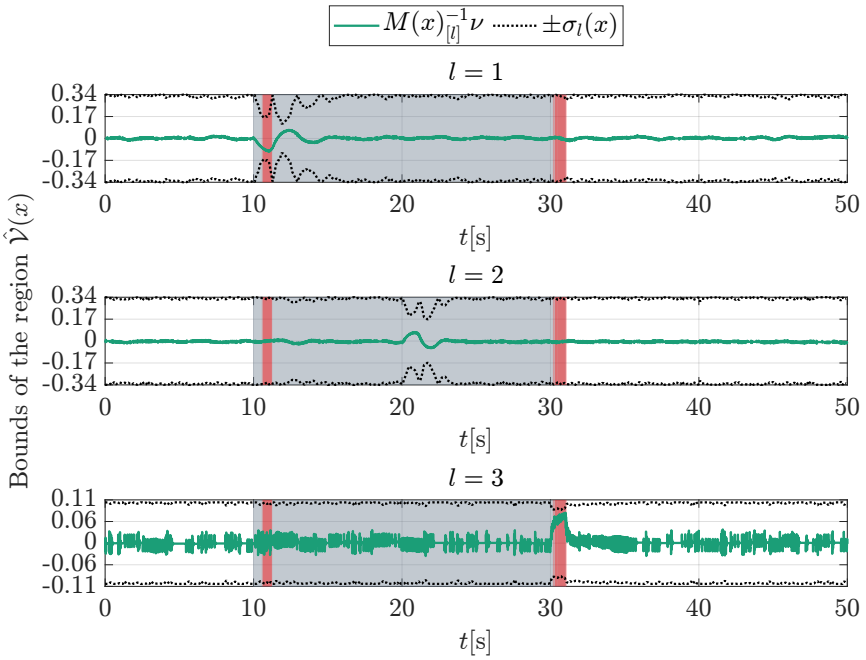

Figure 5.9: Bounds' variation of the region $\hat{\mathcal{V}}(x)$ in (5.23) (Experimental). (The grey background ■ denotes the disturbance time window. The red background ■ represents the time interval where $V(z) > 1$.)

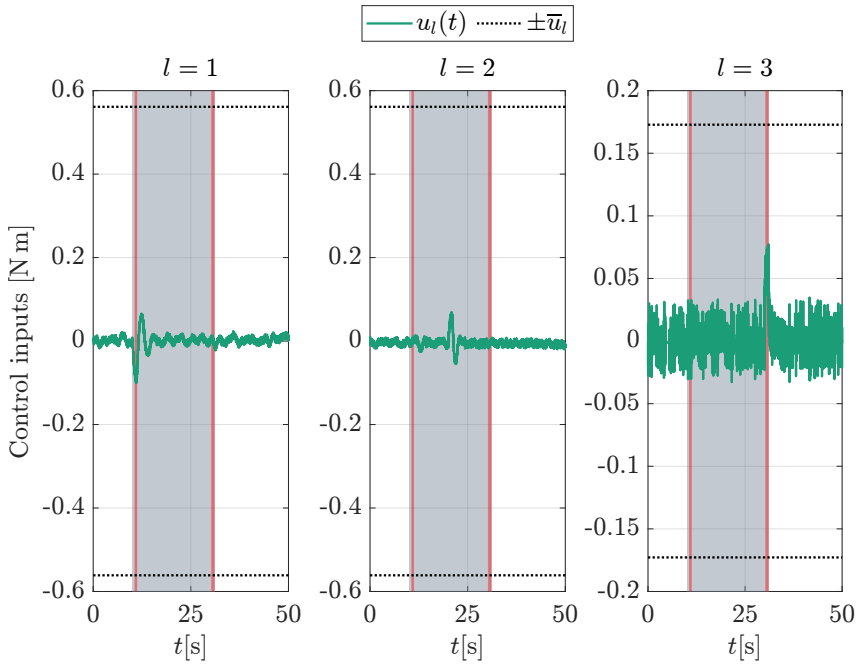

Figure 5.10: Control inputs (Experimental). (The grey background ■ denotes the disturbance time window. The red background ■ represents the time interval where $V(z) > 1$.)

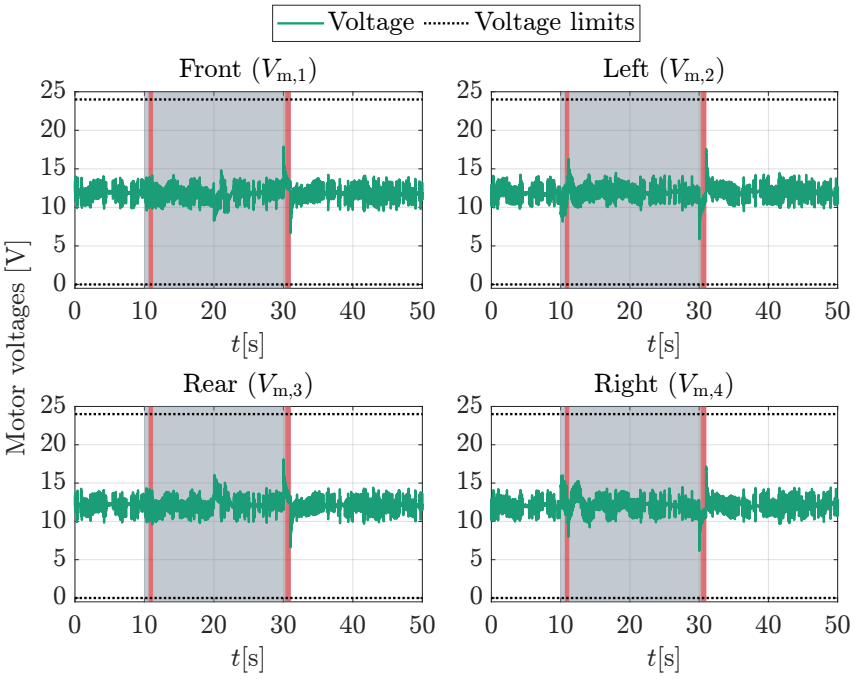

Figure 5.11: Motor voltages (Experimental). (The grey background ■ denotes the disturbance time window. The red background ■ represents the time interval where $V(z) > 1$.)

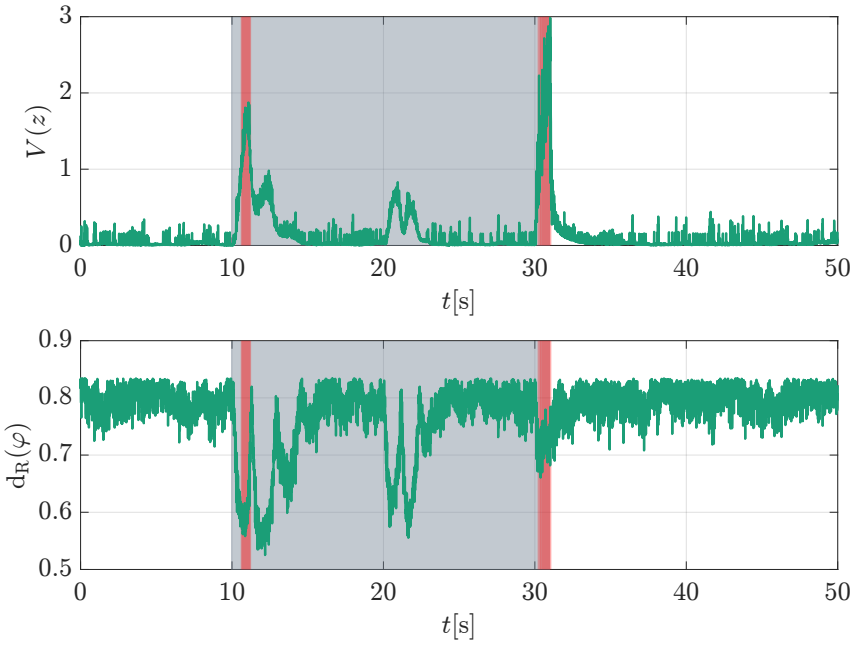

Figure 5.12: Lyapunov function and the guaranteed shifting decay rate (Experimental). (The grey background ■ denotes the disturbance time window. The red background ■ represents the time interval where $V(z) > 1$.)

5.7 Conclusions

The design of a shifting FBL controller for a nonlinear system with input constraints has been investigated in this chapter. The proposed methodology, which is based on the use of the input-output FBL approach, the polytopic representation and the application of the shifting paradigm concept, has been used to design a gain-scheduling state-feedback controller for a fully linearized system subject to a state-dependent input saturation. The simulation and experimental results show that the proposed controller achieves the guaranteed shifting decay rate performance by adjusting the closed-loop response of the system in real time according to the instantaneous values of the time-varying system's region of linearity.

Future research will focus on the development of alternative LMI-based methods to account for asymmetric saturation limits, parameter-dependent Lyapunov functions, and the application of robust techniques.

6 Asymmetric saturations

The content of this chapter is based on the following work:

- [98] A. Ruiz, D. Rotondo, and B. Morcego. "Design of switching state-feedback controllers for linear systems subject to asymmetric saturations". *IFAC-PapersOnLine*, 2023. 22nd IFAC World Congress. Accepted.

6.1 Introduction

Despite the fact that most of the proposed approaches in the literature address the saturation control problem with symmetric actuator saturations in mind (see, for example, works [29, 30, 56], monographs [54, 119], and references therein), asymmetric saturation limits may frequently arise in practical systems. A common approach is to manage the asymmetric saturation functions by treating them as symmetric saturation functions with the most restrictive saturation limits, at the cost of increasing conservatism. For this reason, several researchers have recently focused on this topic in an attempt to reduce conservatism. For example, [25, 73] have suggested a coordinate transformation in order to enlarge the controlled region of attraction. In [15], an LMI-based methodology has been proposed for stabilizing an asymmetrically saturated system by converting it into a saturated one with symmetric saturation limits and a bounded disturbance. Alternatively, a linear system with asymmetric saturations can be converted into a switched linear model with symmetric saturations, as demonstrated in [47, 69, 132], where different LMI-based methodologies have been proposed for designing a switching controller.

The present chapter describes an LMI-based methodology for designing a switching state-feedback controller for a linear system subject to asymmetric input saturations. Although the idea of using a switched model is based on the idea of partitioning the state space into multiple regions, as proposed by Yuan et al. [132], the main difference and contribution of this chapter when compared to existing approaches is that the switching rule is designed based on the attainable closed-loop performance. In particular, the design conditions are obtained through the application of the theory of invariant sets and the use of a QLF, thus guaranteeing that the control action remains in the linearity region of the actuators. Furthermore, a closed-loop performance criterion is established by associating distinct decay rate values to the different possible controller modes, equipping the control system with the ability to change its closed-loop performance in the sense of guaranteed convergence speed.

This chapter is structured as follows: Sections 6.2-6.3 present some preliminary concepts, the formulation of the closed-loop performance specification, and the definition of the control design problem. Section 6.4 provides an LMI-based methodology for the controller design. Section 6.5 explores the extension to the parameter-varying case. Finally, an illustrative example is presented in Section 6.6.

6.2 Preliminaries

Consider the following CT system:

$$\dot{x} = Ax + B\,\mathrm{sat}(u, \underline{u}, \bar{u}), \quad x(0) = x_0, \tag{6.1}$$

where $x \in \mathbb{R}^{n_x}$ is the state vector and $u \in \mathbb{R}^{n_u}$ denotes the control input vector. $A \in \mathbb{R}^{n_x \times n_x}$ and $B \in \mathbb{R}^{n_x \times n_u}$ represent the state and input matrices, respectively, and $\mathrm{sat}(u, \underline{u}, \bar{u}) : \mathbb{R}^{n_u} \to \mathbb{R}^{n_u}$ denotes the standard asymmetric saturation function, defined as in (2.71):

$$\mathrm{sat}(u, \underline{u}, \bar{u}) \triangleq \begin{bmatrix} \mathrm{sat}(u_1, \underline{u}_1, \bar{u}_1) \\ \vdots \\ \mathrm{sat}(u_l, \underline{u}_l, \bar{u}_l) \\ \vdots \\ \mathrm{sat}(u_{n_u}, \underline{u}_{n_u}, \bar{u}_{n_u}) \end{bmatrix}, \quad \mathrm{sat}(u_l, \underline{u}_l, \bar{u}_l) \triangleq \begin{cases} \bar{u}_l, & \text{if } u_l > \bar{u}_l \\ u_l, & \text{if } u_l \in [\underline{u}_l, \bar{u}_l] \\ -\underline{u}_l, & \text{if } u_l < -\underline{u}_l \end{cases} \tag{6.2}$$

for $l \in \mathcal{I}_{[1,n_u]}$ with known saturation limits $\underline{u}_l, \bar{u}_l \in \mathbb{R}_+ \backslash \{0\}$. Note that the standard symmetric saturation function is recovered if $\underline{u}_l = \bar{u}_l \; \forall l \in \mathcal{I}_{[1,n_u]}$, which will be denoted as $\mathrm{sat}(u_l, \bar{u}_l)$.

According to Yuan et al. [132], the asymmetric saturation (6.2) can be characterized by a combination of 2^{n_u} symmetric saturations, the limits of which belong to the set $\mathcal{S}_v \triangleq \{\bar{v}_i\}_{i=1}^{2^{n_u}} \subset \mathbb{R}_+^{n_u} \backslash \{0\}$, and $\bar{v}_i$ is specified as:

$$\bar{v}_i = \Gamma_i \bar{u} + \Gamma_i^- \underline{u}, \quad i \in \mathcal{I}_{[1,2^{n_u}]}, \tag{6.3}$$

where $\bar{v}_i \in \mathcal{S}_v$ corresponds to the i^{th} saturation limit vector, $\Gamma_i \in \mathbb{R}^{n_u \times n_u}$ is a diagonal matrix whose elements take the value 0 or 1 and $\Gamma_i^- = \mathrm{I}_{n_u} - \Gamma_i$.

An example to explain the obtention of vectors $\bar{v}_i \in \mathcal{S}_v$ is provided below.

Example 6.2.1. For $n_u = 2$ and the given vectors $\bar{u} = [\bar{u}_1, \bar{u}_2]^\top$ and $\underline{u} = [\underline{u}_1, \underline{u}_2]^\top$, the matrices Γ_i and Γ_i^- in (6.3) are defined for $i \in \mathcal{I}_{[1,4]}$ by:

$$\Gamma_1 = \begin{bmatrix} 0 & 0 \\ 0 & 0 \end{bmatrix}, \quad \Gamma_2 = \begin{bmatrix} 0 & 0 \\ 0 & 1 \end{bmatrix}, \quad \Gamma_3 = \begin{bmatrix} 1 & 0 \\ 0 & 0 \end{bmatrix}, \quad \Gamma_4 = \begin{bmatrix} 1 & 0 \\ 0 & 1 \end{bmatrix},$$
$$\Gamma_1^- = \begin{bmatrix} 1 & 0 \\ 0 & 1 \end{bmatrix}, \quad \Gamma_2^- = \begin{bmatrix} 1 & 0 \\ 0 & 0 \end{bmatrix}, \quad \Gamma_3^- = \begin{bmatrix} 0 & 0 \\ 0 & 1 \end{bmatrix}, \quad \Gamma_4^- = \begin{bmatrix} 0 & 0 \\ 0 & 0 \end{bmatrix}.$$

Then, the set $\mathcal{S}_v$ contains all the possible combinations of the saturation limit vectors in (6.2) as follows:

$$\mathcal{S}_v = \left\{ \begin{bmatrix} \underline{u}_1 \\ \underline{u}_2 \end{bmatrix}, \begin{bmatrix} \underline{u}_1 \\ \bar{u}_2 \end{bmatrix}, \begin{bmatrix} \bar{u}_1 \\ \underline{u}_2 \end{bmatrix}, \begin{bmatrix} \bar{u}_1 \\ \bar{u}_2 \end{bmatrix} \right\}.$$

▲

Therefore, the system (6.1) can be reformulated as a switched linear system subject to symmetric saturation functions $\mathrm{sat}(u, \bar{v}_i) : \mathbb{R}^{n_u} \to \mathbb{R}^{n_u}$ associated with the vectors $\bar{v}_i \in \mathcal{S}_v$, as follows:

$$\dot{x} = Ax + B\,\mathrm{sat}(u, \bar{v}_i), \quad i \in \mathcal{I}_{[1,2^{n_u}]}. \tag{6.4}$$

6.3 Problem formulation

Let us define the following switching state-feedback controller:

$$u = K_i x, \quad i \in \mathcal{I}_{[1,2^{n_u}]}, \tag{6.5}$$

where $K_i \in \mathbb{R}^{n_u \times n_x}$ corresponds to the i^{th} controller gain matrix. In this way, the closed-loop representation of the switching saturated system (6.4) is obtained, as follows:

$$\dot{x} = Ax + B\,\mathrm{sat}(K_i x, \bar{v}_i),\ \bar{v}_i \in \mathcal{S}_v,\ i \in \mathcal{I}_{[1,2^{n_u}]}. \tag{6.6}$$

The goal of this chapter is to stabilize the closed-loop system (6.6) so that the performance criterion stated in Definition 6.3.1 is fulfilled with the actuators working in their linearity region.

Definition 6.3.1 (Guaranteed switching decay rate (GSWDR))**.** The closed-loop response (6.6) is said to have a desired *guaranteed switching decay rate* if:

$$\dot{V}(x) \leq -2\,\mathrm{d}_{\mathrm{R}i}\,V(x),\ \forall i \in \mathcal{I}_{[1,2^{n_u}]}, \tag{6.7}$$

where $V(x)$ is a parameter-independent Lyapunov candidate function and $\mathrm{d}_{\mathrm{R}i} \in \mathbb{R}_+$ corresponds to the i^{th} desired decay rate value associated to the controller gain K_i in (6.5).

To accomplish this goal, the next section provides an LMI-based methodology for designing a non-saturating switching state-feedback controller (6.5) with the objective of solving the control design problem listed below:

Problem 6.3.1. For the CT system (6.1) under the asymmetric saturation function (6.2) and a given set of admissible initial conditions $\mathcal{X}_0$, design a non-saturating switching state-feedback controller (6.5) and a switching rule such that for any initial state $x_0 \in \mathcal{X}_0$:

1. The closed-loop system response ensures the GSWDR performance (6.7).
2. The computed control action $u(t)$ lies in the region of linearity of the system (6.1), such that $\mathrm{sat}(u, \underline{u}, \bar{u}) = u$, which is characterized by the following polyhedral set:

$$\mathcal{L}(u, \underline{u}, \bar{u}) \triangleq \left\{u \in \mathbb{R}^{n_u} \ :\ -\underline{u}_l \leq u_l \leq \bar{u}_l,\ l \in \mathcal{I}_{[1,n_u]}\right\}. \tag{6.8}$$

□

6.4 Design of a non-saturating switching state-feedback controller

Let us consider the relationship between the input u and the state x given by the control law (6.5), then for the active controller gain K_i and the associated saturation limit $\bar{v}_i \in \mathcal{S}_v$, the region of linearity (6.8) is mapped onto a symmetric region, defined as:

$$\mathcal{L}_s(K_i, \bar{v}_i) \triangleq \left\{x \in \mathbb{R}^{n_x} \ :\ |K_{[l],i}x| \leq \bar{v}_{l,i},\ l \in \mathcal{I}_{[1,n_u]}\right\}, \tag{6.9}$$

which is equivalent to:

$$\mathcal{L}_s(K_i, \bar{v}_i) \triangleq \left\{ x \in \mathbb{R}^{n_x} \ : \ x^\top \frac{K_{[l],i}^\top K_{[l],i}}{\bar{v}_{l,i}^2} x \leq 1, \ l \in \mathcal{I}_{[1,n_u]} \right\}, \tag{6.10}$$

where $\bar{v}_{l,i}$ denotes the l^{th} element of $\bar{v}_i$.

Recalling from Section 2.3.2, the polyhedral set of admissible initial conditions $\mathcal{X}_0$ is defined as in (2.73):

$$\mathcal{X}_0 \triangleq \mathrm{Co}\{v_1, \ldots, v_{n_v}\}, \quad v_s \in \mathbb{R}^{n_x}, \quad \forall s \in \mathcal{I}_{[1,n_v]}, \tag{6.11}$$

where n_v is the number of vertices and v_s represents each vertex of the set. Thereupon, let us propose below a slight modification of Proposition 2.3.1:

Proposition 6.4.1. *Let $\mathcal{L}_s(K_i, \bar{v}_i)$ be a symmetrical polyhedral set defined as in (6.10). If $\mathcal{E}(P, c)$ is a contractively invariant set satisfying $\forall i \in \mathcal{I}_{[1,2^{n_u}]}$:*

$$\mathcal{X}_0 \subset \mathcal{E}(P, c) \subset \mathcal{L}_s(K_i, \bar{v}_i), \tag{6.12}$$

then for any initial condition $x_0 \in \mathcal{X}_0$, and hence $x_0 \in \mathcal{E}(P, c)$, the convergence of the corresponding state trajectory $x(t) \to 0$ when $t \to \infty$ is ensured under saturation avoidance for at least one of the 2^{n_u} computed controller gains K_i.

Proof. Since one of the vectors $\bar{v}_i \in \mathcal{S}_v$ contemplates the case with the most restrictive saturation limits, the region $\mathcal{E}(P, c)$ is forced to reside within the region of linearity that corresponds to the worst-case scenario. Hence, it is ensured that at least one of the computed controllers will perform under saturation avoidance $\forall t$ as long as $x(t) \in \mathcal{E}(P, c)$. The rest of the proof follows the reasoning in Proposition 2.3.1 and is thus omitted. ■

The following theorem gives the conditions for designing the switching state-feedback controller (6.5) in order to solve Problem 6.3.1 considering the performance specification (6.7) and the set of inclusions (6.12) stated in Proposition 6.4.1. To keep things simple, the general design approach is developed with a QLF in mind, as specified in (2.12):

$$V(x) = x^\top P^{-1} x, \tag{6.13}$$

and its unit level set:

$$\mathcal{E}(P, 1) = \{x \in \mathbb{R}^{n_x} \ : \ V(x) \leq 1\}. \tag{6.14}$$

Theorem 6.4.2. *Given the regions (6.10), (6.11) and (6.14) with the known vertices v_s and the desired switching decay rate values $\mathrm{d}_{\mathrm{R}i} \in \mathbb{R}_+$, let there exist decision matrices $P \in \mathbb{S}_+^{n_x}$ and $Y_i \in \mathbb{R}^{n_u \times n_x}$ satisfying $\forall i \in \mathcal{I}_{[1,2^{n_u}]}$ and $\bar{v}_i \in \mathcal{S}_v$:*

$$\mathrm{He}\{AP + BY_i\} + 2\,\mathrm{d}_{\mathrm{R}i} P \prec 0, \tag{6.15}$$

$$\begin{bmatrix} P & v_s \\ \star & 1 \end{bmatrix} \succeq 0, \quad s \in \mathcal{I}_{[1,n_v]}, \tag{6.16}$$

$$\begin{bmatrix} \bar{v}_{l,i}^2 & Y_{[l],i} \\ \star & P \end{bmatrix} \geq 0, \quad l \in \mathcal{I}_{[1,n_u]}. \tag{6.17}$$

Then, the closed-loop system response (6.6) *with the switching state-feedback controller* (6.5) *computed as* $K_i = Y_i P^{-1}$ *has the guaranteed switching decay rate performance expressed by* (6.7)*. Furthermore, the convergence of* $x(t) \to 0$ *when* $t \to \infty$ *is ensured for any* $x_0 \in \mathcal{X}_0$ *such that* $x(t) \in \mathcal{L}_s(K_i, \bar{v}_i)$ *and, hence,* $u \in \mathcal{L}(u, \underline{u}, \bar{u})$*.*

Proof. The proof is split in two parts. The first part demonstrates how the performance criterion (6.7) is guaranteed by the LMI (6.15). The second one shows that any state trajectory $x(t)$ starting from an $x_0 \in \mathcal{X}_0 \subset \mathcal{E}(P, 1)$ belongs to $\mathcal{L}_s(K_i, \bar{v}_i)$, $i \in \mathcal{I}_{[1,2^{n_u}]}$, implying that $x(t) \to 0$ for $t \to \infty$ with $u \in \mathcal{L}(u, \underline{u}, \bar{u})$.

Part 1: By assuming that $\mathrm{sat}(K_i x, \bar{v}_i) = K_i x \ \forall i \in \mathcal{I}_{[1,2^{n_u}]}$, the closed-loop system response (6.6) can be rewritten as:

$$\dot{x} = (A + BK_i)x. \tag{6.18}$$

Then, the following set of BMIs can be obtained by considering (6.7):

$$\mathrm{He}\{P^{-1}A + P^{-1}BK_i\} + 2\,\mathrm{d}_{\mathrm{R}i}\,P^{-1} \prec 0. \tag{6.19}$$

By pre- and post-multiplying (6.19) by P, one gets:

$$\mathrm{He}\{AP + BK_iP\} + 2\,\mathrm{d}_{\mathrm{R}i}\,P \prec 0, \tag{6.20}$$

which can be transformed into the LMI (6.15) by means of the change of variable $Y_i = K_i P$ $\forall i \in \mathcal{I}_{[1,2^{n_u}]}$. Therefore, the feasibility of the LMI (6.15) ensures that the closed-loop response of system (6.6) has the switching guaranteed decay rate performance (6.7).

Part 2: By using Schur's complement, the LMI (6.16) is equivalent to:

$$v_s^\top P^{-1} v_s \leq 1, \quad s \in \mathcal{I}_{[1,n_v]}, \tag{6.21}$$

which leads to the inclusion $\mathcal{X}_0 \subset \mathcal{E}(P, 1)$ (see [54, Chap. 7]). Next, the following condition is obtained by pre- and post-multiplying the LMI (6.17) by $\mathrm{diag}\{1, P^{-1}\}$:

$$\begin{bmatrix} \bar{v}_{l,i}^2 & K_{[l],i} \\ \star & P^{-1} \end{bmatrix} \geq 0, \quad \bar{v}_i \in \mathcal{S}_v, \quad \begin{matrix} l \in \mathcal{I}_{[1,n_u]} \\ i \in \mathcal{I}_{[1,2^{n_u}]} \end{matrix}, \tag{6.22}$$

which by applying Schur's complement and pre- and post-multiplying by $x^\top$ and x, respectively, leads to:

$$x^\top \frac{K_{[l],i}^\top K_{[l],i}}{\bar{v}_{l,i}^2} x \leq x^\top P^{-1} x,$$

which yields $\mathcal{E}(P, 1) \subset \mathcal{L}_s(K_i, \bar{v}_i)$. Consequently, $x \in \mathcal{L}_s(K_i, \bar{v}_i)$ is ensured for any trajectory $x \in \mathcal{E}(P, 1)$ and, hence, $u \in \mathcal{L}(u, \underline{u}, \bar{u})$, thus concluding the proof. ∎

6.4.1 Switching rule

Since $x(t) \in \mathcal{L}_s(K_i, \bar{v}_i)$ is guaranteed $\forall t \geq 0$ by Theorem 6.4.2, the following rule can be defined to select the active controller gain K_σ:

$$\begin{aligned} \sigma &= \arg\max_h \ \mathrm{d}_{\mathrm{R}h} \\ \text{s.t.} \quad h &\in \left\{ i \in \mathcal{I}_{[1,2^{n_u}]} : K_i x \in \mathcal{L}(u, \underline{u}, \bar{u}) \right\} \end{aligned} \tag{6.23}$$

It should be noted that this rule accounts for which one among the controller gains provides an input signal contained in the asymmetric region of linearity (6.8), given the current value of the state. This is a novelty when compared to other existing approaches (see e.g., [132] or [69]), where the switching rule accounts for the control input signs instead. Furthermore, the rule (6.23) selects, among the non-saturating controller gains, the one that provides the largest guaranteed decay rate, therefore adjusting the closed-loop performance according to the criterion given in Definition 6.3.1.

Remark 6.4.1. Note that the situation where rule (6.23) is not defined due to saturating gains is not considered. Future work will address the extension of the provided approach considering saturated control inputs approaches [54, 119].

6.5 Extension to the LPV case

Let us extend the procedure described in Section 6.4 to the LPV case by modifying (6.6) as follows:

$$\dot{x} = A(\vartheta)x + B(\vartheta)\,\mathrm{sat}(K_i(\vartheta)x, \bar{v}_i), \tag{6.24}$$

with $\bar{v}_i \in \mathcal{S}_v$ and $i \in \mathcal{I}_{[1,2^{n_u}]}$. The parameter-dependent matrices $A(\vartheta) \in \mathbb{R}^{n_x \times n_x}$, $B(\vartheta) \in \mathbb{R}^{n_x \times n_u}$ and $K_i(\vartheta) \in \mathbb{R}^{n_u \times n_x}$ can be written as a convex combination of n_μ known vertices:

$$\begin{bmatrix} A(\vartheta) & B(\vartheta) & K_i(\vartheta) \end{bmatrix} = \sum_{j=1}^{n_\mu} \mu_j(\vartheta) \begin{bmatrix} A_j & B_j & K_{ij} \end{bmatrix}, \tag{6.25}$$

where $A_j \in \mathbb{R}^{n_x \times n_x}$, $B_j \in \mathbb{R}^{n_x \times n_u}$ and $K_{ij} \in \mathbb{R}^{n_u \times n_x}$ stand for the given known vertex matrices and $\vartheta \in \Theta \subseteq \mathbb{R}^{n_\vartheta}$ represents the scheduling parameter vector with Θ as a known, bounded and closed set. $\mu(\vartheta) \in \mathbb{R}^{n_\mu}$ corresponds to the polytopic weight vector belonging to the unit simplex, defined as in (2.10):

$$\Delta^{n_\mu} \triangleq \left\{ \mu(\vartheta) \in \mathbb{R}^{n_\mu} \ : \ \sum_{j=1}^{n_\mu} \mu_j(\vartheta) = 1, \ \mu_j(\vartheta) \geq 0, \ j \in \mathcal{I}_{[1,n_\mu]} \right\}. \tag{6.26}$$

Due to the controller gain being parameter-dependent, the symmetric region of linearity (6.10) becomes parameter-dependent as well $\forall i \in \mathcal{I}_{[1,2^{n_u}]}$:

$$\mathcal{L}_s(K_i(\vartheta), \bar{v}_i) \triangleq \left\{ x \in \mathbb{R}^{n_x} \ : \ x^\top \frac{K_i(\vartheta)_{[l]}^\top K_i(\vartheta)_{[l]}}{\bar{v}_{l,i}^2} x \leq 1, \ l \in \mathcal{I}_{[1,n_u]} \right\}, \tag{6.27}$$

so that the set of inclusions (6.12) in Proposition 6.4.1 is modified as:

$$\mathcal{X}_0 \subset \mathcal{E}(P,c) \subset \mathcal{L}_s(K_i(\vartheta), \bar{v}_i), \tag{6.28}$$

which leads to the extension of Theorem 6.4.2 to the LPV case.

Theorem 6.5.1. *Given the regions* (6.11), (6.14) *and* (6.27) *with the known vertices* v_s*, a previously chosen relaxation degree* $d \in \mathbb{N}$*, with* $d \geq 2$*, and the desired switching decay rate values* $\mathrm{d}_{\mathrm{R}i} \in \mathbb{R}_+$*, let there exist the decision matrices* $P \in \mathbb{S}_+^{n_x}$ *and* $Y_{ij} \in \mathbb{R}^{n_u \times n_x}$ *with* $i \in \mathcal{I}_{[1,2^{n_u}]}$ *and* $j \in \mathcal{I}_{[1,n_\mu]}$ *such that the LMI* (6.16) *is satisfied together with:*

$$\sum_{\boldsymbol{q} \in \mathcal{P}(\boldsymbol{j})} [\mathrm{He}\{A_{q_1} P + B_{q_1} Y_{iq_2}\} + 2\,\mathrm{d}_{\mathrm{R}i} P] \prec 0, \quad \boldsymbol{j} \in \mathbb{I}^+_{(d,n_\mu)}, \tag{6.29}$$

$$\begin{bmatrix} \bar{v}_{l,i}^2 & Y_{[l],ij} \\ \star & P \end{bmatrix} \succeq 0, \quad \bar{v}_i \in \mathcal{S}_v,\ l \in \mathcal{I}_{[1,n_u]}. \tag{6.30}$$

Then, the guaranteed switching decay rate performance defined in Definition 6.3.1 holds for all parameter-dependent terms appearing in (6.24), (6.27) *and* (6.28) *with the controller gain computed as* $K_i(\vartheta) = \left(\sum_{j=1}^{n_\mu} \mu_j(\vartheta) Y_{ij}\right) P^{-1}$.

Proof. Similarly to the proof of Theorem 6.4.2, the following BMI can be obtained $\forall i \in \mathcal{I}_{[1,2^{n_u}]}$:

$$\mathrm{He}\{A(\vartheta)P + B(\vartheta)K_i(\vartheta)P\} + 2\,\mathrm{d}_{\mathrm{R}i} P \prec 0, \tag{6.31}$$

which can be transformed into the following LMI by means of the change of variable $Y_i(\vartheta) = K_i(\vartheta)P$:

$$\mathrm{He}\{A(\vartheta)P + B(\vartheta)Y_i(\vartheta)\} + 2\,\mathrm{d}_{\mathrm{R}i} P \prec 0, \tag{6.32}$$

By using the polytopic representation (6.25) of the parameter-dependent matrices appearing in (6.32) and considering $\mu(\vartheta) \in \Delta^{n_\mu}$, one gets:

$$\sum_{j_1=1}^{n_\mu} \sum_{j_2=1}^{n_\mu} \mu_{j_1}(\vartheta)\mu_{j_2}(\vartheta)[\mathrm{He}\{A_{j_1} P + B_{j_1} Y_{ij_2}\} + 2\,\mathrm{d}_{\mathrm{R}i} P] \prec 0. \tag{6.33}$$

Since multiple polytopic summations are involved in the negative-definiteness of (6.33), the use of Lemma 2.2.14 is required for obtaining the LMI (6.29).

By multiplying the left-hand side of the LMI (6.30) by $\mu_j(\vartheta)$ and summing it up to $j \in \mathcal{I}_{[1,n_\mu]}$, one gets:

$$\begin{bmatrix} \bar{v}_{l,i}^2 & Y_i(\vartheta)_{[l]} \\ \star & P \end{bmatrix} \succeq 0, \quad \bar{v}_i \in \mathcal{S}_v, \quad \begin{matrix} i \in \mathcal{I}_{[1,2^{n_u}]} \\ l \in \mathcal{I}_{[1,n_u]} \end{matrix}. \tag{6.34}$$

Then, let us pre- and post-multiply the expression (6.34) by $\mathrm{diag}\{1, P^{-1}\}$, thus obtaining:

$$\begin{bmatrix} \bar{v}_{l,i}^2 & K_i(\vartheta)_{[l]} \\ \star & P^{-1} \end{bmatrix} \succeq 0, \quad \bar{v}_i \in \mathcal{S}_v, \quad \begin{matrix} i \in \mathcal{I}_{[1,2^{n_u}]} \\ l \in \mathcal{I}_{[1,n_u]} \end{matrix}. \tag{6.35}$$

Finally, the following inequality is obtained by using Schur's complement and pre- and post-multiplication by $x^\top$ and x:

$$x^\top \frac{K_i(\vartheta)_{[l]}^\top K_i(\vartheta)_{[l]}}{\bar{v}_{l,i}^2} x \leq x^\top P^{-1} x,$$

which leads to the parameter-dependent inclusions $\mathcal{E}(P,1) \subset \mathcal{L}_s(K_i(\vartheta), \bar{v}_i)$. As a result, $x \in \mathcal{L}_s(K_i(\vartheta), \bar{v}_i)$ is guaranteed for any $x \in \mathcal{E}(P,1)$, and so $u \in \mathcal{L}(u, \underline{u}, \bar{u})$, thus concluding the proof. ■

Note that rule (6.23) can also be applied to the LPV case, although it will lead to the active controller being dependent on the varying parameter ϑ:

$$\begin{aligned} \sigma(\vartheta) &= \arg\max_h \ \mathrm{d}_{\mathrm{R}h} \\ \text{s.t.} \quad & h \in \left\{ i \in \mathcal{I}_{[1,2^{n_u}]} : K_i(\vartheta) x \in \mathcal{L}(u, \underline{u}, \bar{u}) \right\} \end{aligned} \tag{6.36}$$

6.6 Illustrative example

Let us consider the following system [119, Example 1.3], with modified saturation limits:

$$\dot{x} = \begin{bmatrix} 0.1 & -0.1 \\ 0.1 & -3 \end{bmatrix} x + \begin{bmatrix} 5 & 0 \\ 0 & 1 \end{bmatrix} \mathrm{sat}(u, \underline{u}, \bar{u}), \qquad \begin{matrix} \bar{u} = [5,2]^\top \\ \underline{u} = [2,3]^\top \end{matrix} .$$

The characterization of the asymmetric saturation function (6.2) is obtained by a combination of 4 symmetric saturations, thus defining the following matrices:

$$\Gamma_1 = \begin{bmatrix} 0 & 0 \\ 0 & 0 \end{bmatrix}, \quad \Gamma_2 = \begin{bmatrix} 0 & 0 \\ 0 & 1 \end{bmatrix}, \quad \Gamma_3 = \begin{bmatrix} 1 & 0 \\ 0 & 0 \end{bmatrix}, \quad \Gamma_4 = \begin{bmatrix} 1 & 0 \\ 0 & 1 \end{bmatrix},$$
$$\Gamma_1^- = \begin{bmatrix} 1 & 0 \\ 0 & 1 \end{bmatrix}, \quad \Gamma_2^- = \begin{bmatrix} 1 & 0 \\ 0 & 0 \end{bmatrix}, \quad \Gamma_3^- = \begin{bmatrix} 0 & 0 \\ 0 & 1 \end{bmatrix}, \quad \Gamma_4^- = \begin{bmatrix} 0 & 0 \\ 0 & 0 \end{bmatrix}.$$

Then, the symmetric saturation limits $\bar{v}_i \in \mathcal{S}_v$ of the switched closed-loop system (6.6) are obtained for $i \in \mathcal{I}_{[1,4]}$ with $\mathcal{S}_v$ defined as:

$$\mathcal{S}_v = \left\{ \begin{bmatrix} 2 \\ 3 \end{bmatrix}, \begin{bmatrix} 2 \\ 2 \end{bmatrix}, \begin{bmatrix} 5 \\ 3 \end{bmatrix}, \begin{bmatrix} 5 \\ 2 \end{bmatrix} \right\}.$$

Let us now assume that the initial states for the system (6.1) belong to the polyhedral set $\mathcal{X}_0$ defined as:

$$\mathcal{X}_0 = \mathrm{Co}\left\{ \begin{bmatrix} -1 \\ -1 \end{bmatrix}, \begin{bmatrix} 1 \\ -1 \end{bmatrix}, \begin{bmatrix} -1 \\ 1 \end{bmatrix}, \begin{bmatrix} 1 \\ 1 \end{bmatrix} \right\}.$$

Then, for each controller gain K_i in (6.5), let us define the following desired switching decay rate values:

$$\mathrm{d}_{\mathrm{R}1} = 0, \ \mathrm{d}_{\mathrm{R}2} = 1.65, \ \mathrm{d}_{\mathrm{R}3} = 3.30, \ \mathrm{d}_{\mathrm{R}4} = 4.95,$$

which will lead to obtain the fastest guaranteed closed-loop convergence speed for the closed-loop system (6.6) associated with the controller gain K_4 and the saturation limits $\bar{v}_4 \in \mathcal{S}_v$, whereas, the slowest one is established for the system with K_1 and $\bar{v}_1 \in \mathcal{S}_v$. On the other hand, the decay rates $\mathrm{d}_{\mathrm{R}2}$ and $\mathrm{d}_{\mathrm{R}3}$ are chosen by considering 33% and 66% of $\mathrm{d}_{\mathrm{R}4}$, respectively.

Remark 6.6.1. It should be noted that there exists a trade-off between the provided values of the desired switching decay rates and the feasibility of the problem. For example, a larger value of $\mathrm{d}_{\mathrm{R}1}$ implies lower values in the remaining decay rates in order to reach a feasible solution. Furthermore, it is also worth noting that, for a pre-determined design criterion, a linear search technique may be utilized to find values that make Problem 6.3.1 feasible.

After determining the design specifications, Problem 6.3.1 is solved by implementation of Theorem 6.4.2 in MATLAB environment via the YALMIP toolbox [70] and the use of the SeDuMi solver [117]. Then, the Lyapunov matrix P and the controller gains K_i obtained as a feasible solution are:

$$P = \begin{bmatrix} 22.5511 & -0.2223 \\ -0.2223 & 1.0710 \end{bmatrix}, \quad K_1 = \begin{bmatrix} -0.0642 & -0.1346 \\ -0.0819 & -0.5426 \end{bmatrix}, \quad K_2 = \begin{bmatrix} -0.3751 & -0.0815 \\ -0.0785 & -0.5896 \end{bmatrix},$$
$$K_3 = \begin{bmatrix} -0.7214 & -0.2770 \\ -0.0377 & -1.5314 \end{bmatrix}, \quad K_4 = \begin{bmatrix} -1.0289 & -0.4028 \\ -0.0003 & -1.9308 \end{bmatrix}.$$

Simulation results

Let us illustrate the results of the designed switching state-feedback controller under three different initial conditions: $x_0^{(1)} \triangleq [3.5162, 0.6602]^\top$, $x_0^{(2)} \triangleq [2.9, -0.65]^\top$ and $x_0^{(3)} \triangleq [-1, -1]^\top$, denoted by a solid red line (—), a blue dashed line (- -) and a dashed-dotted green line (-·-), respectively.

Figs. 6.1-6.2 show the closed-loop state responses and the behaviour of the obtained control input over time, respectively. It is worth noting that regardless of the initial conditions, all states tend to the origin ensuring closed-loop stabilization. For the case of starting in $x_0^{(1)}$, the computed input signal has three discontinuities due to the activation of three different controller gains, as shown in Fig. 6.3, where the signal $\sigma(t)$ is plotted. Conversely, it can be seen that the input signals do not show any discontinuities in simulation $x_0^{(3)}$ as a result of using the same controller gain for the entire simulation.

Fig. 6.4 illustrates the phase plane delimited by the asymmetric regions of linearity obtained for each designed controller: ■ $\sigma = 1$, ■ $\sigma = 2$, ■ $\sigma = 3$ and ■ $\sigma = 4$. Furthermore, the regions $\mathcal{X}_0$ and $\mathcal{E}(P, 1)$ are represented by the shaded black area and the solid violet line (—), respectively. Then, it can be seen that all region transitions produced by the evolution of the state correspond to the values of the signal $\sigma(t)$ shown in Fig. 6.3.

Remark 6.6.2. During the controller design stage, a unit Lyapunov level set $\mathcal{E}(P, 1)$ has been considered without loss of generality. It should be emphasized, however, that all level sets of the QLF (6.13) completely contained in the illustrated asymmetrical regions of linearity in Fig. 6.4, such as the one bordered by the solid yellow line (—), satisfy the stated closed-loop performance requirement.

Fig. 6.5 shows that the Lyapunov function $V(x)$ is strictly decreasing in all the simulations. Furthermore, note that the closed-loop convergence speed of the state trajectory corresponding to $x_0^{(1)}$ rises from the specified value $\mathrm{d}_{\mathrm{R}2}$ to the value of $\mathrm{d}_{\mathrm{R}4}$ according to current state vector, thus producing abrupt changes in $\dot{V}(x)$. Finally, Fig. 6.6 shows that the guaranteed switching decay rate (6.7) satisfies the desired decay rate values for all the possible non-saturating state trajectories, i.e., $-\dot{V}(x)/(2V(x)) \geq \mathrm{d}_{\mathrm{R}\sigma}\ \forall x \neq 0$. This demonstrates the capacity of online adaptation of the closed-loop system.

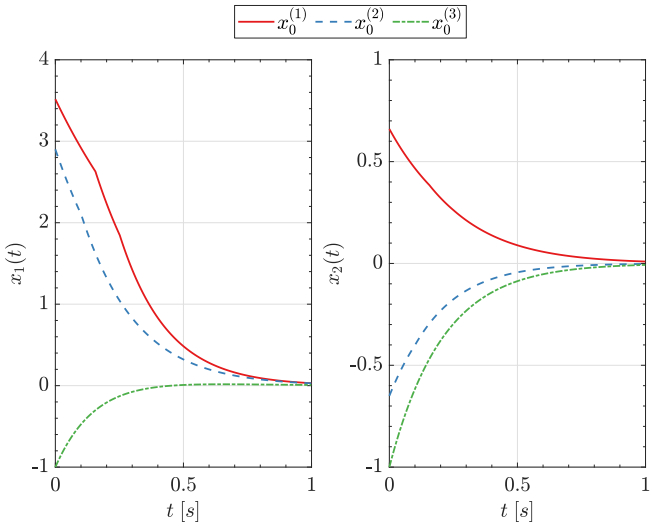

Figure 6.1: Closed-loop state responses.

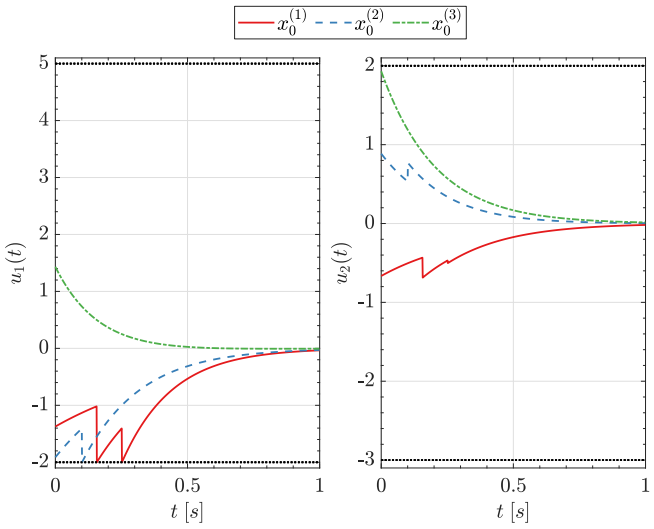

Figure 6.2: Control inputs. (The saturation limits are shown as dotted lines.)

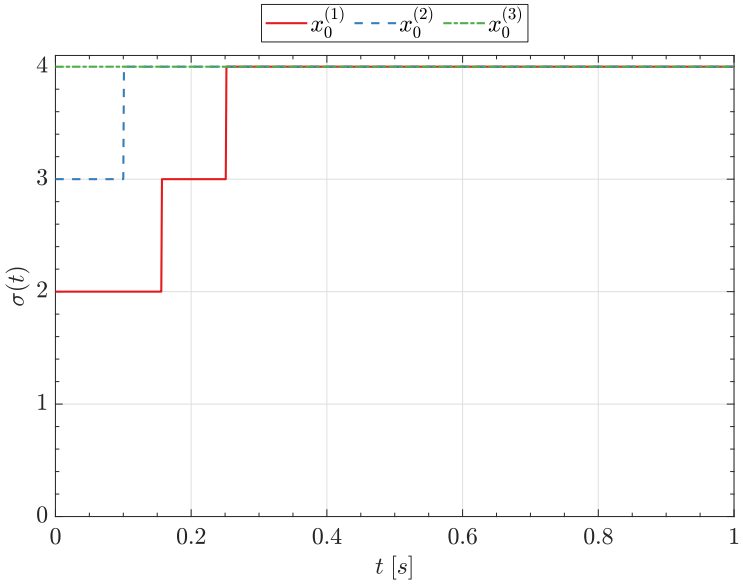

Figure 6.3: Switching control rule signal.

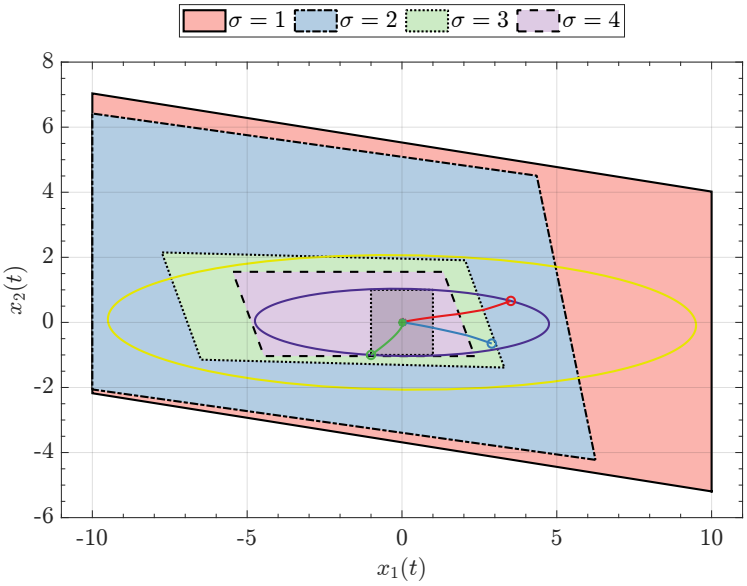

Figure 6.4: Asymmetric regions of linearity.

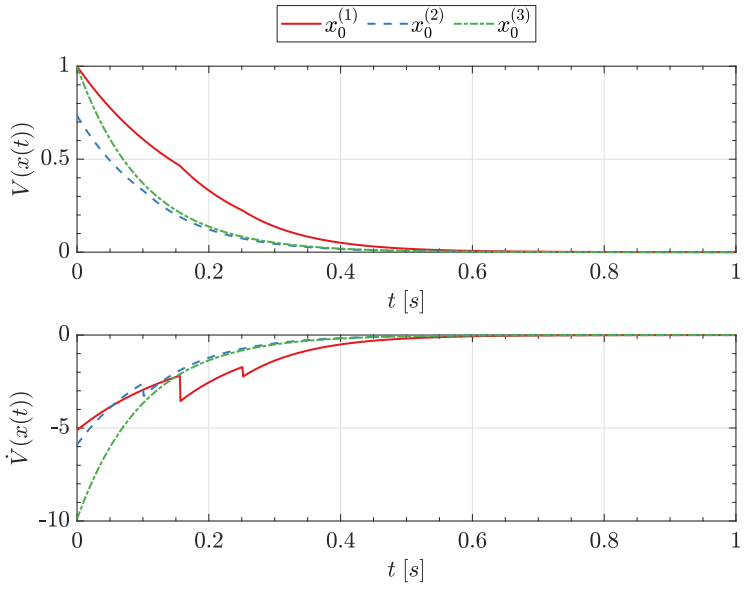

Figure 6.5: Lyapunov function and its derivative.

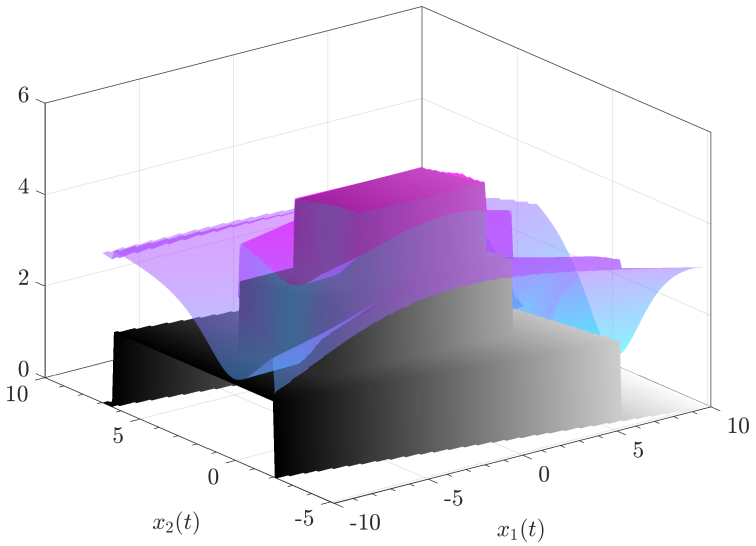

Figure 6.6: Guaranteed switching decay rate. (corresponds to $-\dot{V}(x)/(2V(x))$ and denote $\mathrm{d}_{\mathrm{R}_\sigma}$.)

6.7 Conclusions

This chapter explored the design of a control law for a linear system with asymmetric saturations. The proposed method is based on the transformation of an asymmetrically saturated linear system into an equivalent switched system with symmetric saturations, providing an LMI-based methodology for developing a switching state-feedback controller. The results demonstrate that the proposed switching rule criterion satisfies the guaranteed switching decay rate performance criterion. In this way, the closed-loop system response alters its performance in terms of convergence speed dependent on the current state vector. Furthermore, it has been demonstrated how to extend the proposed methodology to the parameter-varying case.

An important question that has to be addressed further is the consideration of saturated control input with the purpose of obtaining less conservative results, thus allowing the implementation of the designed controllers to real-world systems. Furthermore, the development of alternative LMI-based methodologies to deal with the case where the saturation limits vary over time may be of interest in future work.

7 Conclusions and future work

This thesis has proposed some contributions to the fields of LPV systems and actuator saturation control, with a focus on their application to time-varying saturation avoidance. This chapter provides the main conclusions of the work presented in this dissertation and explores potential lines of research.

7.1 Conclusions

Actuator saturation control has been investigated throughout the last few decades, and several theoretical and experimental results have been presented in the literature. Nevertheless, the presence of time-varying saturation levels still leaves an open direction for further investigation. This thesis has contributed to the advancement of the state-of-the-art in this field.

- In **Chapter 3**, the problem of designing shifting state-feedback controllers has been addressed for time-varying saturated LPV systems. The given solution is based on a convex representation of changes in the saturation limit, enabling the characterization of a parameter-dependent region in which control action saturation does not occur. LMI-based design methodologies have been proposed using both parameter-independent and parameter-dependent QLFs. In addition, an optimization procedure has been proposed for the selection of desired shifting specification vertex values under a pre-established criterion, such as the maximization of the closed-loop convergence speed when the largest saturation limit is available. In order to obtain a finite number of design conditions, the polytopic representation has been employed together with the application of Pólya's relaxation theorem to deal with the presence of products involving multiple polytopic summations, allowing the consideration of, e.g., parameter-dependent input matrices. The proposed design conditions have been effective, with the controller being able to regulate closed-loop convergence speed or disturbance rejection effectiveness according to the instantaneous saturation limit values and closed-loop stabilization under saturation avoidance. It has been observed that the results obtained for the PDQLF case appear to be less conservative than those obtained for the QLF case. However, the computational cost and the mathematical complexity are increased, which may hinder the implementation of the proposed design approach in higher-order plants due to the large number of LMIs required.

- **Chapter 4** has considered the problem of designing shifting output-feedback controllers for time-varying saturated LPV systems, thus extending the procedure proposed in Chap. 3 to the output-feedback case. To this end, a GS dynamic output-feedback control law has been combined with the shifting paradigm concept. Additionally, the conditions for ensuring time-varying saturation avoidance have been stated. The solution to the design problem

has been expressed in terms of LMI-based design procedures, for which a feasible solution should be found, and it has been obtained using a PDQLF. However, the obtained design conditions result in a GS controller whose dependency on the time derivative of scheduling vectors leads to a nonviable implementation. At the expense of adding some degree of conservatism, this issue has been alleviated by imposing some design restrictions on the decision variables. The example has shown the effectiveness of the proposed approach for the shifting guaranteed decay rate criterion. In particular, in contrast with existing results in the literature, the designed controller is able to adjust its closed-loop performance in terms of convergence speed based on the actuator saturation limit values and guarantee closed-loop stability under saturation avoidance.

- In **Chapter 5**, the shifting paradigm concept and the FBL technique have been integrated through the framework proposed in Chap. 3 to solve the problem of designing shifting state-feedback controllers for full-feedback linearized systems under state-dependent input saturations. Specifically, a shifting control strategy and an input constraint mapping have been proposed, thus guaranteeing the stabilization of the full-feedback linearized system under saturation avoidance and achieving a shifting performance such that the combination of the linearizing law and the shifting state-feedback control law remains within the limits of the actuator. The control design has been formulated through LMI-based conditions using a QLF. However, the assumption of symmetrizing the time-varying region of linearity of the constrained linearized system has been considered for obtaining these conditions, thus introducing a certain degree of conservatism. Through simulation and experimental results obtained by using the Quanser 3-DoF hover platform, the potential and efficacy of the designed controller have been demonstrated. It has been shown that the controller guarantees shifting decay rate performance by adjusting the closed-loop response of the system in real time in accordance with the instantaneous values of the time-varying system's region of linearity.

- **Chapter 6** has explored the design of non-saturating switching state-feedback controllers for linear systems under asymmetric saturation. A transformation of an asymmetrically saturated linear system has been used to obtain an equivalent switched system under symmetric saturations. The solution to the design problem has been expressed in terms of LMI-based design conditions using a QLF, which can be solved via the available solvers. Additionally, an extension of the proposed design methodology to the LPV case has been discussed. The main difference between the proposed strategy and others in the literature is that the switching rule has been designed based on achievable closed-loop performance. In particular, the concept of a guaranteed switching decay rate has been introduced. Therefore, the established switching rule selects among the non-saturating controllers the one that provides the largest guaranteed decay rate, thus adjusting the closed-loop performance in terms of closed-loop convergence speed.

7.2 Perspectives and future work

Open issues that could be addressed as potential future research topics are summarized in this section.

- The proposed LMI-based methodologies in **Chapters 3 and 4** for designing shifting controllers have also been developed using PDQLFs, thus resulting in less conservative results in contrast to the QLF case. However, the necessity to deal with the presence of scheduling parameter rates at the design stage increases the computing burden and the mathematical complexity, making it more difficult to implement the suggested design technique in higher-order plants due to the substantial amount of LMIs needed. Through the investigation of polytopic vertex reduction techniques, further study on this subject will try to minimize the number of design conditions.

- An experimental platform has been used to successfully implement the approach proposed in **Chapter 5**. However, the LMI-based design methodology for the controller design has been produced utilizing a QLF and the assumption of symmetric saturation limits of the linearized system, thus introducing a certain conservatism. The extension of the approach to the usage of different kinds of Lyapunov functions, such as parameter-dependent ones, and the consideration of asymmetric saturation limits in order to reduce the conservativeness of the solution would be an intriguing area for further study.

- A non-saturating switching controller for linear systems with asymmetric saturation has been designed thanks to the methodology described in **Chapter 6**. The design criteria, however, do not account for a potential variation in the saturation limits. Additionally, it has been used a QLF for each and every switching region, which is conservative. Creating switching approaches that could deal with the presence of time-varying saturation limitations poses an interesting problem to be addressed. The potential application of switched Lyapunov functions may also be a future research area.

- The selection of the desired shifting specification values associated with each controller vertex gain may not be trivial in situations where there are several vertices. An interesting line for future research would be the exploration of genetic algorithms, swarm-based algorithms, or machine learning techniques for finding an efficient way to assign the desired specifications to each controller's vertex gain.

- The overall suggested design procedure has been developed under the assumption of perfect knowledge of the systems, the absence of uncertainties in the scheduling parameters, the avoidance of actuator saturation, and symmetric saturation limits. However, in many real-world applications, robustness against model uncertainties and sensor noise is required, saturation allowance is desired for obtaining more aggressive performance, and asymmetric saturation limits may appear. Future research will extend the proposed techniques to design saturating, robust controllers for LPV systems subject to actuator saturation with time-varying symmetric/asymmetric saturation limits.

- The conditions for ensuring actuator saturation control have been derived in this thesis using the direct design approach. To avoid placing limitations on the nominal linear con-

troller design, it may be interesting to take into account alternate strategies, such as an anti-windup technique, for extending the suggested methodology. Further investigation into the usage of contractive polyhedral sets throughout the design stage may include a focus on MPC techniques.

Bibliography

1. A. Abdilla, A. Richards, and S. Burrow. "Endurance optimisation of battery-powered rotorcraft". In: *Towards Autonomous Robotic Systems*. Ed. by C. Dixon and K. Tuyls. Springer International Publishing, Cham, 2015, pp. 1–12. ISBN: 978-3-319-22416-9.
2. C. M. Agulhari, A. Felipe, R. C. L. F. Oliveira, and P. L. D. Peres. "Algorithm 998: The Robust LMI Parser—A toolbox to construct LMI conditions for uncertain systems". *ACM Trans. Math. Softw.* 45:3, 2019. ISSN: 0098-3500. DOI: 10.1145/3323925.
3. M. Ali, H. Abbas, and H. Werner. "Controller synthesis for input-output LPV models". In: *49th IEEE Conference on Decision and Control (CDC)*. IEEE. 2010, pp. 7694–7699.
4. H. L. Almeida, A. Bhaya, D. M. Falcao, and E. Kaszkurewicz. "A team algorithm for robust stability analysis and control design of uncertain time-varying linear systems using piecewise quadratic Lyapunov functions". *International Journal of Robust and Nonlinear Control: IFAC-Affiliated Journal* 11:4, 2001, pp. 357–371.
5. P. Apkarian and R. J. Adams. "Advanced gain-scheduling techniques for uncertain systems". In: *Advances in linear matrix inequality methods in control*. SIAM, 2000, pp. 209–228.
6. P. Apkarian, P. Gahinet, and G. Becker. "Self-scheduled $\mathcal{H}_\infty$ control of linear parameter-varying systems: a design example". *Automatica* 31:9, 1995, pp. 1251–1261. ISSN: 0005-1098. DOI: https://doi.org/10.1016/0005-1098(95)00038-X.
7. P. Apkarian and H. D. Tuan. "Parameterized LMIs in control theory". *SIAM journal on control and optimization* 38:4, 2000, pp. 1241–1264.
8. M. ApS. *The MOSEK optimization toolbox for MATLAB manual. Version 9.0.* 2019.
9. C. Arino, E. Perez, A. Sala, and F. Bedate. "Polytopic invariant and contractive sets for closed-loop discrete fuzzy systems". *Journal of the Franklin Institute* 351:7, 2014, pp. 3559–3576.
10. D. Avis and K. Fukuda. "A pivoting algorithm for convex hulls and vertex enumeration of arrangements and polyhedra". In: *Proceedings of the seventh annual symposium on Computational geometry*. 1991, pp. 98–104.
11. S. Azizi. "Sufficient LMI conditions and Lyapunov redesign for the robust stability of a class of feedback linearized dynamical systems". *ISA Transactions* 68, 2017, pp. 90–98. ISSN: 0019-0578. DOI: https://doi.org/10.1016/j.isatra.2017.02.017.
12. G. J. Balas. "Linear, parameter-varying control and its application to a turbofan engine". *International Journal of Robust and Nonlinear Control: IFAC-Affiliated Journal* 12:9, 2002, pp. 763–796.

13. E. A. Basso and K. Y. Pettersen. "MIMO Feedback linearization of redundant robotic systems using task-priority operational space control". *IFAC-PapersOnLine* 53:2, 2020, pp. 5459–5466.
14. J. D. Bendtsen and K. Trangbæk. "Discrete-time LPV current control of an induction motor". In: *42nd IEEE International Conference on Decision and Control (IEEE Cat. No. 03CH37475)*. Vol. 6. IEEE. 2003, pp. 5903–5908.
15. A. Benzaouia, M. Benhayoun, and F. Mesquine. "Stabilization of systems with unsymmetrical saturated control: an LMI approach". *Circuits, Systems, and Signal Processing* 33:10, 2014, pp. 3263–3275.
16. A. Bhardwaj, L. Sam, F. J. Martín-Torres, R. Kumar, et al. "UAVs as remote sensing platform in glaciology: present applications and future prospects". *Remote sensing of environment* 175, 2016, pp. 196–204.
17. F. D. Bianchi, R. J. Mantz, and C. F. Christiansen. "Gain scheduling control of variable-speed wind energy conversion systems using quasi-LPV models". *Control engineering practice* 13:2, 2005, pp. 247–255.
18. F. Blanchini. "Nonquadratic Lyapunov functions for robust control". *Automatica* 31:3, 1995, pp. 451–461.
19. F. Blanchini. "Set invariance in control". *Automatica* 35:11, 1999, pp. 1747–1767.
20. S. Bouabdallah, P. Murrieri, and R. Siegwart. "Design and control of an indoor micro quadrotor". In: *IEEE International Conference on Robotics and Automation, 2004. Proceedings. ICRA '04. 2004*. Vol. 5. 2004, 4393–4398 Vol.5. DOI: 10.1109/ROBOT.2004.1302409.
21. S. Bouabdallah and R. Siegwart. "Full control of a quadrotor". In: *2007 IEEE/RSJ International Conference on Intelligent Robots and Systems*. 2007, pp. 153–158. DOI: 10.1109/IROS.2007.4399042.
22. S. Boyd, V. Balakrishnan, E. Feron, and L. El Ghaoui. "History of linear matrix inequalities in control theory". In: *Proceedings of 1994 American Control Conference - ACC '94*. Vol. 1. 1994, 31–34 vol.1. DOI: 10.1109/ACC.1994.751687.
23. S. Boyd, L. El Ghaoui, E. Feron, and V. Balakrishnan. *Linear matrix inequalities in system and control theory*. eng. SIAM studies in applied mathematics ; 15. SIAM, Philadelphia, Pennsylvania, 1994. ISBN: 089871334X.
24. S. P. Boyd. *Convex optimization*. eng. Cambridge University Press, Cambridge, 2004. ISBN: 0521833787.
25. P. Braun, G. Giordano, C. M. Kellett, and L. Zaccarian. "An asymmetric stabilizer based on scheduling shifted coordinates for single-input linear systems with asymmetric saturation". *IEEE Control Systems Letters* 6, 2021, pp. 746–751.
26. C. Briat. "Linear parameter-varying and time-delay systems". *Analysis, observation, filtering & control* 3, 2014, pp. 5–7.
27. M. L. Brockman and M. Corless. "Quadratic boundedness of nominally linear systems". *International Journal of Control* 71:6, 1998, pp. 1105–1117.

28. Y.-Y. Cao and Z. Lin. "Min–max MPC algorithm for LPV systems subject to input saturation". *IEE Proceedings-Control Theory and Applications* 152:3, 2005, pp. 266–272.
29. Y.-Y. Cao and Z. Lin. "Robust stability analysis and fuzzy-scheduling control for nonlinear systems subject to actuator saturation". *IEEE Transactions on Fuzzy Systems* 11:1, 2003, pp. 57–67.
30. Y.-Y. Cao, Z. Lin, and Y. Shamash. "Set invariance analysis and gain-scheduling control for LPV systems subject to actuator saturation". *Systems & Control Letters* 46:2, 2002, pp. 137–151. ISSN: 0167-6911.
31. R. J. Caverly and J. R. Forbes. "LMI properties and applications in systems, stability, and control theory". *arXiv preprint arXiv:1903.08599*, 2019.
32. Y. Chen, G. Zhang, Y. Zhuang, and H. Hu. "Autonomous flight control for multi-rotor UAVs flying at low altitude". *IEEE Access* 7, 2019, pp. 42614–42625. ISSN: 21693536.
33. G. Chesi, A. Garulli, A. Tesi, and A. Vicino. "Robust stability of time-varying polytopic systems via parameter-dependent homogeneous Lyapunov functions". *Automatica* 43:2, 2007, pp. 309–316.
34. M. Chilali and P. Gahinet. "H_∞ design with pole placement constraints: an LMI approach". *IEEE Transactions on automatic control* 41:3, 1996, pp. 358–367.
35. A. Cristofaro, S. Galeani, S. Onori, and L. Zaccarian. "A switched and scheduled design for model recovery anti-windup of linear plants". *European Journal of Control* 46, 2019, pp. 23–35. ISSN: 0947-3580. DOI: https://doi.org/10.1016/j.ejcon.2018.04.002.
36. A. Dabiri, B. Kulcsár, and H. Köroğlu. "Distributed LPV state-feedback control under control input saturation". *IEEE Transactions on Automatic Control* 62:5, 2016, pp. 2450–2456.
37. D. Dai, T. Hu, A. R. Teel, and L. Zaccarian. "Piecewise-quadratic Lyapunov functions for systems with deadzones or saturations". *Systems & Control Letters* 58:5, 2009, pp. 365–371.
38. J. De Caigny, J. F. Camino, R. C. Oliveira, P. L. Peres, and J. Swevers. "Gain-scheduled dynamic output feedback control for discrete-time LPV systems". *International Journal of Robust and Nonlinear Control* 22:5, 2012, pp. 535–558.
39. D. Efimov, T. Raïssi, and A. Zolghadri. "Control of nonlinear and LPV systems: interval observer-based framework". *IEEE Transactions on Automatic Control* 58:3, 2013, pp. 773–778.
40. J. G. Elliot and R. F. Gans. "Closed-loop control of an underactuated sheet registration device using feedback linearization and gain scheduling". *IEEE Transactions on Control Systems Technology* 16:4, 2008, pp. 589–599. DOI: 10.1109/TCST.2007.912109.
41. M. Faessler, D. Falanga, and D. Scaramuzza. "Thrust mixing, saturation, and body-rate control for accurate aggressive quadrotor flight". *IEEE Robotics and Automation Letters* 2:2, 2017, pp. 476–482. DOI: 10.1109/LRA.2016.2640362.

42. E. Feron, P. Apkarian, and P. Gahinet. "Analysis and synthesis of robust control systems via parameter-dependent Lyapunov functions". *IEEE Transactions on Automatic Control* 41:7, 1996, pp. 1041–1046.
43. G. F. Franklin, J. D. Powell, A. Emami-Naeini, and J. D. Powell. *Feedback control of dynamic systems*. Vol. 4. Prentice hall Upper Saddle River, 2002.
44. P. Gahinet and P. Apkarian. "A linear matrix inequality approach to $\mathcal{H}_\infty$ control". *International journal of robust and nonlinear control* 4:4, 1994, pp. 421–448.
45. J. C. Geromel and P. Colaneri. "Robust stability of time varying polytopic systems". *Systems & Control Letters* 55:1, 2006, pp. 81–85.
46. M. Grant and S. Boyd. *CVX: Matlab Software for Disciplined Convex Programming, version 2.1*. http://cvxr.com/cvx. 2014.
47. L. B. Groff, J. M. G. da Silva, and G. Valmórbida. "Regional stability of discrete-time linear systems subject to asymmetric input saturation". In: *2019 IEEE 58th Conference on Decision and Control (CDC)*. IEEE. 2019, pp. 169–174.
48. T. Gußner, M. Jost, and J. Adamy. "Controller design for a class of nonlinear systems with input saturation using convex optimization". *Systems & Control Letters* 61:1, 2012, pp. 258–265. ISSN: 0167-6911. DOI: https://doi.org/10.1016/j.sysconle.2011.11.003.
49. R. Hann, A. Wenz, K. Gryte, and T. A. Johansen. "Impact of atmospheric icing on UAV aerodynamic performance". In: *2017 Workshop on Research, Education and Development of Unmanned Aerial Systems, RED-UAS 2017*. Institute of Electrical and Electronics Engineers Inc., 2017, pp. 66–71. ISBN: 9781538609392.
50. M. Herceg, M. Kvasnica, C. Jones, and M. Morari. "Multi-Parametric Toolbox 3.0". In: *Proc. of the European Control Conference*. http://control.ee.ethz.ch/~mpt. Zürich, Switzerland, 2013, pp. 502–510.
51. C. Hoffmann and H. Werner. "A survey of linear parameter-varying control applications validated by experiments or high-fidelity simulations". *IEEE Transactions on Control Systems Technology* 23:2, 2014, pp. 416–433.
52. G. Hoffmann, H. Huang, S. Waslander, and C. Tomlin. "Quadrotor helicopter flight dynamics and control: Theory and experiment". In: *AIAA Guidance, Navigation and Control Conference and Exhibit*. 2007, p. 6461.
53. R. A. Horn and C. R. Johnson. *Matrix analysis*. Cambridge university press, 2012.
54. T. Hu and Z. Lin. *Control systems with actuator saturation : analysis and design*. eng. Control engineering (Birkhäuser). Birkhäuser, Boston, 2001. ISBN: 0817642196.
55. T. Hu, Z. Lin, and B. M. Chen. "An analysis and design method for linear systems subject to actuator saturation and disturbance". *Automatica* 38:2, 2002, pp. 351–359.
56. T. Hu, A. R. Teel, and L. Zaccarian. "Regional anti-windup compensation for linear systems with input saturation". In: *Proceedings of the 2005, American Control Conference, 2005.* IEEE. 2005, pp. 3397–3402.

57. A. Isidori, M. Thoma, E. D. Sontag, B. W. Dickinson, A. Fettweis, J. L. Massey, and J. W. Modestino. *Nonlinear Control Systems*. 3rd. Springer-Verlag, Berlin, Heidelberg, 1995. ISBN: 3540199160.

58. D. Joosten, T. van den Boom, and T. Lombaerts. "Effective control allocation in fault-tolerant flight control using feedback linearisation and model predictive control". In: *2007 European Control Conference (ECC)*. 2007, pp. 3552–3559. DOI: 10.23919/ECC.2007.7068917.

59. V. Kapila and K. Grigoriadis. *Actuator saturation control*. eng. Control engineering. Marcel Dekker, New York etc, 2002. ISBN: 0824707516.

60. V. Kapila, A. G. Sparks, and H. Pan. "Control of systems with actuator saturation nonlinearities: An LMI approach". *International Journal of Control* 74:6, 2001, pp. 586–599.

61. F. Karimi Pour, D. Theilliol, V. Puig, and G. Cembrano. "Health-aware control design based on remaining useful life estimation for autonomous racing vehicle". *ISA Transactions*, 2020. ISSN: 0019-0578. DOI: https://doi.org/10.1016/j.isatra.2020.03.032.

62. F. Kendoul. "Survey of advances in guidance, navigation, and control of unmanned rotorcraft systems". *Journal of Field Robotics* 29:2, 2012, pp. 315–378. DOI: https://doi.org/10.1002/rob.20414.

63. H. K. Khalil. *Nonlinear systems*. eng. 3rd ed., international ed. Pearson Education, New Jersey, 2014. ISBN: 9781292039213.

64. M. V. Khlebnikov, B. T. Polyak, and V. M. Kuntsevich. "Optimization of linear systems subject to bounded exogenous disturbances: the invariant ellipsoid technique". *Automation and Remote Control* 72, 2011, pp. 2227–2275.

65. İ. E. Köse and F. Jabbari. "Scheduled controllers for linear systems with bounded actuators". *Automatica* 39:8, 2003, pp. 1377 –1387. ISSN: 0005-1098.

66. A. Kwiatkowski and H. Werner. "LPV control of a 2-DOF robot using parameter reduction". In: *Proceedings of the 44th IEEE Conference on Decision and Control*. IEEE. 2005, pp. 3369–3374.

67. D. J. Leith and W. E. Leithead. "Survey of gain-scheduling analysis and design". *International journal of control* 73:11, 2000, pp. 1001–1025.

68. P. Li, A.-T. Nguyen, H. Du, Y. Wang, and H. Zhang. "Polytopic LPV approaches for intelligent automotive systems: state of the art and future challenges". *Mechanical Systems and Signal Processing* 161, 2021, p. 107931.

69. Y. Li and Z. Lin. "An asymmetric Lyapunov function for linear systems with asymmetric actuator saturation". *International Journal of Robust and Nonlinear Control* 28:5, 2018, pp. 1624–1640.

70. J. Löfberg. "YALMIP : A toolbox for modeling and optimization in MATLAB". In: *2004 IEEE International Conference on Robotics and Automation (IEEE Cat. No.04CH37508)*. 2004, pp. 284–289.

71. A. M. Lyapunov. "Problème général de la stabilité du mouvement". In: *Annales de la Faculté des sciences de Toulouse: Mathématiques*. Vol. 9. 1907, pp. 203–474.

72. M. M. Maia, D. A. Mercado, and F. J. Diez. "Design and implementation of multirotor aerial-underwater vehicles with experimental results". In: *2017 IEEE/RSJ International Conference on Intelligent Robots and Systems (IROS)*. IEEE. 2017, pp. 961–966.

73. S. Mariano, F. Blanchini, S. Formentin, and L. Zaccarian. "Asymmetric state feedback for linear plants with asymmetric input saturation". *IEEE Control Systems Letters* 4:3, 2020, pp. 608–613.

74. L. Martins, C. Cardeira, and P. Oliveira. "Feedback linearization with zero dynamics stabilization for quadrotor control". *Journal of Intelligent & Robotic Systems* 101:1, 2021, pp. 1–17. DOI: https://doi.org/10.1007/s10846-020-01265-2.

75. L. Merino, F. Caballero, J. R. Martínez-de Dios, I. Maza, and A. Ollero. "An unmanned aircraft system for automatic forest fire monitoring and measurement". *Journal of Intelligent & Robotic Systems* 65, 2012, pp. 533–548.

76. J. Mohammadpour and C. W. Scherer. *Control of linear parameter varying systems with applications*. Springer Science & Business Media, 2012.

77. V. F. Montagner, R. C. Oliveira, P. L. Peres, and P.-A. Bliman. "Stability analysis and gain-scheduled state feedback control for continuous-time systems with bounded parameter variations". *International Journal of Control* 82:6, 2009, pp. 1045–1059.

78. M. M. Morato, P. R. Mendes, J. E. Normey-Rico, and C. Bordons. "LPV-MPC fault-tolerant energy management strategy for renewable microgrids". *International Journal of Electrical Power & Energy Systems* 117, 2020, p. 105644.

79. M. M. Morato, M. Jungers, J. E. Normey-Rico, and O. Sename. "A predictive fault tolerant control method for qLPV systems subject to input faults and constraints". *Journal of the Franklin Institute* 359:16, 2022, pp. 9129–9167.

80. Y. Nesterov and A. Nemirovskii. *Interior-point polynomial algorithms in convex programming*. SIAM, 1994.

81. A.-T. Nguyen, P. Chevrel, and F. Claveau. "LPV static output feedback for constrained direct tilt control of narrow tilting vehicles". *IEEE Transactions on Control Systems Technology* 28:2, 2018, pp. 661–670.

82. A.-T. Nguyen, P. Chevrel, and F. Claveau. "Gain-scheduled static output feedback control for saturated LPV systems with bounded parameter variations". *Automatica* 89, 2018, pp. 420–424.

83. R. C. L. F. Oliveira and P. L. D. Peres. "Parameter-dependent LMIs in robust analysis: characterization of homogeneous polynomially parameter-dependent solutions via LMI relaxations". *IEEE Transactions on Automatic Control* 52:7, 2007, pp. 1334–1340. DOI: 10.1109/TAC.2007.900848.

84. R. C. Oliveira, P.-A. Bliman, and P. L. Peres. "Robust LMIs with parameters in multi-simplex: existence of solutions and applications". In: *2008 47th IEEE Conference on Decision and Control*. IEEE. 2008, pp. 2226–2231.

85. A. Packard. "Gain scheduling via linear fractional transformations". *Systems & control letters* 22:2, 1994, pp. 79–92.

86. G. Pappas, J. Lygeros, and D. Godbole. "Stabilization and tracking of feedback linearizable systems under input constraints". In: *Proceedings of 1995 34th IEEE Conference on Decision and Control*. Vol. 1. 1995, 596–601 vol.1. DOI: 10.1109/CDC.1995.478960.

87. K. B. Petersen, M. S. Pedersen, et al. "The matrix cookbook". *Technical University of Denmark* 7:15, 2008, p. 510.

88. X. Ping, P. Wang, and Z. Li. "Quadratic boundedness of LPV systems via saturated dynamic output feedback controller". *Optimal Control Applications and Methods* 38:6, 2017, pp. 1239–1248.

89. M. Podhradský, J. Bone, C. Coopmans, and A. Jensen. "Battery model-based thrust controller for a small, low cost multirotor Unmanned Aerial Vehicles". In: *2013 International Conference on Unmanned Aircraft Systems (ICUAS)*. 2013, pp. 105–113. DOI: 10.1109/ICUAS.2013.6564679.

90. J. D. Powell, N. Fekete, and C.-F. Chang. "Observer-based air fuel ratio control". *IEEE Control Systems Magazine* 18:5, 1998, pp. 72–83.

91. Quanser™. *Quanser 3DOF hover system manual*. [Online; November-2022].

92. D. Rotondo, F. Nejjari, and V. Puig. "Design of parameter-scheduled state-feedback controllers using shifting specifications". *Journal of the Franklin Institute* 352:1, 2015, pp. 93–116.

93. B. Rubí, A. Ruiz, R. Peréz, and B. Morcego. "Path-Flyer: A benchmark of quadrotor path following algorithms". In: *2019 IEEE 15th International Conference on Control and Automation (ICCA)*. 2019, pp. 633–638. DOI: 10.1109/ICCA.2019.8899563.

94. W. J. Rugh and J. S. Shamma. "Research on gain scheduling". *Automatica* 36:10, 2000, pp. 1401–1425.

95. A. Ruiz, D. Rotondo, and B. Morcego. "Design of state-feedback controllers for linear parameter varying systems subject to time-varying input saturation". *Applied Sciences* 9:17, 2019, p. 3606. ISSN: 2076-3417.

96. A. Ruiz, D. Rotondo, and B. Morcego. "Shifting $\mathcal{H}_\infty$ linear parameter varying state-feedback controllers subject to time-varying input saturations". *IFAC-PapersOnLine* 53:2, 2020. 21th IFAC World Congress, pp. 7338–7343. ISSN: 2405-8963. DOI: https://doi.org/10.1016/j.ifacol.2020.12.991.

97. A. Ruiz, D. Rotondo, and B. Morcego. "Design of shifting state-feedback controllers for constrained feedback linearized systems: application to quadrotor attitude control". *International Journal of Robust and Nonlinear Control*, 2023. Under review.

98. A. Ruiz, D. Rotondo, and B. Morcego. "Design of switching state-feedback controllers for linear systems subject to asymmetric saturations". *IFAC-PapersOnLine*, 2023. 22nd IFAC World Congress. Accepted.

99. A. Ruiz, D. Rotondo, and B. Morcego. "Design of shifting state-feedback controllers for LPV systems subject to time-varying saturations via parameter-dependent Lyapunov functions". *ISA Transactions*, 2021. ISSN: 0019-0578. DOI: https://doi.org/10.1016/j.isatra.2021.07.025.

100. A. Ruiz, D. Rotondo, and B. Morcego. "Design of shifting output-feedback controllers for LPV systems subject to time-varying saturations". *IFAC-PapersOnLine* 55:35, 2022. 5th IFAC Workshop on Linear Parameter Varying Systems 2022, pp. 13–18. ISSN: 2405-8963. DOI: https://doi.org/10.1016/j.ifacol.2022.11.283.

101. S. Sajjadi-Kia and F. Jabbari. "Controllers for linear systems with bounded actuators: Slab scheduling and anti-windup". *Automatica* 49:3, 2013, pp. 762 –769. ISSN: 0005-1098.

102. A. Sala and C. Arino. "Asymptotically necessary and sufficient conditions for stability and performance in fuzzy control: Applications of Pólya's theorem". *Fuzzy Sets and Systems* 158:24, 2007, pp. 2671–2686.

103. S. Sastry. *Nonlinear systems : analysis, stability, and control*. eng. Interdisciplinary applied mathematics ; v. 10. Springer, New York, 1999. ISBN: 0387985131.

104. M. Sato. "Design method of gain-scheduled controllers not depending on derivatives of parameters". *International Journal of Control* 81:6, 2008, pp. 1013–1025.

105. M. Sato. "Gain-scheduled output-feedback controllers depending solely on scheduling parameters via parameter-dependent Lyapunov functions". *Automatica* 47:12, 2011, pp. 2786–2790. ISSN: 0005-1098. DOI: https://doi.org/10.1016/j.automatica.2011.09.023.

106. C. Scherer, P. Gahinet, and M. Chilali. "Multiobjective output-feedback control via LMI optimization". *IEEE Transactions on automatic control* 42:7, 1997, pp. 896–911.

107. C. Scherer and S. Weiland. "Linear matrix inequalities in control". *Lecture Notes, Dutch Institute for Systems and Control, Delft, The Netherlands* 3:2, 2000.

108. F. Schnelle and P. Eberhard. "Constraint mapping in a feedback linearization/MPC scheme for trajectory tracking of underactuated multibody systems". *IFAC-PapersOnLine* 48:23, 2015. 5th IFAC Conference on Nonlinear Model Predictive Control NMPC 2015, pp. 446–451. ISSN: 2405-8963. DOI: https://doi.org/10.1016/j.ifacol.2015.11.319.

109. O. Sename, P. Gaspar, and J. Bokor. *Robust control and linear parameter varying approaches: application to vehicle dynamics*. Vol. 437. Springer, 2013.

110. J. S. Shamma. "Analysis and design of gain scheduled control systems". PhD thesis. Massachusetts Institute of Technology, 1988.

111. J. S. Shamma and J. R. Cloutier. "Gain-scheduled missile autopilot design using linear parameter varying transformations". *Journal of guidance, Control, and dynamics* 16:2, 1993, pp. 256–263.

112. J. da Silva and S. Tarbouriech. "Antiwindup design with guaranteed regions of stability: an LMI-based approach". *IEEE Transactions on Automatic Control* 50:1, 2005, pp. 106–111.

113. J. M. G. da Silva and S. Tarbouriech. "Polyhedral regions of local stability for linear discrete-time systems with saturating controls". *IEEE Transactions on Automatic Control* 44:11, 1999, pp. 2081–2085.

114. D. Simon, J. Löfberg, and T. Glad. "Nonlinear model predictive control using Feedback Linearization and local inner convex constraint approximations". In: *2013 European Control Conference (ECC)*. 2013, pp. 2056–2061. DOI: 10.23919/ECC.2013.6669575.

115. J.-J. E. Slotine, W. Li, et al. *Applied nonlinear control*. Vol. 199. 1. Prentice hall Englewood Cliffs, NJ, 1991.

116. G. Stein. "Respect the unstable". *IEEE Control systems magazine* 23:4, 2003, pp. 12–25.

117. J. F. Sturm. "Using SeDuMi 1.02, a MATLAB toolbox for optimization over symmetric cones". *Optimization methods and software* 11:1-4, 1999, pp. 625–653.

118. W. Tan, A. K. Packard, and G. J. Balas. "Quasi-LPV modeling and LPV control of a generic missile". In: *Proceedings of the 2000 American Control Conference. ACC (IEEE Cat. No. 00CH36334)*. Vol. 5. IEEE. 2000, pp. 3692–3696.

119. S. Tarbouriech, G. Garcia, J. M. G. da Silva Jr, and I. Queinnec. *Stability and stabilization of linear systems with saturating actuators*. Springer Science & Business Media, 2011.

120. S. Tarbouriech and M. Turner. "Anti-windup design: an overview of some recent advances and open problems". *IET control theory & applications* 3:1, 2009, pp. 1–19.

121. K.-C. Toh, M. J. Todd, and R. H. Tütüncü. "SDPT3—a MATLAB software package for semidefinite programming, version 1.3". *Optimization methods and software* 11:1-4, 1999, pp. 545–581.

122. R. Tóth, H. S. Abbas, and H. Werner. "On the state-space realization of LPV input-output models: Practical approaches". *IEEE transactions on control systems technology* 20:1, 2011, pp. 139–153.

123. C. Trapiello, V. Puig, and B. Morcego. "Position-heading quadrotor control using LPV techniques". *IET Control Theory & Applications* 13:6, 2019, pp. 783–794.

124. I. L. Turner, M. D. Harley, and C. D. Drummond. "UAVs for coastal surveying". *Coastal Engineering* 114, 2016, pp. 19–24.

125. R. Ungurán, V. Petrović, L. Y. Pao, and M. Kühn. "Smart rotor control of wind turbines under actuator limitations". In: *2019 American Control Conference (ACC)*. 2019, pp. 3474–3481. DOI: 10.23919/ACC.2019.8815001.

126. W. Van Soest, Q. Chu, and J. Mulder. "Combined feedback linearization and constrained model predictive control for entry flight". *Journal of guidance, control, and dynamics* 29:2, 2006, pp. 427–434.

127. A. P. White, G. Zhu, and J. Choi. *Linear parameter-varying control for engineering applications*. SpringerBriefs in Electrical and Computer Engineering. Springer London, London, 2013. ISBN: 978-1-4471-5039-8. DOI: 10.1007/978-1-4471-5040-4.

128. F. Wu, K. M. Grigoriadis, and A. Packard. "Anti-windup controller design using linear parameter-varying control methods". *International Journal of Control* 73:12, 2000, pp. 1104–1114.

129. F. Wu, Z. Lin, and Q. Zheng. "Output feedback stabilization of linear systems with actuator saturation". *IEEE Transactions on Automatic Control* 52:1, 2007, pp. 122–128.

130. F. Wu and B. Lu. "Anti-windup control design for exponentially unstable LTI systems with actuator saturation". *Systems & Control Letters* 52:3-4, 2004, pp. 305–322.

131. F. Wu, X. H. Yang, A. Packard, and G. Becker. "Induced L2-norm control for LPV systems with bounded parameter variation rates". *International Journal of Robust and Nonlinear Control* 6:9-10, 1996, pp. 983–998.

132. C. Yuan and F. Wu. "Switching control of linear systems subject to asymmetric actuator saturation". *International Journal of Control* 88:1, 2015, pp. 204–215.

133. H. Zhang, G. Zhang, and J. Wang. "$\mathcal{H}_\infty$ observer design for LPV systems with uncertain measurements on scheduling variables: application to an electric ground vehicle". *IEEE/ASME Transactions on Mechatronics* 21:3, 2016, pp. 1659–1670.